

Identification and Characterisation of Novel Antibiotic Targets in Multi-Drug Resistant Gram-Negative Bacteria

Submitted by
Rachael Impey

Bachelor of Biomedical Science, 2015
La Trobe University
Bachelor of Biomedical Science (Honours), 2016
La Trobe University

A thesis submitted in total fulfilment of the
requirements for the degree of Doctor of Philosophy

School of Molecular Sciences,
College of Science Health and Engineering

La Trobe University
Victoria, Australia

December 2020

- This page was intentionally left blank -

Table of Contents

| | |
|---|------------|
| <i>Abstract.....</i> | <i>iii</i> |
| <i>Statement of Authorship.....</i> | <i>iv</i> |
| <i>Preface.....</i> | <i>v</i> |
| <i>Acknowledgements.....</i> | <i>vii</i> |
| <i>Abbreviations.....</i> | <i>ix</i> |
| 1 Introduction..... | 1 |
| 1.1 The Need for New Antibiotics..... | 2 |
| 1.1.1 The Golden Era of Antibiotic Discovery | 2 |
| 1.1.2 Antibiotic Modes of Action..... | 3 |
| 1.1.3 Reliance on Antibiotics | 7 |
| 1.1.4 Antibiotic Resistance..... | 7 |
| 1.2 Review: Targeting the Biosynthesis and Incorporation of Amino Acids into the Peptidoglycan as an Antibiotic Approach Against Gram Negative Bacteria..... | 11 |
| 1.2.1 Copyright..... | 11 |
| 1.2.2 Statement of Contribution | 11 |
| 1.3 The Diaminopimelate Pathway..... | 23 |
| 1.3.1 Overview | 23 |
| 1.3.2 DHDPS..... | 23 |
| 1.3.3 DHDPR | 28 |
| 1.3.4 Inhibition Studies of the DAP Pathway | 31 |
| 1.4 Overview | 34 |
| 1.5 References..... | 36 |
| 2 DHDPS enzymes from <i>Pseudomonas aeruginosa</i>..... | 49 |
| 2.1 Published Article..... | 49 |
| 2.1.1 Copyright..... | 49 |
| 2.1.2 Statement of Contribution | 49 |
| 3 DHDPS enzymes from <i>Klebsiella pneumoniae</i> and <i>Acinetobacter baumannii</i> | 65 |
| 3.1 Published Article..... | 65 |
| 3.1.1 Copyright..... | 65 |
| 3.1.2 Statement of Contribution | 65 |
| 4 Validation of DHDPR from <i>Pseudomonas aeruginosa</i> | 77 |
| 4.1 Manuscript for Submission..... | 77 |
| 4.1.1 Statement of Contribution | 77 |
| 5 Discussion and Future Directions..... | 104 |
| 5.1 Final Discussion..... | 104 |
| 5.1.1 Gene Mis-annotations | 104 |
| 5.1.2 Gene Validation and Essentiality | 107 |
| 5.1.3 Protein Structure and Function..... | 109 |
| 5.2 Future Directions | 110 |
| 5.2.1 Genetic Manipulation and Investigation | 111 |
| 5.2.2 Phenotypic Characterisation of Mutant Strains..... | 112 |

| | | |
|--|---------------------------|-------------------|
| 5.2.3 | Inhibitor Discovery | 115 |
| 5.3 | Summary..... | 118 |
| 5.4 | References..... | 119 |
| <i>Appendices.....</i> | | <i>125</i> |
| Appendix I | | 125 |
| Review: Overcoming Intrinsic and Acquired Resistance Mechanisms Associated with the Cell Wall of Gram-Negative Bacteria | | 125 |
| Copyright | | 125 |
| Statement of Contribution..... | | 125 |
| Appendix II - High throughput chemical screen method | | 145 |
| Appendix III – CT1-5 Inhibition Determination | | 146 |
| Appendix IV – CT1-5 Minimum Inhibitory Concentration | | 147 |
| Appendix References | | 147 |

Abstract

There is an urgent need to replenish the antibiotic development pipeline with new products to combat the rise of multi-drug resistant bacteria. Of particular significance are the Gram-negative pathogens in the World Health Organization highest priority list *Pseudomonas aeruginosa*, *Acinetobacter baumannii* and *Klebsiella pneumoniae*. One strategy to overcome resistance in these bacteria is to identify novel antibiotic modes of action. Accordingly, this thesis focuses on the enzymes dihydrodipicolinate synthase (DHDPS) and dihydrodipicolinate reductase (DHDPR), which are responsible for the production of *meso*-diaminopimelate and L-lysine. Given the critical role these metabolites play in cell wall and protein syntheses and the lack of human homologues, DHDPS and DHDPR represent promising antibiotic targets.

Firstly, *P. aeruginosa* was shown to have four annotated DHDPS-encoding genes, with only two encoding functional DHDPS enzymes. Although the isoforms share similar catalytic activities, they are differentially regulated by L-lysine. Using a combination of X-ray crystallography, mutagenesis and homology modelling, the difference in regulation was attributed to a single residue in the allosteric site. Based on these findings, a 7-residue sequence motif was employed to identify mis-annotations of multiple putative DHDPS-encoding genes in *A. baumannii* and *K. pneumoniae*. The mis-annotations were subsequently confirmed using enzyme kinetics and X-ray crystallography. Finally, a gene knockout approach was optimised to address the conflicting evidence around the essentiality of the DHDPR-encoding gene in *P. aeruginosa*. Here, a knockout strain was generated that is unable to survive without the supplementation of *meso*-diaminopimelate, indicating that this gene is indeed essential for *P. aeruginosa*. Moreover, kinetic and binding studies were used to probe the catalytic mechanism of the gene product. In summary, this work provides critical insights into the structure and function of DHDPS and DHDPR from these high-priority multi-drug resistant bacteria for future drug discovery efforts to tackle antibiotic resistance.

Statement of Authorship

Except where reference is made in the text of the thesis, this thesis contains no material published elsewhere or extracted in whole or in part from a thesis accepted for the award of any other degree or diploma. No other person's work has been used without due acknowledgment in the main text of the thesis. This thesis has not been submitted for the award of any degree or diploma in any other tertiary institution.

Rachael Impey

16 December 2020

Preface

Unless otherwise stated in this thesis, all the work presented was performed by the candidate, with the following exceptions:

Chapter 1: A portion of this chapter was published as the following two reviews:

Impey, R. E., Hawkins, D. A., Sutton, J. M. & Soares da Costa, T. P. (2020) “Overcoming intrinsic and acquired resistance mechanisms associated with the cell wall of Gram-negative bacteria”, *Antibiotics*, 9(9), 623

The candidate was responsible for: conceptualisation, drafting and writing of the manuscript in collaboration with Daniel A. Hawkins, preparation of figures and revisions of the manuscript prior to acceptance. J. Mark Sutton and Tatiana P. Soares da Costa were involved in supervision and manuscript preparation and revision.

Impey, R. E. & Soares da Costa, T. P. (2018) “Targeting the biosynthesis and incorporation of amino acids into the peptidoglycan as an antibiotic approach against Gram negative bacteria”, *EC Microbiology*, 14(4), 200-209

The candidate was responsible for: conceptualisation, drafting and writing of the manuscript, preparation of figures and revisions of the manuscript prior to acceptance. Tatiana P. Soares da Costa was involved in supervision and manuscript preparation and revision.

Chapter 2: This chapter is a published manuscript in *The FEBS Journal* as follows:

Impey, R. E., Panjikar, S., Hall, C. J., Bock, L. J., Sutton, J. M., Perugini, M. A. & Soares da Costa, T. P. (2020) “Identification of two dihydrodipicolinate synthase isoforms from *Pseudomonas aeruginosa* that differ in allosteric regulation”, *FEBS Journal*, 287(2), 386-400

The candidate was responsible for all experimental work, except for the homology model generation that was performed by Cody J. Hall (Figure 11). Furthermore, refinement of the PaDHDPS2-H56Q structure was assisted by Santosh Panjikar. Lucy J. Bock, J. Mark Sutton, Matthew A. Perugini and Tatiana P. Soares da Costa were responsible for assistance in experimental design, manuscript preparation as well as candidate supervision.

Chapter 3: This chapter is a published manuscript in *FEBS Letters* as follows:

Impey, R. E., Lee, M., Hawkins, D.A., Sutton, J. M., Panjikar, S., Perugini, M. A. & Soares da Costa, T. P. (2020) “Mis-annotations of a promising antibiotic target in high-priority Gram-negative pathogens”, *FEBS Letters*, 594(9), 1453-1463

All experimental work was completed by the candidate with the exception of the overexpression of recombinant KpDapA3 and KpDapA4 proteins, which was performed by Daniel A. Hawkins. Refinement of the KpDHDPS structure was assisted by Mihwa Lee, with beamline time provided by Santosh Panjikar at the Australian Synchrotron. J. Mark Sutton, Matthew A. Perugini and Tatiana P. Soares da Costa were responsible for assistance in experimental design, manuscript preparation as well as candidate supervision.

Chapter 4: This chapter is a draft manuscript for to be submitted to *The FEBS Journal* entitled “Validation and characterisation of a novel antibiotic target in *Pseudomonas aeruginosa*” by Rachael E. Impey, Sarah Licul, Lucy J. Bock, Matthew A. Perugini, J. Mark Sutton and Tatiana P. Soares da Costa.

The candidate was responsible for all experimental work with the exception of the circular dichroism spectroscopy data for the recombinant PaDHDPR protein (Figure 4), which was collected and analysed by Sarah Licul. Lucy J. Bock, J. Mark Sutton, Matthew A. Perugini and Tatiana P. Soares da Costa were responsible for assistance in experimental design, manuscript preparation as well as candidate supervision.

Chapter 5: A portion of this chapter contains unpublished experimental work conducted by Matthew A. Perugini and Tatiana P. Soares da Costa. Matthew A. Perugini was responsible for the high throughput chemical screen in collaboration with the Walter and Eliza Hall Institute High Throughput Chemical Screening Facility (Melbourne, Australia). Tatiana P. Soares da Costa was responsible for the lead optimisation and bacterial screening of the CT1-5 inhibitor against *P. aeruginosa*. All work is credited where applicable.

This work was supported by an Australian Government Research Training Program Scholarship and the British Society for Antimicrobial Chemotherapy Overseas Scholarship.

Acknowledgements

First, I would like to acknowledge my primary supervisor Dr. Tatiana Soares da Costa. Throughout this whole journey you have been a source of wisdom, guidance and a fantastic mentor. You have dealt with my numerous questions and always put a positive spin on every result. Your enthusiasm for science and wanting to change the world is so strong, it has motivated me for the last 5 years. From the walks during lockdown, to the many iced chocolates and soy chais, I am pleased that at the end of this journey I can not only call you my supervisor, but a close friend as well!

I would also like to extend my thanks to the rest of my progress panel, including my co-supervisors Associate Professor Matthew Perugini and Dr. Mihwa Lee, as well as my mentor Professor Patrick Humbert. Thank you all for pushing me when you thought I was too comfortable, for attending the many talk rehearsals and always being there to answer my questions. In particular Mihwa, thank you for all of your help with crystallography and structure refinement. Whenever I got frustrated with Coot, and simply just didn't understand, all it would take was an email to you and you would put me on the right track again.

To the rest of the Soares da Costa/Perugini lab members, every one of you has helped me on this journey and I certainly wouldn't be here without you all. Cody, you and I started this endeavour together and it looks like we will finish it together! Thank you for always being willing to go see Marvel movies the first day they came out, but I won't thank you for making me sit through the 3-hour extended addition of Batman versus Superman. Never again. Seb, thank you for always watching something interesting on YouTube that I can snoop on, and thank you for teaching us all how to play Tarot. It's debatable that I might have been able to finish much sooner if I didn't spend all that time at tea parties. To Dan, my partner in crime and dual pronged knockout buddy. Your unwavering positivity has always been a huge support and it's been great to pass on projects to you to continue. Em, thank you for appreciating my dancing and never missing an opportunity to point out when I've said something stupid. You always encourage me and make me feel like I have achieved a lot, even when I may not have had anything work that week. To Jess, thank you for always taking the elevator with me, even though it was definitely slower, and being the early bird with me. The mornings in the lab would have been very lonely without you in as well! To Andrew, thank you for answering my many chemistry questions despite the fact I rarely understood the answers. Thank you for the

many hours of endless proof reading and motivating me to keep going. To the hiking (and I guess now climbing?) crew, thank you for all of the outings, laughing at me falling over and all of the hot chocolates afterwards. Little Matt, thank you for making me laugh and always finding the most inappropriate thing to say at that moment. To all the other lab members, past and present, thank you for putting up with me even if I extended roundtable by at least an hour at some points.

None of this would have been possible without the absolute unwavering support from my family. Mum and Dad, thank you for always being there, letting me come home when it had been a hard week in the lab and always trying to understand my science. Dad, thank you for only falling asleep once when I practiced my talk to you – I hope I've improved since then! David and Sam, thank you for bringing my two favourite nephews into the world and always bringing them to see me whenever I came home! I appreciate all the Christmas lunches where you never made me feel bad for not hosting.

To my chosen family, my two best friends, Emma and Cassie. Thank you for dealing with all of the meltdowns, the many tea breaks, the dog park trips and takeaway food. It certainly hasn't been a healthy journey, but you both have been there from the start – and look how far this potato has come now! To my other two best friends, Amy and Cristina, you have both always been only a message away. Thank you for all of the lunches, the tea breaks and the movie nights. We are finally all on the home stretch of this journey together!

Thank you to everyone on this adventure. Everyone has helped in their own way and I wouldn't be here without every single one of you.

Abbreviations

| | |
|----------------------|---|
| 2,6-PDC | 2,6-pyridinedicarboxylic acid |
| 3D | 3-dimensional |
| 3MB | <i>m</i> -toluic acid |
| ABC | ATP binding cassette |
| Abs _{340nm} | Absorbance at 340nm |
| AGRF | Australian Genome Research Facility |
| Alr | Alanine racemase |
| AMR | Antimicrobial resistance |
| ASA | Aspartate semialdehyde |
| ATP | Adenosine triphosphate |
| AUC | Analytical ultracentrifugation |
| Bam | β-barrel assembly machinery |
| bp | Base pair |
| CD | Circular dichroism |
| DAP | Diaminopimelate |
| DAP-DC | Diaminopimelate decarboxylase |
| DAP-EP | DAP epimerase |
| Dat | D-aminotransferase |
| Ddl | D-Ala-D-Ala ligase |
| DHDP | Dihydrodipicolinate |
| DHDPR | Dihydrodipicolinate reductase |
| DHDPS | Dihydrodipicolinate synthase |
| DNA | Deoxyribonucleic acid |
| ECDC | European Centers for Disease Prevention and Control |
| EPI | Efflux pump inhibitor |
| ESBL | Extended spectrum β-lactamase |
| GDH | Glutamate dehydrogenase |
| GlcNAc | <i>N</i> -acetylglucosamine |
| | Gram-negative bacteria |
| GOGAT | Glutamate synthase |
| GPB | Gram-positive bacteria |
| GS | Glutamine synthetase |
| HTPA | 4-hydroxy-2,3,4,5-tetrahydrodipicolinic acid |
| IC ₅₀ | Inhibition concentration 50% |
| IMAC | Immobilised metal affinity chromatography |
| k _{cat} | Catalytic constant - enzymatic turnover |
| kDa | Kilodalton |
| K _i | Inhibitor constant |
| K _M | Michaelis-Menten constant |
| KPC | <i>Klebsiella pneumoniae</i> carbapenemases |
| LB | Luria-Bertani |

| | |
|---------------|---|
| LL-DAP | L, L,-2,6-diaminopimelate |
| LPS | Lipopolysaccharide |
| MCR | Mobile colistin resistance |
| MDR | Multi-drug resistant |
| MFS | Major facilitator superfamily |
| MIC | Minimum inhibitory concentration |
| MRE | Mean residue ellipticity |
| mRNA | Messenger RNA |
| MST | Microscale thermophoresis |
| MurNAc | <i>N</i> -acetylmuramic acid |
| NADH | Nicotinamide adenine dinucleotide |
| NADPH | Nicotinamide adenine dinucleotide phosphate |
| NEB | New England Biolabs |
| NSDAP | <i>N</i> -succinyl-L,L-2,6-diaminopimelate |
| NSDAP-AS | <i>N</i> -succinyldiaminopimelate aminotransferase |
| NSKAP | <i>N</i> -succinyl-L-2-amino-6-ketopimelate |
| <i>o</i> -ABA | <i>o</i> -aminobenzaldehyde |
| OMP | Outer membrane protein |
| ORF | Open reading frame |
| PAβN | Phenylalanine-arginine beta-naphthylamide |
| PBP | Penicillin binding protein |
| PCR | Polymerase chain reaction |
| PDB | Protein Data Bank |
| PDR | Pan-drug resistant |
| PEP | Phosphoenolpyruvate |
| PLP | Pyridoxal-5`-phosphate |
| PMBN | Polymyxin B nonapeptide |
| PmrC | Phosphoethanolamine transferase |
| Pyr4H2C | 1-pyrroline-4-hydroxy-2-carboxylate |
| RNA | Ribonucleic acid |
| RND | Resistance nodulation cell division |
| rRNA | Ribosomal RNA |
| SAR | Structure activity relationship |
| SDAP-DS | Succinyldiaminopimelate desuccinylase |
| SDS-PAGE | Sodium dodecyl sulfate-polyacrylamide electrophoresis |
| sRNA | Small RNA |
| TCS | Two-component system |
| THDP | 2,3,4,5-tetrahydrodipicolinate |
| THPC-NST | Tetrahydrodipicolinate <i>N</i> -succinyltransferase |
| tRNA | Transfer RNA |
| TYS | Tryptone, yeast and sucrose |
| UDP | Uridine diphosphate |
| V_{\max} | Maximum velocity |

| | |
|-----|---------------------------|
| WHO | World Health Organization |
| WT | Wildtype |
| XDR | Extremely drug resistant |

- This page was intentionally left blank -

1 Introduction

A portion of this chapter was published as the following two reviews:

Impey, R. E., Hawkins, D. A., Sutton., J. M. & Soares da Costa, T. P. (2020) “Overcoming intrinsic and acquired resistance mechanisms associated with the cell wall of Gram-negative bacteria”, *Antibiotics*, 9(9), 623

Impey, R. E. & Soares da Costa, T. P. (2018) “Targeting the biosynthesis and incorporation of amino acids into the peptidoglycan as an antibiotic approach against Gram negative bacteria”, *EC Microbiology*, 14(4), 200-209

1.1 The Need for New Antibiotics

1.1.1 The Golden Era of Antibiotic Discovery

The first known use of antibacterials was the application of mouldy soybean curd to ailments, including carbuncles and furuncles in Chinese medicine [1]. However, it was not until Alexander Fleming discovered *Penicillium notatum* in 1928, that the first clinical antibiotic would soon be developed [2]. His discovery was closely followed by that of the sulfonamide antibiotics in the 1930s, before Howard Florey and Ernst Chain established mass production of penicillin for use during World War II [1,3]. By the 1950s, the “golden era” of antibiotics had begun. The 20 years following the emergence of penicillin as a viable treatment saw the discovery of almost every known class of antibiotic in use today (Fig. 1). The isolation of streptomycin from *Streptomyces griseus* in 1944 allowed for the development of the first aminoglycosides [4]. This was quickly followed by the discovery of cephalosporins, chloramphenicol, macrolides and streptogramins (Fig. 1) [5]. Another five antibiotic classes were approved prior to 1968, including glycopeptides, rifamycin, nitroimidazoles, quinolones and trimethoprim (Fig 1) [5]. Many of these antibiotic classes were discovered by “mining” for new agents from organisms themselves. However, by 1968, many of the compounds being discovered were similar or redundant when compared to the already discovered antibiotics [6]. This marked the end of the “golden era”, with no new classes of antibiotics approved in over 32 years, until the introduction of the oxazolidinones in 2000 (Fig. 1) [5]. Since then, antibiotic development has become substantially more challenging, resulting in only one additional class of antibiotics, lipopeptides, which received approval in 2003 [5]. This is coupled with reduced interest from pharmaceutical companies, with minimal financial incentives to continue antibiotic development [7].

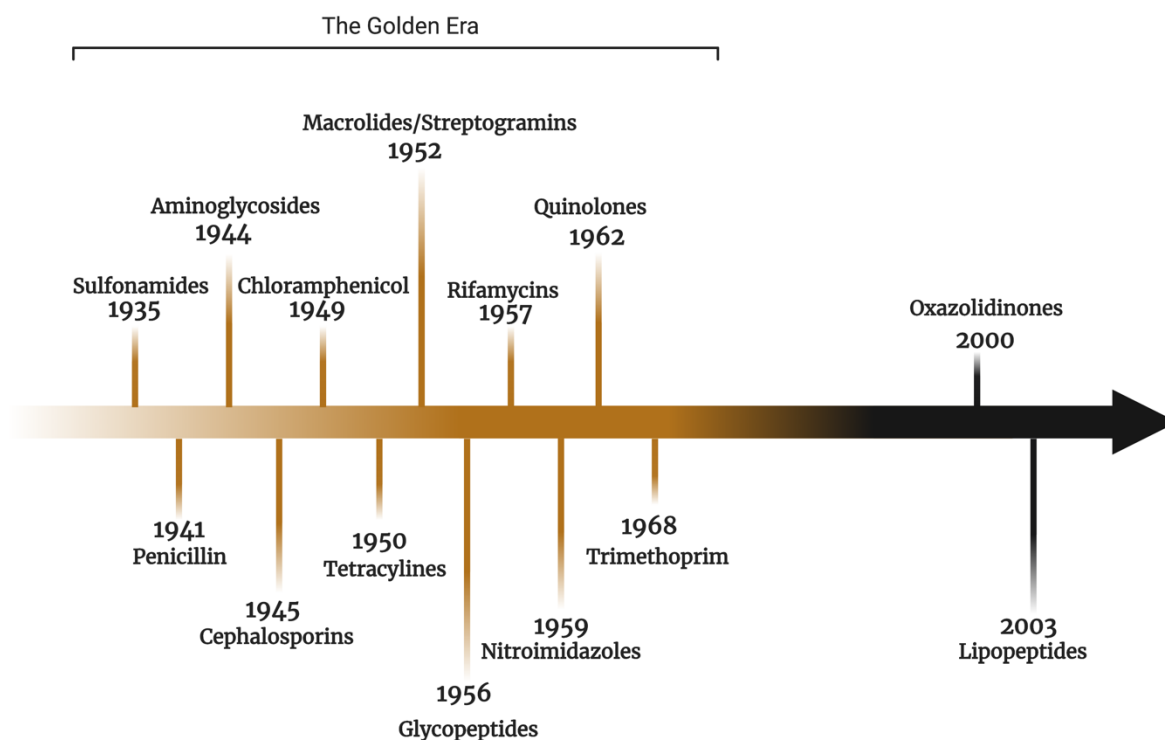


Figure 1. Antibiotic development timeline.

1.1.2 Antibiotic Modes of Action

The antibiotic classes mentioned above are typically composed of a variety of analogues sharing similar structural motifs and modes of action, to increase the range of available treatments. This allows for broader species specificity, potency and reduced cross-resistance. Moreover, the current clinically relevant antibiotics have one of four main modes of action; inhibiting cell wall synthesis/disruption, inhibiting protein synthesis, inhibiting nucleic acid synthesis or antimetabolite activity. These modes of action are described in detail below.

1.1.2.1 Cell Wall Synthesis and Disruption

Many antibiotic classes target the peptidoglycan layer of the cell wall, comprised of long sugar polymers crosslinked with a pentapeptide chain [8,9]. For example, the β -lactam antibiotics, which includes penicillin, bind to the penicillin binding proteins (PBPs) that are responsible for the crosslinking of the peptidoglycan layer, resulting in cell wall disruption and bacterial cell lysis (Fig. 2) [10]. The β -lactam class of antibiotics includes several subclasses, including cephalosporins, carbapenems and monobactams, which differ in their potency and species

specificity. For instance, carbapenem antibiotics have the greatest potency and broadest spectrum of activity, and as a result are often used as “last resort” treatments [11].

Another class of antibiotics targeting the cell wall is a group of glycosylated peptides known as glycopeptides, whose members include vancomycin, teicoplanin and their derivatives [12]. Glycopeptides interact with the peptidoglycan precursor lipid II, which contains a pentapeptide chain terminating in a dipeptide moiety D-alanyl-D-alanine (D-Ala-D-Ala) (Fig. 2) [12]. Specifically, glycopeptides bind to the D-Ala-D-Ala motif, inhibiting the interaction with the PBPs responsible for crosslinking the precursor via the pentapeptide chain, into the peptidoglycan layer [12]. This causes membrane destabilisation and subsequently bacterial cell death [12]. Glycopeptides are only effective against Gram-positive bacteria, as Gram-negative bacteria contain an additional outer membrane that hinders glycopeptides from traversing it due their size and chemical composition [12].

Another notable class of peptide antibiotic that target cell wall synthesis is the polymyxins, which include polymyxin B and E, also known as colistin. Unlike glycopeptides, polymyxins have a dual mode of action by permeabilising the outer membrane and causing a bactericidal effect on the cytoplasmic membrane [13,14]. The LPS molecules of the outer membrane of Gram-negative bacteria are bridged by divalent cations that are crucial for membrane integrity [13–15]. Polymyxins are positively charged and interact with the outward facing lipid A portion of the LPS, causing displacement of these divalent cations [13,14]. This increases the permeability of the membrane and allows the polymyxins to cross the outer membrane and exert their effects on the cytoplasmic membrane [13,16]. The direct mechanism of the antibacterial effect on the cytoplasmic membrane is still unknown [13,16]. Use of polymyxin antibiotics was originally halted due to renal and neurological toxicity, however improvements in manufacturing and dosages have allowed a resurgence in its use as another last resort antibiotic [13,14].

1.1.2.2 Protein Synthesis

The essentiality of protein synthesis makes it another attractive antibiotic target. Given that protein synthesis from mRNA occurs at the ribosome, several antibiotic classes have been developed targeting either the 30S or 50S ribosomal subunit (Fig. 2) [4]. Specifically, aminoglycosides bind to the 16S ribosomal RNA (rRNA) of the 30S subunit, resulting in a conformational change that induces codon misreading [4]. There is also some evidence that

different aminoglycosides can directly block initiation or elongation depending on the chemical structure [4]. Alternatively, while tetracyclines also bind to the 16S rRNA, they act by preventing attachment of the aminoacyl-tRNA to this site [17]. The low cost of aminoglycosides and tetracyclines and broad spectrum activity against Gram-negative and Gram-positive bacteria have resulted in them being two of the most commonly used antibiotic classes [4,17].

Unlike aminoglycosides and tetracyclines, there are multiple antibiotic classes that interact with the 50S ribosome. The antibiotic chloramphenicol blocks several important ribosomal functions, including binding and movement of ribosomal substrates and peptidyltransferase activity by its interaction with the 50S subunit [18]. Moreover, macrolides, which include erythromycin, azithromycin, clarithromycin and roxithromycin, are macrocyclic lactone rings that interrupt protein synthesis by blocking the ribosomal peptide exit tunnel [19–21]. Clindamycin also binds competitively at this site, making chloramphenicol, macrolides and clindamycin antagonistic of one another [22]. Furthermore, streptogramins are often used synergistically as streptogramin A inactivates the donor and acceptor sites of the peptidyltransferase, while streptogramin B inhibits peptide bond formation similarly to the macrolides mentioned above [23]. Alternatively, oxazolidinones exert a different mode of action at the 50S subunit, including linezolid that binds and prevents formation of the initiation complex with the other necessary components involved in protein synthesis [24].

1.1.2.3 Nucleic Acid Synthesis

Both DNA and RNA synthesis are targeted by clinically available antibiotics. DNA gyrase, which is responsible for the supercoiling of DNA strands to allow replication, is the target of fluoroquinolones [25]. In Gram-positive bacteria, the preferred target is topoisomerase IV, which after replication, separates the daughter DNA strand [26]. Fluoroquinolones bind to either the DNA gyrase or topoisomerase IV when bound to DNA, forming a trapped complex [26]. This ultimately results in chromosomal fragmentation, causing bacterial cell death [26]. Alternatively, the antibiotic rifampicin, part of the rifamycin family, binds allosterically to RNA polymerase (Fig. 2). [27]. Other antibiotics, including actinomycin and mitomycin, also interact with RNA polymerase but result in toxic effects, and as such, have been repurposed as chemotherapeutic agents [27].

1.1.2.4 Antimetabolite Activity

Antimetabolite antibiotics are those that inhibit the synthesis of the nucleotides required for DNA and RNA synthesis [28]. Two examples are sulfonamides and trimethoprim, which act through their inhibition of folic acid synthesis. Sulfonamides inhibit dihydropteroate synthase competitively against its natural substrate, p-aminobenzoic acid [28]. Alternatively, trimethoprim blocks the production of the active form of folic acid, tetrahydrofolate, by competitive inhibition of dihydrofolate reductase (Fig. 2) [29]. Trimethoprim is highly effective against Gram-positive bacteria, however has limited antimicrobial activity against Gram-negative bacteria [29].

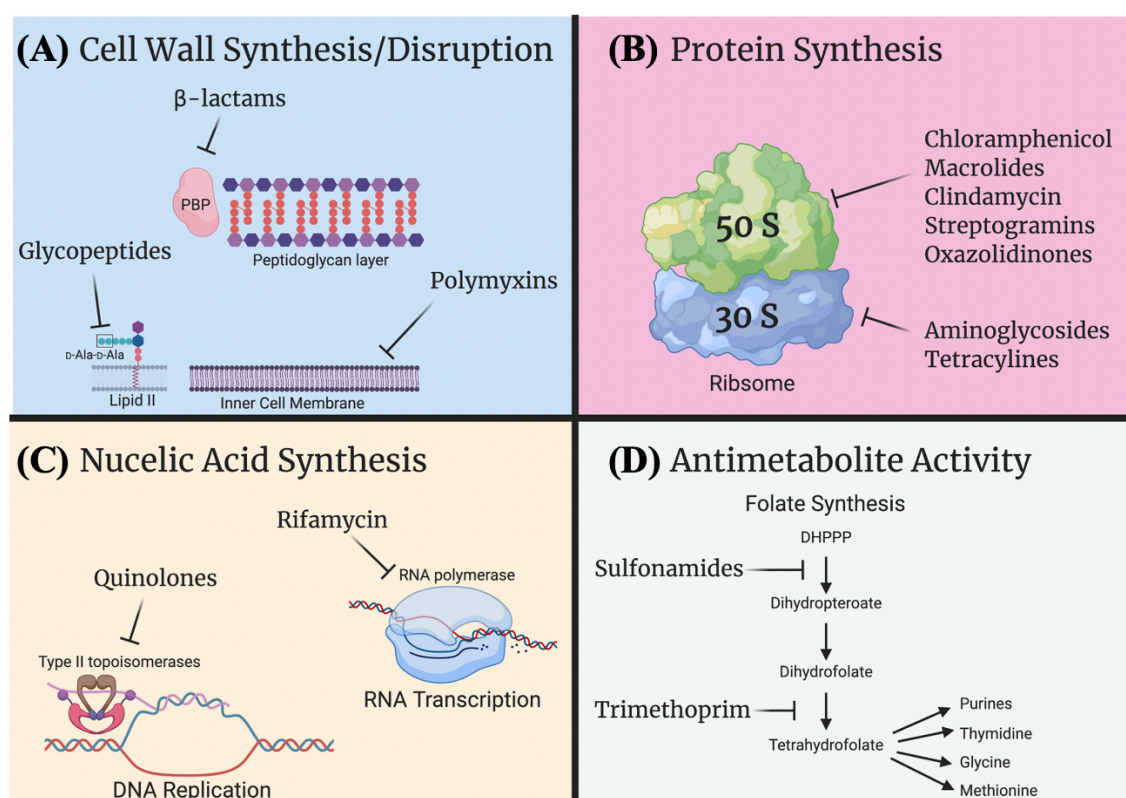


Figure 2. Antibiotic modes of action. (A) β-lactams target the penicillin binding proteins (PBPs) involved in peptidoglycan synthesis, while glycopeptides bind to the D-Ala-D-Ala terminal dipeptide in complex with lipid II. Polymyxins bind to the outer membrane, however, are believed to exert their antimicrobial effects on the cytoplasmic membrane. (B) Aminoglycosides and tetracyclines target the 30S subunit of the ribosome to inhibit protein synthesis, whilst chloramphenicol, macrolides, streptogramins and oxazolidinones act on the 50S subunit. (C) Quinolones target the type II topoisomerases, DNA gyrase and topoisomerase IV, to halt DNA synthesis, as opposed to rifamycin antibiotics, which target RNA polymerase

and RNA synthesis. **(D)** Sulfonamides and trimethoprim inhibit different enzymes in folic acid synthesis, an important precursor for metabolite synthesis.

1.1.3 Reliance on Antibiotics

Prior to the widespread use of antibiotics in the 20th century, diseases such as pneumonia, diarrhoea and diphtheria were the leading causes of death [30]. Furthermore, infections such as endocarditis and those caused by *Staphylococcus aureus* had mortality rates of 97% and 80%, respectively [31,32], and the standard treatment for wound infections was amputation [33]. Indeed, 70% of amputations performed during World War I were due to bacterial wound infection [33]. The introduction of penicillin reduced the death rate of *S. aureus* infections to 30%, which has reduced further with improved antibiotic efficacy and treatment [31]. Moreover, post-surgical infection rates have decreased from 40% to 2% [34], with the use of prophylactic antibiotics now routine for many surgeries [35,36]. Antibiotics have successfully treated or prevented infections in “at-risk” patients, such as those receiving chemotherapy, diabetics or those with rheumatoid arthritis and with end stage renal disease [37]. Prophylactic antibiotic treatment for caesarean births has also been shown to substantially reduce febrile morbidity, wound infections and severe maternal complications [38]. These statistics demonstrate the reliance that modern medicine has had on the use of antibiotics. However, the dwindling number of antibiotics in the drug development pipeline and the rise in antibiotic resistance are of serious concern.

1.1.4 Antibiotic Resistance

During his 1945 Nobel lecture, Alexander Fleming warned of the dangers of resistance [2]. After the clinical introduction of penicillin in the 1940s, approximately 50% of *S. aureus* infections were resistant by 1950, swiftly followed by resistance to tetracycline and macrolides, before resistance to methicillin only two years after its introduction [39,40]. Since then, antibiotic resistance has been rapidly on the rise. The 2016 antimicrobial resistance (AMR) review predicts that by 2050, 10 million lives and over US\$100 trillion worth of economic output could be lost due to antibiotic resistance every year [41]. However, due to inadequate global surveillance of resistant infections, it is difficult to accurately predict the current burden, with fears this prediction could be an underestimate. Some drug resistance is inevitable, even without antibiotic use, due to random mutagenesis and evolution [42]. Nevertheless,

epidemiological studies have shown that antibiotic use, even when used correctly, has dramatically accelerated this process [42]. Moreover, resistance has been attributed to the misuse of antimicrobials in several scenarios, including primary care [43,44], agriculture [45,46] and urban and farm runoffs [47,48].

1.1.4.1 Multi-drug Resistance

The emergence of multi-drug resistance (MDR) is increasing at an alarming rate. Due to previous inconsistencies in the reporting of MDR strains, a standardised classification system has recently been adopted [49]. A bacterium is considered MDR if it is resistant to one agent in three or more therapeutically relevant antimicrobial classes [49]. Meanwhile, to be classified as either extremely drug-resistant (XDR) or pan-drug resistant (PDR), the isolate must be resistant to one agent in all but two or fewer antimicrobial classes or resistant to all antimicrobial agents in all classes, respectively [49]. The increased prevalence of these resistant strains represents a serious threat to the healthcare system as it results in higher mortality rate and increased hospital stays [50–53].

A significant portion of MDR, XDR and PDR infections are attributed to Gram-negative bacteria. Despite this, the World Health Organization (WHO) reports that only 12 of the 50 agents currently on the clinical pipeline target Gram-negative bacteria [54]. Furthermore, of these 12, only two meet the WHO criteria of being innovative, which includes the absence of any known existing cross-resistance within an antibiotic class or a novel target/mode of action [54].

1.1.4.2 High Priority Gram-Negative Pathogens

Unlike Gram-positive bacteria, Gram-negative bacteria have an additional outer membrane layer, which directly contributes to their increased antibiotic resistance [55,56]. The resistance mechanisms associated with the cell wall of Gram-negative bacteria is described in detail in Appendix I. In an attempt to guide antibiotic discovery efforts, the WHO proposed a priority list of bacteria based on mortality, healthcare and community burdens, prevalence and trends of resistance as well as treatability and drugs already in the pipeline [57]. The highest category, critical, comprises three Gram-negative bacteria; *Acinetobacter baumannii*, *Pseudomonas aeruginosa* and the Enterobacteriaceae family, which includes *Klebsiella pneumoniae* [57]. These three bacterial species form the focus of this thesis and are described in brief below, specifically in relation to their impact on the MDR healthcare crisis.

Pseudomonas aeruginosa

P. aeruginosa is an opportunistic pathogen, responsible for both chronic and potentially lethal infections in susceptible patients [58,59]. It is listed as the most common cause of septicemia in immunodeficient patients and is the most frequent isolate in burn units [60]. Treatment typically involves a β -lactam antibiotic alone or in combination with aminoglycosides, depending on the location and type of infection [58]. However, resistance to one or more antibiotic classes frequently emerges in *P. aeruginosa* via innate and acquired resistance mechanisms. The European Centers for Disease Prevention and Control (ECDC) reported that over 13% of isolates tested were MDR, while 5.5% were resistant to all five antimicrobial classes tested [61]. A South China study found 54% of *P. aeruginosa* infections to be MDR and had a significantly higher mortality rate (49%) when compared to susceptible strains (20%) [62].

Acinetobacter baumannii

Similar to *P. aeruginosa*, *A. baumannii* is an opportunistic pathogen responsible for a variety of infections including blood, urinary tract and surgical site infections [63]. Carbapenems, including imipenem and meropenem, were frequently used for treatment of *A. baumannii* infections, however resistance profiling reveals that 44-49% of isolates tested were resistant to these antibiotics [64]. In most cases, carbapenem resistant isolates are also resistant to penicillins, cephalosporins, aminoglycosides and fluoroquinolones [64]. Other surveillance reports indicate ~45% of *A. baumannii* isolates worldwide are MDR, with rates as high as 70% in the Middle East and Latin America [65,66]. PDR *A. baumannii* has also been reported in nosocomial outbreaks in Germany [67], France [68], Iran [69], Taiwan [70] and Spain [71], indicating that this issue is widespread.

Klebsiella pneumoniae

K. pneumoniae is a member of the Gram-negative *Enterobacteriaceae* family of bacteria, which also includes other pathogenic species like *Escherichia coli* and *Salmonella* [72]. *K. pneumoniae* and other *Enterobacteriaceae* species are of concern due to their highly transmissible carbapenem resistance. Carbapenems are often prescribed as first line treatments for extended spectrum β -lactamase (ESBL) producing infections, which provide resistance to many β -lactam antibiotics [73]. However, carbapenem resistance due to *K. pneumoniae*

carbapenemases (KPCs) has now been observed worldwide [73,74]. KPCs are often plasmid encoded, and thus have high motility to other bacteria previously susceptible to carbapenems [73,74]. This is dangerous in nosocomial environments as KPC resistance can spread easily throughout the *Enterobacteriaceae* species, and also occasionally to *P. aeruginosa*, causing outbreaks with high mortality rates [74]. Moreover, infections with MDR *K. pneumoniae* are estimated to have mortality rates above 40% [75]. Although not as common as PDR *A. baumannii*, PDR *K. pneumoniae* has been reported in several countries, including Brazil [76] and Turkey [77]. Moreover, carbapenem resistance for all three bacteria, *P. aeruginosa*, *A. baumannii* and *K. pneumoniae*, is associated with cross-resistance to other antimicrobial classes [61].

A key contributing factor to the resistance profiles of these Gram-negative bacteria is their almost impenetrable outer cell wall, also referred to as cell envelope, and efflux mechanisms, which actively limit the concentration of antibiotics within the cell. Section 1.2 is a published review of direct relevance to the experimental work in this thesis, which describes novel approaches in antibiotic development targeting amino acid biosynthesis and their incorporation into the peptidoglycan of the cell wall. This review not only outlines potential targets and pathways, but also provides an update of the current stage of inhibitor development.

1.2 Review: Targeting the Biosynthesis and Incorporation of Amino Acids into the Peptidoglycan as an Antibiotic Approach Against Gram Negative Bacteria

1.2.1 Copyright

This article was published in *EC Microbiology*, Vol 14(4), Impey, R. E. & Soares da Costa, T. P., “Targeting the biosynthesis and incorporation of amino acids into the peptidoglycan as an antibiotic approach against Gram negative bacteria”, pp. 200-209. Copyright ECronicon 2018.

Copyright authorisation obtained on:


10th November 2020

1.2.2 Statement of Contribution

I confirm that Rachael Impey has made the following contributions:

- Conceptualisation and drafting of the manuscript
- Preparation of figures
- Revisions of manuscript prior to acceptance

Tatiana Soares da Costa

Signed: 

Date: 14/12/2020

(Executive Author)

Review: Targeting the Biosynthesis and Incorporation of Amino Acids into Peptidoglycan as an Antibiotic Approach Against Gram Negative Bacteria

Rachael E Impey and Tatiana P Soares da Costa*

Department of Biochemistry and Genetics, La Trobe Institute for Molecular Science, La Trobe University, Melbourne, Australia

***Corresponding Author:** Tatiana P Soares da Costa, Department of Biochemistry and Genetics, La Trobe Institute for Molecular Science, La Trobe University, Melbourne, Australia.

Received: February 05, 2018; **Published:** March 23, 2018

Abstract

The rise of multi-drug resistant bacteria causing life threatening infections is instigating researchers to shift their attention towards previously unexplored antimicrobial targets. Targeting the synthesis of peptidoglycan that contributes to the structure of the bacterial cell wall has been and is still an attractive pathway due to its essentiality in bacteria and absence in humans. Here, we examine the pathways involved in the synthesis of three key amino acids and their incorporation into the peptide stem in Gram negative bacteria. This review also summarises the current research investigating these pathways as novel antibiotic targets.

Keywords: Biosynthesis; Amino Acids; Peptidoglycan; Antibiotic; Gram Negative Bacteria

Introduction

In the last few decades, there has been a significant increase in antibiotic resistance, resulting in multi drug resistant (MDR) and extremely drug resistant (XDR) bacteria [1]. Due to these increasing levels of resistance, the need for new antibiotic targets is more urgent than ever before. Ever since the development of the first antibiotic over 70 years ago, peptidoglycan synthesis has been a major target of antibiotics. It is regarded as an ideal target due to its essentiality to bacterial survival and its absence in humans and other eukaryotes. However, with the emergence of resistance against many antibiotics that target peptidoglycan and its synthesis, researchers started to examine other antibiotic targets upstream to the synthesis of the peptidoglycan precursors and their components.

Peptidoglycan itself consists of long strands of alternating N-acetylglucosamine (GlcNAc) and N-acetylmuramic acid (MurNAc) residues. Interestingly, the length of these glycan strands is not indicative of the thickness of the peptidoglycan layer, with both Gram positive and Gram negative bacteria having long and short strands depending on the species [2]. The length of these strands can also vary depending on the strain and growth conditions [3]. The strands of MurNAc and GlcNAc are cross-linked by a pentapeptide stem, connecting two opposing strands. This peptide stem varies between species, but is most commonly found to be L-alanine-D-glutamate-meso-DAP-D-alanine-D-alanine in Gram negative bacteria, with the terminal D-alanine cleaved during the formation of the mature peptidoglycan [4]. In the majority of Gram negative bacteria, the crosslinking between the peptide stems is a direct link between the side chain of the third amino acid, meso-DAP, and the carboxyl group of the fourth residue, D-Ala, on the opposing strand [2]. This is in contrast to the inter-bridge between residues found in Gram positive species [2]. Penicillin binding proteins are responsible for catalysing these crosslinking reactions, and as the target for many established antibiotics, have been comprehensively studied [5]. This review will focus upstream of the crosslinking, specifically on the biosynthesis of the three key amino acids found in the peptide stem and their incorporation into the peptidoglycan layer in Gram negative bacteria. We will also explore the targeting of the biosynthesis of these amino acids and their incorporation into the peptide stem as novel antimicrobial strategies. Although this review will focus primarily on Gram negative bacteria, it will also include *Mycobacterium* as they contain a similar pentapeptide to that of other Gram negative bacteria [6].

Citation: Rachael E Impey and Tatiana P Soares da Costa. "Review: Targeting the Biosynthesis and Incorporation of Amino Acids into Peptidoglycan as an Antibiotic Approach Against Gram Negative Bacteria". *EC Microbiology* 14.4 (2018): 200-209.

Alanine

Synthesis

Alanine plays many key roles in eukaryotes, including humans, and bacteria. In most Gram positive and Gram negative bacteria, the L- and the D- isomers of alanine are found in the first and last positions of the peptide stem, respectively [7]. The first L-alanine is responsible for binding to the peptidoglycan precursor; UDP-MurNAc, and in a subsequent reaction, binds to D-Glutamate, the next amino acid in the peptide chain [2]. L-Alanine is typically synthesised by transaminases (also referred to as aminotransferases) from pyruvate via the transamination of L-glutamate or L-valine to L-alanine (Figure 1) [8]. *E. coli* contains both AlaA and AlaC glutamate-pyruvate aminotransferases, which can reversibly convert L-glutamate and pyruvate into L-alanine and α -ketoglutarate (Figure 1) [8]. Transaminase C (an alanine-valine transaminase) is believed to catalyse the last step in valine synthesis, producing pyruvate and valine from 3-methyl-2-oxobutanoate and alanine [9]. However, it also plays a significant role in synthesising alanine due to the reversibility of this reaction (Figure 1) [9]. Up to eight other possible alanine synthesis pathways have been described in *E. coli*, however this is believed to be a secondary function for these enzymes, with the physiological contribution of these reactions remaining unclear [8].

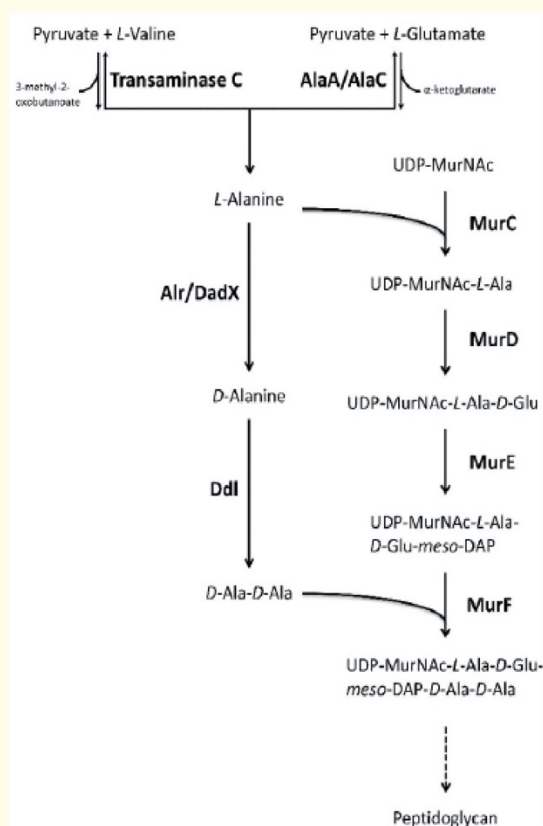


Figure 1: L-alanine synthesis in Gram negative bacteria. L-alanine biosynthesis in *E. coli* by transaminase C and AlaA/AlaC enzymes followed by the conversion to D-alanine and ligation of the D-Ala-D-Ala dipeptide before incorporation of both to the peptide stem of the UDP-MurNAc peptidoglycan precursor.

Citation: Rachael E Impey and Tatiana P Soares da Costa. "Review: Targeting the Biosynthesis and Incorporation of Amino Acids into Peptidoglycan as an Antibiotic Approach Against Gram Negative Bacteria". *EC Microbiology* 14.4 (2018): 200-209.

As mentioned previously, in addition to L-alanine, D-alanine is present in the peptidoglycan crosslink. D amino acids are formed by either racemases or aminotransferase enzymes, with the racemase enzymes being the most prominent for D-alanine production [10]. Several Gram negative bacteria, including *Escherichia coli*, *Pseudomonas aeruginosa* and *Salmonella typhimurium*, have two alanine racemases, encoded for by the *alr* and the *dadX* genes [7]. The *dadX*-encoded racemase has been found to be inducible, and expressed only when L-Ala has been sequestered as a carbon source [7]. On the other hand, the *alr* racemase is expressed constitutively, and thus, thought to be of more physiological importance [7]. This has led to *Alr* being more thoroughly studied. These racemases are pyridoxal-5'-phosphate (PLP)-dependent, involving a two-step binding event with the co-factor and the substrate [10]. Once L-alanine has been converted to D-alanine, it is ligated together to form a D-Ala-D-Ala dipeptide by the enzyme D-Ala-D-Ala ligase (Ddl) for use in the peptidoglycan peptide stem [7]. Typically, the Ddls synthesise the D-Ala-D-Ala in bacteria, yet some vancomycin resistant Gram positive bacteria have D-Ala-D-Ser or D-Ala-D-Lac in these terminal positions [11]. Two Ddl genes (*ddlA* and *ddlB*) have been observed in multiple Gram negative bacteria, including *E. coli* [12] and *S. typhimurium* [13]. While the products are of different sizes, both have been purified and shown to have similar kinetic characteristics, including comparable substrate affinities [7]. Despite the fact that the terminal D-ala of the pentapeptide chain is cleaved in mature peptidoglycan, it is added to the precursor UDP-MurNAc-L-Ala-D-Glu-meso-DAP as a dipeptide [2].

Addition of L-Ala onto the peptidoglycan precursor UDP-MurNAc is commenced by the MurC enzyme, which exhibits high specificity for L-Ala, lower affinity for glycine and L-serine, but no affinity for D-Ala [7,14]. *Mycobacterium tuberculosis* and *Mycobacterium leprae* show a higher affinity for a glycine substrate than other MurC enzymes, however it has been noted that glycine is the first residue of the peptide stem for *M. tuberculosis*, which could explain this difference in affinities [15]. The MurF enzyme ligates the D-Ala-D-Ala dipeptide to the peptide stem, and is similar between Gram positive and Gram negative bacteria. These enzymes show equal affinity for both the meso-DAP and L-Lys containing substrates [16].

Inhibition

A vast amount of research has focused on the development of inhibitors of Alrs and Ddls, as these enzymes are not found in humans. One such inhibitor, which was further developed into a treatment, is cycloserine, marketed as the drug Seromycin. Cycloserine is a structural analogue of D-Ala, which inhibits both *Alr* and *Ddl* *in vitro*, while exhibiting a higher affinity for *Ddl* *in vivo* [17]. While mainly used as a treatment for MDR tuberculosis, questions have been raised about its safety [18], indicating that to target these enzymes, the development of new inhibitors is required. Accordingly, *de novo* drug design has been employed for the development of inhibitors against *Ddl*, but resulting compounds displayed weaker potency compared to the current *Alr* and *Ddl* inhibitors [19].

Further downstream of L- and D-alanine synthesis, the MurC and MurF enzymes also represent promising antimicrobial targets. Phosphinate inhibitors for MurC have been reported to have IC_{50} values as low as 49 nM, utilising phosphinate inhibitors from other Mur enzymes as a structural backbone [20]. Identification of an inhibitor of MurF was achieved by virtual screening of compound libraries. The identified compound has an IC_{50} of 63 μ M against the *E. coli* MurF enzyme, but lacks antimicrobial activity [21]. Affinity-based high-throughput screening was also employed, with resulting inhibitors reported to have IC_{50} values between 20 - 70 nM, but again, little to no antibacterial activity [22]. Little progress was made for almost a decade after this until MurF inhibitors were developed that showed promising antimicrobial activity. These inhibitors were reported to have MIC values ranging between 4 - 64 μ g/ml for the different *E. coli* strains tested [23]. While gaining antimicrobial activity was a success, these compounds are unlikely to undergo any further development due to off-target effects caused by eukaryotic cytoplasmic membrane damage [23].

Glutamate

Synthesis

Several Gram negative bacteria have two primary pathways for glutamate synthesis; via the glutamate dehydrogenase (GDH) or glutamine synthetase (GS)-glutamate synthase (GOGAT) enzymes. The GDH enzyme catalyses the formation of glutamate through the reductive amination of 2 oxoglutarate (Figure 2) [24]. On the other hand, the GOGAT pathway results in the amidation of L-glutamate to glutamine by GS, before GOGAT catalyses the transfer of the amide group to 2 oxoglutarate (Figure 2) [24]. Previous work indicated that mutations in both the GDH and GOGAT encoding genes in *E. coli* required supplementation with external glutamate for survival. However,

mutations in only one of either of the genes showed glutamate production equivalent to the wildtype [25]. This indicates that only one of the two pathways is necessary for sufficient glutamate production. This is further validated by studies done on the Gram negative bacteria *Erwinia carotovora*, which lacks the GDH enzyme and, as such, only contains the GOGAT pathway for glutamate production [26]. Other pathways for glutamate synthesis exist, with the transamination reactions involving the transfer of the amino groups from other amino acids to 2-oxoglutarate to produce glutamate. An example of this is the aspartate aminotransferase reaction (Figure 2) [24]. This reaction is similar to that of the amino-transferases involved in alanine synthesis and is also dependant on the PLP cofactor for activity [26]. However, as glutamate synthesis is present in many organisms, including humans, the most common antibiotic target for glutamate synthesis is the pathway that synthesises the bacteria-specific D-glutamate.

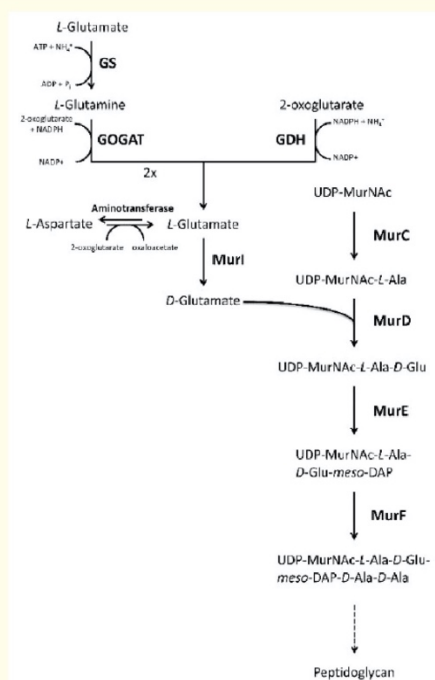


Figure 2: D-glutamate synthesis in Gram negative bacteria. D-glutamate synthesis by glutamate dehydrogenase (GDH) and the glutamine synthetase-glutamate synthase (GOGAT) pathways, and the incorporation into the peptide stem of peptidoglycan precursor glycan strands.

D-glutamate is synthesised by two enzymes; glutamate racemase (MurI) and D-aminotransferase (Dat). Unlike the alanine racemase discussed earlier, the MurI enzyme is PLP-independent and, as such, requires no cofactor to function [27]. Typically for Gram negative bacteria, the glutamate racemase is the only route for D-glutamate synthesis, however, several studies on Gram positive species report the synthesis of D-γ-glutamate using D-aminotransferase (Dat) [7].

Citation: Rachael E Impey and Tatiana P Soares da Costa. "Review: Targeting the Biosynthesis and Incorporation of Amino Acids into Peptidoglycan as an Antibiotic Approach Against Gram Negative Bacteria". *EC Microbiology* 14.4 (2018): 200-209.

Subsequently, D-glutamate is added to the L-Ala component of the peptide chain by the enzyme MurD [7]. When compared to the Gram positive MurD enzymes, those from the Gram negative bacteria *E. coli* and *Haemophilus influenzae* have been found to be more highly regulated [28]. This could indicate that Gram negative bacteria have a tighter overall regulation on peptidoglycan synthesis than Gram positive bacteria.

Inhibition

Disruption of the *murI* gene ultimately leads to cell lysis as a result of alteration of peptidoglycan synthesis, making it a promising antibiotic target [29]. It also has a high protein sequence similarity at the active site between many species, including *E. coli*, *Helicobacter pylori* and *Aquifex pyrophilus*, giving rise to the potential development of a broad spectrum inhibitor [30]. The first attempts to inhibit the MurI enzyme involved the development of substrate analogues that were able to covalently modify the enzyme, but these were shown to be ineffective [27,31]. Other inhibitors were designed based on the product, D-glutamate, to avoid any off-target effects resulting from L-glutamate [32]. These compounds were effective against *S. pneumoniae* strains, however inhibition did not translate to any other tested bacterial strains [32]. Allosteric inhibitors were then developed against *H. pylori*, though again these had selectivity for *H. pylori* only [33]. Recently, a whole-cell vaccine strategy against *Pseudomonas aeruginosa*, *Acinetobacter baumannii*, and *Staphylococcus aureus* has been developed. The proposed vaccine would involve inactivating genes encoding both MurI and the Dat enzymes (if applicable), resulting in an attenuated strain dependent on supplemented D-Glu [34]. This promising strategy has shown that the attenuated strains yield significant immune responses combined with a reduced virulence and no observed phenotypic reversion to the wildtype [34].

In addition to MurI, the MurD enzyme has also been targeted for antibiotic development. The first inhibitors were developed based on the intermediate product and bound to the transition state of the enzyme [35]. This included the phosphinate based inhibitors, with the best compound reporting an IC_{50} of 0.68 μ M [35]. This was optimised through the incorporation of muramic acid, resulting in an IC_{50} of 20 nM [36]. This spurred further development of phosphinate inhibitors, however these alterations were often ineffective and resulted in no improvement in the inhibition of MurD. To design a new class of inhibitor against MurD from *P. aeruginosa*, techniques such as phage display, coupled with extensive biopanning, were used [37]. This resulted in peptides with IC_{50} values of ~ 4 μ M, however much optimisation is still required for these to be able to cross the bacterial membrane [37]. Virtual screening has also been employed to target the MurD enzyme, with design aimed towards the ATP-binding site as opposed to the active site [38]. While these inhibitors showed weak activity, they provide a novel pharmacophore for drug development.

Lysine

Synthesis

The third position of the pentapeptide chain is typically the point of difference between most Gram positive and Gram negative cell walls. Lysine or meso-DAP generally occupy this position, respectively, although there are exceptions [7]. Peptide stems from the Gram positive bacteria *Thermotoga maritima* have revealed L-Lys or D-Lys in the third position, as opposed to meso-DAP [39]. In bacteria, both L-Lys and D-Lys residues are synthesised via the diaminopimelate (DAP) pathway (Figure 3). The first committed step of the DAP pathway involves the condensation reaction between pyruvate and L-aspartate semialdehyde (ASA) catalysed by the enzyme dihydrodipicolinate synthase (DHDPS) [40,41]. The product of this reaction, 4-hydroxy-2,3,4,5-tetrahydro-L-L-dipicolinic acid (HTPA), is then reduced to L-2,3,4,5-tetrahydrodipicolinate (THDP) by dihydrodipicolinate reductase (DHDPR) [42,43]. Depending on the organism, L,L-2,6-diaminopimelate (LL-DAP) is produced by one of four different sub-pathways. Since all documented Gram negative bacteria use the succinyl pathway, this will be the focus in this review. The succinyl sub-pathway commences with the enzyme 2,3,4,5-tetrahydropyridine-2-carboxylate N-succinyltransferase (THPC-NST) catalysing the production of N-succinyl-L-2-amino-6-ketopimelate (NSKAP) from THDP [44]. NSKAP is then converted to N-succinyl-L,L-2,6-diaminopimelate (NSDAP), before desuccinylation to LL-DAP by N-succinyldiaminopimelate aminotransferase (NSDAP-AT) and succinyldiaminopimelate desuccinylase (SDAP-DS), respectively [44]. DAP epimerase then catalyses the conversion of LL-DAP to meso-DAP, which can then be incorporated into the peptide chain covalently linked to UDP-MurNAc in Gram negative bacteria [44]. It is important to note that in Gram negative bacteria, meso-DAP can be converted to lysine by the enzyme DAP decarboxylase (DAP-DC) for use in protein synthesis as opposed to incorporation into the peptidoglycan layer [45].

Citation: Rachael E Impey and Tatiana P Soares da Costa. "Review: Targeting the Biosynthesis and Incorporation of Amino Acids into Peptidoglycan as an Antibiotic Approach Against Gram Negative Bacteria". *EC Microbiology* 14.4 (2018): 200-209.

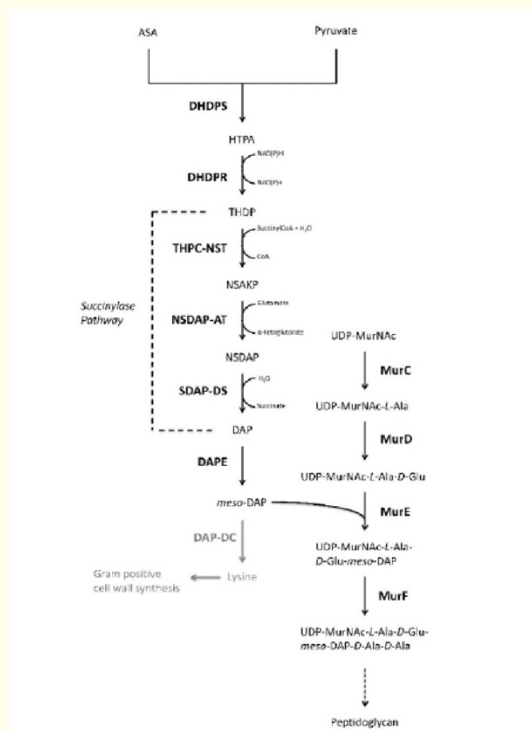


Figure 3: meso-DAP and L-lysine biosynthesis via the diaminopimelate (DAP) pathway in bacteria. Synthesis in Gram negative bacteria occurs through the succinyl sub pathway before the incorporation of meso-DAP into the peptide stem of precursor peptidoglycan.

The MurE enzyme catalyses the covalent linkage of meso-DAP to D-Glu on the peptide stem, with this enzyme displaying a species-dependent preference for either meso-DAP or lysine. Previous work suggested that incorrect incorporation of L-lys into the *E. coli* peptide chain resulted in lethality [46]. There are exceptions for this in Gram negative bacteria, with the MurE enzyme from *T. maritima* showing similar *in vitro* efficiency for adding L-Lys and meso-DAP, despite no meso-DAP being found in the peptidoglycan layer [39]. A preference for the addition of meso-DAP or lysine to the peptidoglycan layer has been hypothesised to be due to a difference in intracellular concentrations of these metabolites [39].

Inhibition

Similar to the other Mur class enzymes, MurE has been targeted in efforts to produce novel antimicrobials. The first MurE inhibitor, like the MurD inhibitors, was a phosphinate compound, which targeted the transition state of the enzyme. This inhibitor has an IC_{50} value $\sim 1 \mu M$, but lacks antibacterial activity [47]. Phage display studies resulted in the discovery of a peptide with MurE inhibitory properties, but the degree of inhibition was reduced compared to published inhibitors. Despite this, this work provided another avenue of investigation for novel inhibitor development. More recently, other compounds that exhibit MurE inhibitory activity, such as tetrahydroisoquinolones, have been investigated for treatment of *M. tuberculosis*. The inhibitors have been shown to display moderate antibacterial activity *in vivo*, but they lack broad spectrum activity against Gram negative bacteria [48].

Citation: Rachael E Impey and Tatiana P Soares da Costa. "Review: Targeting the Biosynthesis and Incorporation of Amino Acids into Peptidoglycan as an Antibiotic Approach Against Gram Negative Bacteria". *EC Microbiology* 14.4 (2018): 200-209.

Unlike alanine and glutamate synthesis, meso-DAP and lysine are not synthesised by humans, thus making the DAP pathway an ideal target for antibiotic development upstream of the MurE enzyme. The first enzyme in the DAP pathway, DHDPS, is considered a prime target for antibiotic development since it catalyses the rate limiting step of the pathway. Several groups have previously attempted to develop DHDPS inhibitors by targeting either the active or allosteric site [49-51]. The first inhibitors were generated by analogy to its substrates, pyruvate and ASA, or to dihydrodipicolinate, which was originally thought to be the product of the DHDPS-catalysed reaction [51]. Until recently, the most successful of these compounds were planar and heterocyclic, but these were not effective at sub-millimolar concentrations [49]. With the identification of HTPA as the DHDPS product, various heterocycles with oxygen functionality have been tested [49]. However, these compounds were only marginally more effective at inhibiting DHDPS than the first generation substrate analogues [49]. Recently, rational inhibitor design approaches have been employed to demonstrate that α -ketopimelic acid, a structural analogue of pyruvate, binds the active site of *Mycobacterium tuberculosis* DHDPS and partially inhibits the enzyme with micromolar potency [52].

Additionally, a bislysine analogue that binds to the allosteric site of *Campylobacter jejuni* DHDPS has recently been described with sub- μ M potency [50].

While less explored than DHDPS, the subsequent enzyme DHDPR also presents as a promising antibiotic target due to its essentiality to bacteria and absence in humans [53]. Several inhibitors have been designed to target both the substrate and the cofactor binding sites simultaneously [54]. One such example is 2, 6-pyridinedicarboxylic acid (2,6-PDC), with a K_i of 0.9 mM against *E. coli* DHDPR [51]. A molecular modelling approach has also been employed to identify several sulphonamides that inhibit DHDPR, with the most potent of these having IC_{50} values ranging from 10 to 90 μ M [53]. These inhibitors provide a platform for future inhibitor development against DHDPR.

As DHDPS and DHDPR are positioned above the junction of the multiple sub-pathways employed in all bacteria to produce meso-DAP, they remain the focus for new broad spectrum antimicrobial development. However, despite extensive research into the structural and functional characterisation of these enzymes, there have been no published DAP pathway inhibitors with antibacterial activity to date.

Conclusion

In this review, we have summarised how peptidoglycan synthesis can be targeted upstream of the crosslinking of the glycan strands by examining the precursors and their components. While over 3 decades of research has focussed on inhibiting the Mur class of enzymes and their role in the addition of amino acids onto the peptide stem, there are still promising under-explored avenues for antibiotic discovery targeting peptidoglycan synthesis. Exciting new research is emerging, including the development of the bacterial whole cell vaccine against the MurI enzyme as well as lysine biosynthesis inhibitors, which further validate the importance of targeting pathways not directly involved in peptidoglycan synthesis. Further exploration of these areas could yield new classes of antibiotics, which are urgently needed to negate the steady rise in antibiotic resistance worldwide.

Bibliography

1. Banin E., *et al.* "Editorial: bacterial pathogens, antibiotics and antibiotic resistance". *FEMS Microbiology Reviews* 41.3 (2017): 450-452.
2. Vollmer W., *et al.* "Peptidoglycan structure and architecture". *FEMS Microbiology Reviews* 32.2 (2008): 149-167.
3. Glauner, B. *et al.* "The composition of the murein of escherichia coli". *The Journal of Biological Chemistry* 263.21 (1988): 10088-10095.
4. Scheffers DJ and Pinho MG. "Bacterial cell wall synthesis: new insights from localization studies". *Microbiology and Molecular Biology Reviews* 69.4 (2005): 585-607.

Citation: Rachael E Impey and Tatiana P Soares da Costa. "Review: Targeting the Biosynthesis and Incorporation of Amino Acids into Peptidoglycan as an Antibiotic Approach Against Gram Negative Bacteria". *EC Microbiology* 14.4 (2018): 200-209.

5. Sauvage E., *et al.* "The penicillin-binding proteins: structure and role in peptidoglycan biosynthesis". *FEMS Microbiology Reviews* 32.2 (2008): 234-258.
6. Alderwick LJ., *et al.* "The mycobacterial cell wall-peptidoglycan and arabinogalactan". *Cold Spring Harbor Perspectives in Medicine* 5.8 (2015): a021113.
7. Barreteau H., *et al.* "Cytoplasmic steps of peptidoglycan biosynthesis". *FEMS Microbiology Reviews* 32.2 (2008): 168-207.
8. Kim SH., *et al.* "Genetics and regulation of the major enzymes of alanine synthesis in *Escherichia coli*". *Journal of Bacteriology* 192.20 (2010): 5304-5311.
9. Whalen WA and Berg CM. "Analysis of an *avta::mu d1(ap lac)* mutant: metabolic role of transaminase *c*". *Journal of Bacteriology* 150.2 (1982): 739-746.
10. Radkov AD and Moe LA. "Bacterial synthesis of d-amino acids". *Applied Microbiology and Biotechnology* 98.12 (2014): 5363-5374.
11. Tytgat I., *et al.* "DD-ligases as a potential target for antibiotics: past, present and future". *Current Medicinal Chemistry* 16.20 (2009): 2566-2580.
12. Zawadzke LE., *et al.* "Existence of two d-alanine:d-alanine ligases in *Escherichia coli*: cloning and sequencing of the *ddlA* gene and purification and characterization of the *ddlA* and *ddlB* enzymes". *Biochemistry* 30.6 (1991): 1673-1682.
13. Daub E., *et al.* "Isolation, cloning, and sequencing of the *Salmonella typhimurium ddlA* gene with purification and characterization of its product, d-alanine:d-alanine ligase (adp forming)". *Biochemistry* 27.10 (1988): 3701-3708.
14. Liger D., *et al.* "Over-production, purification and properties of the uridine-diphosphate-n -acetylmuramate: l-alanine ligase from *Escherichia coli*". *European Journal of Biochemistry* 230.1 (1995): 80-87.
15. Mahapatra S., *et al.* "Comparison of the *udp-n-acetylmuramate:l-alanine* ligase enzymes from *Mycobacterium tuberculosis* and *Mycobacterium leprae*". *Journal of Bacteriology* 182.23 (2000): 6827-6830.
16. Anderson MS., *et al.* "Kinetic mechanism of the *Escherichia coli* *udpmurnac-tripeptide d-alanyl-d-alanine*-adding enzyme: use of a glutathione *s*-transferase fusion". *Biochemistry* 35.50 (1996): 16264-16269.
17. Prosser GA and de Carvalho LPS. "Metabolomics reveal d-alanine:d-alanine ligase as the target of d-cycloserine in *Mycobacterium tuberculosis*". *ACS Medicinal Chemistry Letters* 4.12 (2013): 1233-1237.
18. Hwang TJ., *et al.* "Safety of cycloserine and terizidone for the treatment of drug-resistant tuberculosis: a meta-analysis". *The International Journal of Tuberculosis and Lung Disease* 17.10 (2013): 1257-1266.
19. Besong GE., *et al.* "A de novo designed inhibitor of d-ala-d-ala ligase from *E. coli*". *Angewandte Chemie International Edition* 44.39 (2005): 6403-6406.
20. Reck F., *et al.* "Inhibitors of the bacterial cell wall biosynthesis enzyme *murC*". *Bioorganic and Medicinal Chemistry Letters* 11.11 (2001): 1451-1454.
21. Turk S., *et al.* "Discovery of new inhibitors of the bacterial peptidoglycan biosynthesis enzymes *murD* and *murF* by structure-based virtual screening". *Bioorganic and Medicinal Chemistry* 17.5 (2009): 1884-1889.
22. Gu YG., *et al.* "Structure-activity relationships of novel potent *murF* inhibitors". *Bioorganic and Medicinal Chemistry Letters* 14.1 (2004): 267-270.

Citation: Rachael E Impey and Tatiana P Soares da Costa. "Review: Targeting the Biosynthesis and Incorporation of Amino Acids into Peptidoglycan as an Antibiotic Approach Against Gram Negative Bacteria". *EC Microbiology* 14.4 (2018): 200-209.

23. Hrast M., *et al.* "Design, synthesis and evaluation of second generation murf inhibitors based on a cyanothiophene scaffold". *European Journal of Medicinal Chemistry* 73 (2014): 83-96.
24. Helling RB. "Why does Escherichia coli have two primary pathways for synthesis of glutamate?" *Journal of Bacteriology* 176.15 (1994): 4664-4668.
25. Berberich MA. "A glutamate-dependent phenotype in e. coli k12: the result of two mutations". *Biochemical and Biophysical Research Communications* 47.6 (1972): 1498-1503.
26. Meers JL, *et al.* "'Glutamine(amide): 2-oxoglutarate amino transferase oxido-reductase (nadp)', an enzyme involved in the synthesis of glutamate by some bacteria". *Microbiology* 64.2 (1970): 187-194.
27. Glavas, S. and Tanner, M. E. "The inhibition of glutamate racemase by d-n-hydroxyglutamate". *Bioorganic and Medicinal Chemistry Letters* 7.17 (1997): 2265-2270.
28. Walsh AW, *et al.* "Comparison of the d-glutamate-adding enzymes from selected gram-positive and gram-negative bacteria". *Journal of Bacteriology* 181.17 (1999): 5395-5401.
29. Doublet P, *et al.* "The muri gene of escherichia coli is an essential gene that encodes a glutamate racemase activity". *Journal of Bacteriology* 175.10 (1993): 2970-2979.
30. Fisher SL. "Glutamate racemase as a target for drug discovery". *Microbial Biotechnology* 1.5 (2008): 345-360.
31. Ashiuchi M., *et al.* "Inactivation of glutamate racemase of pediococcus pentosaceus with l-serine o-sulfate". *Bioscience, Biotechnology, and Biochemistry* 57.11 (1993): 1978-1979.
32. de Dios A., *et al.* "4-substituted d-glutamic acid analogues: the first potent inhibitors of glutamate racemase (muri) enzyme with antibacterial activity". *Journal of Medicinal Chemistry* 45.20 (2002): 4559-4570.
33. de Jonge BLM, *et al.* "Pyrazolopyrimidinediones are selective agents for helicobacter pylori that suppress growth through inhibition of glutamate racemase (muri)". *Antimicrobial Agents and Chemotherapy* 53.8 (2009): 3331-3336.
34. Cabral MP, *et al.* "Design of live attenuated bacterial vaccines based on d-glutamate auxotrophy". *Nature Communications* 8 (2017): 15480.
35. Tanner ME, *et al.* "Phosphinate inhibitors of the d-glutamic acid-adding enzyme of peptidoglycan biosynthesis". *The Journal of Organic Chemistry* 61.5 (1996): 1756-1760.
36. Gegnas LD, *et al.* "Inhibitors of the bacterial cell wall biosynthesis enzyme mur D". *Bioorganic and Medicinal Chemistry Letters* 8.13 (1998): 1643-1648.
37. Paradis-Bleau C., *et al.* "Selection of peptide inhibitors against the pseudomonas aeruginosa murD cell wall enzyme". *Peptides* 27.7 (2006): 1693-1700.
38. Tomašić T, *et al.* "Virtual screening for potential inhibitors of bacterial murC and murD ligases". *Journal of Molecular Modeling* 18.3 (2012): 1063-1072.
39. Boniface A., *et al.* "The mure synthetase from thermotoga maritima is endowed with an unusual d-lysine adding activity". *Journal of Biological Chemistry* 281.23 (2006): 15680-15686.
40. Soares da Costa TP, *et al.* "Molecular evolution of an oligomeric biocatalyst functioning in lysine biosynthesis". *Biophysical Reviews* (2017): 1-10.

Citation: Rachael E Impey and Tatiana P Soares da Costa. "Review: Targeting the Biosynthesis and Incorporation of Amino Acids into Peptidoglycan as an Antibiotic Approach Against Gram Negative Bacteria". *EC Microbiology* 14.4 (2018): 200-209.

41. Gupta R., *et al.* "Comparison of untagged and his-tagged dihydrodipicolinate synthase from the enteric pathogen *Vibrio cholerae*". *Protein Expression and Purification* 145 (2018): 85-93.
42. Devenish SRA., *et al.* "NMR studies uncover alternate substrates for dihydrodipicolinate synthase and suggest that dihydrodipicolinate reductase is also a dehydratase". *Journal of Medicinal Chemistry* 53.12 (2010): 4808-4812.
43. Christensen JB., *et al.* "Structure and function of cyanobacterial dhds and dhdsr". *Scientific Reports* 6 (2016): 37111.
44. Dogovski C., *et al.* "Enzymology of bacterial lysine biosynthesis". *Biochemistry, InTech* (2012).
45. Peverelli MG., *et al.* "Dimerization of bacterial diaminopimelate decarboxylase is essential for catalysis". *Journal of Biological Chemistry* 291.18 (2016): 9785-9795.
46. Mengin-Lecreulx D., *et al.* "Expression of the *Staphylococcus aureus* *sdpN*-acetylmuramoyl-L-alanyl-D-glutamate:L-lysine ligase in *Escherichia coli* and effects on peptidoglycan biosynthesis and cell growth". *Journal of Bacteriology* 181.19 (1999): 5909-5914.
47. Zeng B., *et al.* "A phosphinate inhibitor of the meso-diaminopimelic acid-adding enzyme (mure) of peptidoglycan biosynthesis". *The Journal of Organic Chemistry* 63.26 (1998): 10081-10085.
48. Guzman JD., *et al.* "Tetrahydroisoquinolines affect the whole-cell phenotype of *Mycobacterium tuberculosis* by inhibiting the ATP-dependent mure ligase". *Journal of Antimicrobial Chemotherapy* 70.6 (2015): 1691-1703.
49. Turner JJ., *et al.* "Heterocyclic inhibitors of dihydrodipicolinate synthase are not competitive". *Bioorganic and Medicinal Chemistry* 13.6 (2005): 2133-2140.
50. Skovpen YV., *et al.* "Biomimetic design results in a potent allosteric inhibitor of dihydrodipicolinate synthase from *Campylobacter jejuni*". *Journal of the American Chemical Society* 138.6 (2016): 2014-2020.
51. Couper L., *et al.* "Pyridine and piperidine derivatives as inhibitors of dihydrodipicolinic acid synthase, a key enzyme in the diaminopimelate pathway to L-lysine". *Bioorganic and Medicinal Chemistry Letters* 4.19 (1994): 2267-2272.
52. Shrivastava P., *et al.* "Inhibition of *Mycobacterium tuberculosis* dihydrodipicolinate synthase by α -ketopimelic acid and its other structural analogues". *Scientific Reports* 6 (2016): 30827.
53. Paiva AM., *et al.* "Inhibitors of dihydrodipicolinate reductase, a key enzyme of the diaminopimelate pathway of *Mycobacterium tuberculosis*". *Biochimica et Biophysica Acta (BBA) - Protein Structure and Molecular Enzymology* 1545.1 (2001): 67-77.
54. Sem DS., *et al.* "Systems-based design of bi-ligand inhibitors of oxidoreductases: filling the chemical proteomic toolbox". *Chemistry and Biology* 11.2 (2004): 185-194.

Volume 14 Issue 4 April 2018

©All rights reserved by Rachael E Impey and Tatiana P Soares da Costa.

Citation: Rachael E Impey and Tatiana P Soares da Costa. "Review: Targeting the Biosynthesis and Incorporation of Amino Acids into Peptidoglycan as an Antibiotic Approach Against Gram Negative Bacteria". *EC Microbiology* 14.4 (2018): 200-209.

- This page was intentionally left blank -

1.3 The Diaminopimelate Pathway

1.3.1 Overview

As described in Section 1.2, the diaminopimelate (DAP) pathway represents a promising antibiotic target for numerous reasons. Firstly, the end metabolites, *meso*-DAP and L-lysine (herein referred to as lysine), are essential for bacterial survival given their roles in peptidoglycan crosslinking and protein synthesis. Secondly, the pathway is absent in animals, including humans, thus off target effects due to chemical inhibition should be minimised. Lastly, as inhibitors of the DAP pathway act upstream of current antibiotic targets within cell wall synthesis, they are expected to not be subject to existing resistance mechanisms. This thesis focuses on the first two enzymes of the DAP pathway, DHDPS and DHDPR.

1.3.2 DHDPS

1.3.2.1 The *dapA* Gene

The first enzyme in the DAP pathway, DHDPS, is encoded by the *dapA* gene. The gene from *E. coli* (*EcdapA*) was first mapped in 1971 [78] and then subsequently cloned in 1986 [79]. *EcdapA* has since been recombinantly expressed routinely in many studies and has formed the basis for much of the discovery work on DHDPS. Additionally, *dapA* genes have also been identified, sequenced and cloned from *Agrobacterium tumefaciens* [80], *Anabaena variabilis* [81], *Bacillus subtilis* [82], *Bacillus anthracis* [83], *Mycobacterium tuberculosis* [84], *P. aeruginosa* [85], *S. aureus* [86], *Streptococcus pneumoniae* [87] and others.

Typically, bacteria only have a single *dapA* gene, encoding one DHDPS enzyme. Alternatively, plants typically have two *dapA* genes, which is hypothesised to increase metabolic flux [88]. Gene knockout studies have shown the essentiality of the *dapA* gene for both Gram-positive bacteria and Gram-negative bacteria species including *S. pneumoniae* [87], *B. subtilis* [89], *E. coli* [90], *Salmonella enterica* [91] and *Helicobacter pylori* [92]. Furthermore, a *dapA* mutant of *Yersinia pestis* showed avirulence in mouse infection models of both the bubonic and septicæmic plague, as well as an inability to grow without *meso*-DAP supplementation [93].

1.3.2.2 Catalytic Mechanism

DHDPS enzymes belong to the class I aldolases, which are characterised by the formation of a Schiff base between a lysine residue and the keto acid group of the substrate [94]. DHDPS

catalyses the condensation reaction of pyruvate and ASA, resulting in the product, HTPA (Section 1.2, Fig. 3) [95,96]. The reaction follows a bi-bi ping-pong mechanism [95]. Specifically, Schiff base formation is initiated by a nucleophilic attack of the ϵ -amino group of the highly conserved active site lysine (Lys161, *E. coli* numbering) on the keto group of pyruvate. A catalytic triad (Thr44, Tyr133 and Tyr107, *E. coli* numbering) has been hypothesised to transfer protons to and from the active site through a water filled channel. Following dehydration, the imine (Schiff base) tautomerises to an enamine intermediate to allow ASA to bind [95]. Arg138 (*E. coli* numbering) facilitates binding of the aldehyde group of ASA to the enamine via interaction with the carboxyl group of ASA [97]. Finally, an aldol-like condensation reaction leads to the cyclisation and the release of the product, HTPA [98]. Other key residues, including Tyr106 and Thr45 (*E. coli* numbering), stabilise the orientation of the catalytic triad through hydrophobic stacking and hydrogen bonding with the adjacent residues, respectively [97,99].

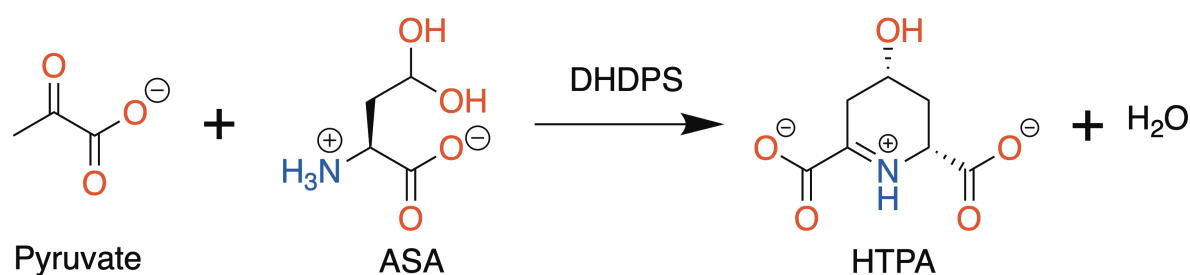


Figure 3. The DHDPS-catalysed reaction. DHDPS catalyses the condensation of pyruvate and ASA to form the product, HTPA, with the release of a water molecule. Figure generated using ChemDraw (version 20.0).

Given the importance of these 7 active site residues for DHDPS activity, namely Thr44, Thr45, Tyr106, Tyr107, Tyr133, Arg138 and Lys161 (*E. coli* numbering), they represent a unique sequence representative and unique to DHDPS enzymes, termed a signature motif. Desbois and colleagues recently used this motif to demonstrate the absence of DHDPS enzymes in the fungi kingdom, despite having annotated *dapA* genes in several species [100]. This indicates that this motif could be a useful tool in predicting gene products that encode for DHDPS.

1.3.2.3 Allosteric Regulation

As described in Section 1.2, DHDPS represents a key regulatory point in the DAP pathway. This occurs through a feedback inhibition mechanism via the allosteric binding of the end

product of the pathway, lysine [101]. The level of inhibition of DHDPS by lysine varies greatly between bacteria and plants. Plant enzymes are strongly inhibited by lysine with IC_{50} values between 10 and 50 μ M [102,103]. On the contrary, bacterial DHDPS enzymes are either moderately inhibited by lysine (IC_{50} values in the mid-micromolar range) or not inhibited at all. The original dogma suggested that DHDPS enzymes from Gram-negative bacteria were inhibited by lysine with mid-micromolar potency, while DHDPS enzymes from Gram-positive bacteria were insensitive to allosteric regulation [104]. However, the discovery that DHDPS from *S. pneumoniae*, a Gram-positive bacterium, was inhibited by lysine, while that from the Gram-negative bacterium *Legionella pneumophila* was not, led to a re-evaluation of the dogma [104]. This resulted in the identification of a key allosteric site residue at position 56 that defines allostery in DHDPS [104]. Specifically, the presence of a histidine or glutamate at position 56 imbues allosteric inhibition, whereas the presence of a basic residue results in no inhibition [104]. The position 56 residue has now been termed as the allosteric determinant for lysine inhibition [104].

Despite several studies focusing on the inhibition potency of lysine, the mechanism underpinning allostery remains unclear. To this date, there have been three mechanisms proposed to explain the lysine-mediated allosteric regulation of DHDPS. The increased flexibility of the active site residue Arg138 has been hypothesised to affect lysine inhibition, however mutations to a histidine or alanine yielded proteins that were still inhibited by lysine [97]. Nevertheless, these mutant proteins retained 35% of activity at saturating lysine concentrations, in comparison to the wildtype protein that only had 8% of activity remaining [97]. Further investigation revealed an alternative hypothesis, in which the observed re-orientation of Tyr107 could potentially interrupt the protein relay required for catalysis [97]. In a comparison of the apo and lysine bound EcDHDPS structures, the phenyl ring of Tyr107 is twisted approximately 20° [97,105]. This is believed to be due to the loss of hydrophobic stacking with Tyr106 as this residue moves towards the carboxyl group of the lysine molecule upon binding [105]. In the Arg138 mutants described above, this effect was more prominent, with Tyr107 rotating up to 40°, potentially explaining the reduced maximum inhibition [97]. Alternatively, the overlay of the apo and lysine bound EcDHDPS structures also revealed the presence of a water channel connecting the allosteric and active sites [105]. The exact effect of the water channel is still unclear, as mutational studies to attempt to block this channel have failed to hinder allosteric inhibition [106]. As none of these mechanisms fully explain the mechanism of lysine inhibition, more research is required.

1.3.2.4 Structural Characterisation

The first DHDPS crystal structure was that of EcDHDPS determined to a resolution of 2.5 Å in 1995, but since refined to 1.9 Å [105,107]. In the past 25 years, there have been several structures determined from multiple bacterial and plant species. The DHDPS enzyme exists predominantly as a homotetramer, with a tighter dimerisation interface joining two monomers and a weak tetramerisation interface, which connects the dimer of dimers together (Fig. 4) [102]. Each monomer consists of two domains. The N-terminal domain folds into a typical $(\beta/\alpha)_8$ - or TIM-barrel, which contains the active site, whilst the C-terminal domain forms three α helices that contain residues that mediate tetramerisation [102].

While both bacterial and plant DHDPS enzymes are typically homotetramers, they adopt different quaternary structures. The bacterial enzymes adopt a ‘head-to-head’ conformation, while plant enzymes conform to a ‘back-to-back’ quaternary structure (Fig. 4) [102]. It was predicted that this quaternary structure was evolved to reduce increased dynamic movement across the dimerisation interface, known as a “breathing motion”, which is associated with the dimeric form [102,108]. This breathing motion is hypothesised to not only disrupt the catalytic triad, interfering with catalytic activity, but also to alter the narrow substrate channel to the active site [108]. Thus, the tetramerisation interface stabilises the dimeric form, quenching this breathing motion [102]. This diversity in structure results in the allosteric site being located on the exterior of the bacterial isoforms, while it is located on the interior of the dimerisation interface of plant DHDPS enzymes (Fig. 4) [102]. The active sites are found in similar positions across both kingdoms. Interestingly, the DHDPS enzymes from *S. aureus* and *P. aeruginosa* have both been crystallised as dimers (Fig. 4) [85,86]. It has been proposed that these enzymes have evolved as an alternate method of stabilising this breathing motion given the increase in buried surface area at the dimerisation interface [86].

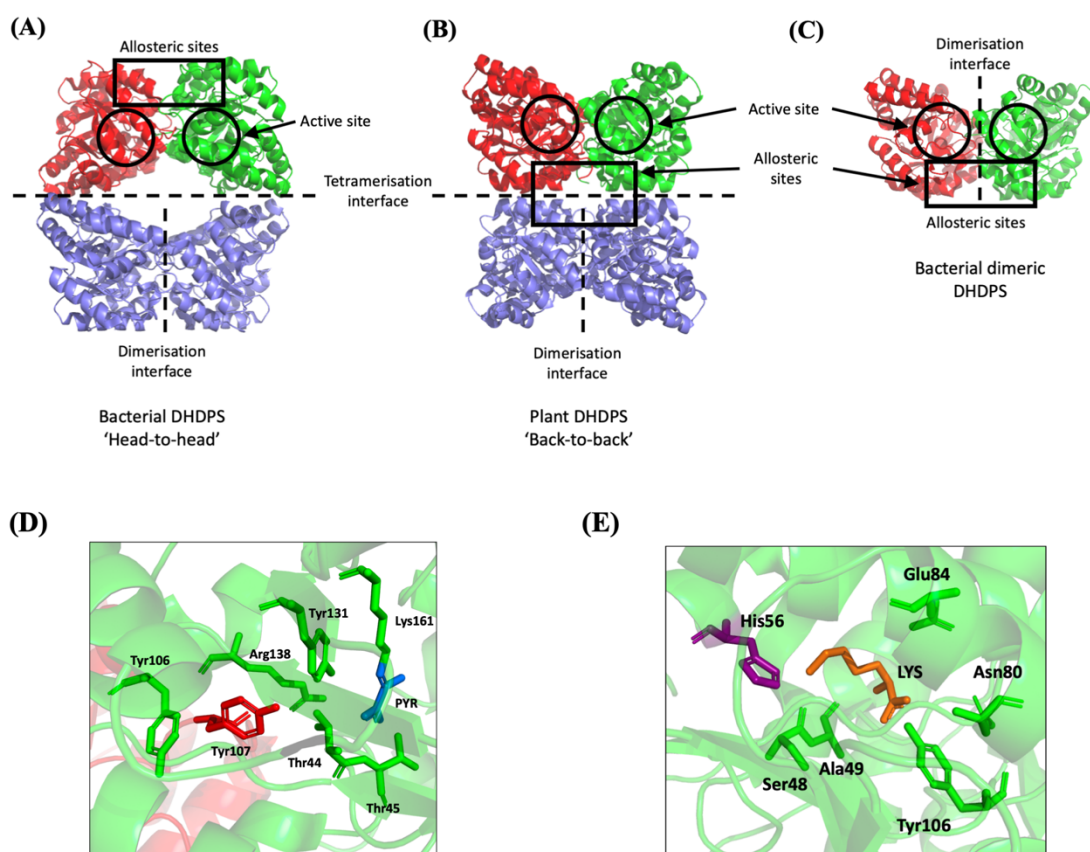


Figure 4. Structure of DHDPS enzymes. The crystal structures of (A) *E. coli* DHDPS (EcDHDPS; PDB: 1YXC), (B) *Arabidopsis thaliana* DHDPS (PDB: 4DPP) and (C) *Staphylococcus aureus* DHDPS (PDB: 3DAQ) showing the ‘head-to-head’, ‘back-to-back’ and the dimeric quaternary structures of DHDPS enzymes, respectively. The allosteric site (square), active site (circles), dimerisation interface and tetramerisation interface (dashed lines) are highlighted in each structure. (D) The active site of pyruvate bound EcDHDPS located in the centre of each monomer (PDB: 3DU0). Key catalytic residues are shown as sticks against the protein backbone (shown as cartoon). The interdigitating tyrosine 107 from the adjacent monomer is shown in red. The bound substrate pyruvate is shown in blue forming a Schiff base with lysine 161. (E) The allosteric site of lysine bound EcDHDPS located at the top of the dimerisation interface (PDB: 1YXD). Key allosteric residues are labelled and shown as sticks, with the allosteric determinant (position 56) shown in purple, and the bound lysine molecule shown in orange.

1.3.3 DHDPR

1.3.3.1 The *dapB* gene

The enzyme DHDPR was first identified and partially purified from *E. coli* by Farkas and Gilvarg in 1965 [109]. Subsequent investigation led to the identification, sequencing and subcloning of the encoding gene, *dapB* [110]. Since then, DHDPR has been cloned from several bacterial species including *A. variabilis* [81], *Bacillus cereus* [111], *B. subtilis* [82], *Corynebacterium glutamicum* [112], *M. tuberculosis* [113], *S. aureus* [114,115] and *Thermotoga maritima* [116].

Similar to the *dapA* gene, bacteria typically have one *dapB* gene. Although some studies have listed the *dapB* gene as essential in different bacterial species [89–91], transposon libraries provide conflicting conclusions with Skurnik and colleagues classing it as non-essential [117]. Moreover, unlike the *dapA* gene, there has been no complete deletion of the *dapB* gene to adequately assess its essentiality in a bacterial species.

1.3.3.2 Catalytic Mechanism

DHDPR catalyses the reduction of DHDP to generate THDP, as discussed in Section 1.2. The substrate, DHDP, is the non-enzymatic product resulting from the dehydration of HTPA, the product of the preceding DHDPs reaction [118,119]. The DHDPR kinetic mechanism has been shown to be sequential in several species [81,115], with the initial binding of the nucleotide co-factor NAD(P)H, followed by the substrate, DHDP [119]. Specifically, DHDPR catalyses the rapid hydride ion transfer from NAD(P)H to the C4 position of DHDP [119]. The product, THDP, is then formed by tautomerisation and protonation in a slower manner, before being released (Fig. 5) [119,120]. One of the residues hypothesised to play a key role in the DHDPR-catalysed reaction is His159 (*E. coli* numbering), which is proposed to assist in the activation of a proton donor water molecule (Fig. 6) [120]. The proton provided is used after the hydride addition to the double bond of DHDP [121]. The mechanism of the non-enzymatic dehydration of HTPA to form DHDP remains unclear. There is some evidence that DHDPR is also a dehydratase, with His159 acting as a base for the deprotonation of HTPA and the subsequent hydroxide loss results in DHDP (Fig. 5) [121]. Mutation of His159 to an alanine or glutamine results in a ~200-fold decrease in maximum velocity and a ~6 fold higher substrate affinity constant (K_M), highlighting its importance [120].

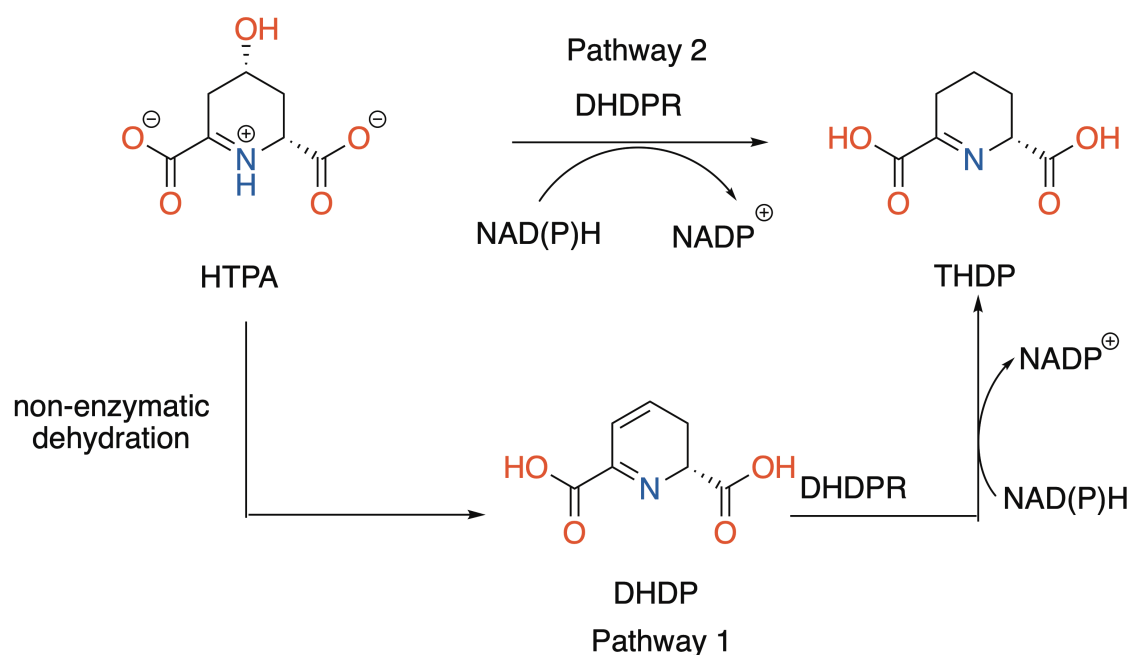


Figure 5. The DHDPR-catalysed reaction. DHDP is reduced to form the product THDP (Pathway 1). It remains unclear whether DHDPR also has an additional dehydratase activity, and as such, the true substrate may be HTPA as illustrated in Pathway 2. Figure generated using ChemDraw (version 20.0).

1.3.3.3 Co-factor Preference

Similar to other nucleotide-dependant enzymes, DHDPR has been reported to either have dual specificity or a preference for either NADH or the phosphorylated NADPH co-factor [113,115,119]. Two residues implicated in the binding to the co-factor are Glu38 and Arg39 (*E. coli* numbering). The 2' and 3' adenosyl ribose hydroxyl groups from NADH are believed to interact with Glu38 [113,120]. Meanwhile, the 2' phosphate of NADPH is hypothesised to interact with Arg39 and the backbone of the glycine rich region (GXXGXXG) typical of nucleotide-dependant enzymes [113,120]. Indeed, when the Arg39 residue was mutated in *E. coli* DHDPR (EcDHDPR), a 31-fold decrease in specificity for NADPH was observed [112].

1.3.3.4 Structure of DHDPR

Bacterial DHDPR enzymes typically adopt a tetrameric quaternary structure, which has been observed in both crystallisation [113,120] and in solution studies [81]. Each monomer contains an N-terminal domain, which includes the co-factor binding site, with an alternating β -strand- α -helix secondary structure, also known as a Rossmann-fold (Fig. 6) [118]. A sharp four

residue loop, from Ala127 to Ser130 (*E. coli* numbering), connects the N-terminal domain to the substrate binding site [118], which is located within the C-terminal domain [113,118,120].

The four monomers interact to form a mixed barrel core [120]. NMR binding studies using 2,6-pyridinedicarboxylic acid (2,6-PDC) as a substrate analogue demonstrate that upon binding, there is a monomeric shift around this core, allowing for open, and thus accessible, or closed protein conformations [122].

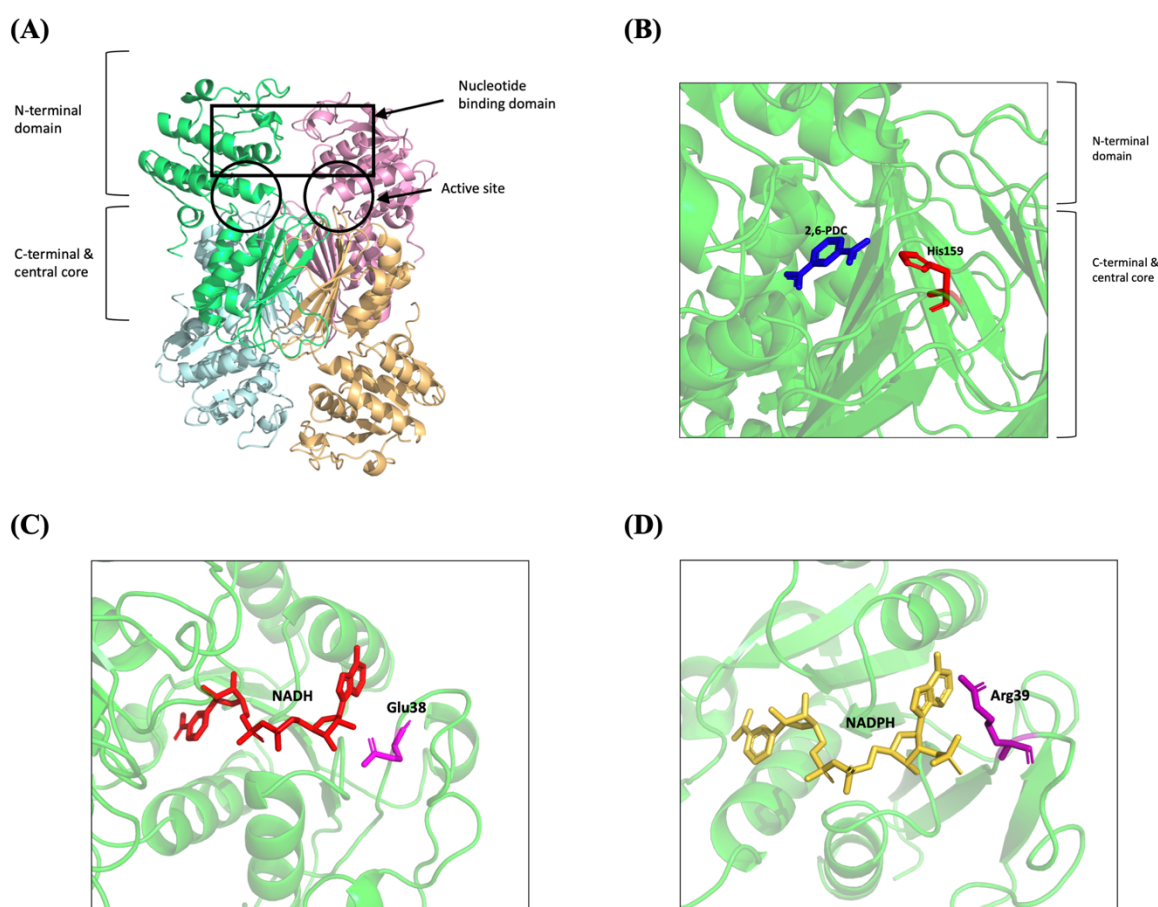


Figure 6. Structure of DHDPR enzymes. (A) The tetrameric structure of EcDHDPR (PDB: 1ARZ) with the nucleotide binding domain in the top two monomers highlighted with a box and the active sites shown by circles. The four C-terminal domains interact to form the central core of the protein. (B) The crystal structure of *E. coli* DHDPR (EcDHDPR; PDB: 1ARZ) in complex with the substrate analogue 2,6-pyridinedicarboxylic acid (2,6-PDC, blue), shown interacting with the active site residue His159. (C-D) EcDHDPR in complex with (C) NADH (red, PDB: 1ARZ) and (D) NADPH (yellow, PDB: 1DIH) showing the binding site within the

N-terminal domain. Highlighted as sticks are the key interacting residues Glu38 (pink) and Arg39 (purple) for each co-factor, respectively.

1.3.4 Inhibition Studies of the DAP Pathway

Substrate analogues of both pyruvate and ASA have been tested for inhibitory effects against DHDPS, with little to no success. These include phosphoenolpyruvate, phenylpyruvate, α -ketoglutarate, oxaloacetate, L-glutamate semialdehyde and *N*-acetyl-L-ASA [123]. Inhibition was observed with some pyruvate analogues, including fluoropyruvate, ketobutyrate and glyoxalate, but none with desired potency (Fig. 7 (1)-(3)) [95]. However, the discovery that the dehydrated form of HTPA, DHDP (Fig. 7 (4)), had a modest effect on EcDHDPS, stimulated investigation of product analogues. A series of substituted pyridine and piperidine analogues were shown to display mid-micromolar potency, but failed to progress further [123,124]. Inhibitors inspired by the product HTPA followed a similar path, with Turner and colleagues reporting two irreversible inhibitors [125]. An extended series of analogues were synthesised, but none reported an IC_{50} below 1 mM [126]. Alternatively, phenylene bis(ketoacid) derivatives were able to inhibit with low micromolar potency in a slow time dependant manner against EcDHDPS [127]. Development of these inhibitors was not continued, as this mode of inhibition is not desirable for drug discovery. Another product analogue of DHDPS, tetrahydroisophthalic acid (Fig. 7 (5)), was investigated against both DHDPS and DHDPR activity [128]. Interestingly, the analogue inhibited DHDPR more tightly, with an IC_{50} of 4 mM, compared to 15 mM for DHDPS [128]. While the inhibition potency of these inhibitors is not considered 'drug-like', it did encourage further investigation into DHDPR inhibition.

Exploration of the DHDPR active site as a druggable target has been less extensive. To date, the substrate analogue 2,6-PDC has received the most attention and acted as a starting point for lead identification (Fig. 7 (6)). Both MtDHDPR and EcDHDPR have been co-crystallised with 2,6-PDC in an attempt to determine the key interacting residues. Paiva and colleagues performed molecular dynamic screening to dock potential ligands into this site [129]. One of the most potent group of inhibitors found was several sulfonamide compounds, which had sulfonamide groups occupying the same space as 2,6-PDC [129]. The most potent compound had a sulfone replacing one of the sulfonamide groups, which had similar *in vitro* potency against EcDHDPR and MtDHDPR [129]. Other competitive inhibitors were also identified, with a common motif of a benzene ring with one or more nitro groups occurring in multiple

hits [129]. However, these compounds had higher IC_{50} values than the sulfonamides identified [129]. While none of these compounds resulted in antimicrobial activity against a wildtype strain of *E. coli* [129], the low micromolar potency *in vitro* and the wide structural motif range of these compounds demonstrates the potential that the DHDPR active site could be targeted for antibiotic development.

Alternative to the active site, DHDPS also contains the allosteric site that allows inhibition upon lysine binding (Section 1.3.2.3). Several inhibitors that target this site have been identified. Initially investigated as an ASA analogue, homoserine lactone was found to inhibit EcDHDPS non-competitively, and thus was hypothesised to be an allosteric inhibitor (Fig. 7 (7)) [128]. This spurred further investigation into other analogues, including cysteine sulfonic acid, aspartic acid and glutamic acid, all of which allosterically inhibited EcDHDPS, however only with millimolar potency (Fig. 7 (8)-(10)) [128]. Given that for many DHDPS enzymes lysine remains the most potent inhibitor, analogues of lysine have also been considered. Thialysine, a sulfur containing lysine mimetic, did inhibit EcDHDPS, however it had a 10-fold weaker potency *in vitro* in comparison to lysine (Fig. 7 (11)) [95]. More recently however, Skovpen and colleagues developed a bis-lysine inhibitor of *Campylobacter jejuni* DHDPS involving two lysine molecules joined by a two-carbon bridge in a back-to-back conformation (Figure 7 (12)) [130]. This represents the first sub-micromolar allosteric inhibitor of DHDPS, reporting a K_i value of approximately 200 nM [130]. While potent *in vitro*, the *in vivo* potency of this inhibitor against intact bacteria remains to be investigated.

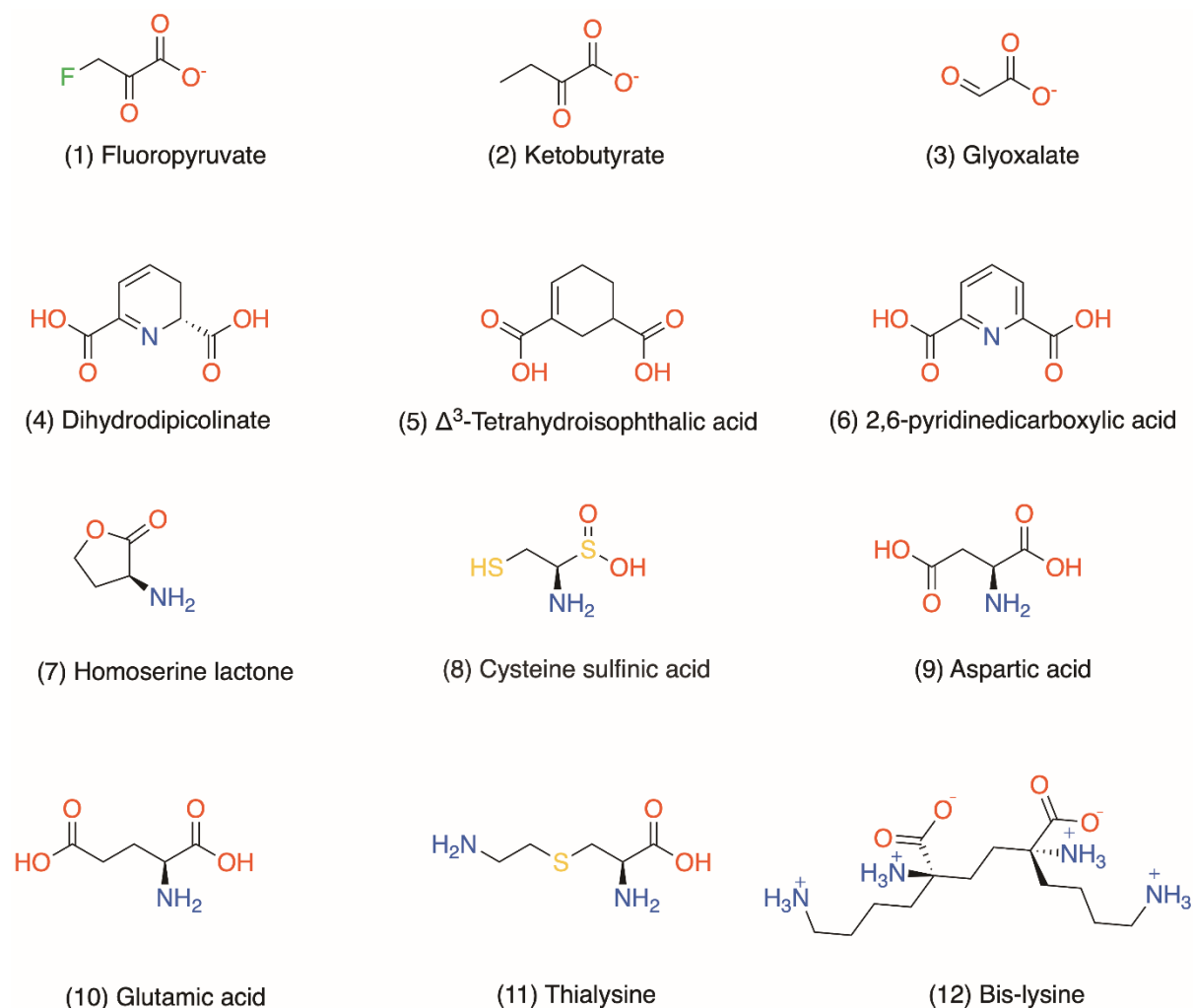


Figure 7. Current DHDPS and DHDPR inhibitors.

The presence of multiple druggable targets both within each enzyme and among the different enzymes of the DAP pathway is promising as it provides an avenue for a multi-targeted antibiotic discovery approach. The use of multi-targeted drugs is expected to negate or slow resistance generation, given mutation of a single site or enzyme is unlikely to generate resistance [131]. However, as it currently stands, all previous drug discovery attempts targeting DHDPS and DHDPR enzymes have failed to yield antimicrobial activity (Section 1.2). This highlights the need for more research into probing the structure and function of the enzymes, specifically from the pathogenic Gram-negative bacteria discussed in this chapter. Much of the previous research has been based on the model EcDHDPS enzyme and therefore is lacking in fundamental knowledge of species-specific nuances that are critical for drug discovery. By investigating DHDPS and DHDPR from these key pathogens, this thesis hopes to significantly contribute to the drug discovery efforts targeting the DAP pathway.

1.4 Overview

Due to increasing levels of antibiotic resistance, there is an urgent need for new antibiotic classes with novel modes of action in an attempt to avoid cross-resistance. As described here, the DAP pathway represents a promising target as it is implicated in both cell wall and protein syntheses. These two processes are validated antibiotic targets, exemplified by antibiotic classes such as β -lactams and aminoglycosides. In this project, my aims were to identify, validate and characterise novel antibiotic targets within the DAP pathway. Specifically, I have focussed on the enzymes DHDPS and DHDPR from the high priority Gram-negative pathogens *P. aeruginosa*, *A. baumannii* and *K. pneumoniae*. To achieve these aims, I used a combination of biochemical and biophysical techniques, including protein expression and purification, site-directed mutagenesis, enzyme kinetics, circular dichroism spectroscopy, X-ray crystallography, analytical ultracentrifugation and microscale thermophoresis, in addition to microbiology techniques such as genome modification, plasmid complementation and growth curve analysis.

Chapter Two is a published paper in *The FEBS Journal* entitled “Identification of two dihydrodipicolinate synthase isoforms from *Pseudomonas aeruginosa* that differ in allosteric regulation”. In this paper, I utilised the DHDPS signature motif to identify two *bona fide* *dapA* genes in *P. aeruginosa*, from among the four annotated genes. Furthermore, these DHDPS enzymes were functionally characterised, including probing differences in allosteric regulation by lysine.

Chapter Three is a published paper in *FEBS Letters* entitled “Mis-annotations of a promising antibiotic target in high-priority Gram-negative pathogens”. This paper uses the principles learned from Chapter Two to identify the *dapA* genes that encode for functional DHDPS enzymes in *K. pneumoniae* and *A. baumannii*. For both species, I revealed that of the four annotated *dapA* genes, only one from each species contained the DHDPS signature motif and thus encoded a single functional DHDPS enzyme. Using a combination of enzyme kinetics and X-ray crystallography, I confirmed these *dapA* mis-annotations. The *bona fide* DHDPS enzymes were then functionally characterised to aid future drug discovery efforts.

Chapter Four is a draft manuscript to be submitted to *The FEBS Journal* entitled “Validation and characterisation of a novel antibiotic target in *Pseudomonas aeruginosa*”. In this chapter,

I aimed to clarify the conflicting literature concerning the essentiality of the DHDPR-encoding gene, *dapB*, in *P. aeruginosa*. In contrast to published transposon libraries, I created a seamless gene deletion of the *dapB* gene for the first time and characterised the resulting mutant bacterial strain to assess essentiality. Subsequent functional characterisation of the recombinant enzyme revealed crucial substrate and co-factor binding information.

In summary, the work described in this thesis lays the foundation for future inhibitor discovery studies in our pursuit for much needed new antibiotics against these high priority species. We hope that by investigating a novel mechanism of action and a multi-targeted approach that we will be able to reduce resistance and circumvent resistance mechanisms.

1.5 References

- 1 Conly JM & Johnston BL (2004) Coming full circle: From antibiotics to probiotics and prebiotics. *Can J Infect Dis Med Micro* **15**, 161–163.
- 2 Fleming A (1945) Penicillin - Nobel Lecture.
(<https://www.nobelprize.org/uploads/2018/06/fleming-lecture.pdf>)
- 3 Stanwell-Smith R (2007) From the golden age of antibiotics to the era of the superbug: The lessons of antibiotic resistance. *Health and Hygiene; London* **28**, 11–12.
- 4 Krause KM, Serio AW, Kane TR & Connolly LE (2016) Aminoglycosides: an overview. *Cold Spring Harb Perspect Med* **6**.
- 5 Conly J & Johnston B (2005) Where are all the new antibiotics? The new antibiotic paradox. *Canadian J Infect Dis Med Microbiol* **16**, 159–160.
- 6 Lyddiard D, Jones GL & Greatrex BW (2016) Keeping it simple: lessons from the golden era of antibiotic discovery. *FEMS Microbiol Lett* **363**.
- 7 Årdal C, Balasegaram M, Laxminarayan R, McAdams D, Outtersson K, Rex JH & Sumpradit N (2020) Antibiotic development — economic, regulatory and societal challenges. *Nat Rev Microbiol* **18**, 267–274.
- 8 Vollmer W & Seligman SJ (2010) Architecture of peptidoglycan: more data and more models. *Trends Microbiol* **18**, 59–66.
- 9 Vollmer W, Blanot D, Pedro De MA (2008) Peptidoglycan structure and architecture. *FEMS Microbiol Rev* **32**, 149–167.
- 10 Tipper D (1985) Mode of action of β -lactam antibiotics. *Pharmacol Ther* **27**, 1–35.
- 11 Papp-Wallace KM, Endimiani A, Taracila MA & Bonomo RA (2011) Carbapenems: Past, Present, and Future. *Antimicrob Agents Chemother* **55**, 4943–4960.
- 12 Zeng D, DeBabov D, Hartsell TL, Cano RJ, Adams S, Schuyler JA, McMillan R & Pace JL (2016) Approved glycopeptide antibacterial drugs: mechanism of action and resistance. *Cold Spring Harb Perspect Med* **6**, a026989.
- 13 Trimble MJ, Mlynářčík P, Kolář M & Hancock REW (2016) Polymyxin: alternative mechanisms of action and resistance. *Cold Spring Harb Perspect Med* **6**, a025288.
- 14 Poirel L, Jayol A & Nordmann P (2017) Polymyxins: Antibacterial activity, susceptibility testing, and resistance mechanisms encoded by plasmids or chromosomes. *Clin Microbiol Reviews* **30**, 557–596.

- 15 Clifton LA, Skoda MWA, Le Brun AP, Ciesielski F, Kuzmenko I, Holt SA & Lakey JH (2015) Effect of divalent cation removal on the structure of Gram-negative bacterial outer membrane models. *Langmuir* **31**, 404–412.
- 16 Zhang L, Dhillon P, Yan H, Farmer S & Hancock REW (2000) Interactions of bacterial cationic peptide antibiotics with outer and cytoplasmic membranes of *Pseudomonas aeruginosa*. *Antimicrob Agents Chemother* **44**, 3317–3321.
- 17 Chopra I & Roberts M (2001) Tetracycline antibiotics: mode of action, applications, molecular biology, and epidemiology of bacterial resistance. *Microbiol Mol Biol Rev* **65**, 232–260.
- 18 Xaplanteri MA, Andreou A, Dinos GP & Kalpaxis DL (2003) Effect of polyamines on the inhibition of peptidyltransferase by antibiotics: revisiting the mechanism of chloramphenicol action. *Nucleic Acids Res* **31**, 5074–5083.
- 19 Retsema J, Girard A, Schelkly W, Manousos M, Anderson M, Bright G, Borovoy R, Brennan L & Mason R (1987) Spectrum and mode of action of azithromycin (CP-62,993), a new 15-membered-ring macrolide with improved potency against Gram-negative organisms. *Antimicrob Agents Chemother* **31**, 1939–1947.
- 20 Kannan K, Kanabar P, Schryer D, Florin T, Oh E, Bahroos N, Tenson T, Weissman JS & Mankin AS (2014) The general mode of translation inhibition by macrolide antibiotics. *Proc Nat Acad Sci* **111**, 15958–15963.
- 21 Pestka S (1974) Binding of [¹⁴C]erythromycin to *Escherichia coli* ribosomes. *Antimicrob Agents Chemother* **6**, 474–478.
- 22 Kasten MJ (1999) Clindamycin, metronidazole, and chloramphenicol. *Mayo Clin Proc* **74**, 825–833.
- 23 Bonfiglio G & Furneri PM (2001) Novel streptogramin antibiotics. *Expert Opin Investig Drugs* **10**, 185–198.
- 24 Livermore DM (2002) Multiple mechanisms of antimicrobial resistance in *Pseudomonas aeruginosa*: our worst nightmare? *Clin Infect Dis* **34**, 634–640.
- 25 Wolfson JS & Hooper DC (1985) The fluoroquinolones: structures, mechanisms of action and resistance, and spectra of activity in vitro. *Antimicrob Agents Chemother* **28**, 581–586.
- 26 Redgrave LS, Sutton SB, Webber MA & Piddock LJV (2014) Fluoroquinolone resistance: mechanisms, impact on bacteria, and role in evolutionary success. *Trends Microbiol* **22**, 438–445.

- 27 Wehrli W (1983) Rifampin: Mechanisms of action and resistance. *Rev Infect Dis* **5**, S407–S411.
- 28 Kapoor G, Saigal S & Elongavan A (2017) Action and resistance mechanisms of antibiotics: A guide for clinicians. *J Anaesthesiol Clin Pharmacol* **33**, 300–305.
- 29 Gleckman R, Blagg N & Joubert DW (1981) Trimethoprim: Mechanisms of action, antimicrobial activity, bacterial resistance, pharmacokinetics, adverse reactions, and therapeutic indications. *Pharmacotherapy: J Human Pharmacol Drug Therap* **1**, 14–19.
- 30 Zaffiri L, Gardner J & Toledo-Pereyra LH (2012) History of antibiotics. From Salvarsan to cephalosporins. *J Invest Surg* **25**, 67–77.
- 31 Karchmer AW (1991) *Staphylococcus aureus* and vancomycin: The sequel. *Ann Intern Med* **115**, 739–741.
- 32 Newman W, Torres JM & Guck JK (1954) Bacterial endocarditis: An analysis of fifty-two cases. *American J Infect* **16**, 535–542.
- 33 Hirsch EF (2008) “The Treatment of Infected Wounds,” Alexis Carrel’s contribution to the care of wounded soldiers during World War I. *J Trauma Acute Care Surg* **64**, S209.
- 34 Wallace WC, Cinat ME, Nastanski F, Gornick WB & Wilson SE (2000) New epidemiology for postoperative nosocomial infections. *Am Surg* **66**, 874–8.
- 35 Prokuski L (2008) Prophylactic antibiotics in orthopaedic surgery. *J Am Acad Orthop Surg* **16**, 283–293.
- 36 Classen DC, Evans RS, Pestotnik SL, Horn SD, Menlove RL & Burke JP (1992) The timing of prophylactic administration of antibiotics and the risk of surgical-wound infection. *New England J Med* **326**, 281–286.
- 37 Ventola CL (2015) The antibiotic resistance crisis. *P&T* **40**, 277–283.
- 38 Salam RA, Mansoor T, Mallick D, Lassi ZS, Das JK & Bhutta ZA (2014) Essential childbirth and postnatal interventions for improved maternal and neonatal health. *Reprod Health* **11**, S3.
- 39 Shallcross LJ & Davies DSC (2014) Antibiotic overuse: a key driver of antimicrobial resistance. *Br J Gen Pract* **64**, 604–605.
- 40 Friedman ND, Temkin E & Carmeli Y (2016) The negative impact of antibiotic resistance. *Clin Microbiol Infect* **22**, 416–422.
- 41 O’Neil J (2016) *Tackling drug-resistant infections globally: final report and recommendations* Wellcome Trust, HM Government, London, England.
- 42 Shlaes DM, Gerding DN, John JF, Craig WA, Bornstein DL, Duncan RA, Eckman MR, Farrer WE, Greene WH, Lorian V, Levy S, McGowan JE, Paul SM, Ruskin J, Tenover

- FC & Watanakunakorn C (1997) Society for healthcare epidemiology of America and infectious diseases society of America joint committee on the prevention of antimicrobial resistance: guidelines for the prevention of antimicrobial resistance in hospitals. *Clin Infect Dis* **25**, 584–599.
- 43 Hawker JJ, Smith S, Smith GE, Morbey R, Johnson AP, Fleming DM, Shallcross L & Hayward AC (2014) Trends in antibiotic prescribing in primary care for clinical syndromes subject to national recommendations to reduce antibiotic resistance, UK 1995-2011: analysis of a large database of primary care consultations. *J Antimicrob Chemother* **69**, 3423–3430.
- 44 Duong DV, Binns CW & Le TV (1997) Availability of antibiotics as over-the-counter drugs in pharmacies: a threat to public health in Vietnam. *Trop Med Int Health* **2**, 1133–1139.
- 45 Witte W (1998) Medical consequences of antibiotic use in agriculture. *Science* **279**, 996–997.
- 46 Arthur M, Reynolds P & Courvalin P (1996) Glycopeptide resistance in enterococci. *Trends Microbiol* **4**, 401–407.
- 47 Gillings MR (2013) Evolutionary consequences of antibiotic use for the resistome, mobilome and microbial pangenome. *Front Microbiol* **4**, 4.
- 48 Michael CA, Dominey-Howes D & Labbate M (2014) The antimicrobial resistance crisis: causes, consequences, and management. *Front Public Health* **2**.
- 49 Magiorakos A-P, Srinivasan A, Carey RB, Carmeli Y, Falagas ME, Giske CG, Harbarth S, Hindler JF, Kahlmeter G, Olsson-Liljequist B, Paterson DL, Rice LB, Stelling J, Struelens MJ, Vatopoulos A, Weber JT & Monnet DL (2012) Multidrug-resistant, extensively drug-resistant and pandrug-resistant bacteria: an international expert proposal for interim standard definitions for acquired resistance. *Clin Microbiol Infect* **18**, 268–281.
- 50 Hirsch EB & Tam VH (2010) Impact of multidrug-resistant *Pseudomonas aeruginosa* infection on patient outcomes. *Exp Rev Pharmacoecon Outcomes Res* **10**, 441–451.
- 51 Nathwani D, Raman G, Sulham K, Gavaghan M & Menon V (2014) Clinical and economic consequences of hospital-acquired resistant and multidrug-resistant *Pseudomonas aeruginosa* infections: a systematic review and meta-analysis. *Antimicrob Resist Infect Control* **3**, 32.
- 52 Dantas RC, Ferreira ML, Gontijo-Filho PP & Ribas RM (2014) *Pseudomonas aeruginosa* bacteraemia: independent risk factors for mortality and impact of resistance on outcome. *J Med Microbiol*, **63**, 1679–1687.

- 53 Horcajada JP, Montero M, Oliver A, Sorlí L, Luque S, Gómez-Zorrilla S, Benito N & Grau S (2019) Epidemiology and treatment of multidrug-resistant and extensively drug-resistant *Pseudomonas aeruginosa* infections. *Clin Microbiol Rev* **32**, e00031-19.
- 54 2019 antibacterial agents in clinical development: an analysis of the antibacterial clinical development pipeline (2019) World Health Organization, Geneva. (<https://www.who.int/publications/i/item/9789240000193>).
- 55 Li X-Z, Plésiat P & Nikaido H (2015) The challenge of efflux-mediated antibiotic resistance in Gram-negative bacteria. *Clin Microbiol Rev* **28**, 337–418.
- 56 Zgurskaya HI, López CA & Gnanakaran S (2015) Permeability barrier of Gram-negative cell envelopes and approaches to bypass it. *ACS Infect Dis* **1**, 512–522.
- 57 Tacconelli E, Carrara E, Savoldi A, Harbarth S, Mendelson M, Monnet DL, Pulcini C, Kahlmeter G, Kluytmans J, Carmeli Y, Ouellette M, Outtersson K, Patel J, Cavaleri M, Cox EM, Houchens CR, Grayson ML, Hansen P, Singh N, Theuretzbacher U, Magrini N, Aboderin AO, Al-Abri SS, Awang Jalil N, Benzonana N, Bhattacharya S, Brink AJ, Burkert FR, Cars O, Cornaglia G, Dyar OJ, Friedrich AW, Gales AC, Gandra S, Giske CG, Goff DA, Goossens H, Gottlieb T, Guzman Blanco M, Hryniewicz W, Kattula D, Jinks T, Kanj SS, Kerr L, Kieny M-P, Kim YS, Kozlov RS, Labarca J, Laxminarayan R, Leder K, Leibovici L, Levy-Hara G, Littman J, Malhotra-Kumar S, Manchanda V, Moja L, Ndoye B, Pan A, Paterson DL, Paul M, Qiu H, Ramon-Pardo P, Rodríguez-Baño J, Sanguinetti M, Sengupta S, Sharland M, Si-Mehand M, Silver LL, Song W, Steinbakk M, Thomsen J, Thwaites GE, van der Meer JW, Van Kinh N, Vega S, Villegas MV, Wechsler-Fördös A, Wertheim HFL, Wesangula E, Woodford N, Yilmaz FO & Zorzet A (2018) Discovery, research, and development of new antibiotics: the WHO priority list of antibiotic-resistant bacteria and tuberculosis. *Lancet Infect Dis* **18**, 318–327.
- 58 Bassetti M, Vena A, Croxatto A, Righi E & Guery B (2018) How to manage *Pseudomonas aeruginosa* infections. *Drugs Context* **7**, 212527.
- 59 Paterson DL (2006) The epidemiological profile of infections with multidrug-resistant *Pseudomonas aeruginosa* and *Acinetobacter* species. *Clin Infect Dis* **43**, S43–S48.
- 60 Driscoll JA, Brody SL & Kollef MH (2007) The epidemiology, pathogenesis and treatment of *Pseudomonas aeruginosa* infections. *Drugs* **67**, 351–368.
- 61 Surveillance Report. Surveillance of antimicrobial resistance in Europe 2018, 110.
- 62 Peng Y, Bi J, Shi J, Li Y, Ye X, Chen X & Yao Z (2014) Multidrug-resistant *Pseudomonas aeruginosa* infections pose growing threat to health care-associated infection control in

- the hospitals of Southern China: a case-control surveillance study. *Am J Infect Control* **42**, 1308–1311.
- 63 Howard A, O'Donoghue M, Feeney A & Sleator RD (2012) *Acinetobacter baumannii*. *Virulence* **3**, 243–250.
 - 64 Doi Y, Murray GL & Peleg AY (2015) *Acinetobacter baumannii*: Evolution of antimicrobial resistance—treatment options. *Semin Respir Crit Care Med* **36**, 85–98.
 - 65 Harding CM, Hennon SW & Feldman MF (2018) Uncovering the mechanisms of *Acinetobacter baumannii* virulence. *Nat Rev Microbiol* **16**, 91–102.
 - 66 Giammanco A, Calà C, Fasciana T & Dowzicky MJ (2017) Global assessment of the activity of tigecycline against multidrug-resistant Gram-negative pathogens between 2004 and 2014 as part of the tigecycline evaluation and surveillance trial. *mSphere* **2**, e00310-16.
 - 67 Götting S, Gruber TM, Higgins PG, Wachsmuth M, Seifert H & Kempf VAJ (2014) Detection of pan drug-resistant *Acinetobacter baumannii* in Germany. *J Antimicrob Chemother* **69**, 2578–2579.
 - 68 Rolain J-M, Diene SM, Kempf M, Gimenez G, Robert C & Raoult D (2013) real-time sequencing to decipher the molecular mechanism of resistance of a clinical pan-drug-resistant *Acinetobacter baumannii* isolate from Marseille, France. *Antimicrob Agents Chemother* **57**, 592–596.
 - 69 Japoni-Nejad A, Sofian M, Belkum A van & Ghaznavi-Rad E (2013) Nosocomial outbreak of extensively and pan drug-resistant *Acinetobacter baumannii* in tertiary hospital in central part of Iran. *Jundishapur J Microbiol* **6**.
 - 70 Chan P-C, Huang L-M, Lin H-C, Chang L-Y, Chen M-L, Lu C-Y, Lee P-I, Chen J-M, Lee C-Y, Pan H-J, Wang J-T, Chang S-C & Chen Y-C (2007) Control of an outbreak of pandrug-resistant *Acinetobacter baumannii* colonization and infection in a neonatal intensive care unit. *Infect Control Hosp Epidemiol* **28**, 423–429.
 - 71 Valencia R, Arroyo LA, Conde M, Aldana JM, Torres M-J, Fernández-Cuenca F, Garnacho-Montero J, Cisneros JM, Ortiz C, Pachón J & Aznar J (2009) nosocomial outbreak of infection with pan-drug-resistant *Acinetobacter baumannii* in a tertiary care university hospital. *Infect Control Hosp Epidemiol* **30**, 257–263.
 - 72 Tzouveleakis LS, Markogiannakis A, Psychogiou M, Tassios PT & Daikos GL (2012) Carbapenemases in *Klebsiella pneumoniae* and other *Enterobacteriaceae*: an Evolving crisis of global dimensions. *Clin Microbiol Rev* **25**, 682–707.
 - 73 Nordmann P, Cuzon G & Naas T (2009) The real threat of *Klebsiella pneumoniae* carbapenemase-producing bacteria. *Lancet Infect Dis* **9**, 228–236.

- 74 Munoz-Price LS, Poirel L, Bonomo RA, Schwaber MJ, Daikos GL, Cormican M, Cornaglia G, Garau J, Gniadkowski M, Hayden MK, Kumarasamy K, Livermore DM, Maya JJ, Nordmann P, Patel JB, Paterson DL, Pitout J, Villegas MV, Wang H, Woodford N & Quinn JP (2013) Clinical epidemiology of the global expansion of *Klebsiella pneumoniae* carbapenemases. *Lancet Infect Dis* **13**, 785–796.
- 75 Bassetti M, Righi E, Canelutti A, Graziano E & Russo A (2018) Multidrug-resistant *Klebsiella pneumoniae*: challenges for treatment, prevention and infection control. *Expert Rev Anti Infect Ther* **16**, 749–761.
- 76 Longo LGA, de Sousa VS, Kraychete GB, Justo-da-Silva LH, Rocha JA, Superti SV, Bonelli RR, Martins IS & Moreira BM (2019) Colistin resistance emerges in pandrug-resistant *Klebsiella pneumoniae* epidemic clones in Rio de Janeiro, Brazil. *Int J of Antimicrobial Agents* **54**, 579–586.
- 77 Guducuoglu H, Gursoy NC, Yakupogullari Y, Parlak M, Karasin G, Sunnetcioglu M & Otlu B (2018) Hospital outbreak of a colistin-resistant, ndm-1- and oxa-48-producing *Klebsiella pneumoniae*: high mortality from pandrug resistance. *Microb Drug Resist* **24**, 966–972.
- 78 Bukhari AI & Taylor AL (1971) Genetic analysis of diaminopimelic acid- and lysine-requiring mutants of *Escherichia coli*. *J Bacteriol* **105**, 844–854.
- 79 Richaud F, Richaud C, Ratet P & Patte JC (1986) Chromosomal location and nucleotide sequence of the *Escherichia coli* *dapA* gene. *J Bacteriol* **166**, 297–300.
- 80 Atkinson SC, Dogovski C, Dobson RCJ & Perugini MA (2012) Cloning, expression, purification and crystallization of dihydrodipicolinate synthase from *Agrobacterium tumefaciens*. *Acta Crystallogr Sect F Struct Biol Cryst Commun* **68**, 1040–1047.
- 81 Christensen JB, Soares da Costa TP, Faou P, Pearce FG, Panjikar S & Perugini MA (2016) Structure and function of cyanobacterial DHDPS and DHDPR. *Sci Rep* **6**, 37111.
- 82 Chen NY, Jiang SQ, Klein DA & Paulus H (1993) Organization and nucleotide sequence of the *Bacillus subtilis* diaminopimelate operon, a cluster of genes encoding the first three enzymes of diaminopimelate synthesis and dipicolinate synthase. *J Biol Chem* **268**, 9448–9465.
- 83 Domigan LJ, Scally SW, Fogg MJ, Hutton CA, Perugini MA, Dobson RCJ, Muscroft-Taylor AC, Gerrard JA & Devenish SRA (2009) Characterisation of dihydrodipicolinate synthase (DHDPS) from *Bacillus anthracis*. *Biochim Biophys Acta Proteins Proteom* **1794**, 1510–1516.

- 84 Kefala G, Evans GL, Griffin MDW, Devenish SRA, Pearce FG, Perugini MA, Gerrard JA, Weiss MS & Dobson RCJ (2008) Crystal structure and kinetic study of dihydrodipicolinate synthase from *Mycobacterium tuberculosis*. *Biochem J* **411**, 351–360.
- 85 Kaur N, Gautam A, Kumar S, Singh A, Singh N, Sharma S, Sharma R, Tewari R & Singh TP (2011) Biochemical studies and crystal structure determination of dihydrodipicolinate synthase from *Pseudomonas aeruginosa*. *Int J Biol Macromol* **48**, 779–787.
- 86 Burgess BR, Dobson RCJ, Bailey MF, Atkinson SC, Griffin MDW, Jameson GB, Parker MW, Gerrard JA & Perugini MA (2008) Structure and evolution of a novel dimeric enzyme from a clinically important bacterial pathogen. *J Biol Chem* **283**, 27598–27603.
- 87 Dogovski C, Atkinson SC, Dommaraju SR, Downton M, Hor L, Moore S, Paxman JJ, Peverelli MG, Qiu TW & Reumann M (2012) Enzymology of bacterial lysine biosynthesis. In *Biochemistry (D Ekinici, ed.)* InTech Open Access Publisher, London, UK.
- 88 Jones-Held S, Ambrozevicius LP, Campbell M, Drumheller B, Harrington E & Leustek T (2012) Two *Arabidopsis thaliana* dihydrodipicolinate synthases, DHDPS1 and DHDPS2, are unequally redundant. *Funct Plant Biol* **39**, 1058–1067.
- 89 Kobayashi K, Ehrlich SD, Albertini A, Amati G, Andersen KK, Arnaud M, Asai K, Ashikaga S, Aymerich S, Bessieres P, Boland F, Brignell SC, Bron S, Bunai K, Chapuis J, Christiansen LC, Danchin A, Débarbouillé M, Dervyn E, Deuerling E, Devine K, Devine SK, Dreesen O, Errington J, Fillinger S, Foster SJ, Fujita Y, Galizzi A, Gardan R, Eschevins C, Fukushima T, Haga K, Harwood CR, Hecker M, Hosoya D, Hullo MF, Kakeshita H, Karamata D, Kasahara Y, Kawamura F, Koga K, Koski P, Kuwana R, Imamura D, Ishimaru M, Ishikawa S, Ishio I, Coq DL, Masson A, Mauël C, Meima R, Mellado RP, Moir A, Moriya S, Nagakawa E, Nanamiya H, Nakai S, Nygaard P, Ogura M, Ohanan T, O'Reilly M, O'Rourke M, Pragai Z, Pooley HM, Rapoport G, Rawlins JP, Rivas LA, Rivolta C, Sadaie A, Sadaie Y, Sarvas M, Sato T, Saxild HH, Scanlan E, Schumann W, Seegers JFML, Sekiguchi J, Sekowska A, Séror SJ, Simon M, Stragier P, Studer R, Takamatsu H, Tanaka T, Takeuchi M, Thomaides HB, Vagner V, Dijnl JM van, Watabe K, Wipat A, Yamamoto H, Yamamoto M, Yamamoto Y, Yamane K, Yata K, Yoshida K, Yoshikawa H, Zuber U & Ogasawara N (2003) Essential *Bacillus subtilis* genes. *Proc Nat Acad Sci* **100**, 4678–4683.

- 90 Gerdes SY, Scholle MD, Campbell JW, Balázsi G, Ravasz E, Daugherty MD, Somera AL, Kyrpides NC, Anderson I, Gelfand MS, Bhattacharya A, Kapatral V, D'Souza M, Baev MV, Grechkin Y, Mseeh F, Fonstein MY, Overbeek R, Barabási A-L, Oltvai ZN & Osterman AL (2003) Experimental determination and system level analysis of essential genes in *Escherichia coli* MG1655. *J Bacteriol* **185**, 5673–5684.
- 91 Becker D, Selbach M, Rollenhagen C, Ballmaier M, Meyer TF, Mann M & Bumann D (2006) Robust Salmonella metabolism limits possibilities for new antimicrobials. *Nature* **440**, 303–307.
- 92 Salama NR, Shepherd B & Falkow S (2004) Global transposon mutagenesis and essential gene analysis of *Helicobacter pylori*. *J Bacteriol* **186**, 7926–7935.
- 93 Bland DM, Eisele NA, Keleher LL, Anderson PE & Anderson DM (2011) Novel genetic tools for diaminopimelic acid selection in virulence studies of *Yersinia pestis*. *PLOS ONE* **6**, e17352.
- 94 Gefflaut T, Blonski C, Perie J & Willson A (1995) Class I aldolases: Substrate specificity, mechanism, inhibitors and structural aspects. *Prog Biophys Mol Bio* **63**, 301–340.
- 95 Karsten WE (1997) Dihydrodipicolinate synthase from *Escherichia coli*: pH dependent changes in the kinetic mechanism and kinetic mechanism of allosteric inhibition by L-lysine. *Biochemistry* **36**, 1730–1739.
- 96 Frisch DA, Gengenbach BG, Tommey AM, Sellner JM, Somers DA & Myers DE (1991) Isolation and characterization of dihydrodipicolinate synthase from maize. *Plant Physiol* **96**, 444–452.
- 97 Dobson RCJ, Devenish SRA, Turner LA, Clifford VR, Pearce FG, Jameson GB & Gerrard JA (2005) Role of arginine 138 in the catalysis and regulation of *Escherichia coli* dihydrodipicolinate synthase. *Biochemistry* **44**, 13007–13013.
- 98 Dobson RCJ, Griffin MDW, Roberts SJ & Gerrard JA (2004) Dihydrodipicolinate synthase (DHDPS) from *Escherichia coli* displays partial mixed inhibition with respect to its first substrate, pyruvate. *Biochimie* **86**, 311–315.
- 99 Dobson RCJ, Valegård K & Gerrard JA (2004) The crystal structure of three site-directed mutants of *Escherichia coli* dihydrodipicolinate synthase: further evidence for a catalytic triad. *J Mol Biol* **338**, 329–339.
- 100 Desbois S, John UP & Perugini MA (2018) Dihydrodipicolinate synthase is absent in fungi. *Biochimie* **152**, 73–84.
- 101 Hutton CA, Perugini MA & Gerrard JA (2007) Inhibition of lysine biosynthesis: an evolving antibiotic strategy. *Mol Biosyst* **3**, 458–465.

- 102 Soares da Costa TP, Abbott BM, Gendall AR, Panjikar S & Perugini MA (2017) Molecular evolution of an oligomeric biocatalyst functioning in lysine biosynthesis. *Biophys Rev* **4**, 153–162.
- 103 Atkinson SC, Dogovski C, Downton MT, Czabotar PE, Dobson RCJ, Gerrard JA, Wagner J & Perugini MA (2013) Structural, kinetic and computational investigation of *Vitis vinifera* DHDPS reveals new insight into the mechanism of lysine-mediated allosteric inhibition. *Plant Mol Biol* **81**, 431–446.
- 104 Soares da Costa TP, Desbois S, Dogovski C, Gorman MA, Ketaren NE, Paxman JJ, Siddiqui T, Zammit LM, Abbott BM, Robins-Browne RM, Parker MW, Jameson GB, Hall NE, Panjikar S & Perugini MA (2016) Structural determinants defining the allosteric inhibition of an essential antibiotic target. *Structure* **24**, 1282–1291.
- 105 Dobson RCJ, Griffin MDW, Jameson GB & Gerrard JA (2005) The crystal structures of native and (S)-lysine-bound dihydrodipicolinate synthase from *Escherichia coli* with improved resolution show new features of biological significance. *Acta Crystallogr* **61**, 1116–1124.
- 106 Board A (2018) Mapping the uncharted water channel of dihydrodipicolinate synthase: a proposed mechanism of allostery. *Masters Thesis, University of Canterbury, New Zealand*.
- 107 Mirwaldt C, Korndorfer I & Huber R (1995) The crystal structure of dihydrodipicolinate synthase from *Escherichia coli* at 2.5 Å resolution. *J Mol Bio* **246**, 227–239.
- 108 Griffin MDW, Dobson RCJ, Pearce FG, Antonio L, Whitten AE, Liew CK, Mackay JP, Trehwella J, Jameson GB, Perugini MA & Gerrard JA (2008) Evolution of quaternary structure in a homotetrameric enzyme. *J Mol Biol* **380**, 691–703.
- 109 Farkas W & Gilvarg C (1965) The reduction step in diaminopimelic acid biosynthesis. *J Biol Chem* **240**, 4717–4722.
- 110 Bouvier J, Richaud C, Richaud F, Patte JC & Stragier P (1984) Nucleotide sequence and expression of the *Escherichia coli* *dapB* gene. *J Biol Chem* **259**, 14829–14834.
- 111 Kimura K & Goto T (1977) dihydrodipicolinate reductases from *Bacillus cereus* and *Bacillus megaterium*. *J Biochem* **81**, 1367–1373.
- 112 Xu J-Z, Yang H-K, Liu L-M, Wang Y-Y & Zhang W-G (2018) Rational modification of *Corynebacterium glutamicum* dihydrodipicolinate reductase to switch the nucleotide-cofactor specificity for increasing L-lysine production. *Biotech Bioeng* **115**, 1764–1777.

- 113 Cirilli M, Zheng R, Scapin G & Blanchard JS (2003) The three-dimensional structures of the *Mycobacterium tuberculosis* dihydrodipicolinate reductase–NADH–2,6-PDC and –NADPH–2,6-PDC complexes. Structural and mutagenic analysis of relaxed nucleotide specificity. *Biochemistry* **42**, 10644–10650.
- 114 Girish TS, Sharma E & Gopal B (2008) Structural and functional characterization of *Staphylococcus aureus* dihydrodipicolinate synthase. *FEBS Lett* **582**, 2923–2930.
- 115 Dommaraju SR, Dogovski C, Czabotar PE, Hor L, Smith BJ & Perugini MA (2011) Catalytic mechanism and cofactor preference of dihydrodipicolinate reductase from methicillin-resistant *Staphylococcus aureus*. *Arch Biochem Biophys* **512**, 167–174.
- 116 Pearce FG, Sprissler C & Gerrard JA (2008) Characterization of dihydrodipicolinate reductase from *Thermotoga maritima* reveals evolution of substrate binding kinetics. *J Biochem* **143**, 617–623.
- 117 Skurnik D, Roux D, Aschard H, Cattoir V, Yoder-Himes D, Lory S & Pier GB (2013) A comprehensive analysis of *in vitro* and *in vivo* genetic fitness of *Pseudomonas aeruginosa* using high-throughput sequencing of transposon libraries. *PLOS Pathog* **9**, e1003582.
- 118 Scapin G, Blanchard JS & Sacchettini JC (1995) Three-dimensional structure of *Escherichia coli* dihydrodipicolinate reductase. *Biochemistry* **34**, 3502–3512.
- 119 Reddy SG, Sacchettini JC & Blanchard JS (1995) Expression, purification, and characterization of *Escherichia coli* dihydrodipicolinate reductase. *Biochemistry* **34**, 3492–3501.
- 120 Scapin G, Reddy SG, Zheng R & Blanchard JS (1997) Three-dimensional structure of *Escherichia coli* dihydrodipicolinate reductase in complex with NADH and the inhibitor 2,6-pyridinedicarboxylate. *Biochemistry* **36**, 15081–15088.
- 121 Devenish SRA, Gerrard JA, Jameson GB & Dobson RCJ (2008) The high-resolution structure of dihydrodipicolinate synthase from *Escherichia coli* bound to its first substrate, pyruvate. *Acta Cryst F* **64**, 1092–1095.
- 122 Ge X, Olson A, Cai S & Sem DS (2008) Binding synergy and cooperativity in dihydrodipicolinate reductase: implications for mechanism and the design of biligand inhibitors. *Biochemistry* **47**, 9966–9980.
- 123 Cox RJ (1996) The DAP pathway to lysine as a target for antimicrobial agents. *Nat Prod Rep* **13**, 29.

- 124 Christoff RM, Gardhi CK, Soares da Costa TP, Perugini MA & Abbott BM (2019) Pursuing DHDPS: an enzyme of unrealised potential as a novel antibacterial target. *MedChemComm* **10**, 1581–1588.
- 125 Turner JJ, Gerrard JA & Hutton CA (2005) Heterocyclic inhibitors of dihydrodipicolinate synthase are not competitive. *Bioorg Med Chem* **13**, 2133–2140.
- 126 Boughton BA, Griffin MDW, O'Donnell PA, Dobson RCJ, Perugini MA, Gerrard JA & Hutton CA (2008) Irreversible inhibition of dihydrodipicolinate synthase by 4-oxo-heptenedioic acid analogues. *Bioorg Med Chem* **16**, 9975–9983.
- 127 Boughton BA, Hor L, Gerrard JA & Hutton CA (2012) 1,3-Phenylene bis(ketoacid) derivatives as inhibitors of *Escherichia coli* dihydrodipicolinate synthase. *Bioorg Med Chem* **20**, 2419–2426.
- 128 Coulter CV, Gerrard JA, Kraunsoe JAE & Pratt AJ (1999) *Escherichia coli* dihydrodipicolinate synthase and dihydrodipicolinate reductase: kinetic and inhibition studies of two putative herbicide targets. *J Pest Sci* **55**, 887–895.
- 129 Paiva AM, Vanderwall DE, Blanchard JS, Kozarich JW, Williamson JM & Kelly TM (2001) Inhibitors of dihydrodipicolinate reductase, a key enzyme of the diaminopimelate pathway of *Mycobacterium tuberculosis*. *Biochim Biophys Acta Protein Struct Mol Enzymol* **1545**, 67–77.
- 130 Skovpen YV, Conly CJT, Sanders DAR & Palmer DRJ (2016) Biomimetic design results in a potent allosteric inhibitor of dihydrodipicolinate synthase from *Campylobacter jejuni*. *J Am Chem Soc* **138**, 2014–2020.
- 131 Oldfield E & Feng X (2014) Resistance-resistant antibiotics. *Trends Pharmacol Sci* **35**, 664–674.

- This page was intentionally left blank -

2 DHDPs enzymes from *Pseudomonas aeruginosa*

2.1 Published Article

2.1.1 Copyright

This article was published in *FEBS Journal*, Vol. 287(2), Impey, R. E., Panjikar, S., Hall, C. J., Bock, L. J., Sutton, J. M., Perugini, M. A. & Soares da Costa, T. P. “Identification of two dihydrodipicolinate synthase isoforms from *Pseudomonas aeruginosa* that differ in allosteric regulation”, pp 386-400. Copyright *FEBS Journal* 2020 (c/o John Wiley and Sons).

Copyright authorisation obtained on:


13th December 2020

2.1.2 Statement of Contribution

I confirm that Rachael Impey has made the following contributions:

- Completion of experimental work (95%) with the exception of Figure 11, in which the homology models were generated by Cody J. Hall
- Data analysis (95%), assisted by Santosh Panjikar for structural refinement of the PaDHDPs2-H56Q enzyme
- Conceptualisation and drafting of the manuscript (60%)
- Preparation of figures
- Revisions of manuscript prior to acceptance



Tatiana Soares da Costa

Signed: 

Date: 14/12/2020

(Executive Author)

Identification of two dihydrodipicolinate synthase isoforms from *Pseudomonas aeruginosa* that differ in allosteric regulation

Rachael E. Impey¹, Santosh Panjikar^{2,3}, Cody J. Hall¹, Lucy J. Bock⁴, J. Mark Sutton⁴, Matthew A. Perugini¹  and Tatiana P. Soares da Costa¹ 

¹ Department of Biochemistry and Genetics, La Trobe Institute for Molecular Science, La Trobe University, Bundoora, Australia

² Australian Synchrotron, ANSTO, Clayton, Australia

³ Department of Molecular Biology and Biochemistry, Monash University, Melbourne, Australia

⁴ National Infection Service, Public Health England, Porton Down, Salisbury, UK

Keywords

4-hydroxy-tetrahydrodipicolinate synthase; allosteric regulation; antibiotic resistance; diaminopimelate; lysine biosynthesis

Correspondence

T. P. Soares da Costa and M. A. Perugini, Department of Biochemistry and Genetics, La Trobe University, Bundoora, Vic. 3086, Australia

Tel: (+61) 3 9479 2227 (TPSC); (+61) 3 9479 6570 (MAP)

E-mails: T.SoaesdaCosta@latrobe.edu.au (TPSC); M.Perugini@latrobe.edu.au (MAP)

Website: <https://www.latrobe.edu.au/biochemistry-and-genetics/research/soares-da-costa-antibiotic-and-herbicide-discovery> (TPSC); <https://www.latrobe.edu.au/biochemistry-and-genetics/research/perugini> (MAP)

(Received 4 February 2019, revised 12 June 2019, accepted 19 July 2019)

doi:10.1111/febs.15014

Pseudomonas aeruginosa is one of the leading causes of nosocomial infections, accounting for 10% of all hospital-acquired infections. Current antibiotics against *P. aeruginosa* are becoming increasingly ineffective due to the exponential rise in drug resistance. Thus, there is an urgent need to validate and characterize novel drug targets to guide the development of new classes of antibiotics against this pathogen. One such target is the diaminopimelate (DAP) pathway, which is responsible for the biosynthesis of bacterial cell wall and protein building blocks, namely *meso*-DAP and lysine. The rate-limiting step of this pathway is catalysed by the enzyme dihydrodipicolinate synthase (DHDPS), typically encoded for in bacteria by a single *dapA* gene. Here, we show that *P. aeruginosa* encodes two functional DHDPS enzymes, PaDHDPS1 and PaDHDPS2. Although these isoforms have similar catalytic activities ($k_{\text{cat}} = 29 \text{ s}^{-1}$ and 44 s^{-1} for PaDHDPS1 and PaDHDPS2, respectively), they are differentially allosterically regulated by lysine, with only PaDHDPS2 showing inhibition by the end product of the DAP pathway ($\text{IC}_{50} = 130 \text{ }\mu\text{M}$). The differences in allostery are attributed to a single amino acid difference in the allosteric binding pocket at position 56. This is the first example of a bacterium that contains multiple *bona fide* DHDPS enzymes, which differ in allosteric regulation. We speculate that the presence of the two isoforms allows an increase in the metabolic flux through the DAP pathway when required in this clinically important pathogen.

Databases

PDB ID: 6P90.

Abbreviations

ASA, (S)-aspartate semialdehyde; CD, circular dichroism; DAP, diaminopimelate; DAPDC, diaminopimelate decarboxylase; DHDPR, dihydrodipicolinate reductase; DHDPS, dihydrodipicolinate synthase; HTPA, 4-hydroxy-2,3,4,5-tetrahydro-(2S)-dipicolinic acid; L-lysine, lysine; NADPH, nicotinamide adenine dinucleotide phosphate; NSDAP, *N*-succinyl-L-L-2,6-diaminopimelate; NSDAP-AT, *N*-succinyl-diaminopimelate aminotransferase; NSKAP, *N*-succinyl-L-2-amino-6-ketopimelate; PEP, phosphoenolpyruvate; Pyr4H2C, 1-pyrroline-4-hydroxy-2-carboxylate; SDAP-DS, succinyl-diaminopimelate desuccinylase; THDP, 2,3,4,5-tetrahydrodipicolinate; THPC-NST, 2,3,4,5-tetrahydropyridine-2-carboxylate *N*-succinyltransferase.

Introduction

Pseudomonas aeruginosa is an opportunistic Gram-negative bacterium that causes a wide range of acute and chronic infections. It commonly affects immunocompromised patients, including those with cystic fibrosis, cancer, AIDS and burn wounds [1–4]. *P. aeruginosa* infections have been frequently treated over the past 70 years using antibiotic classes, such as aminoglycosides, carbapenems and cephalosporins, that target the synthesis of bacterial cell wall and proteins. However, these antipseudomonal agents are becoming increasingly ineffective, due to a combination of intrinsic antibiotic resistance (efflux pumps and membrane permeability) and acquisition of new traits, with up to one quarter of infections classified as extremely drug resistant [5–7]. Nevertheless, the effectiveness of these antibiotics, that have dominated the market since their discovery, provides proof of concept that targeting cell wall and amino acid biosynthesis is an excellent strategy for antibiotic development against *P. aeruginosa*.

A promising, but as yet unexploited, antibiotic target is the diaminopimelate (DAP) pathway, which yields essential metabolic building products, namely *meso*-DAP and lysine (Fig. 1). In Gram-negative bacteria, including *P. aeruginosa*, *meso*-DAP is found in the penta-peptide moieties used to cross-link peptidoglycan chains in the cell wall, whilst lysine is critical for protein synthesis [8–12]. Importantly, *meso*-DAP and lysine are only synthesized in bacteria and plants via the DAP pathway, and thus, chemical inhibition of this pathway is unlikely to result in toxicity to the human host [8,12,13]. The DAP pathway commences with the condensation of pyruvate and (*S*)-aspartate semialdehyde (ASA) to form 4-hydroxy-2,3,4,5-tetrahydro-(2*S*)-dipicolinic acid (HTPA) (Fig. 1). This first committed and rate-limiting step is catalysed by 4-hydroxy-tetrahydrodipicolinate synthase (EC 4.3.3.7), commonly referred to as dihydrodipicolinate synthase (DHDPS) [9,14]. HTPA is then reduced to 2,3,4,5-tetrahydrodipicolinate (THDP) in an NADPH-dependant reaction by 4-hydroxy-tetrahydrodipicolinate reductase (EC 1.17.1.8), commonly known as dihydrodipicolinate reductase (DHDPR) (Fig. 1) [12,13,15,16]. From this point on, the pathway diverges depending on the organism until *meso*-DAP is formed [12]. Gram-negative bacteria, including *P. aeruginosa*, are proposed to utilize the succinyl pathway to produce *LL*-DAP (Fig. 1) [12]. *LL*-DAP is converted to *meso*-DAP, which is then used in the cross-linking of the peptidoglycan layer [11,17,18]. Finally, *meso*-DAP is decarboxylated to *L*-lysine (referred to as lysine herein) by diaminopimelate decarboxylase (DAPDC, EC 4.1.1.20)

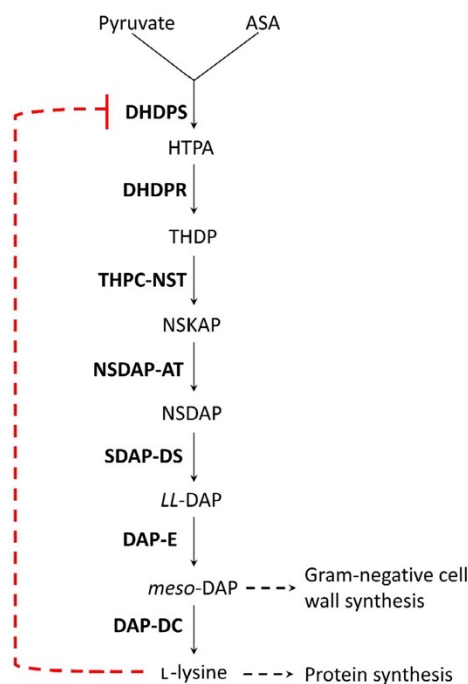


Fig. 1. Diaminopimelate (DAP) pathway in Gram-negative bacteria. Dihydrodipicolinate synthase (DHDPS) catalyses the first step in the pathway, involving the condensation of pyruvate and (*S*)-aspartate semialdehyde (ASA) to the product 4-hydroxy-2,3,4,5-tetrahydro-(2*S*)-dipicolinic acid (HTPA). HTPA is subsequently converted to 2,3,4,5-tetrahydrodipicolinate (THDP) by dihydrodipicolinate reductase (DHDPR) in an NADPH-dependent reaction. THDP undergoes several enzymatic steps in the succinyl subpathway, before *meso*-DAP is formed, which can be utilized for cell wall synthesis or be further decarboxylated to lysine for protein synthesis. The pathway can be allosterically regulated by lysine via the inhibition of DHDPS (dashed line).

(Fig. 1) [12,13,19]. Interestingly, the final product, lysine, can allosterically inhibit DHDPS from some bacterial species via a negative feedback loop [20–22]. The current dogma suggests that the DHDPS residue in position 56 (*E. coli* DHDPS numbering) is a key molecular determinant for allosteric regulation [20], as the presence of a histidine or glutamate allows allosteric inhibition, whereas a lysine or arginine at this position results in no inhibition [20].

Gene knockout studies have shown either directly or indirectly that the *dapA* gene encoding DHDPS is essential in a number of bacterial species, including

Salmonella typhimurium [23], *Bacillus subtilis* [24], *Escherichia coli* [25] and *Streptococcus pneumoniae* [26]. However, a recent study demonstrated that a *dapA* knockout in *P. aeruginosa* results in no change in bacterial counts or virulence [27]. Interestingly, unlike other bacterial species that encode for a single *dapA* gene, there are four annotated *dapA* genes in *P. aeruginosa* genomes. Thus far, only the *dapA2* gene product (GenBank: PA1010) from *P. aeruginosa* has been functionally and structurally characterized as a DHDPS enzyme, displaying similar catalytic properties to other bacterial orthologues [28]. Interestingly, despite *dapA3* (GenBank: PA1254) being annotated as a *dapA* gene, it has been shown to have 1-pyrroline-4-hydroxy-2-carboxylate (Pyr4H2C) deaminase (EC 3.5.4.22) activity [29]. It remains to be explored whether this gene product has Pyr4H2C deaminase/DHDPS dual activity. The proposed DHDPS activity for the products of *dapA1* (GenBank: PALES_34361) and *dapA4* (GenBank: PA0223) genes is also yet to be elucidated.

In this study, we set out to validate the existence of multiple isoforms of DHDPS from *P. aeruginosa* and compare the aforementioned four putative *dapA* genes and their products by employing a combination of bioinformatics, RT-PCR, circular dichroism spectroscopy, enzyme kinetics, complementation assays, allosteric inhibition assays, mutagenesis studies, X-ray crystallography and homology models. Firstly, we show that the presence and expression of the *dapA* genes vary between *P. aeruginosa* strains. Subsequently, we expressed and purified the four *dapA*-encoding recombinant proteins and showed that only the *dapA1* and *dapA2* gene products (referred to as PaDHDPS1 and PaDHDPS2, respectively) have *bona fide* DHDPS activity. Moreover, these isoforms display similar catalytic efficiencies but are differentially allosterically regulated by lysine, with only PaDHDPS2 subject to allosteric inhibition. We then employed site-directed mutagenesis, X-ray crystallography and homology models to further investigate the molecular determinants defining lysine-mediated allosteric inhibition. Thus, this work provides important insights into the future design of *P. aeruginosa* DHDPS inhibitors and, importantly, the metabolic regulation of the DAP pathway in this pathogen.

Results

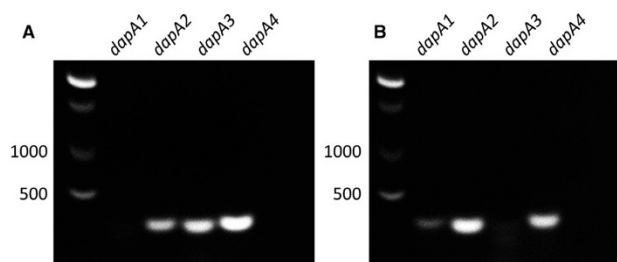
Annotated *dapA* genes in *P. aeruginosa* genomes

To identify the genes encoding for DHDPS in *P. aeruginosa*, we searched for annotated *dapA* genes

in the *Pseudomonas* Genome Database [30] and NCBI. The search yielded four putative *dapA* genes, of which *dapA2* (PA1010), *dapA3* (PA1254) and *dapA4* (PA0223) were universally present. The *dapA2* gene was found to be consistently located in the same operon in all annotated *Pseudomonas* species. In contrast, *dapA1* (PALES_34361) was found in 144 of 335 (43%) complete *Pseudomonas* species genomes available through the *Pseudomonas* Genome Database (version 18.1; 2019-03-12; <http://www.pseudomonas.com/> [30]), and is widely distributed across species with 57 *P. aeruginosa* isolates and 83 isolates from other *Pseudomonas* species. A comparison between PAO1 and LESB58 showed the *dapA1* gene is inserted as a 1180 base pair fragment, which contains a putative promoter and the gene itself. This fragment and the site of insertion is highly conserved with isolates of the Liverpool Epidemic Strain (LES), such as the seven genome sequenced isolates found in cystic fibrosis (CF) patients in both the United Kingdom and Canada [31], and CF isolates including NCTC 13618 and NCTC 13620 [32]. This does not appear to be part of any of the known or predicted genomic islands or other mobile genetic elements within this epidemic clone [33]. The fragment also appears in isolates from other high-risk international clones, such as the colistin-resistant NDM-1 expressing ST654 isolate described previously [34]. It remains unclear whether this is conserved in all isolates of this sequence type. Next, we set out to assess whether the annotated *dapA* genes were indeed expressed in *P. aeruginosa* using RT-PCR. The two strains employed in this study were (a) PAO1, a standard lab strain that contains *dapA2*, *dapA3* and *dapA4*, and (b) 372261, a clinical strain that has the 4 *dapA* genes annotated. The RT-PCR analyses showed that all *dapA* genes present are transcribed in PAO1 during exponential phase, while only *dapA1*, *dapA2* and *dapA4* are expressed in 372261 (Fig. 2).

To assess whether the *dapA* gene products are likely to encode for functional DHDPS enzymes, sequence alignments were performed at the protein sequence level and compared to the sequence of *E. coli* (Ec) DHDPS (Fig. 3). The amino acid sequences of the putative DHDPS enzymes show a high degree of variation, with identity ranging from 19 to 32% (Fig. 3). Interestingly, only the *dapA1* and *dapA2* gene products were shown to have the seven residues that are critical for DHDPS catalytic function [35], with *dapA3* and *dapA4* gene-encoded proteins containing only two and four of these residues respectively (Fig. 3). This suggests that only *dapA1* and *dapA2* encode for functional DHDPS enzymes. We, therefore, set out to express,

Fig. 2. RT-PCR analyses showing the expression of *dapA2*, *dapA3* and *dapA4* in PAO1 (A), and *dapA1*, *dapA2* and *dapA4* in 372261 (B).



purify and characterize these *dapA* gene products to validate their putative DHDPS function.

Expression, purification and characterization of *dapA* gene products

The putative *dapA* genes were overexpressed in *E. coli* and purified to > 98% homogeneity as described in the Methods (Fig. 4A). The secondary structure of the recombinant proteins was assessed using circular

dichroism (CD) spectroscopy. The CD spectra show a broad minimum spanning approximately 208–225 nm, which is consistent with the α/β secondary motif reported for the previously characterized *P. aeruginosa* DHDPS enzyme (i.e. the *dapA2* gene product), as well as other bacterial orthologues (Fig. 4B) [28,36–38]. Having confirmed the recombinant proteins were folded, they were next assessed for DHDPS activity using the qualitative *o*-aminobenzaldehyde assay, which measures activity based upon the production of

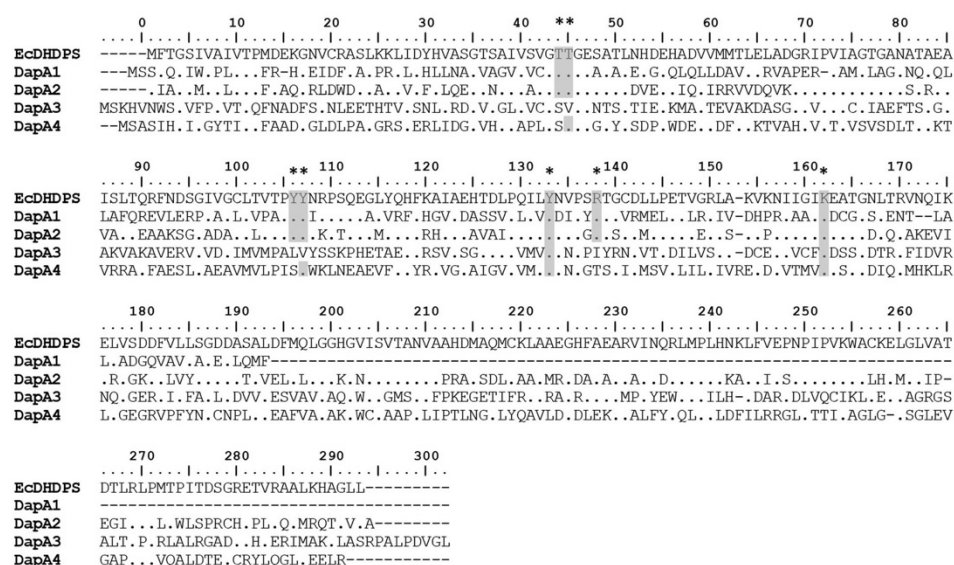


Fig. 3. Multiple sequence alignment of the four annotated *dapA* gene products from *P. aeruginosa* (DapA1 UNIPROT ID: A0A3G5V4H5, DapA2 UNIPROT ID: Q914W3, DapA3 UNIPROT ID: Q91490, DapA4 UNIPROT ID: Q916R5) compared to the single *dapA* gene product from *E. coli* (UNIPROT ID: P0A6L2). Identical residues are shown by a dot (.), while gaps are shown by a dash (-). Active site residues shown to be important for DHDPS function are denoted with asterisks and conserved residues highlighted by grey boxes. Sequence alignment was performed using the CLUSTALW algorithm incorporated in BIOEDIT (v7.2.0).

a purple chromophore [20,39,40]. Both *dapA1* and *dapA2* gene products are shown to produce a purple colour relative to the positive control EcDHDPS, while the *dapA3* and *dapA4* gene products result in no discernible colour change (Fig. 5A). To further validate this, the DHDPS activity of all four gene products was quantitatively assessed using the DHDPS-DHDPR coupled assay [38,41,42]. The *dapA1* and *dapA2* gene products are shown to have comparable activity to EcDHDPS, whilst the *dapA3* and *dapA4* gene products have no detectable activity (Fig. 5B).

To confirm that neither the *dapA3* or *dapA4* gene products could complement DHDPS activity *in vivo*, a complementation assay was performed using the AT997r⁻ *E. coli* strain that lacks a functional *dapA* gene [43–45]. The pET28a vectors containing the *dapA1–4* genes were transformed into the AT997r⁻ strain and expression was induced using IPTG. As expected, all cells grew on the DAP supplemented media (Fig. 6A), while only the cells transformed with the pET28a-*dapA1* or pET28a-*dapA2* plasmids were able to grow without DAP (Fig. 6B). This demonstrates that only the *dapA1* and *dapA2* genes encode for functional DHDPS enzymes – PaDHDPS1 and PaDHDPS2.

Catalytic efficiency of PaDHDPS1 and PaDHDPS2

Having determined that the recombinant PaDHDPS1 and PaDHDPS2 enzymes were homogenous, folded and catalytically active, we set out to determine their enzyme kinetic parameters using the DHDPS-DHDPR coupled assay [38,41,46]. Initial rates were monitored

while varying the concentrations of the DHDPS substrates, pyruvate and ASA (Fig. 7). The resulting Michaelis–Menten curves were analysed globally to a bisubstrate ping-pong model without substrate inhibition to yield the kinetic parameters summarized in Table 1. The K_M values for PaDHDPS1 were 230 μM for pyruvate and 120 μM for ASA, whilst for PaDHDPS2 the K_M values were 150 μM and 53 μM , respectively (Table 1). The turnover numbers for the two isoforms were comparable, with PaDHDPS1 having a k_{cat} of 29 s^{-1} compared to 44 s^{-1} for PaDHDPS2 (Table 1). Interestingly, the enzyme kinetic data reported here for PaDHDPS2 is significantly different to an earlier report that employed pseudokinetic analyses, where only one substrate was titrated at a time (Table 1) [28].

Allosteric inhibition by lysine

In order to determine whether PaDHDPS1 and PaDHDPS2 are allosterically inhibited by lysine, the end product of the DAP pathway (Fig. 1), the DHDPS-DHDPR coupled assay was performed in the presence of increasing lysine concentrations. We show for the first time that PaDHDPS2 is inhibited by lysine with an IC_{50} value of 130 μM (Fig. 8), consistent with other bacterial DHDPS enzymes [20,26,39]. On the other hand, PaDHDPS1 is shown to be insensitive to lysine even up to 2 mM (Fig. 8).

To probe the molecular determinants for this differential allosteric regulation, we compared the amino acid sequences of PaDHDPS1 and PaDHDPS2 with other bacterial DHDPS enzymes. This revealed that a

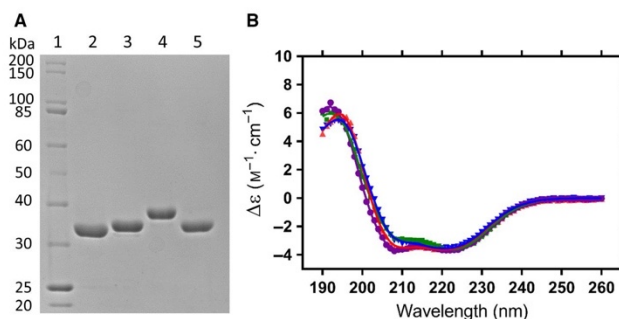


Fig. 4. (A) SDS/PAGE summary showing the pure recombinant *P. aeruginosa* *dapA1*, *dapA2*, *dapA3* and *dapA4* gene products (lanes 2, 3, 4 and 5 respectively) with the expected molecular weights between 35–40 kDa as shown by the Broad Range Molecular Weight (10–200 kDa) ladder (lane 1). (B) Circular dichroism spectroscopy analyses of recombinant *dapA1* (purple), *dapA2* (green), *dapA3* (red) and *dapA4* (blue) encoding proteins, with the mean residue ellipticity ($\text{M}^{-1}\cdot\text{cm}^{-1}$) shown as a function of wavelength (nm). The data were fitted using the CONTINILL database using the SP22x reference set (line).

Fig. 5. (A) Qualitative *o*-aminobenzaldehyde assay of the *P. aeruginosa* proteins. Purple colour indicates DHDPS activity. (I) *E. coli* DHDPS-positive control; (II) *E. coli* DHDPS-negative control; (III) *P. aeruginosa* *dapA1* gene product; (IV) *P. aeruginosa* *dapA2* gene product; (V) *P. aeruginosa* *dapA3* gene product; (VI) *P. aeruginosa* *dapA4* gene product. (B) The DHDPS-DHDPR coupled assay was used to quantitatively assess DHDPS catalytic activity for the putative *dapA* gene products from *P. aeruginosa* compared to the *EcDHDPS* control (*Ec-dapA*).

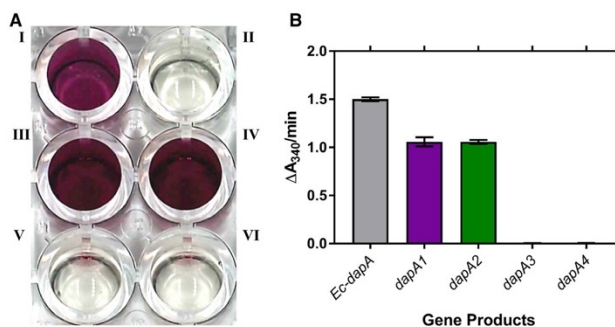
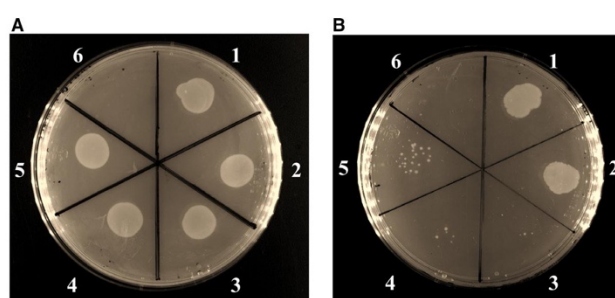


Fig. 6. Complementation assay performed with the DHDPS-deficient AT997r- *E. coli* cells plated on 50 $\mu\text{g}\cdot\text{mL}^{-1}$ kanamycin with 0.5 mM DAP (A) or without DAP (B). Each sector contains AT997r⁻¹ cells transformed with either (1) pET28a-*dapA1*, (2) pET28a-*dapA2*, (3) pET28a-*dapA3*, (4) pET28a-*dapA4* or (5) no insert. (6) represents an empty sector (no bacteria).



histidine at position 56 (*E. coli* DHDPS numbering), which has been shown to be the key molecular determinant for lysine inhibition [20], is found in PaDHDPS2 but not PaDHDPS1 (Fig. 9A). Interestingly, PaDHDPS1 has a glutamine at the equivalent position, which has not been observed in previously characterized DHDPS enzymes (Fig. 9A). Other known lysine-insensitive DHDPS enzymes, including *Legionella pneumophila* and *Coxiella burnetii* [20], contain a lysine and arginine at the equivalent position, respectively (Fig. 9A). To confirm the effect of these residues at position 56 in lysine-mediated allosteric inhibition, three mutants were generated; PaDHDPS2-H56Q, PaDHDPS2-H56K and PaDHDPS2-H56R. As predicted, mutant enzymes lacking a histidine at position 56 are insensitive to lysine even at 2 mM concentration (Fig. 9B). Moreover, to examine why the presence of these residues at position 56 result in lysine insensitivity in DHDPS enzymes, we determined the crystal structure of PaDHDPS2-H56Q to 1.9 Å resolution (PDB ID: 6P90, Fig. 10A). The data collection, processing and scaling are presented in Table 2, and refinement statistics in Table 3. An overlay with the

lysine-bound PaDHDPS2 structure (PDB ID: 3PUO) demonstrates that a glutamine at this position causes steric hindrance with a lysine ligand in the allosteric site (Fig. 10B). Furthermore, homology models of PaDHDPS2-H56K (Fig. 11A) and PaDHDPS2-H56R (Fig. 11B) generated using SWISS-MODEL predict that a lysine or arginine at this position adopts a similar conformation to glutamine, also resulting in steric clash.

Discussion

Multiple DHDPS isoforms have been commonly observed in plants [47–49], and the retention of the genes have been attributed to a beneficial increase in metabolic flux [50]. However, bacteria typically contain only a single *dapA* gene. Even when multiple *dapA* genes have been annotated in a bacterium, such as in *Agrobacterium tumefaciens*, only one *dapA* gene has been shown to have *bona fide* DHDPS activity [36]. In this study, we identified and characterized the four putative *dapA* genes encoding DHDPS proteins in *P. aeruginosa*.

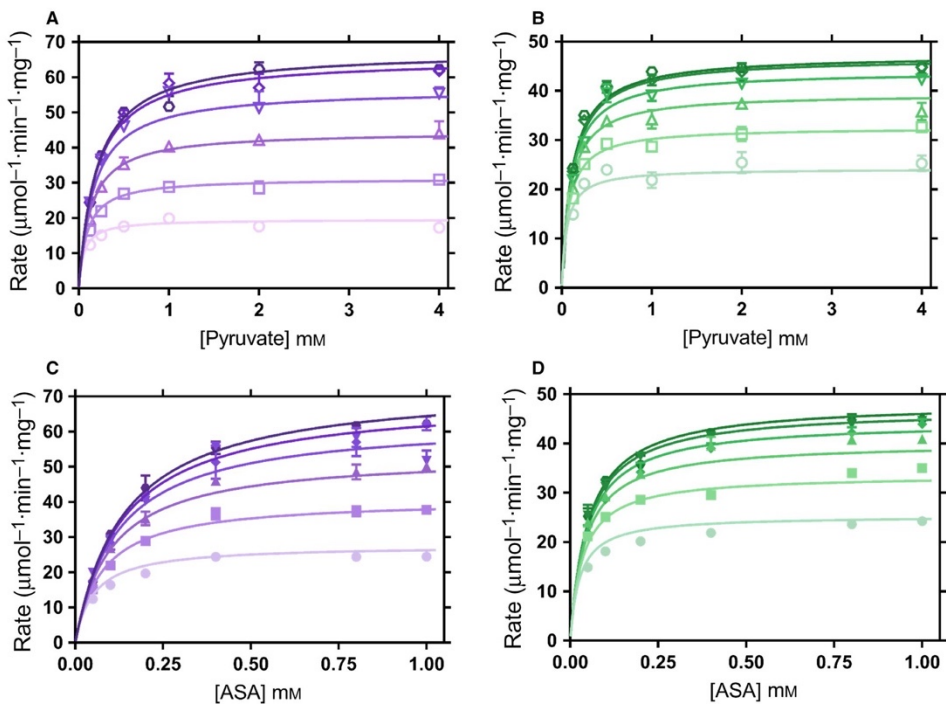


Fig. 7. Enzyme kinetic profiles of recombinant PaDHDPS1 and PaDHDPS2. The initial velocity is plotted for PaDHDPS1 (A) and PaDHDPS2 (B) at varying pyruvate concentrations of 4 mM (□), 2 mM (○), 1 mM (▽), 0.5 mM (△), 0.25 mM (◻), 0.125 mM (◊). The initial velocity is plotted for PaDHDPS1 (C) and PaDHDPS2 (D) at varying ASA concentrations of 1.0 mM (□), 0.8 mM (▼), 0.4 mM (◆), 0.2 mM (▲), 0.1 mM (■) and 0.05 mM (●). The global nonlinear best-fit using the *ENZIFTER* software v2.0.18 (Biosoft) were fitted to a bisubstrate ping-pong model without substrate inhibition and resulted in R^2 values of 0.98 and 0.97 for PaDHDPS1 and PaDHDPS2, respectively. Data are represented as mean \pm standard deviation ($n = 3$).

Table 1. Kinetic parameters for PaDHDPS1 and PaDHDPS2 obtained in this study compared to parameters obtained for PaDHDPS2 in Kaur *et al.* [28]. Data are shown as mean \pm standard deviation ($n = 3$).

| Kinetic parameter | PaDHDPS1 | PaDHDPS2 | PaDHDPS2 ^a |
|---|-------------------|-------------------|-----------------------|
| K_M Pyruvate (μ M) | 230 (\pm 15) | 120 (\pm 8.0) | 900 (\pm 13) |
| K_M ASA (μ M) | 150 (\pm 9.0) | 53 (\pm 3.0) | 170 (\pm 20) |
| k_{cat} (s^{-1}) | 44 (\pm 1.0) | 29 (\pm 0.50) | NR |
| k_{cat}/K_M Pyruvate ($s^{-1}\cdot M^{-1}$) | 1.9×10^5 | 2.4×10^5 | NR |
| k_{cat}/K_M ASA ($s^{-1}\cdot M^{-1}$) | 2.9×10^5 | 5.5×10^5 | NR |

^aData obtained from [24], NR = not reported.

Alignments of multiple *P. aeruginosa* strains demonstrate that *dapA2*, *dapA3* and *dapA4* are universally present, whereas *dapA1* is annotated in only 47% of

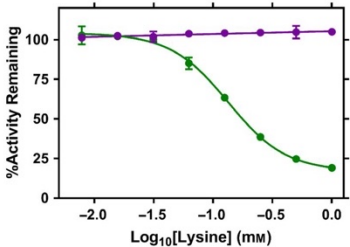


Fig. 8. Inhibition curves of DHDPS enzymes in the presence of lysine. Activity remains constant for PaDHDPS1 (purple) in the presence of increasing lysine concentrations. This is in contrast to PaDHDPS2 (green), which displays an IC_{50} of 130 μ M. Data are represented as mean and \pm standard deviation ($n = 3$).

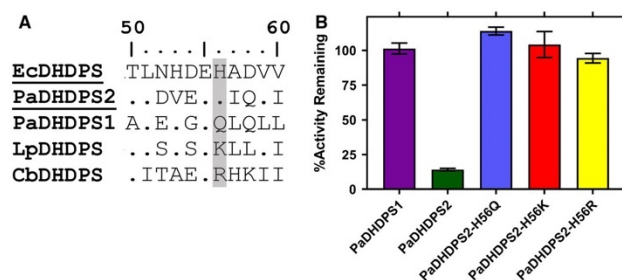


Fig. 9. (A) Multiple sequence alignment of allosteric site residues in PaDHDPS1 (UNIPROT ID: A0A3G5V4H5), PaDHDPS2 (UNIPROT ID: Q9I4W3), EcDHDPS (UNIPROT ID: P0A6L2), *Legionella pneumophila* (Lp) DHDPS (UNIPROT ID: Q5ZT5A) and *Coxiella burnetii* (Cb) DHDPS (UNIPROT ID: Q83CA6), with enzymes known to be inhibited by lysine underlined. The residue at position 56 (*E. coli* numbering) is highlighted by the grey box. Sequence alignment was performed using the CLUSTALW algorithm incorporated in BIOEDIT (v7.2.0). (B) Plot of activity remaining for PaDHDPS1 (purple), PaDHDPS2 (green), PaDHDPS2-H56Q (blue), PaDHDPS2-H56K (red) and PaDHDPS2-H56R (yellow) in the presence of 2 mM lysine. Data are represented as mean \pm standard deviation ($n = 3$).

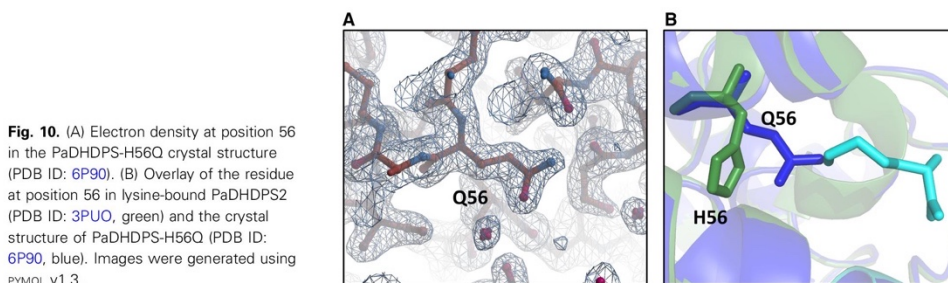


Fig. 10. (A) Electron density at position 56 in the PaDHDPS-H56Q crystal structure (PDB ID: 6P90). (B) Overlay of the residue at position 56 in lysine-bound PaDHDPS2 (PDB ID: 3PUO, green) and the crystal structure of PaDHDPS-H56Q (PDB ID: 6P90, blue). Images were generated using PYMOL v1.3.

strains. Moreover, the fragment containing the *dapA2* gene appears in isolates from high-risk international clones. However, the significance of this additional copy of the gene in these epidemic strains is unknown. Employing DHDPS catalytic activity and complementation assays, it was revealed that only *dapA1* and *dapA2* encode functional DHDPS enzymes. These enzymes have similar catalytic efficiencies, which are consistent with other DHDPS orthologues [16,36,51,52]. Thus, *P. aeruginosa* is the first reported bacterium to have two functional DHDPS enzymes.

Interestingly, PaDHDPS1 was shown in this study to be insensitive to allosteric regulation, whilst PaDHDPS2 displays mid-micromolar inhibition by lysine. Mutagenesis experiments confirmed that the differential regulation can be attributed to a single residue at position 56 (*E. coli* DHDPS numbering), which has been shown to be critical for allosteric inhibition [20]. Specifically, mutation of histidine 56 to a glutamine in PaDHDPS2, the equivalent residue in PaDHDPS1, results in the abolishment of lysine

inhibition. The presence of a glutamine at this position has never been reported in other bacterial or plant DHDPS enzymes, and the crystal structure of PaDHDPS2-H56Q demonstrates that steric hindrance prevents lysine binding into the allosteric cleft. Furthermore, mutation of histidine 56 in PaDHDPS2 to a lysine or arginine, which are residues found in other lysine-insensitive DHDPS orthologues, also abolish lysine inhibition. These findings not only further support the current dogma regarding the importance of position 56 as an allosteric determinant in bacterial DHDPS enzymes [20] but also expand it by adding glutamine to the list of residues that prevent allosteric inhibition. The allosteric site of DHDPS enzymes has recently been targeted for the development of new antibacterial agents with the discovery of a bis-lysine compound that inhibits *Campylobacter jejuni* DHDPS *in vitro* [53]. The presence of DHDPS enzymes that are not inhibited by lysine, such as PaDHDPS1, indicates that this approach cannot be employed to develop broad-spectrum bacterial DHDPS inhibitors.

Table 2. Data collection and processing statistics for PaDHDPS2-H56Q.

| | |
|--|-----------------------------|
| Diffraction source | MX2, Australian Synchrotron |
| Wavelength (Å) | 0.953654 |
| Temperature (K) | 100 |
| Detector | EIGER-16M |
| Crystal-to-detector distance (mm) | 150 |
| Total rotation range (°) | 180 |
| Space group | P2 ₁ |
| <i>a</i> , <i>b</i> , <i>c</i> (Å) | 43.2, 123.3, 57.4 |
| α , β , γ (°) | 90.0, 107.6, 90.0 |
| Mosaicity (°) | 0.23 |
| Resolution range (Å) | 20–1.9 (1.94–1.90) |
| Total no. of reflections | 282 620 (18 555) |
| No. of unique reflections | 44 202 (2979) |
| Completeness (%) | 98.8 (98.5) |
| Multiplicity | 6.4 (6.2) |
| $\langle I/\sigma(I) \rangle$ | 8.9 (2.6) |
| CC _{1/2} | 0.994 (0.913) |
| <i>R</i> _{merge} | 0.121 (0.448) |
| Overall <i>B</i> factor from Wilson plot (Å ²) | 31.0 |

Table 3. Refinement statistics for PaDHDPS2-H56Q.

| | |
|--|--------|
| Resolution range (Å) | 20–1.9 |
| No. of reflections, working set | 43 257 |
| No. of reflections, test set | 945 |
| Final <i>R</i> _{cryst} | 0.186 |
| Final <i>R</i> _{free} | 0.219 |
| No. of non-H atoms | |
| Protein | 4408 |
| Glycerol | 12 |
| Chloride | 2 |
| Water | 302 |
| Total | 4726 |
| R.m.s. deviations | |
| Bonds (Å) | 0.009 |
| Angles (°) | 1.644 |
| Average <i>B</i> factors (Å ²) | |
| Protein | 31.084 |
| Glycerol | 41.557 |
| Chloride | 40.440 |
| Water | 35.396 |
| Ramachandran plot | |
| Most favoured (%) | 98.0 |
| Allowed (%) | 2.0 |
| PDB code | 6P90 |

Importantly, we speculate that the presence of two differentially regulated DHDPS enzymes in *P. aeruginosa* allows a means to control the flux of pyruvate and ASA into the DAP pathway as observed in plants [48,49,54]. Pyruvate and ASA are used in multiple other biosynthetic pathways, including alanine and lactate synthesis [55–57], as well as threonine, isoleucine

and methionine synthesis [58–60]. Limiting ASA and pyruvate entry into the DAP pathway ensures substrate availability for other pathways. This principle is supported by previous studies showing that single *dapA* gene knockouts of the diploid plant, *Arabidopsis thaliana*, result in increased levels of both aspartate- and pyruvate-derived amino acids [48,49,54]. Allosteric regulation is also hypothesized to affect the metabolic flux of other biosynthetic pathways in *P. aeruginosa* that have multiple genes encoding for each enzyme, including the shikimate pathway responsible for the synthesis of aromatic amino acids [61]. The fitness advantages associated with having two differentially regulated DHDPS enzymes in this important pathogen remains to be elucidated.

Methods

Sequence analysis

Sequence alignments were performed using the CLUSTALW algorithm [62] incorporated in BIOEDIT (v7.2.0). Protein sequences were obtained from UniProt for *E. coli* DHDPS (UNIPROT ID: P0A6L2), *L. pneumophila* DHDPS (UNIPROT ID: Q5ZT5A) and *C. burnetii* DHDPS (UNIPROT ID: Q83CA6). All alignments used *E. coli* residue numbering. Putative annotated *dapA* genes were identified in the genome for PAO1 (*dapA1*, 3 and 4) with an additional *dapA* gene (*dapA2*) identified in the annotation of strain LESB58. The distribution of the genes was assessed using BLASTN searches of the complete *Pseudomonas* species genomes available on the *Pseudomonas* Genome Database (<https://www.pseudomonas.com/search/sequences>; DB version 18.1; searched 7 June 2019). The genome context was explored by aligning the sequences of LESB58 flanking the *dapA2* gene with PAO1 as a reference and with other genomes, using MEGALIGN (DNASTAR Lasergene v14).

Protein expression and purification

Recombinant proteins were expressed in *E. coli* BL21 (DE3) cells as hexa-histidine-tagged constructs and purified using immobilized metal affinity chromatography (IMAC) as previously described [16,63,64]. In brief, the synthetic genes coding for the *P. aeruginosa* proteins and the PaDHDPS2 mutants H56Q and H56K were purchased from Bioneer (Bioneer Pacific, Kew East, Vic., Australia) ligated in the pET28a expression vector. The PaDHDPS2-H56R mutant was generated using QuikChange mutagenesis (Stratagene, La Jolla, CA, USA) as per manufacturer's protocol. Primers are listed in Table 4. Recombinant proteins were produced in *E. coli* BL21 (DE3) cells upon treatment with 0.5 mM isopropyl β-D-1-thiogalactopyranoside (IPTG) in Luria–Bertani (LB) broth at 16 °C for 18 h for the *P. aeruginosa* proteins or 37 °C for 4 h for the

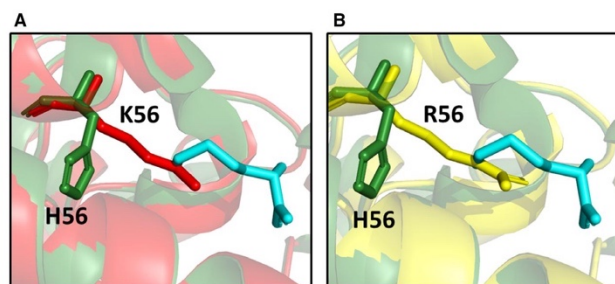


Fig. 11. Overlay of the residue at position 56 in lysine-bound PaDHDPS2 (PDB ID: 3PUO, green) and the homology models for (A) PaDHDPS2-H56K (red) and (B) PaDHDPS2-H56R (yellow). Images were generated using PYMOL v1.3.

E. coli proteins. Cells were harvested by centrifugation at 5000 *g* at 4 °C and sonicated in 20 mM Tris, 150 mM NaCl, 20 mM imidazole, pH 8.0 using a Vibra Cell VC40 (Sonics & Materials, Newtown, CT, USA). Recombinant His-tagged proteins were purified using a 5 mL IMAC column (GE Healthcare, Silverwater, NSW, Australia) and stored in 20 mM Tris, 150 mM NaCl, 1 mM EDTA, pH 8.0 or 20 mM Tris, 150 mM NaCl, pH 8.0 for EcDHDPS and EcDHDPR.

Circular dichroism (CD) spectroscopy

Circular dichroism spectroscopy was performed using 1-mm quartz cuvettes in the Aviv Model 420 CD spectrometer as previously described [20,35,42]. Protein samples were prepared in 20 mM NaH₂PO₄, 50 mM KF, pH 8.0 at 150–200 µg·mL⁻¹. Wavelength scans were conducted between 190 and 260 nm in 1-nm increments with 4 s averaging time at a temperature of 20 °C. Data were fitted using the CDPro software employing the CONTINLL algorithm and SP22X database [65,66].

RT-PCR

Pseudomonas aeruginosa strains PAO1 and 372261 were grown in LB broth to an optical density at 600 nm (OD₆₀₀) of 0.5 before harvesting via centrifugation at 3000 *g* for 10 min followed by lysis using sonication. RNA was isolated using the PureLink RNA Mini Kit (Thermo Fisher Scientific Australia, Scoresby, Vic., Australia) as per manufacturer's protocol. An iScript reverse transcription supermix was used to create a cDNA library using 500 ng of RNA per reaction. PCR was then performed using a Thermo Fisher Scientific PCR master mix following the

Table 4. Mutagenesis primers employed to generate PaDHDPS2-H56R.

| Primer sequence (5'-3') | |
|-------------------------|-------------------------------------|
| Forward | GTTAGATGTTGAAGAACGTATTCAGGTTATACGCC |
| Reverse | GGCGTATAACCTGAATACGTTCTTCAACATCTAAC |

manufacturer's protocol. Briefly, each reaction contained ~120 ng cDNA template and 0.4 µM primer DNA. Primers were designed to amplify specific 100 bp regions in each *dapA* gene. Primers are listed in Table 5. PCR conditions involved 35 cycles of the following: 95 °C for 5 min, 95 °C for 15 s, 58 °C for 20 s, 72 °C for 90 s and a final extension step of 72 °C for 5 min. PCR products were run on a 1% (w/v) agarose gel for 45 min at 90 V using GelGreen nucleic acid stain (Biotium, Hayward, CA, USA).

o-aminobenzaldehyde assay

The colourimetric *o*-aminobenzaldehyde (*o*-ABA) assay was used to qualitatively assess DHDPS activity [20,40]. Assays were performed in 96-well plates with the addition of 100 µL of mastermix containing 200 mM Tris pH 6.8, 30 mM pyruvate, 10 mM *o*-ABA and 5 mM ASA and reactions initiated with 5 µL of 0.5 mg·mL⁻¹ of protein sample. Reactions were incubated for 30 min at 37 °C before they were terminated with 10 µL of 10% (v/v) trichloroacetic acid. Recombinant *E. coli* DHDPS was used as a positive control and *E. coli* DHDPR as a negative control. DHDPS enzyme activity was confirmed by observation of a purple chromophore, whilst absence of colour indicated no DHDPS activity.

Table 5. Primers used for RT-PCR experiments.

| Primer target | Primer sequence (5'-3') |
|---------------|-------------------------|
| <i>dapA1</i> | |
| Forward | TACTACATCCGCCCTCC |
| Reverse | CACCGGTGCGATAGGGAATG |
| <i>dapA2</i> | |
| Forward | CGATCCCGCAGATCCTCTAC |
| Reverse | ATGATGTTCCGCACCTTGGA |
| <i>dapA3</i> | |
| Forward | TGCCGGTGATGGTCTACAAC |
| Reverse | AAGCAGACGATGTTCTCGCA |
| <i>dapA4</i> | |
| Forward | CCCGGGTGTGTAGAGCAT |
| Reverse | GCCGATCTCTACTGGAAGC |

Enzyme kinetics

Dihydrodipicolinate synthase enzyme activity was quantified using the DHDPS-DHDPR coupled assay [37,38,41] that measures substrate turnover spectrophotometrically at Abs_{340 nm} ($\epsilon_{340 \text{ nm}} = 6220 \text{ M}^{-1}\text{cm}^{-1}$) via the associated oxidation of NADPH as previously reported. Assays were performed in triplicate ($n = 3$) at 37 °C in a temperature-controlled Cary 4000 UV/Vis spectrophotometer (Varian, Mulgrave, Vic., Australia). All reactions were incubated at 37 °C for 12 min before initiating the reaction by the addition of ASA.

Preliminary DHDPS enzyme activity determination of the *dapA1-4* gene products was performed using excess amounts of pyruvate (4 mM) and ASA (1.25 mM) with a final protein concentration of 6.5 and 4.1 $\mu\text{g}\cdot\text{mL}^{-1}$ for EcDHDPS as previously reported [39]. For the determination of the Michaelis–Menten constant (K_M) determination, pyruvate and ASA were varied simultaneously ranging from 0.125 to 4 mM and 0.05 to 1 mM respectively. PaDHDPS1 and PaDHDPS2 were used at a final concentration of 5 $\mu\text{g}\cdot\text{mL}^{-1}$. Initial velocity data were analysed using ENZFITTER (Biosoft, Cambridge, UK) and fitted to the ping-pong mechanism using Eqn 1.

$$v = (V_{\max} * A * B) / (K_{M,A} * B + K_{M,B} * A + A * B) \quad (1)$$

here v = initial velocity, V_{\max} = limiting maximal velocity, A = [pyruvate], B = [ASA], $K_{M,A}$ = limiting Michaelis–Menten constant for A, $K_{M,B}$ = limiting Michaelis–Menten constant for B.

Lysine inhibition was measured by titrating concentrations of lysine ranging from 0.078 to 2 mM against PaDHDPS1, PaDHDPS2, PaDHDPS2-H56Q, PaDHDPS2-H56K and PaDHDPS2-H56R. Initial velocity data for PaDHDPS2 were analysed using GRAPHPAD PRISM and fitted to the log(inhibitor) vs response (variable slope) using Eqn 2, while PaDHDPS1 data were fitted using linear regression. Data were plotted using GRAPHPAD PRISM version 7.03 (GraphPad Software, La Jolla, CA, USA).

$$Y = \text{Bottom} + (\text{Top} - \text{Bottom}) / (1 + 10^{((\text{Log}(IC_{50} - X) * \text{HillSlope}))}) \quad (2)$$

where X = log of lysine concentration, Y = response, Top and Bottom = Plateaus in same units as Y , Hill slope = slope factor.

Complementation assay

The pET28a vector containing each of the four *dapA* genes and an empty vector were transformed into the *E. coli* *dapA* knockout strain AT997r[−] [43–45,51] for the complementation assay as previously described [35]. The transformed cells were grown at 37 °C in LB supplemented with 0.5 mM DAP and 50 $\text{mg}\cdot\text{mL}^{-1}$ kanamycin until an OD₆₀₀

of 0.6 was attained. At this point, the cells were harvested by centrifugation (3000 g , 10 min, 4 °C) before resuspension in either LB with 0.5 mM DAP or 0.5 mM IPTG to induce protein expression. After incubation at 37 °C for 15 min, 20 μL of the culture was plated onto LB agar containing 50 $\text{mg}\cdot\text{mL}^{-1}$ kanamycin with or without 0.5 mM DAP before overnight incubation.

X-ray crystallography

PaDHDPS2-H56Q was crystallized using the hanging-drop vapour diffusion method in Hampton 24-well crystallization plates. Diffraction-quality crystals of PaDHDPS2-H56Q grew after 7 days in drops consisting of equal volumes (1 μL) of PaDHDPS2-H56Q (12 $\text{mg}\cdot\text{mL}^{-1}$ in 20 mM Tris, 150 mM NaCl, 1 mM EDTA, pH 8.0) and reservoir (100 mM Tris pH 8.5, 200 mM MgCl_2 , PEG 8000) solutions equilibrated against 500 μL of reservoir solution. Crystals were soaked in reservoir solution containing 20% (v/v) glycerol prior to data collection. X-ray diffraction experiments were performed at the microfocus beamline (MX2) of the Australian Synchrotron [67]. The crystals were then flash-cooled in liquid nitrogen and transferred to a stream of nitrogen gas at 100 K. X-ray data were collected at a wavelength of 0.9537 Å at 100 K using an EIGER-16M detector with 0.1° oscillation and 0.1-s exposure of 0% attenuated beam per frame. The data were indexed and integrated with XDS [68] and scaled using AIMLESS [69]. Data collection and processing statistics are detailed in Table 2. The crystal belongs to space group P2₁. Molecular replacement was performed using the MR phasing protocol of the AUTO-RICKSHAW software [70,71] with wild-type PaDHDPS2 employed as the search model (PDB ID: 3QZE). The resulting model from AUTO-RICKSHAW was refined using REFMAC5 [72] and manual building was carried out in Coot [73]. The quality of the structure was determined by MolProbity [74]. The refinement statistics are summarized in Table 3. Images were generated using PYMOL version 1.3 (Schrödinger, San Diego, CA, USA).

Homology modelling

Homology models of PaDHDPS2-H56K and PaDHDPS2-H56R were generated using SWISS-MODEL [75–77] employing the highest resolution PaDHDPS2 structure (PDB ID: 3QZE) as a template. The lowest energy rotamer for the residue at position 56 is shown aligned to the lysine-bound PaDHDPS2 structure (PDB ID: 3PUO) using PYMOL version 1.3.

Acknowledgements

We thank Prof Juliet Gerrard (The University of Auckland) for providing the *dapA* and *dapB* plasmids from *E. coli*. TPSC acknowledges the National Health

and Medical Research Council of Australia (APP1091976) and Australian Research Council (DE190100806) for fellowship support, and MAP the Australian Research Council for funding support (DP150103313). REI is supported by an Australian Research Training scholarship and acknowledges the British Society for Antimicrobial Chemotherapy for funding support. We acknowledge the use of the MX2 beamline at the Australian Synchrotron and the CSIRO Collaborative Crystallisation Centre (www.csiro/C3; Melbourne, Australia). We also thank the La Trobe University Comprehensive Proteomics Platform for providing infrastructure support.

Conflicts of interest

The authors declare no conflict of interest.

Author contributions

TPSC, MAP, REI, LJB and JMS planned the experiments; REI, SP and CJH performed the experiments; TPSC, MAP, REI, SP and LJB analysed the data; TPSC, MAP, JMS and REI wrote the paper.

References

- Emerson J, Rosenfeld M, McNamara S, Ramsey B & Gibson RL (2002) *Pseudomonas aeruginosa* and other predictors of mortality and morbidity in young children with cystic fibrosis. *Pediatr Pulmonol* **34**, 91–100.
- Eshabbanati HK, Kashani PP & Ghanaatpisheh F (2002) Frequency of *Pseudomonas aeruginosa* serotypes in burn wound infections and their resistance to antibiotics. *Burns* **28**, 340–348.
- Mittal R, Aggarwal S, Sharma S, Chhibber S & Harjai K (2009) Urinary tract infections caused by *Pseudomonas aeruginosa*: a minireview. *J Infect Public Health* **2**, 101–111.
- Buhl M, Peter S & Willmann M (2015) Prevalence and risk factors associated with colonization and infection of extensively drug-resistant *Pseudomonas aeruginosa*: a systematic review. *Expert Rev Anti Infect Ther* **13**, 1159–1170.
- Palavutitotai N, Jitmuang A, Tongsa S, Kiratisin P & Angkasekwinai N (2018) Epidemiology and risk factors of extensively drug-resistant *Pseudomonas aeruginosa* infections. *PLoS ONE* **13**, e0193431.
- Livermore DM (2002) Multiple mechanisms of antimicrobial resistance in *Pseudomonas aeruginosa*: our worst nightmare? *Clin Infect Dis* **34**, 634–640.
- Poole K (2007) Efflux pumps as antimicrobial resistance mechanisms. *Ann Med* **39**, 162–176.
- Hutton CA, Perugini MA & Gerrard JA (2007) Inhibition of lysine biosynthesis: an evolving antibiotic strategy. *Mol Biosyst* **3**, 458–465.
- Soares da Costa TP, Abbott BM, Gendall AR, Panjikar S & Perugini MA (2017) Molecular evolution of an oligomeric biocatalyst functioning in lysine biosynthesis. *Biophys Rev* **4**, 153–162.
- Hermann M, Thevenet NJ, Coudert-Maratier MM & Vandecasteele J-P (1972) Consequences of lysine oversynthesis in *Pseudomonas* mutants insensitive to feedback inhibition. *Eur J Biochem* **30**, 100–106.
- Impey RE & Soares da Costa TP (2018) Review: Targeting the biosynthesis and incorporation of amino acids into peptidoglycan as an antibiotic approach against Gram negative bacteria. *EC Microbiol* **14**, 200–209.
- Dogovski C, Atkinson SC, Dommaraju SR, Downton M, Hor L, Moore S, Paxman JJ, Peverelli MG, Qiu TW, Reumann M *et al.* (2012) Enzymology of bacterial lysine biosynthesis. In *Biochemistry* (Ekinici D, ed.), pp. 225–262. InTech Open Access Publisher, London, UK.
- Dogovski C, Atkinson SC, Dommaraju SR, Hor L, Dobson RCJ, Hutton CA, Gerrard JA & Perugini MA (2009) Lysine biosynthesis in bacteria: an uncharted pathway for novel antibiotic design. *Encyclopedia of Life Support Systems* (Doelle H, ed.), pp. 116–136. EOLSS Publishers, Paris, France.
- Gupta R, Soares da Costa TP, Faou P, Dogovski C & Perugini MA (2018) Comparison of untagged and his-tagged dihydrodipicolinate synthase from the enteric pathogen *Vibrio cholerae*. *Protein Expr Purif* **145**, 85–93.
- Devenish SRA, Blunt JW & Gerrard JA (2010) NMR studies uncover alternate substrates for dihydrodipicolinate synthase and suggest that dihydrodipicolinate reductase is also a dehydratase. *J Med Chem* **53**, 4808–4812.
- Christensen JB, Soares da Costa TP, Faou P, Pearce FG, Panjikar S & Perugini MA (2016) Structure and function of cyanobacterial DHDPS and DHDPR. *Sci Rep* **6**, 37111.
- Vollmer W & Seligman SJ (2010) Architecture of peptidoglycan: more data and more models. *Trends Microbiol* **18**, 59–66.
- Royet J & Dziarski R (2007) Peptidoglycan recognition proteins: pleiotropic sensors and effectors of antimicrobial defences. *Nat Rev Microbiol* **5**, 264–277.
- Peverelli MG, da Costa TPS, Kirby N & Perugini MA (2016) Dimerization of bacterial diaminopimelate decarboxylase is essential for catalysis. *J Biol Chem* **291**, 9785–9795.
- Soares da Costa TP, Desbois S, Dogovski C, Gorman MA, Ketaren NE, Paxman JJ, Siddiqui T, Zammit LM, Abbott BM, Robins-Browne RM *et al.* (2016) Structural determinants defining the allosteric inhibition

- of an essential antibiotic target. *Structure* **24**, 1282–1291.
- 21 Dobson RCJ, Griffin MDW, Jameson GB & Gerrard JA (2005) The crystal structures of native and (S)-lysine-bound dihydrodipicolinate synthase from *Escherichia coli* with improved resolution show new features of biological significance. *Acta Crystallogr* **61**, 1116–1124.
 - 22 Karsten WE (1997) Dihydrodipicolinate synthase from *Escherichia coli*: pH dependent changes in the kinetic mechanism and kinetic mechanism of allosteric inhibition by L-lysine. *Biochemistry* **36**, 1730–1739.
 - 23 Becker D, Selbach M, Rollenhagen C, Ballmaier M, Meyer TF, Mann M & Bumann D (2006) Robust Salmonella metabolism limits possibilities for new antimicrobials. *Nature* **440**, 303–307.
 - 24 Kobayashi K, Ehrlich SD, Albertini A, Amati G, Andersen KK, Arnaud M, Asai K, Ashikaga S, Aymerich S, Bessieres P *et al.* (2003) Essential *Bacillus subtilis* genes. *Proc Natl Acad Sci* **100**, 4678–4683.
 - 25 Gerdes SY, Scholle MD, Campbell JW, Balázs G, Ravasz E, Daugherty MD, Somera AL, Kyrpides NC, Anderson I, Gelfand MS *et al.* (2003) Experimental determination and system level analysis of essential genes in *Escherichia coli* MG1655. *J Bacteriol* **185**, 5673–5684.
 - 26 Dogovski C, Gorman MA, Ketaren NE, Praszkie J, Zammit LM, Mertens HD, Bryant G, Yang J, Griffin MDW, Pearce FG *et al.* (2013) From knock-out phenotype to three-dimensional structure of a promising antibiotic target from *Streptococcus pneumoniae*. *PLoS ONE* **8**, e83419.
 - 27 Schnell R, Oehlmann W, Sandalova T, Braun Y, Huck C, Maringer M, Singh M & Schneider G (2012) Tetrahydrodipicolinate N- and dihydrodipicolinate synthase from *Pseudomonas aeruginosa*: structure analysis and gene deletion. *PLoS ONE* **7**, e31133.
 - 28 Kaur N, Gautam A, Kumar S, Singh A, Singh N, Sharma S, Sharma R, Tewari R & Singh TP (2011) Biochemical studies and crystal structure determination of dihydrodipicolinate synthase from *Pseudomonas aeruginosa*. *Int J Biol Macromol* **48**, 779–787.
 - 29 Watanabe S, Morimoto D, Fukumori F, Shinomiya H, Nishiwaki H, Kawano-Kawada M, Sasai Y, Tozawa Y & Watanabe Y (2012) Identification and characterization of d-hydroxyproline dehydrogenase and δ 1-pyrroline-4-hydroxy-2-carboxylate deaminase involved in novel l-hydroxyproline metabolism of bacteria. *J Biol Chem* **287**, 32674–32688.
 - 30 Winsor GL, Griffiths EJ, Lo R, Dhillon BK, Shay JA & Brinkman FSL (2016) Enhanced annotations and features for comparing thousands of *Pseudomonas* genomes in the Pseudomonas genome database. *Nucleic Acids Res* **44**, D646–D653.
 - 31 Freschi L, Bertelli C, Jeukens J, Moore MP, Kukavica-Ibrulj I, Emond-Rheault J-G, Hamel J, Fothergill JL, Tucker NP, McClean S *et al.* (2018) Genomic characterisation of an international *Pseudomonas aeruginosa* reference panel indicates that the two major groups draw upon distinct mobile gene pools. *FEMS Microbiol Lett* **365**, <https://doi.org/10.1093/femsle/fny120>
 - 32 Martin K, Baddal B, Mustafa N, Perry C, Underwood A, Constantidou C, Loman N, Kenna DT & Turton JF (2013) Clusters of genetically similar isolates of *Pseudomonas aeruginosa* from multiple hospitals in the UK. *J Med Microbiol* **62**, 988–1000.
 - 33 Jani M, Mathee K & Azad RK (2016) Identification of novel genomic islands in Liverpool epidemic strain of *Pseudomonas aeruginosa* using segmentation and clustering. *Front Microbiol* **7**, 1210.
 - 34 Mataseje LF, Peirano G, Church DL, Conly J, Mulvey M & Pitout JD (2016) Colistin-nonsusceptible *Pseudomonas aeruginosa* sequence type 654 with blandm-1 arrives in North America. *Antimicrob Agents Chemother* **60**, 1794–1800.
 - 35 Desbois S, John UP & Perugini MA (2018) Dihydrodipicolinate synthase is absent in fungi. *Biochimie* **152**, 73–84.
 - 36 Atkinson SC, Hor L, Dogovski C, Dobson RCJ & Perugini MA (2014) Identification of the *bona fide* DHDPS from a common plant pathogen. *Proteins* **82**, 1869–1883.
 - 37 Dobson RCJ, Griffin MDW, Roberts SJ & Gerrard JA (2004) Dihydrodipicolinate synthase (DHDPS) from *Escherichia coli* displays partial mixed inhibition with respect to its first substrate, pyruvate. *Biochimie* **86**, 311–315.
 - 38 Burgess BR, Dobson RCJ, Bailey MF, Atkinson SC, Griffin MDW, Jameson GB, Parker MW, Gerrard JA & Perugini MA (2008) Structure and evolution of a novel dimeric enzyme from a clinically important bacterial pathogen. *J Biol Chem* **283**, 27598–27603.
 - 39 Soares da Costa TP, Muscroft-Taylor AC, Dobson RCJ, Devenish SRA, Jameson GB & Gerrard JA (2010) How essential is the 'essential' active-site lysine in dihydrodipicolinate synthase? *Biochimie* **92**, 837–845.
 - 40 Yugari Y & Gilvarg C (1965) The condensation step in diaminopimelate synthesis. *J Biol Chem* **240**, 4710–4716.
 - 41 Coulter CV, Gerrard JA, Kraunsoe JAE & Pratt AJ (1999) *Escherichia coli* dihydrodipicolinate synthase and dihydrodipicolinate reductase: kinetic and inhibition studies of two putative herbicide targets. *J Pest Sci* **55**, 887–895.
 - 42 Voss JE, Scally SW, Taylor NL, Atkinson SC, Griffin MDW, Hutton CA, Parker MW, Alderton MR, Gerrard JA, Dobson RCJ *et al.* (2010) Substrate-mediated stabilization of a tetrameric drug target

- reveals Achilles heel in anthrax. *J Biol Chem* **285**, 5188–5195.
- 43 Bukhari AI & Taylor AL (1971) Genetic analysis of diaminopimelic acid- and lysine-requiring mutants of *Escherichia coli*. *J Bacteriol* **105**, 844–854.
 - 44 García-Rodríguez FM, Zekri S & Toro N (2000) Characterization of the *Sinorhizobium meliloti* genes encoding a functional dihydrodipicolinate synthase (*dapA*) and dihydrodipicolinate reductase (*dapB*). *Arch Microbiol* **173**, 438–444.
 - 45 Yeh P, Sicard AM & Sinskey AJ (1988) General organization of the genes specifically involved in the diaminopimelate-lysine biosynthetic pathway of *Corynebacterium glutamicum*. *Mol Gen Genet* **212**, 105–111.
 - 46 Dobson RCJ, Valegård K & Gerrard JA (2004) The crystal structure of three site-directed mutants of *Escherichia coli* dihydrodipicolinate synthase: further evidence for a catalytic triad. *J Mol Biol* **338**, 329–339.
 - 47 Griffin MDW, Billakanti JM, Wason A, Keller S, Mertens HDT, Atkinson SC, Dobson RCJ, Perugini MA, Gerrard JA & Pearce FG (2012) Characterisation of the first enzymes committed to lysine biosynthesis in *Arabidopsis thaliana*. *PLoS ONE* **7**, e40318.
 - 48 Jones-Held S, Ambrozecius LP, Campbell M, Drumheller B, Harrington E & Leustek T (2012) Two *Arabidopsis thaliana* dihydrodipicolinate synthases, DHDPS1 and DHDPS2, are unequally redundant. *Funct Plant Biol* **39**, 1058–1067.
 - 49 Craciun A, Jacobs M & Vauterin M (2000) *Arabidopsis* loss-of-function mutant in the lysine pathway points out complex regulation mechanisms. *FEBS Lett* **487**, 234–238.
 - 50 Panchy N, Lehti-Shiu M & Shiu S-H (2016) Evolution of gene duplication in plants. *Plant Physiol* **171**, 2294–2316.
 - 51 Girish TS, Sharma E & Gopal B (2008) Structural and functional characterization of *Staphylococcus aureus* dihydrodipicolinate synthase. *FEBS Lett* **582**, 2923–2930.
 - 52 Devenish SRA, Huisman FHA, Parker EJ, Hadfield AT & Gerrard JA (2009) Cloning and characterisation of dihydrodipicolinate synthase from the pathogen *Neisseria meningitidis*. *Biochim Biophys Acta* **1794**, 1168–1174.
 - 53 Skovpen YV, Conly CJT, Sanders DAR & Palmer DRJ (2016) Biomimetic design results in a potent allosteric inhibitor of dihydrodipicolinate synthase from *Campylobacter jejuni*. *J Am Chem Soc* **138**, 2014–2020.
 - 54 Sarrobert C, Thibaud M-C, Contard David P, Gineste S, Bechtold N, Robaglia C & Nussaume L (2000) Identification of an *Arabidopsis thaliana* mutant accumulating threonine resulting from mutation in a new dihydrodipicolinate synthase gene. *Plant J* **24**, 357–368.
 - 55 Hutcherson JA, Sinclair KM, Belvin BR, Gui Q, Hoffman PS & Lewis JP (2017) Amixicile, a novel strategy for targeting oral anaerobic pathogens. *Sci Rep* **7**, 10474.
 - 56 Liu SQ (2003) Practical implications of lactate and pyruvate metabolism by lactic acid bacteria in food and beverage fermentations. *Int J Food Microbiol* **83**, 115–131.
 - 57 Fowler EB & Werkman CH (1952) Bacterial synthesis of alanine and glutamate. *Arch Biochem Biophys* **41**, 42–47.
 - 58 Clepet C, Borne F, Krishnapillai V, Baird C, Patte JC & Cami B (1992) Isolation, organization and expression of the *Pseudomonas aeruginosa* threonine genes. *Mol Micro* **6**, 3109–3119.
 - 59 Oogai Y, Yamaguchi M, Kawada-Matsuo M, Sumitomo T, Kawabata S & Komatsuzawa H (2016) Lysine and threonine biosynthesis from aspartate contributes to *Staphylococcus aureus* growth in calf serum. *Appl Environ Microbiol* **82**, 6150–6157.
 - 60 Malumbres M & Martin JF (1996) Molecular control mechanisms of lysine and threonine biosynthesis in amino acid-producing corynebacteria: redirecting carbon flow. *FEMS Microbiol Lett* **143**, 103–114.
 - 61 Sterritt OW, Kessans SA, Jameson GB & Parker EJ (2018) A pseudoisostuctural type II DAH7PS enzyme from *Pseudomonas aeruginosa*: alternative evolutionary strategies to control shikimate pathway flux. *Biochemistry* **57**, 2667–2678.
 - 62 Thompson JD, Higgins DG & Gibson TJ (1994) CLUSTAL W: improving the sensitivity of progressive multiple sequence alignment through sequence weighting, position-specific gap penalties and weight matrix choice. *Nucleic Acids Res* **22**, 4673–4680.
 - 63 Atkinson SC, Dogovski C, Dobson RCJ & Perugini MA (2012) Cloning, expression, purification and crystallization of dihydrodipicolinate synthase from *Agrobacterium tumefaciens*. *Acta Crystallogr F* **68**, 1040–1047.
 - 64 Wubben JM, Dogovski C, Dobson RCJ, Codd R, Gerrard JA, Parker MW & Perugini MA (2010) Cloning, expression, purification and crystallization of dihydrodipicolinate synthase from the psychrophile *Shewanella benthica*. *Acta Crystallogr F* **66**, 1511–1516.
 - 65 Sreerama N & Woody RW (2000) Estimation of protein secondary structure from circular dichroism spectra: comparison of CONTIN, SELCON, and CDSSTR methods with an expanded reference set. *Anal Biochem* **287**, 252–260.
 - 66 Johnson WC (1999) Analyzing protein circular dichroism spectra for accurate secondary structures. *Proteins* **35**, 307–312.
 - 67 Aragão D, Aishima J, Cherukuvada H, Clarken R, Clift M, Cowieson NP, Ericsson DJ, Gee CL, Macedo S, Mudie N *et al.* (2018) MX2: a high-flux undulator

- microfocus beamline serving both the chemical and macromolecular crystallography communities at the Australian Synchrotron. *J Synchrotron Radiat* **25**, 885–891.
- 68 Kabsch W (2010) XDS. *Acta Crystallogr D* **66**, 125–132.
- 69 Evans PR & Murshudov GN (2013) How good are my data and what is the resolution? *Acta Crystallogr D Biol Crystallogr* **69**, 1204–1214.
- 70 Panjikar S, Parthasarathy V, Lamzin VS, Weiss MS & Tucker PA (2005) Auto-Rickshaw: an automated crystal structure determination platform as an efficient tool for the validation of an X-ray diffraction experiment. *Acta Crystallogr D* **61**, 449–457.
- 71 Panjikar S, Parthasarathy V, Lamzin VS, Weiss MS & Tucker PA (2009) On the combination of molecular replacement and single-wavelength anomalous diffraction phasing for automated structure determination. *Acta Crystallogr D* **65**, 1089–1097.
- 72 Murshudov GN, Skubák P, Lebedev AA, Pannu NS, Steiner RA, Nicholls RA, Winn MD, Long F & Vagin AA (2011) REFMAC5 for the refinement of macromolecular crystal structures. *Acta Crystallogr D* **67**, 355–367.
- 73 Emsley P, Lohkamp B, Scott WG & Cowtan K (2010) Features and development of Coot. *Acta Crystallogr D* **66**, 486–501.
- 74 Chen VB, Arendall WB, Headd JJ, Keedy DA, Immormino RM, Kapral GJ, Murray LW, Richardson JS & Richardson DC (2010) MolProbity: all-atom structure validation for macromolecular crystallography. *Acta Crystallogr D* **66**, 12–21.
- 75 Waterhouse A, Bertoni M, Bienert S, Studer G, Tauriello G, Gumienny R, Heer FT, de Beer TAP, Rempfer C, Bordoli L *et al.* (2018) SWISS-MODEL: homology modelling of protein structures and complexes. *Nucleic Acids Res* **46**, W296–W303.
- 76 Bienert S, Waterhouse A, de Beer TAP, Tauriello G, Studer G, Bordoli L & Schwede T (2017) The SWISS-MODEL Repository—new features and functionality. *Nucleic Acids Res* **45**, D313–D319.
- 77 Benkert P, Biasini M & Schwede T (2011) Toward the estimation of the absolute quality of individual protein structure models. *Bioinformatics* **27**, 343–350.

3 DHDPS enzymes from *Klebsiella pneumoniae* and *Acinetobacter baumannii*

3.1 Published Article

3.1.1 Copyright

This article was published in *FEBS Letters*, Vol. 594(9), Impey, R. E., Lee, M. Hawkins, D. A., Sutton, J. M., Panjikar, S., Perugini, M. A. & Soares da Costa, T. P. “Mis-annotations of a promising antibiotic target in high-priority gram-negative pathogens”, pp 1453-1463. Copyright *FEBS Letters* 2020 (c/o John Wiley and Sons).

Copyright authorisation obtained on:


13th December 2020

3.1.2 Statement of Contribution

I confirm that Rachael Impey has made the following contributions:

- Completion of experimental work (90%), with the exception of the overexpression of recombinant KpDapA3 and KpDapA4 proteins
- Data analysis (95%), assisted by Mihwa Lee for structural refinement of the KpDHDPS enzyme
- Conceptualisation and drafting of the manuscript (60%)
- Preparation of figures
- Revisions of manuscript prior to acceptance

Tatiana Soares da Costa

Signed: 

Date: 14/12/2020

(Executive Author)

COMMUNICATION

Mis-annotations of a promising antibiotic target in high-priority gram-negative pathogens

Rachael E. Impey¹, Mihwa Lee¹, Daniel A. Hawkins¹, J. Mark Sutton² , Santosh Panjikar^{3,4}, Matthew A. Perugini¹ and Tatiana P. Soares da Costa¹ 

¹ Department of Biochemistry and Genetics, La Trobe Institute for Molecular Science, La Trobe University, Melbourne, VIC, Australia

² National Infection Service, Research and Development Institute, Public Health England, Salisbury, UK

³ Australian Synchrotron, ANSTO, Clayton, VIC, Australia

⁴ Department of Molecular Biology and Biochemistry, Monash University, Melbourne, VIC, Australia

Correspondence

T. P. Soares da Costa, Department of Biochemistry and Genetics, La Trobe University, Bundoora, VIC 3086, Australia
Tel. (+61) 3 9479 2227
E-mail: T.SoareshdaCosta@latrobe.edu.au
M. A. Perugini, Department of Biochemistry and Genetics, La Trobe University, Bundoora, VIC 3086, Australia
Tel. (+61) 3 9479 6570
E-mail: M.Perugini@latrobe.edu.au

(Received 15 November 2019, revised 17 December 2019, accepted 17 December 2019, available online 24 January 2020)

doi:10.1002/1873-3468.13733

Edited by Stuart Ferguson

The rise of antibiotic resistance combined with the lack of new products entering the market has led to bacterial infections becoming one of the biggest threats to global health. Therefore, there is an urgent need to identify novel antibiotic targets, such as dihydrodipicolinate synthase (DHDPS), an enzyme involved in the production of essential metabolites in cell wall and protein synthesis. Here, we utilised a 7-residue sequence motif to identify mis-annotation of multiple DHDPS genes in the high-priority Gram-negative bacteria *Acinetobacter baumannii* and *Klebsiella pneumoniae*. We subsequently confirmed these mis-annotations using a combination of enzyme kinetics and X-ray crystallography. Thus, this study highlights the need to ensure genes encoding promising drug targets, like DHDPS, are annotated correctly, especially for clinically important pathogens.

PDB ID
6UE0.

Keywords: 4-hydroxy-tetrahydrodipicolinate synthase; antibiotic resistance; cell wall; diaminopimelate pathway; lysine

Bacterial resistance to antibiotics is increasing, with widespread resistance no longer a threat but a reality, contributing significantly to patient morbidity and mortality [1]. Moreover, few new antibiotics are in development, with pharmaceutical companies failing to meet current clinical needs. As such, the World Health Organization (WHO) has released a priority list of bacteria that require urgent antibiotic research and development, with the top three pathogens being carbapenem-resistant *Acinetobacter baumannii*, *Pseudomonas aeruginosa*, and *Enterobacteriaceae* spp. [1]. These Gram-negative bacteria cause several nosocomial infections, particularly in

immunocompromised patients, including meningitis, pneumonia, bacteraemia, and urinary tract and wound infections [1]. The range and severity of these infections highlight the importance of identifying novel drug targets against these high-priority Gram-negative pathogens.

A promising target for new antibiotic development is the enzymes in the diaminopimelate (DAP) pathway that is responsible for the production of *meso*-DAP and *L*-lysine (lysine) (Fig. 1) [2–7]. In the majority of Gram-negative bacteria, *meso*-DAP is a constituent of the peptidoglycan chains within the cell wall, whilst

Abbreviations

ASA, (S)-aspartate semialdehyde; DAP, diaminopimelate; DAP-DC, diaminopimelate decarboxylase; DHDPR, dihydrodipicolinate reductase; DHDPS, dihydrodipicolinate synthase; HTPA, 4-hydroxy-2,3,4,5-tetrahydro-(2S)-dipicolinic acid; *L*-lysine, lysine; *o*-ABA, *o*-aminobenzaldehyde; THDP, 2,3,4,5-tetrahydrodipicolinate.

lysine is essential for protein synthesis [2–9]. Importantly, the synthesis of these metabolites *via* the DAP pathway is unique to bacteria and plants, thus minimising potential off-target effects in humans [3,4,6,7]. The first committed step of this pathway is the condensation of pyruvate and (S)-aspartate semialdehyde (ASA) to produce 4-hydroxy-2,3,4,5-tetrahydro-(2S)-dipicolinic acid (HTPA) catalysed by the class I aldolase 4-hydroxy-tetrahydrodipicolinate synthase (EC 4.3.3.7), commonly referred to as dihydrodipicolinate synthase (DHDPS) (Fig. 1) [2,10]. HTPA is subsequently reduced to 2,3,4,5-tetrahydrodipicolinate (THDP) using the NAD(P)H-dependent enzyme 4-hydroxy-tetrahydrodipicolinate reductase (EC 1.17.1.8), herein referred to as dihydrodipicolinate reductase (DHDPR) (Fig. 1) [6,11,12]. At this point, the DAP pathway diverges into one of four subpathways, with each resulting in the production of *meso*-DAP (Fig. 1) [6,7,10]. The subpathways are organism-dependent [6,7,10] with, for example, Gram-negative bacteria utilising the succinyl subpathway that yields *LL*-DAP before conversion to *meso*-DAP by DAP epimerase (EC 5.1.1.7) (Fig. 1) [4,6]. Finally, *meso*-DAP is used either directly in the crosslinking of the peptidoglycan layer in Gram-negative bacteria, or decarboxylated to lysine by DAP decarboxylase (DAP-DC, EC 4.1.1.20) (Fig. 1) [4,13,14]. The production of lysine in this final step also serves as a negative feedback loop, where lysine can bind and allosterically inhibit the DHDPS enzyme [15–17].

Given DHDPS is involved in the first committed and rate-limiting step of the DAP pathway, several studies have focused on demonstrating the essentiality of its encoding gene, *dapA*, for bacterial survival [18–22]. Typically, bacteria contain a single *dapA* gene. However, we have recently identified that *P. aeruginosa* has up to 4 annotated *dapA* genes, of which only two encode functional DHDPS enzymes [23]. Mis-annotated *dapA* genes have also been previously observed in *Agrobacterium tumefaciens*, with 9 out of the 10 annotated *dapA* genes yielding enzymes that lacked DHDPS activity [24]. Another recent study showed that fungi do not contain an active DHDPS gene despite being annotated in various sequence and structure databases [25]. Indeed, this study postulated a 7-residue motif (TTX₍₅₇₋₆₁₎YYX₍₂₂₋₂₆₎YX₍₃₋₅₎RX₍₁₈₋₂₂₎K, where X represents the length, shown by the numbers in brackets, of the undefined amino acid sequences separating the signature residues) to identify functional DHDPS sequences [25]. Without accurate and reliable similarity-based assignments, the amount of mis-annotation errors in genomes could account for up to 30% of annotated protein functions [26]. There

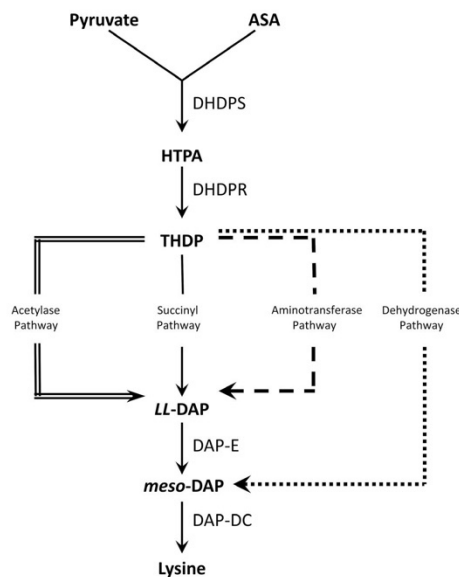


Fig. 1. DAP pathway in bacteria. The DAP pathway begins with the condensation of pyruvate and ASA by DHDPS to produce HTPA. DHDPR then converts HTPA to THDP. At this point, the pathway branches into four subpathways; the acetylase (double line), dehydrogenase (dotted line), amino transferase (dashed line), or succinyl pathway (solid line), which is commonly observed in Gram-negative bacteria. The subpathways all converge at the production of *meso*-DAP, which is irreversibly decarboxylated to lysine by DAP-DC.

is also conjecture about using descriptions of genes as ‘putative’ or ‘like’, as currently there are no defined parameters for this classification [27]. The use of these terms further enhances the potential for mis-annotations [27].

In this study, we have identified that *A. baumannii* and *K. pneumoniae* have been suggested to contain multiple *dapA* genes. We then set out to characterise the gene products from these priority Gram-negative pathogens using a combination of sequence analysis, CD spectroscopy, enzyme kinetics, and X-ray crystallography. Importantly, this work supports recent studies that have used a combination of sequence and structure/function workflows to reliably identify the annotated *dapA* genes that encode functional DHDPS enzymes [24,25]. Such strategies are critical to ensure correct gene annotations are based on key signature motifs that are validated experimentally.

Materials and methods

Sequence analysis

Three putative *dapA* genes were identified in the *K. pneumoniae* (Kp) genome Ecl8, with a further *dapA* gene found in the CDH3823 genome [28]. All four putative *dapA* genes for *A. baumannii* (Ab) were identified in the AB030 genome [29]. Sequence alignments with *Escherichia coli* (Ec) DHDPS (UNIPROT ID: P0A6L2) were performed using the ClustalW algorithm [30] incorporated in BIOEDIT (v.7.2.0) [31]. All alignments used *E. coli* residue numbering.

Protein expression and purification

The synthetic genes coding for *K. pneumoniae* and *A. baumannii* proteins with a hexa-histidine tag were codon optimised, synthesised, and ligated into a pET28a expression vector by Bioneer Pacific (Kew East, Vic, Australia). Recombinant proteins were expressed in *E. coli* BL21 (DE3) cells and purified using immobilised metal affinity chromatography (IMAC) as previously described [32]. Briefly, recombinant proteins were expressed upon the addition of 0.5 mM IPTG in Luria-Bertani broth at 16 °C for 18 h for *K. pneumoniae* and *A. baumannii* proteins or 37 °C for 4 h for *E. coli* proteins. Cells were harvested *via* centrifugation at 5000 *g* at 4 °C and sonicated in 20 mM Tris, 150 mM NaCl, 20 mM imidazole, pH 8.0 using a Vibra Cell VC40 (Sonics and Material, Newtown, CT, USA). Recombinant His-tagged proteins were purified using a 5 mL IMAC column (Bio-Rad Laboratories, Gladesville, NS, Australia) and stored in 20 mM Tris, 150 mM NaCl, pH 8.0.

Circular Dichroism (CD) spectroscopy

CD spectroscopy was performed as previously described [12,33] in an Aviv Model 420 CD spectrometer. Protein samples were prepared at 150–200 µg·mL⁻¹ in 20 mM NaH₂PO₄, 50 mM KF, pH 8.0. Spectra were obtained between 190 and 250 nm in 1-nm increments with 5-s averaging time at a temperature of 20 °C using 1-mm quartz cuvettes. The analysis was performed employing CDPro, and the data were fitted using the CONTINLL database with the SP22X reference set [34,35].

o-Aminobenzaldehyde assay

To qualitatively assess for DHDPS activity, the colorimetric *o*-aminobenzaldehyde (*o*-ABA) assay was employed as previously described [17,36,37]. Assays were performed in a 96-well plate with reactions initiated with the addition of 5 µL of 0.5 mg·mL⁻¹ protein sample to 100 µL of master-mix. Reactions were terminated after 30 min with 10 µL of 10% (v/v) trichloroacetic acid. Recombinant *E. coli*

DHDPS and *E. coli* DHDPR were used as a positive and negative controls, respectively. DHDPS activity was confirmed by the production of a purple chromophore.

Coupled assay

The DHDPS-DHDPR coupled assay was used to quantify DHDPS activity as previously described [38–40]. Briefly, the substrate turnover was measured *via* the associated oxidation of NADPH at Abs_{340 nm} (ε_{340 nm} = 6220 M⁻¹·cm⁻¹) in a Cary 4000 UV/Vis spectrophotometer (Varian, Mulgrave, Vic, Australia). All assays were performed in triplicate (*n* = 3) and incubated at 37 °C for 12 min before initiating the reaction by the addition of ASA. For the determination of the Michaelis–Menten constants (*K_M*), pyruvate and ASA were varied simultaneously ranging from 0.125–4 mM to 0.05–1 mM, respectively, with KpDHDPS kept constant at 5 µg·mL⁻¹ and AbDHDPS at 3 µg·mL⁻¹. Initial velocity data were analysed employing ENZFITTER v.2.0.18 (Biosoft, Cambridge, UK) and fitted to the ping-pong mechanism using Equation 1.

$$v = (V_{\max} \times A \times B) / (K_{M,A} \times B + K_{M,B} \times A + A \times B) \quad (1)$$

where *v* = initial velocity, *V_{max}* = limiting maximal velocity, *A* = [pyruvate], *B* = [ASA], *K_{M,A}* = limiting Michaelis–Menten constant for *A*, *K_{M,B}* = limiting Michaelis–Menten constant for *B*.

Lysine inhibition was measured by titrating concentrations of lysine ranging from 0.078 to 1 mM against KpDHDPS and AbDHDPS. Initial velocity data were analysed using GRAPHPAD PRISM v.8.2 (GraphPad, San Diego, CA, USA) and fitted to the log(inhibitor) vs response (variable slope) using Equation 2.

$$Y = \text{Bottom} + (\text{Top} - \text{Bottom}) / (1 + 10^{((\text{LogIC}_{50} - X) \times \text{Hill Slope})}) \quad (2)$$

where *X* = log of lysine concentration, *Y* = response, Top and Bottom = plateaus in the same units as *Y*, Hill slope = slope factor.

Crystallisation and X-ray diffraction data collection

KpDHDPS was crystallised using the hanging-drop vapour diffusion method at 20 °C. Diffraction-quality crystals grew after 2 days in drops consisting of equal volume (2 µL) of KpDHDPS (10 mg·mL⁻¹ in 20 mM Tris, 150 mM NaCl, pH 8.0) and reservoir solution (100 mM Tris pH 7.5, 2 M ammonium sulphate, 5 mM pyruvate) equilibrated against 1 mL of reservoir solution. X-ray diffraction was performed at the microfocus beamline (MX2) of the Australian Synchrotron [41]. The crystals were flash-cooled in

liquid nitrogen and transferred to a stream of nitrogen gas at 100 K at the goniometer. 180° of the diffraction data were collected at a wavelength of 0.9537 Å using an EIGER-16M detector with 0.1° oscillation and 0.1-s exposure of 0% attenuated beam per frame. The data were indexed and integrated with XDS [42] and scaled using AIMLESS [43]. The data were processed in space group $P2_12_12$, with unit-cell parameters $a = 105.6$, $b = 114.2$, $c = 55.3$ Å. The asymmetric unit is estimated to contain two monomers, with a corresponding crystal volume per protein weight of $2.67 \text{ Å}^3 \text{ Da}^{-1}$ and a solvent content of 54.0%. Data collection and processing statistics are detailed in Table 2.

Structure solution and refinement

Molecular replacement was performed using PHASER [44] within the CCP4 suite [45]. Chain A of the EcDHDPS structure (PDB ID: 1YXC) was used as a search model after removing all nonprotein atoms. CHAINSAW was used to replace all nonidentical residues with alanine [46]. Two monomers were found in the asymmetric unit with a log-likelihood gain of 59 712 and a Z-score of 72.7. Iterative model building with COOT [47] and refinement using REFMAC [48] were performed. The quality of the model was validated using MOLPROBITY [49]. The refinement statistics are included in Table 3. The atomic co-ordinates and experimental structure factors were deposited in the Protein Data Bank under accession code 6UE0.

Results

Annotated *dapA* genes

The annotated *dapA* genes in *K. pneumoniae* were identified using the NCBI database. The search yielded four putative genes, with *KpdapA1* (GENBANK ID: CCN30951.1), *KpdapA2* (GENBANK ID: WP_107318840.1), and *KpdapA4* (GENBANK ID: CCN29687.1) found in the genome of the reference strain Ecl8 (GENBANK ID: GCA_000315385.1), whilst *KpdapA3* (GENBANK ID: KGJ39907.1) was identified in the CDH3823 genome (GENBANK ID: JQDX000000000). To further investigate the putative function of these genes, we performed an alignment with their translated protein sequences compared to *E. coli* DHDPS (Fig. 2). KpDapA1 was shown to possess the highest sequence identity (87.6%) to EcDHDPS. The sequence alignment also shows low similarity between the KpDapA proteins, with KpDapA1 and KpDapA4 displaying the highest identity to one another (29.5%). Interestingly, KpDapA3 has a high degree of similarity to the mis-annotated *P. aeruginosa* (Pa) DapA3 protein (UNIPROT ID: Q9I490) (data not shown), which encodes a 1-pyrroline-4-

hydroxy-2-carboxylate (Pyr4H2C) deaminase enzyme [23]. Nevertheless, based on our previous findings [23–25], sequence similarity alone is an unreliable determinant of DHDPS function. Therefore, we examined whether these sequences contained a 7-residue signature sequence motif that has been proposed to be essential in *bona fide* DHDPS enzymes [25]. KpDapA1 was found to be the only protein with all SEVEN active site residues that are critical for DHDPS catalysis, whilst both KpDapA2 and KpDapA4 have four of the seven residues and KpDapA3 contains only two of the seven (Fig. 2).

Similar to *K. pneumoniae*, our investigation revealed that *A. baumannii* had four annotated *dapA* genes: *AbdapA1* (GENBANK ID: KMV04290.1), *AbdapA2* (GENBANK ID: KRJ74652.1), *AbdapA3* (GENBANK ID: KMV01952.1), and *AbdapA4* (GENBANK ID: AZK38617.1). The crystal structure of AbdapA1 has been deposited (PDB ID: 3TAK), although there is no accompanying functional data. A comparison of all four gene products revealed that the sequence with the highest similarity to EcDHDPS was that of the gene product of *AbdapA1*, displaying ~50% identity. Furthermore, we confirmed that only this protein contains the 7-residue DHDPS functional signature motif (Fig. 2). We therefore hypothesise that *KpdapA1* and *AbdapA1* encode functional DHDPS enzymes. We set out to confirm this by characterising the corresponding recombinant proteins.

Validation of DHDPS activity

To experimentally validate the 7-residue motif, recombinant KpDapA1-4 proteins were overexpressed in *E. coli* and purified to >90% homogeneity (Fig. 3A). CD spectroscopy showed a single maximum at ~195 nm and a broad minimum spanning ~205–225 nm. This confirms that the recombinant proteins were folded to form a mixed α/β secondary structure (Fig. 3B), which is known for aldolase or TIM-barrel enzymes, such as DHDPS [50,51]. Next, the qualitative *o*-ABA assay was used to assess DHDPS enzymatic activity *in vitro*. Activity is indicated by the production of a purple chromophore, with no discernible colour change indicative of no DHDPS activity [36,37]. A purple colour change was only observed for KpDapA1, which was similar to the positive control (Fig. 3C). This confirms our hypothesis that *KpdapA1* encodes the only functional DHDPS from *K. pneumoniae*. This protein will be referred to from herein as KpDHDPS.

Given that the 7-residue signature prediction was validated experimentally in *K. pneumoniae*, the predicted functional DHDPS enzyme from *A. baumannii*,

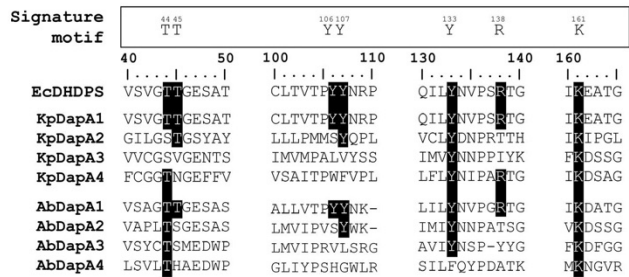


Fig. 2. Multiple sequence alignment of the putative *dapA* gene products from *Klebsiella pneumoniae* (KpDapA1 UNIPROT ID: A6TCA1, KpDapA2 UNIPROT ID: A0A0H3GS49, KpDapA3 UNIPROT ID: B5Y2B8, KpDapA4 UNIPROT ID: W1DHJ6) and *A. baumannii* (AbDapA1 UNIPROT ID: S3TLB4, AbDapA2 UNIPROT ID: A0A372IOL7, AbDapA3 UNIPROT ID: S3TI37, AbDapA4 UNIPROT ID: A0A022J7S0), compared to *E. coli* DHDPS (UNIPROT ID: P0A6L2). Conservation of the active site residues required for catalysis is highlighted in black, with the DHDPS signature motif displayed above the alignment. Sequence alignment was performed using the ClustalW software embedded in BIOEDIT (v.7.2.0).

AbDapA1, was subsequently overexpressed in *E. coli* and purified to > 90% homogeneity (Fig. 4A). CD spectroscopy again confirmed a mixed α/β secondary structure (Fig. 4B), consistent with the previously solved structure (PDB ID: 3TAK), whilst the *o*-ABA assay was used to qualitatively ascertain the production of DHDPS enzymatic activity (Fig. 4C). This confirms that *AbdapA1* codes for a functional DHDPS enzyme, hereafter referred to as AbDHDPS.

DHDPS functional characterisation

To further characterise the confirmed DHDPS enzymes, their kinetic parameters were quantified using the DHDPS-DHDPR coupled assay [12,38]. Initial rate was monitored by varying the concentrations of both

substrates, pyruvate and ASA, and data were globally fitted to a bisubstrate ping-pong model without substrate inhibition (Fig. 5) [52]. For KpDHDPS, the resulting K_M values for pyruvate and ASA were calculated to be 1.2 mM and 0.34 mM, respectively, with a turnover number (k_{cat}) of 290 s^{-1} . These yielded catalytic efficiency (k_{cat}/K_M) values of $2.4 \times 10^5\text{ s}^{-1}\cdot\text{M}^{-1}$ and $1.9 \times 10^6\text{ s}^{-1}\cdot\text{M}^{-1}$ for pyruvate and ASA, respectively, which are consistent with previously characterised bacterial DHDPS enzymes [24,53]. Kinetic characterisation of AbDHDPS yielded a K_M value for pyruvate of 0.25, and 0.036 mM for ASA, resulting in a k_{cat} of 48 s^{-1} (Fig. 5). Calculated catalytic efficiency values of 1.9×10^5 and $1.3 \times 10^6\text{ s}^{-1}\cdot\text{M}^{-1}$ for pyruvate and ASA, respectively, were determined, which are consistent with what we observe for KpDHDPS and

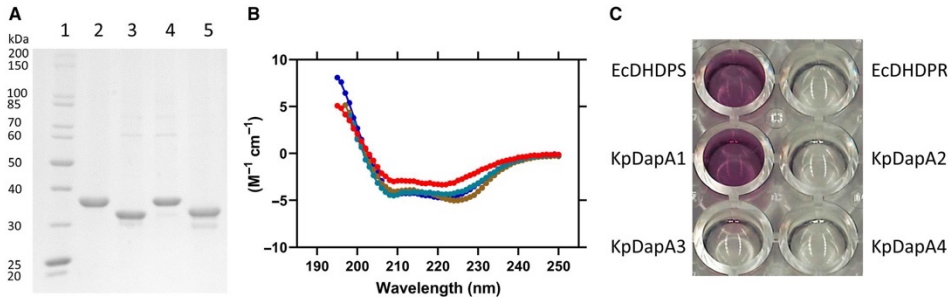


Fig. 3. (A) SDS/PAGE summary showing the recombinant *K. pneumoniae* *dapA1-4* gene products (lanes 2–5, respectively) compared to the Broad Range Molecular Weight (10–200 kDa) ladder (Lane 1). (B) CD spectra of recombinant KpDapA1 (blue), KpDapA2 (brown), KpDapA3 (teal) and KpDapA4 (red). The solid line represents the fit produced using the CONTINLL database and the SP22x reference set. (C) *o*-ABA assay of KpDapA1–4 proteins, with *E. coli* DHDPS used as a positive control and *E. coli* DHDPR as a negative control.

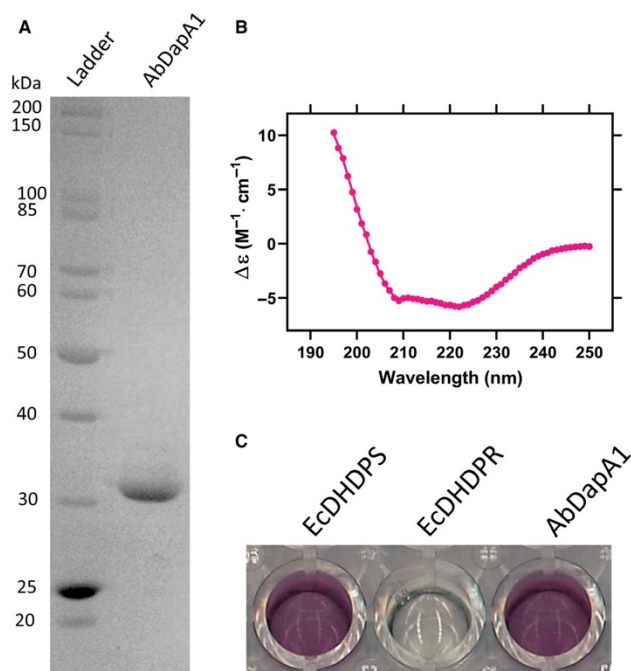


Fig. 4. (A) SDS/PAGE summary showing purified recombinant AbDapA1 compared to the Broad Range Molecular Weight (10–200 kDa) ladder, indicating a purity of > 90%. (B) CD spectrum of AbDapA1 with the fit produced using the CONTINLL database and the SP22x reference set (line). (C) o-ABA assay of AbDapA1, with *E. coli* DHDPS and *E. coli* DHDPR as positive and negative controls, respectively.

previously reported values for other bacterial DHDPS orthologues [23,54]. To determine the allosteric inhibition of these enzymes, increasing concentrations of lysine were titrated in the DHDPS-DHDPR coupled assay. The resulting IC_{50} value for both KpDHDPS and AbDHDPS was 160 μM (Table 1). This is consistent with previously reported bacterial DHDPS enzymes, including EcDHDPS and PaDHDPS2 (Table 1) [23,54].

Implications for inhibitor design

Although some DHDPS enzymes are not inhibited by lysine, the high degree of conservation at the active site across bacterial species allows for the potential identification of broad-spectrum inhibitors [55]. To illustrate this, KpDHDPS was crystallised in the presence of the substrate pyruvate, and the structure was solved using molecular replacement and refined to 1.89 Å resolution (Tables 2 and 3). The overall quaternary structure of KpDHDPS is consistent with previously characterised bacterial DHDPS enzymes, including orthologues from *E. coli* (PDB ID: 3DU0,

root-mean-square-deviation (r.m.s.d.) of 0.50 Å for 584 C α atoms) and *A. baumannii* (PDB ID: 3TAK, r.m.s.d. of 1.19 Å for 582 C α atoms), with a head-to-head dimer-of-dimers arrangement to form the tetramer (Fig. 6A). The active site is located at the C-terminal end of the α/β TIM-barrel, with tyrosine 107 (*E. coli* numbering) interdigitating between the two monomers across the dimerisation interface, forming the complete catalytic triad required for enzymatic activity [56]. The pyruvate molecule was found to form a Schiff base with lysine 161 (*E. coli* numbering) in the active site, which is consistent with other pyruvate-bound DHDPS enzymes [56].

We first superposed the active site of KpDHDPS with the structures of the now validated AbDHDPS (PDB ID: 3TAK) and EcDHDPS (PDB ID: 3DU0) in pyruvate-bound forms, and the apo PaDHDPS2 structure (PDB: 3NOE). As shown in Fig. 6B, the active site residues in these high-priority Gram-negative pathogens are 100% conserved, representing a possible 'druggable' site for novel broad-spectrum antibiotic development. Subsequently, we superposed the structure of EcDHDPS (PDB ID: 3DU0) with that of the

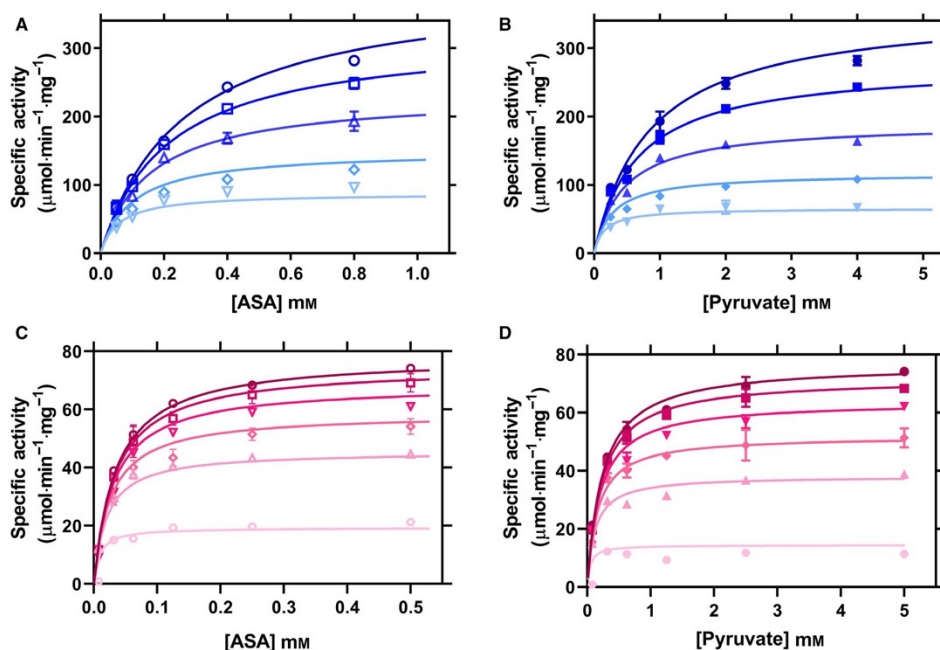


Fig. 5. (A, B) Kinetic profile of KpDHDPS plotted as initial velocity ($\mu\text{mol}\cdot\text{min}^{-1}\cdot\text{mg}^{-1}$) at varying concentrations of (A) pyruvate at 4.0 mM (○), 2.0 mM (□), 1.0 mM (△), 0.50 mM (◇) and 0.25 mM (▽) plotted as a function of ASA concentration and (B) ASA at 0.80 mM (●), 0.40 mM (■), 0.20 mM (▲), 0.10 mM (◆) and 0.05 mM (▼) plotted as a function of pyruvate concentration. (C-D) Kinetic profile of AbDHDPS plotted as initial velocity ($\mu\text{mol}\cdot\text{min}^{-1}\cdot\text{mg}^{-1}$) at varying concentrations of (C) pyruvate at 5.0 mM (○), 2.5 mM (□), 1.3 mM (△), 0.63 mM (◇), 0.32 (▽) and 0.078 mM (○) plotted as a function of ASA concentration and (D) ASA at 0.50 mM (●), 0.25 mM (■), 0.13 mM (▲), 0.063 mM (◆), 0.032 (▼) and 0.0078 mM (●) plotted as a function of pyruvate concentration. All data was fitted to a bisubstrate ping-pong model without substrate inhibition using ENZFITTER software (v.2.0.18), which resulted in an R^2 value of 0.98. Data are represented as mean \pm standard deviation ($n = 3$).

Table 1. Lysine inhibition affinities (IC_{50}) of DHDPS enzymes from Gram-negative bacteria.

| | IC_{50} (μM) |
|---------------|------------------------------------|
| KpDHDPS | 160 |
| AbDHDPS | 160 |
| EcDHDPS [54] | 180 |
| PaDHDPS2 [23] | 130 |

mis-annotated PaDapA4 enzyme (PDB ID: 3NA8), which has previously been shown not to possess DHDPS activity and only contains four of the seven key DHDPS residues [23]. Not surprisingly, we observe a low level of conservation in the active site with differences at positions 45, 106, and 138 (*E. coli* numbering) (Fig. 6C). Most notably, tyrosine 106 is

replaced by a serine, which in turn changes the position of the interdigitating tyrosine 107 from the adjacent monomer (*E. coli* numbering) (Fig. 6C). These differences significantly alter the conformation of the active site, highlighting the need for correct annotations and validation of the activity of promising drug targets.

Discussion

The development of whole-genome sequencing in the late 1990s led to a boom in gene annotations based often on limited homology [57]. Sequencing is now relatively routine and typically involves automatic computerised annotations. However, this method relies on the assumption that sequence similarity equates to a similar function [58]. This has resulted in an

Table 2. Data collection and processing statistics for KpDHDPS. Values in parentheses are for the highest resolution shell.

| | |
|------------------------------------|--|
| Diffraction source | MX2, Australian Synchrotron |
| Wavelength (Å) | 0.95374 |
| Temperature (K) | 100 |
| Detector | EIGER-16M |
| Crystal-to-detector distance (mm) | 150 |
| Total rotation range (°) | 180 |
| Space group | <i>P</i> 2 ₁ 2 ₁ 2 |
| <i>a</i> , <i>b</i> , <i>c</i> (Å) | 105.6, 114.2, 55.3 |
| α , β , γ (°) | 90, 90, 90 |
| Mosaicity (°) | 0.15 |
| Resolution range (Å) | 48.99–1.89 (1.93–1.89) |
| Total no. of reflections | 362 343 (20 999) |
| No. of unique reflections | 54 102 (3259) |
| Completeness (%) | 99.7 (95.3) |
| Multiplicity | 6.7 (6.4) |
| $\langle I/\sigma(I) \rangle$ | 11.4 (1.9) |
| <i>CC</i> _{1/2} | 0.998 (0.827) |
| <i>R</i> _{merge} (%) | 8.0 (62.9) |
| <i>R</i> _{pim} (%) | 5.0 (39.6) |

Table 3. Refinement statistics for KpDHDPS. Values in parentheses are for the highest resolution shell.

| | |
|--|------------------------|
| Resolution range (Å) | 49.04–1.89 (1.94–1.89) |
| Completeness (%) | 99.7 (96.3) |
| <i>R</i> (%) | 17.0 (29.7) |
| <i>R</i> _{free} (%) | 20.0 (31.7) |
| No. (%) of reflections in test set | 3608 (4.7) |
| No. of protein molecules per asu | 2 |
| R.m.s.d. bond length (Å) | 0.01 |
| R.m.s.d. bond angle (°) | 1.40 |
| Average <i>B</i> -factors (Å ²) ^a | 24.4 |
| Protein molecules | 23.7 |
| Water molecules | 31.3 |
| Ramachandran plot ^b | |
| Residues other Gly and Pro in: | |
| Most favoured regions (%) | 98.6 |
| Additionally allowed regions (%) | 1.4 |
| PDB code entry | 6UE0 |

^aCalculated by BAVEAGE in CCP4 Suite [45]; ^bCalculated using MolProbity [49].

astounding number of gene mis-annotations across multiple species. One striking example is the annotation of *Haemophilus influenzae*, which had over 148 amendments within just 4 weeks of publication [59]. More recently, a study highlighted that one out of eight genes in the human genome are annotated differently among different database sets [60]. Statistical analysis of genome annotations has estimated the error rate to even be as high as 49% [61]. This is exemplified with the investigation of carbohydrate-active enzyme genes in *Fibrobacter succinogenes*, in which out of the

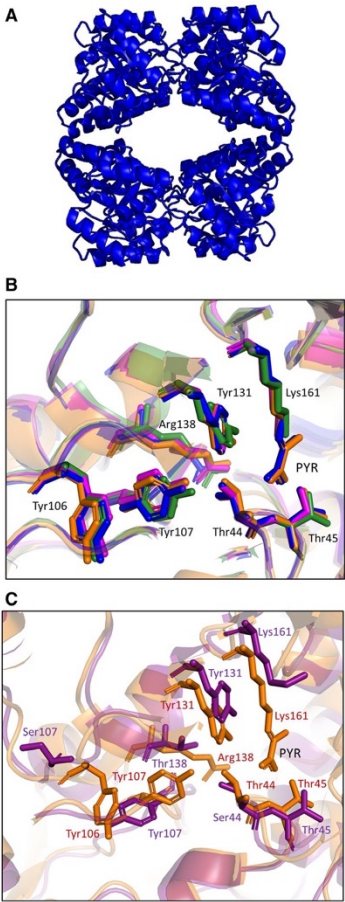


Fig. 6. (A) Overall structure of KpDHDPS in a head-to-head dimer-of-dimer arrangement (PDB ID: 6UE0). (B) Superposition of the active sites of pyruvate-bound EcDHDPS (orange) (PDB ID: 3DU0), pyruvate-bound AbDHDPS (pink) (PDB ID: 3TAK), pyruvate-bound KpDHDPS (blue) (PDB ID: 6UE0) and apo PaDHDPS2 (green) (PDB ID: 3NOE), highlighting the key residues involved in catalytic activity. (C) Superposition of EcDHDPS (orange) (PDB ID: 3DU0) and PaDapA4 (purple) (PDB: 3NAB) demonstrates the differences in the active site residues. Images were generated using PyMOL v.1.3 (Schrodinger, New York, NY, USA).

20 novel genes discovered, 12 were annotated to functions unrelated to the observed enzymatic activity [62]. These mis-annotations can lead to what is described as ‘the snowball effect’ [63]. Simply, when a single gene is

mis-annotated, a multitude of similar genes are then subsequently mis-annotated based on the first [63].

Here, we describe the repeated mis-annotation of the DHDPS-encoding *dapA* gene in two clinically important Gram-negative pathogens, *A. baumannii*, and *K. pneumoniae*. Specifically, we used a recently reported 7-residue signature motif [25] to predict DHDPS activity for the *dapA* gene encoding products in *A. baumannii* and *K. pneumoniae*, followed by experimental validations *in vitro*. In summary, despite sequence databases suggesting *A. baumannii* and *K. pneumoniae* contain 4 *dapA* genes, we show that these pathogens only possess a single gene encoding a functional DHDPS enzyme. Importantly, we determined the crystal structure of the *bona fide* DHDPS enzyme from *K. pneumoniae* DHDPS, which formed a tetrameric structure consistent with other bacterial DHDPS enzymes. Indeed, comparison to the structures of the validated DHDPS enzymes from *A. baumannii*, *P. aeruginosa*, and *E. coli* reveal a high degree of conservation, especially within the active site. We then further compared the active site of the *E. coli* DHDPS enzyme to the mis-annotated *P. aeruginosa* DapA4, illustrating a lesser degree of conservation as expected given the lack of DHDPS activity observed with this enzyme. Thus, this study highlights the need to validate the enzymatic activity of annotated drug targets, like DHDPS, and provides an important platform for the rational design of broad-spectrum DHDPS inhibitors as an emerging class of antibiotics for the treatment of infections caused by these high-priority Gram-negative pathogens.

Acknowledgements

TPSC would like to thank the National Health and Medical Research Council of Australia (APP1091976) and Australian Research Council (DE190100806) for fellowship and funding support, and MAP and SP the Australian Research Council for funding support (DP150103313). REI is supported by an Australian Research Training scholarship and acknowledges the British Society for Antimicrobial Chemotherapy for funding support. ML is supported by the Tracey Bani-vanua Mar fellowship from La Trobe University. We thank Dr. Janni Christensen for the insurgent technical support. We acknowledge the use of the MX2 beam-line at the Australian Synchrotron and the CSIRO Collaborative Crystallisation Centre (www.csiro/C3; Melbourne, Australia). We also thank the La Trobe University Comprehensive Proteomics Platform for providing infrastructure support.

Author contributions

TPSC, MAP and REI planned the experiments; REI and DAH performed the experiments; REI, TPSC, MAP, ML, SP and JMS analysed the data; REI, MAP and TPSC wrote the paper.

References

- 1 Tacconelli E, Carrara E, Savoldi A, Harbarth S, Mendelson M, Monnet DL, Pulcini C, Kahlmeter G, Kluytmans J, Carmeli Y *et al.* (2018) Discovery, research, and development of new antibiotics: the WHO priority list of antibiotic-resistant bacteria and tuberculosis. *Lancet Infect Dis* **18**, 318–327.
- 2 Soares da Costa TP, Abbott BM, Gendall AR, Panjikar S and Perugini MA (2017) Molecular evolution of an oligomeric biocatalyst functioning in lysine biosynthesis. *Biophys Rev* **4**, 153–162.
- 3 Impey RE and Soares da Costa T (2018) Review: Targeting the biosynthesis and incorporation of amino acids into peptidoglycan as an antibiotic approach against Gram negative bacteria. *EC Microbiol*, **10**, 200–209.
- 4 Hutton CA, Perugini MA and Gerrard JA (2007) Inhibition of lysine biosynthesis: an evolving antibiotic strategy. *Mol Biosyst* **3**, 458–465.
- 5 Hermann M, Thevenet NJ, Coudert-Maratier MM and Vandecasteele J-P (1972) Consequences of lysine oversynthesis in *Pseudomonas* mutants insensitive to feedback inhibition. *Eur J Biochem* **30**, 100–106.
- 6 Dogovski C, Atkinson SC, Dommaraju SR, Downton M, Hor L, Moore S, Paxman JJ, Peverelli MG, Qiu TW and Reumann M (2012) Enzymology of bacterial lysine biosynthesis. In *Biochemistry* (Ekinici D, ed), pp. 225–262. InTech Open Access Publisher, London.
- 7 Dogovski C, Atkinson SC, Dommaraju SR, Hor L, Dobson RCJ, Hutton CA, Gerrard JA and Perugini MA (2009) Lysine biosynthesis in bacteria: an uncharted pathway for novel antibiotic design. In *Encyclopedia of Life Support Systems* (Doell H, ed), pp. 116–136. EOLSS Publishers, Paris.
- 8 Vollmer W and Seligman SJ (2010) Architecture of peptidoglycan: more data and more models. *Trends Microbiol* **18**, 59–66.
- 9 Royet J and Dziarski R (2007) Peptidoglycan recognition proteins: pleiotropic sensors and effectors of antimicrobial defences. *Nat Rev Microbiol* **5**, 264–277.
- 10 Hall C and Soares da Costa TP (2018) Lysine: biosynthesis, catabolism and roles. *WikiJ Sci* **1**, 4.
- 11 Devenish SRA, Blunt JW and Gerrard JA (2010) NMR studies uncover alternate substrates for dihydrodipicolinate synthase and suggest that dihydrodipicolinate reductase is also a dehydratase. *J Med Chem* **53**, 4808–4812.

- 12 Christensen JB, Soares da Costa TP, Faou P, Pearce FG, Panjikar S and Perugini MA (2016) Structure and function of cyanobacterial DHDPS and DHDPR. *Sci Rep* **6**, 37111.
- 13 Peverelli MG, da Costa TPS, Kirby N and Perugini MA (2016) Dimerization of bacterial diaminopimelate decarboxylase is essential for catalysis. *J Biol Chem* **291**, 9785–9795.
- 14 Ray SS, Bonanno JB, Rajashankar KR, Pinho MG, He G, De Lencastre H, Tomasz A and Burley SK (2002) Cocystal structures of diaminopimelate decarboxylase: mechanism, evolution, and inhibition of an antibiotic resistance accessory factor. *Structure* **10**, 1499–1508.
- 15 Karsten WE (1997) Dihydrodipicolinate synthase from *Escherichia coli*: pH dependent changes in the kinetic mechanism and kinetic mechanism of allosteric inhibition by L-lysine. *Biochemistry* **36**, 1730–1739.
- 16 Dobson RCJ, Griffin MDW, Jameson GB and Gerrard JA (2005) The crystal structures of native and (S)-lysine-bound dihydrodipicolinate synthase from *Escherichia coli* with improved resolution show new features of biological significance. *Acta Crystallogr* **61**, 1116–1124.
- 17 Soares da Costa TP, Desbois S, Dogovski C, Gorman MA, Ketaren NE, Paxman JJ, Siddiqui T, Zammit LM, Abbott BM, Robins-Browne RM *et al.* (2016) Structural determinants defining the allosteric inhibition of an essential antibiotic target. *Structure* **24**, 1282–1291.
- 18 Dogovski C, Gorman MA, Ketaren NE, Praszker J, Zammit LM, Mertens HD, Bryant G, Yang J, Griffin MDW, Pearce FG *et al.* (2013) From knock-out phenotype to three-dimensional structure of a promising antibiotic target from *Streptococcus pneumoniae*. *PLoS ONE* **8**, e83419.
- 19 Gerdes SY, Scholle MD, Campbell JW, Balázs G, Ravasz E, Daugherty MD, Somera AL, Kyrpides NC, Anderson I, Gelfand MS *et al.* (2003) Experimental determination and system level analysis of essential genes in *Escherichia coli* MG1655. *J Bacteriol* **185**, 5673–5684.
- 20 Bukhari AI and Taylor AL (1971) Genetic analysis of diaminopimelic acid- and lysine-requiring mutants of *Escherichia coli*. *J Bacteriol* **105**, 844–854.
- 21 Kobayashi K, Ehrlich SD, Albertini A, Amati G, Andersen KK, Arnaud M, Asai K, Ashikaga S, Aymerich S, Bessieres P *et al.* (2003) Essential *Bacillus subtilis* genes. *Proc Natl Acad Sci USA* **100**, 4678–4683.
- 22 Becker D, Selbach M, Rollenhagen C, Ballmaier M, Meyer TF, Mann M and Bumann D (2006) Robust *Salmonella* metabolism limits possibilities for new antimicrobials. *Nature* **440**, 303–307.
- 23 Impey RE, Panjikar S, Hall CJ, Bock LJ, Sutton JM, Perugini MA and Soares da Costa TP (2020) Identification of two dihydrodipicolinate synthase isoforms from *Pseudomonas aeruginosa* that differ in allosteric regulation. *FEBS J* **287**, 386–400.
- 24 Atkinson SC, Hor L, Dogovski C, Dobson RCJ and Perugini MA (2014) Identification of the *bona fide* DHDPS from a common plant pathogen. *Proteins* **82**, 1869–1883.
- 25 Desbois S, John UP and Perugini MA (2018) Dihydrodipicolinate synthase is absent in fungi. *Biochimie* **152**, 73–84.
- 26 Devos D and Valencia A (2001) Intrinsic errors in genome annotation. *Trends Genet* **17**, 429–431.
- 27 Schnoes AM, Brown SD, Dodevski I and Babbitt PC (2009) Annotation error in public databases: misannotation of molecular function in enzyme superfamilies. *PLoS Comp Biol* **5**, e1000605.
- 28 Greninger AL, Chorny I, Knowles S, Ng VL and Chaturvedi V (2015) Draft genome sequences of four NDM-1-producing *Klebsiella pneumoniae* strains from a health care facility in Northern California. *Genome Announc* **3**.
- 29 Loewen PC, Alsaadi Y, Fernando D and Kumar A (2014) Genome sequence of an extremely drug-resistant clinical isolate of *Acinetobacter baumannii* strain AB030. *Genome Announc* **2**, 1.
- 30 Thompson JD, Higgins DG and Gibson TJ (1994) CLUSTAL W: improving the sensitivity of progressive multiple sequence alignment through sequence weighting, position-specific gap penalties and weight matrix choice. *Nucleic Acids Res.* **22**, 4673–4680.
- 31 Hall T (2011) BioEdit: An important software for molecular biology. *GERF Bull BioSci* **2**, 60–61.
- 32 Gupta R, Soares da Costa TP, Faou P, Dogovski C and Perugini MA (2018) Comparison of untagged and his-tagged dihydrodipicolinate synthase from the enteric pathogen *Vibrio cholerae*. *Protein Expr Purif* **145**, 85–93.
- 33 Atkinson SC, Dogovski C, Downton MT, Czabotar PE, Dobson RCJ, Gerrard JA, Wagner J and Perugini MA (2013) Structural, kinetic and computational investigation of *Vitis vinifera* DHDPS reveals new insight into the mechanism of lysine-mediated allosteric inhibition. *Plant Mol Biol* **81**, 431–446.
- 34 Sreerama N and Woody RW (2000) Estimation of protein secondary structure from circular dichroism spectra: comparison of CONTIN, SELCON, and CDSSTR methods with an expanded reference set. *Anal Biochem* **287**, 252–260.
- 35 Johnson WC (1999) Analyzing protein circular dichroism spectra for accurate secondary structures. *Proteins* **35**, 307–312.
- 36 Mitsakos V, Devenish SRA, O'Donnell PA, Gerrard JA and Hutton CA (2011) LC-MS and NMR characterization of the purple chromophore formed in the *o*-aminobenzaldehyde assay of dihydrodipicolinate synthase. *Bioorg Med Chem* **19**, 1535–1540.

- 37 Yugari Y and Gilvarg C (1965) The condensation step in diaminopimelate synthesis. *J Biol Chem* **240**, 4710–4716.
- 38 Coulter CV, Gerrard JA, Kraunsoe JAE and Pratt AJ (1999) *Escherichia coli* dihydrodipicolinate synthase and dihydrodipicolinate reductase: kinetic and inhibition studies of two putative herbicide targets. *J Pest Sci* **55**, 887–895.
- 39 Pearce FG, Perugini MA, Mckerchar HJ and Gerrard JA (2006) Dihydrodipicolinate synthase from *Thermotoga maritima*. *Biochem J* **400**, 359–366.
- 40 Dobson RCJ, Devenish SRA, Turner LA, Clifford VR, Pearce FG, Jameson GB and Gerrard JA (2005) Role of arginine 138 in the catalysis and regulation of *Escherichia coli* dihydrodipicolinate synthase. *Biochemistry* **44**, 13007–13013.
- 41 Aragão D, Aishima J, Cherukuvada H, Clarken R, Clift M, Cowieson NP, Ericsson DJ, Gee CL, Macedo S, Mudie N *et al.* (2018) MX2: a high-flux undulator microfocus beamline serving both the chemical and macromolecular crystallography communities at the Australian Synchrotron. *J Synchrotron Radiat* **25**, 885–891.
- 42 Kabsch W (2010) XDS. *Acta Crystallogr D Biol Crystallogr* **66**, 125–132.
- 43 Evans PR and Murshudov GN (2013) How good are my data and what is the resolution? *Acta Crystallogr D Biol Crystallogr* **69**, 1204–1214.
- 44 McCoy AJ, Grosse-Kunstleve RW, Adams PD, Winn MD, Storoni LC and Read RJ (2007) Phaser crystallographic software. *J Appl Cryst* **40**, 658–674.
- 45 Winn MD, Ballard CC, Cowtan KD, Dodson EJ, Emsley P, Evans PR, Keegan RM, Krissinel EB, Leslie AGW, McCoy A *et al.* (2011) Overview of the CCP4 suite and current developments. *Acta Crystallogr D Biol Crystallogr* **67**, 235–242.
- 46 Stein N (2008) CHAINSAW: a program for mutating pdb files used as templates in molecular replacement. *J Appl Cryst* **41**, 641–643.
- 47 Emsley P, Lohkamp B, Scott WG and Cowtan K (2010) Features and development of Coot. *Acta Crystallogr D Biol Crystallogr* **66**, 486–501.
- 48 Murshudov GN, Skubák P, Lebedev AA, Pannu NS, Steiner RA, Nicholls RA, Winn MD, Long F and Vagin AA (2011) REFMAC5 for the refinement of macromolecular crystal structures. *Acta Crystallogr D Biol Crystallogr* **67**, 355–367.
- 49 Chen VB, Arendall WB, Headd JJ, Keedy DA, Immormino RM, Kapral GJ, Murray LW, Richardson JS and Richardson DC (2010) MolProbity: all-atom structure validation for macromolecular crystallography. *Acta Crystallogr D Biol Crystallogr* **66**, 12–21.
- 50 Dobson RCJ, Griffin MDW, Roberts SJ and Gerrard JA (2004) Dihydrodipicolinate synthase (DHDPS) from *Escherichia coli* displays partial mixed inhibition with respect to its first substrate, pyruvate. *Biochimie* **86**, 311–315.
- 51 Burgess BR, Dobson RCJ, Bailey MF, Atkinson SC, Griffin MDW, Jameson GB, Parker MW, Gerrard JA and Perugini MA (2008) Structure and evolution of a novel dimeric enzyme from a clinically important bacterial pathogen. *J Biol Chem* **283**, 27598–27603.
- 52 Muscroft-Taylor AC, Soares da Costa TP and Gerrard JA (2010) New insights into the mechanism of dihydrodipicolinate synthase using isothermal titration calorimetry. *Biochimie* **92**, 254–262.
- 53 Voss JE, Scally SW, Taylor NL, Atkinson SC, Griffin MDW, Hutton CA, Parker MW, Alderton MR, Gerrard JA, Dobson RCJ *et al.* (2010) Substrate-mediated stabilization of a tetrameric drug target reveals Achilles heel in anthrax. *J Biol Chem* **285**, 5188–5195.
- 54 Soares da Costa TP, Muscroft-Taylor AC, Dobson RCJ, Devenish SRA, Jameson GB and Gerrard JA (2010) How essential is the 'essential' active-site lysine in dihydrodipicolinate synthase? *Biochimie* **92**, 837–845.
- 55 Christoff RM, Gardhi CK, Soares da Costa TP, Perugini MA and Abbott BM (2019) Pursuing DHDPS: an enzyme of unrealised potential as a novel antibacterial target. *MedChemComm* **10**, 1581–1588.
- 56 Dobson RCJ, Valegård K and Gerrard JA (2004) The crystal structure of three site-directed mutants of *Escherichia coli* dihydrodipicolinate synthase: further evidence for a catalytic triad. *J Mol Biol* **338**, 329–339.
- 57 Nobre T, Campos MD, Lucic-Mercy E and Arnholdt-Schmitt B (2016) Misannotation awareness: a tale of two gene-groups. *Front Plant Sci* **7**, 868.
- 58 Gilks WR, Audit B, De Angelis D, Tsoka S and Ouzounis CA (2002) Modeling the percolation of annotation errors in a database of protein sequences. *Bioinformatics* **18**, 1641–1649.
- 59 Casari G, Andrade MA, Bork P, Boyle J, Daruvar A, Ouzounis C, Schneider R, Tamames J, Valencia A and Sander C (1995) Challenging times for bioinformatics. *Nature* **376**, 647–648.
- 60 Abascal F, Juan D, Jungreis I, Martinez L, Rigau M, Rodriguez JM, Vazquez J and Tress ML (2018) Loose ends: almost one in five human genes still have unresolved coding status. *Nucleic Acids Res* **46**, 7070–7084.
- 61 Jones CE, Brown AL and Baumann U (2007) Estimating the annotation error rate of curated GO database sequence annotations. *BMC Bioinformatics* **8**, 170.
- 62 Brumm P, Mead D, Boyum J, Drinkwater C, Gowda K, Stevenson D and Weimer P (2011) Functional annotation of *Fibrobacter succinogenes* S85 carbohydrate active enzymes. *Appl Biochem Biotechnol* **163**, 649–657.
- 63 Jabbari K, Cruveiller S, Clay O, Le Saux J and Bernardi G (2004) The new genes of rice: a closer look. *Trends Plant Sci* **9**, 281–285.

4 Validation of DHDPR from *Pseudomonas aeruginosa*

4.1 Manuscript for Submission

This chapter is a paper for submission to *FEBS Journal* titled “Validation and characterisation of a novel antibiotic target in *Pseudomonas aeruginosa*” by Rachael E. Impey, Sarah Licul, Lucy J. Bock, Matthew A. Perugini, J. Mark Sutton and Tatiana P. Soares da Costa.


This paper is yet to be submitted and as such is not under copyright.

4.1.1 Statement of Contribution

I confirm that Rachael Impey has made the following contributions:

- Completion of experimental work (95%), with the exception of the collection of the circular dichroism spectroscopy data (Figure 4), which was performed by Sarah Licul
- Data analysis (100%)
- Conceptualisation and drafting of the manuscript (60%)
- Preparation of figures
- Revisions of manuscript prior to acceptance

Tatiana Soares da Costa

Signed: 

Date: 14/12/2020

(Executive Author)

Title: Validation and Characterisation of a Novel Antibiotic Target in *Pseudomonas aeruginosa*

Running title: DHDPR as a novel antibiotic target

Rachael E. Impey¹, Sarah Licul¹, Lucy J. Bock², Matthew A. Perugini¹, J. Mark Sutton² & Tatiana P. Soares da Costa^{1*}

¹Department of Biochemistry and Genetics, La Trobe Institute for Molecular Science, La Trobe University, Melbourne, VIC 3086, Australia.

²National Infection Service, Public Health England, Porton Down, Salisbury, Wiltshire SP4 0JG, UK.

* Correspondence:

T. P. Soares da Costa, Department of Biochemistry and Genetics, La Trobe University, Bundoora, VIC 3086, Australia

Tel: (+61) 3 9479 2227

E-mail: T.SoareshdaCosta@latrobe.edu.au

ABSTRACT

Antibiotic resistance represents one of the biggest threats facing modern medicine. This is exacerbated by the lack of new therapeutics entering the market in the past 30 years. Therefore, the validation of novel antibiotic targets is of the highest priority. In this study, we focus on the enzyme dihydrodipicolinate reductase (DHDPR) from the clinically important pathogen *Pseudomonas aeruginosa*. DHDPR is involved in the production of the essential metabolites *meso*-diaminopimelate and L-lysine that are critical for bacterial cell wall and protein synthesis. However, studies employing transposon libraries present conflicting evidence for the essentiality of the DHDPR-encoding gene for bacterial survival. Although such libraries allow us to quickly screen for essential bacterial genes, it has drawbacks depending on the transposon location. To address this issue, we performed for the first time, a complete knockout of the *P. aeruginosa* DHDPR-encoding gene using a two-step allelic exchange method. The knockout resulted in a lethal phenotype that could be rescued with supplementation of the downstream metabolite *meso*-diaminopimelate but not L-lysine alone. Given its essentiality in this pathogen, we subsequently characterised the catalytic mechanism of the gene product using enzyme kinetics and microscale thermophoresis. This allowed us to ascertain novel insights into substrate and co-factor binding, which are critical for future drug discovery efforts. Thus, this study provides the first step towards the identification of much needed new antibiotic classes by validating and characterising a promising target in the high priority pathogen *P. aeruginosa*.

Keywords:

antibiotic resistance, catalysis, cell wall, gene knockout, lysine biosynthesis

Abbreviations:

2,6-PDC, 2,6-pyridinedicarboxylic acid; THDP, 2,3,4,5-tetrahydrodipicolinate; 3MB, *m*-toluic acid; ASA, aspartate semialdehyde; AUC, analytical ultracentrifugation; CD, circular dichroism; DAP, diaminopimelate; DAPDC, diaminopimelate decarboxylase; DHDP, dihydrodipicolinate; DHDPR, dihydrodipicolinate reductase; DHDPS, dihydrodipicolinate synthase; HTPA, 4-hydroxy-2,3,4,5-tetrahydrodipicolinic acid; IMAC, immobilised metal affinity chromatography; LB, Luria-Bertani; MST, microscale thermophoresis; TYS, tryptone yeast and sucrose; WT, wildtype.

INTRODUCTION

The continuous rise of antibiotic resistant bacteria combined with a lack of antibiotics in the development pipeline is threatening our ability to treat common bacterial infections. One critical pathogen is *Pseudomonas aeruginosa*, which is a leading cause of mortality in cystic fibrosis patients and is commonly associated with nosocomial infections [1]. Both intrinsic and acquired resistance mechanisms contribute to the pathogenicity of *P. aeruginosa* that, in turn, has led to an increase in reports of extremely drug resistant strains [2–5]. Thus, the identification and characterisation of novel antibiotic targets in this pathogen is of the utmost importance to tackle the global antibiotic resistance crisis.

One promising novel target is the diaminopimelate (DAP) pathway. The pathway begins with the condensation of pyruvate and aspartate semialdehyde (ASA) to 4-hydroxy-2,3,4,5-tetrahydrodipicolinic acid (HTPA), which is catalysed by HTPA synthase, also commonly referred to as dihydrodipicolinate synthase (DHDPS, E.C. **4.3.3.7**) (Fig. 1) [6–9]. Following this, the dehydrated product, dihydrodipicolinate (DHDP), is reduced to 2,3,4,5-tetrahydrodipicolinate in a NAD(P)H-dependent reaction by dihydrodipicolinate reductase (DHDPR, E.C. **1.17.1.8**) (Fig. 1) [10,11]. The pathway then diverges into four sub-pathways in a species-specific manner, before converging for the formation of *meso*-diaminopimelate (DAP), which is utilised by Gram-negative bacteria, including *P. aeruginosa*, for crosslinking of the cell wall (Fig.1) [6,12–14]. Finally, DAP is converted to L-lysine (hereinafter referred to as lysine) by diaminopimelate decarboxylase (DAPDC, E.C. **4.1.1.20**) for protein production (Fig. 1) [12,13]. Given that the synthesis of bacterial cell wall and proteins are targets of current antibiotics, including β -lactams and aminoglycosides (Fig. 1) [15,16], we postulate that the inhibition of the DAP pathway could represent a novel antibiotic discovery approach as it would interfere with these two essential processes concurrently [6]. This study focuses on examining the potential of the second enzyme in the pathway, DHDPR, as an antibiotic target.

Unlike DHDPS, where two *bona fide* genes have been recently identified in *P. aeruginosa* [17], there is a single gene coding for DHDPR, namely *dapB*. Although several studies employing transposon libraries have flagged *dapB* as essential in *P. aeruginosa* [18–21], Skurnik and colleagues list *dapB* as non-essential using the same approach [22]. We hypothesise that the conflicting evidence arises from the limitations of transposon mutant libraries to assess essentiality, and consequently identify potential antibiotic targets. For instance, a gene could be considered essential if there were no successful transposon mutants

obtained for that locus [23]. An alternative approach is to generate complete gene knockouts, which negate any effects of the transposon DNA placement and eliminates the reliance on the number of mutants generated. This has long been considered more difficult in *P. aeruginosa*, compared to other bacterial species, due to the inefficiency and time dedication of the established lambda red system commonly used for *Escherichia coli* [24]. Recently, a streamlined method was developed using a double homologous recombination event with a suicide vector utilising *sacB* for counterselection [24], which has since been optimised by allowing transformation via electroporation [25]. However, to our knowledge, this approach is yet to be employed for the validation of an essential bacterial gene to identify novel antibiotic targets. In this study, we optimised this methodology to generate a seamless knockout of the *dapB* gene in the *P. aeruginosa* PAO1 strain to assess its essentiality. Furthermore, we utilised media supplementation to characterise the knockout phenotype. Following the validation of *dapB* as an essential gene in this pathogen, we used a combination of *in vitro* biochemical and biophysical techniques, including circular dichroism (CD) spectroscopy, analytical ultracentrifugation (AUC), enzyme kinetics and microscale thermophoresis (MST), to characterise the in-solution structure and catalytic mechanism of *P. aeruginosa* DHDPR (PaDHDPR) to aid in future drug development efforts.

RESULTS

Generation of Δ dapB Knockout

The Δ *dapB* mutant was generated using the two-step allelic exchange method [24], incorporating the optimised electroporation protocol [25]. To allow for the first recombination event into the genome, the upstream and downstream regions of the *dapB* gene were amplified from PAO1 (Fig. 2A) and cloned into the pEX18Tc plasmid. After transformation, the surviving colonies were subjected to colony PCR to determine the presence of the pEX18Tc plasmid (Fig. 2B), either upstream (~1250 bp) or downstream (~3000 bp) within the *dapB* operon. In the 5 colonies generated, 3 had integrated the plasmid upstream, while 2 had integrated the plasmid downstream (Fig. 2B). Another recombination event was induced by subjecting the bacteria to tryptone yeast and sucrose (TYS) media, thus making them susceptible to *sacB*-induced toxicity if the plasmid remains within the genome [24,25]. In addition to the original protocol and to allow for bacterial survival without the *dapB* gene, the media was supplemented with DAP and lysine. Colonies were then screened by colony PCR, which revealed 6 successful Δ *dapB* mutants out of 60 colonies examined (Fig. 2C). Our 10% success rate is lower than that reported in the protocol papers [24,25], which may be attributed

to the deletion of the *dapB* gene being selected against, despite the supplementation. As expected, when the second counterselection was performed on non-supplemented media lacking DAP and lysine, no successful mutants were obtained when similar numbers of bacteria were screened (data not shown). This indicates that the supplementation of the media is a critical step to allow for the assessment of a knockout of a potentially essential gene.

Phenotypic Characterisation of Δ dapB Knockout

To initially assess the phenotype of the Δ dapB knockout strains, overnight cultures were set up of the mutants, alongside wildtype (WT) bacteria as a control, with and without supplementation. Visual inspection of the overnight cultures revealed that there was no growth for the Δ dapB mutants without supplementation, whilst the opaque appearance, which is indicative of increased cell density, of the WT and supplemented Δ dapB cultures indicated that the bacteria were able to survive and grow (Fig. 3A). To assess differences in their growth rates, we measured the change in absorbance at 600 nm over 24 hrs (Fig. 3B). The WT bacteria show a typical growth rate curve with a plateau occurring at approximately 18 hrs. The flat growth line for the Δ dapB mutant indicates that without supplementation, the bacteria are unable to replicate. Supplementation with both end products, DAP and lysine, rescued growth, albeit with a slight growth delay compared to WT. Supplementation with DAP alone was also able to rescue growth to a similar extent, however lysine supplementation alone could not, indicating that DAP is essential for bacterial replication. To confirm that the observed phenotype was due to the loss of the *dapB* gene, a complementation plasmid with the wildtype PAO1 *dapB* gene under the control of XylS/Pm regulator and promoter system was generated (pSEVA658-*dapB*). Induction of *dapB* expression with the use of *m*-toluic acid (3MB) rescued the growth of the PAO1 Δ dapB mutant strain. Moreover, absence of 3MB, and thus no expression of the *dapB* gene, resulted in no bacterial growth (Fig. 3A & C). These phenotypic analyses indicate that the *dapB* gene is essential for *P. aeruginosa* growth in environments lacking supplemented DAP, and that the DHDPR-catalysed conversion of DHDP to THDP, and consequently, the production of DAP and subsequently, lysine, are critical for the survival of this pathogen.

Recombinant Protein Production and Structural Characterisation

Given the essentiality of *dapB* in *P. aeruginosa*, we set out to recombinantly produce the PaDHDPR enzyme and perform *in vitro* structural and kinetic characterisation studies. Firstly,

the enzyme with a monomeric size of ~31 kDa was purified to >99% homogeneity (Fig. 4A), before being subjected to CD spectroscopy and AUC to assess its structural integrity in solution. The resulting CD spectrum reveals an α/β fold (Fig. 4B) and the AUC data shows a single peak at approximately 5.5 S (Fig. 4C), indicative of a tetrameric species. These in-solution data are in agreement with the structural features observed in the deposited crystal structure of PaDHDPR (PDB ID: [4YWJ](#)).

Kinetic Analysis of PaDHDPR

To aid future drug discovery efforts, we probed the kinetic mechanism of PaDHDPR using the well-established DHDPS-DHDPR coupled assay [26–28]. First, we set out to assess the co-factor preference for this enzyme. Some previously investigated bacterial DHDPR orthologues, including *Staphylococcus aureus* DHDPR (SaDHDPR) [28,29] and *Anabaena variabilis* DHDPR (AvDHDPR) [26], show a preference for NADPH over NADH; whereas other bacterial DHDPR enzymes, namely *E. coli* DHDPR (EcDHDPR) [30] and *Mycobacterium tuberculosis* DHDPR (MtDHDPR) [31], display dual co-factor specificity. Given these observed differences, initial velocity studies were conducted with PaDHDPR by varying the concentration of ASA (and thus DHDP) at several fixed concentrations of either NADPH or NADH. The resulting Michaelis-Menten constant (K_M) values for DHDP were calculated to be 0.050 ± 0.009 mM in the presence of NADPH and 0.025 ± 0.005 mM in the presence of NADH, with a turnover number (k_{cat}) of 76 s^{-1} and 42 s^{-1} for each co-factor, respectively. Nevertheless, the catalytic efficiencies were comparable, with a k_{cat}/K_M of $1.5 \times 10^6\text{ s}^{-1}\cdot\text{M}^{-1}$ when using NADPH and $1.6 \times 10^6\text{ s}^{-1}\cdot\text{M}^{-1}$ with NADH. This indicates that PaDHDPR, similarly to EcDHDPR and MtDHDPR, does not show a co-factor preference.

Substrate and Co-factor Binding Order

To further investigate the catalytic mechanism of PaDHDPR, MST was employed to assess the binding of the substrate to the apo and co-factor bound enzyme. Specifically, we wanted to ascertain whether the pre-formation of the enzyme:co-factor complex is required to allow for substrate binding, as it has been observed for SaDHDPR and AvDHDPR [26,28]. Given that DHDP is unstable, the substrate analogue 2,6-pyridinedicarboxylic acid (2,6-PDC) was used in the binding studies. Initially, a concentration range of 2,6-PDC was titrated against the apo enzyme, which yielded a dissociation constant (K_D) of 0.95 ± 0.068 mM (Fig. 6). Pre-incubation of the enzyme with the oxidised co-factors, NADP⁺ and NAD⁺, resulted in similar

K_D values of 0.80 ± 0.071 mM and 0.58 ± 0.051 mM, respectively (Fig. 6). This indicates that the substrate can bind to PaDHDPR independently of the co-factor.

DISCUSSION

It is evident that there is an urgent need to identify and validate novel antibiotic targets to combat the rise in antibiotic resistance that is threatening our global health system. This is particularly pertinent for high priority Gram-negative bacteria such as *P. aeruginosa*, for which effective treatments are rapidly diminishing. As many antibiotic targets are the products of essential genes, genome wide studies have attempted to identify possible targets in *P. aeruginosa*. These studies often utilise transposon libraries, which are generated via the insertion of transposon DNA into the bacterial genome to disrupt normal gene function [32]. Gene essentiality is then determined either by the frequency of transposon insertion or via assessment of growth defects for each individual transposon mutant [18,19,21,22]. However, such approaches come with limitations. Determining essentiality by the absence or low frequency of transposon insertions is heavily influenced by the breadth of the library itself [23]. Furthermore, assessing growth defects relies on the constitution of the media, which could result in the mutant being inadvertently supplemented [23].

The conflicting evidence around the DHDPR-encoding gene, *dapB*, led us to investigate the essentiality of this potential antibiotic target by generating a complete gene knockout. Employing the optimised allelic exchange method [24,25], we were able to create seamless $\Delta dapB$ mutants in *P. aeruginosa* for the first time. The generation of a seamless knockout allows us to overcome the limitation of relying upon a transposon insertion into the *dapB* gene to determine essentiality. We then characterised the growth phenotype of the $\Delta dapB$ mutants in minimal media, with the controlled addition of DAP and/or lysine to avoid any unintentional supplementation within the media. This revealed that no growth was observed unless DAP was added. Moreover, the ability to supplement the knockout strain with metabolites, as well as induced *dapB* expression, indicated that the lethal phenotype was due to the removal of the *dapB* gene, as opposed to any downstream effects in the genome due to operon disruption. Although Hmelo and colleagues suggested that this method of allelic exchange could not be used to screen for essential genes [24], we have shown that this is possible by using supplementation during and after the generation of the gene knockout, as long as there is a suitable metabolite for the disrupted function. Another potential method would be to utilise the controlled expression of the gene of interest via the complementation plasmid during the

knockout generation protocol. This may require strong counterselection against the plasmid carrying the complementing gene and/or the use of tightly regulated promoters, as demonstrated for the XylS/Pm regulator and 3MB induction shown here, to establish whether the target is essential. This strategy could be employed to assess the essentiality of other potential antibiotic targets, especially when supplementation is unavailable.

Given that our data indicates that DHDPR represents an essential enzyme in *P. aeruginosa* in environments lacking supplemented DAP, it could be pursued for the development of new classes of antibacterial agents. To assist in future drug development, the in-solution structure and catalytic mechanism of recombinant PaDHDPR was characterised. The recombinant enzyme was first purified to >99% homogeneity. CD spectroscopy and AUC were subsequently used to confirm the secondary and quaternary structural features in solution. We then sought to functionally characterise the catalytic mechanism employing a combination of enzyme kinetics and MST. Using the DHDPS-DHDPR coupled assay, we were able to show that PaDHDPR displayed similar catalytic efficiencies when either NADH or NADPH was used as a co-factor. This dual co-factor specificity is in agreement with studies performed on EcDHDPR and MtDHDPR, but in contrast to what is observed with SaDHDPR and AvDHDPR, which show a preference for NADPH over NADH [26,28,30,31]. In an attempt to elucidate the mechanism responsible for co-factor preference, studies on EcDHDPR proposed that Glu38 can interact with the 2' and 3' hydroxyl groups of NADH [30]. PaDHDPR has an aspartate residue at the equivalent position, which would still allow for NADH binding [31]. For NADPH, Arg39 (*E. coli* numbering) is hypothesised to bind to the 2' phosphate, as well as the backbone of a N-terminal glycine rich region (GXXGXXG), which has been proposed to be responsible for anchoring this phosphate moiety [30,31,33]. These features are again conserved in PaDHDPR, supporting our findings that NADPH can be used as a co-factor as well as NADH. MST studies revealed that the substrate analogue, 2,6-PDC, can bind to both the apo and co-factor:enzyme complex with relatively similar affinities, which has important implications for inhibitor design.

In conclusion, this study provides the first steps towards the identification of new antibiotic modes of action to overcome resistance. Specifically, we have shown that the DHDPR-catalysed reaction is essential for the survival of *P. aeruginosa*. Furthermore, we have characterised the in-solution structure and function of PaDHDPR, providing key insights into substrate and co-factor binding. Such studies pave the way for future work aimed at developing

inhibitors of PaDHDPR that could be used to treat infections caused by multi-drug resistant strains of *P. aeruginosa*.

EXPERIMENTAL PROCEDURES

Gene Knockouts

Gene knockouts were generated using a recently optimised protocol [24,25]. Briefly, the 500 bp upstream and downstream regions flanking the *dapB* gene were amplified using primer sets 1&2 and 3&4 (Table 1) with Phusion DNA polymerase (NEB). These fragments were then cloned into an EcoRI-digested pEX18Tc plasmid using the NEB Hi-Fi assembly master mix. The assembled plasmid was transformed into *P. aeruginosa* PAO1 employing previously established electroporation parameters [25]. Colonies were then plated on Luria-Bertani (LB) agar containing 100 $\mu\text{g}\cdot\text{mL}^{-1}$ tetracycline and grown at 37 °C for 48 hrs. To determine the genome integration location, colony PCR was performed using One-Taq master mix (NEB) with primers 5 and 7 (Table 1). Colonies were re-streaked onto TYS agar plates (10 g tryptone, 5 g yeast, 10% (w/v) filtered sucrose), supplemented with 1 mM DAP (>96% purity, Thermofisher Scientific) and 1 mM lysine (>99% purity, Sigma Aldrich). Plates were left at room temperature for 72 hrs and any colonies were subjected to colony PCR to screen for the *dapB* knockout using primers 6&7 (Table 1). Complete gene knockout was confirmed by Sanger sequencing using primers 6&7 (Table 1) performed by the Australian Genomic Research Facility.

Complementation plasmid

The wildtype *dapB* gene was amplified from *P. aeruginosa* PAO1 using primers 8&9 (Table 1) with Phusion polymerase (NEB) as per manufacturer's protocol. The pSEVA658 plasmid was digested with AvrII and BamHI (NEB) at 37 °C for 1 hr. Both the amplified *dapB* and digested plasmid were gel purified using the Monarch Gel Purification Kit (Monarch). The final plasmid (pSEVA658-*dapB*) was constructed using NEB Hi-Fi Assembly as per manufacturer's protocol. Sanger sequencing was used to confirm the correct plasmid assembly (Australian Genomic Research Facility). The pSEVA658-*dapB* plasmid was transformed into the PAO1 ΔdapB strain using the transformation protocol previously described [34]. Transformants were selected using tryptic soy agar containing 30 $\mu\text{g}\cdot\text{mL}^{-1}$ gentamycin. The resulting PAO1 ΔdapB - pSEVA658-*dapB* strain was maintained with 30 $\mu\text{g}\cdot\text{mL}^{-1}$ gentamycin in all subsequent experiments.

Bacterial Cultures

Overnight bacterial cultures were set up by inoculating a 10 mL aliquot of M9 minimal media [35] with a single colony of either PAO1 WT or PAO1 $\Delta dapB$, both with and without supplementation of 1 mM DAP and 1 mM lysine. The PAO1 $\Delta dapB$ - pSEVA658-*dapB* strain was set up in MOPS minimal media [36], with and without induction with 1 mM 3MB (Sigma Aldrich). Each culture was then grown overnight at 37 °C while shaking at 165 rpm. Bacterial growth was assessed visually by observation of density.

Growth Curve Analysis

A fresh bacterial colony of PAO1 WT or PAO1 $\Delta dapB$ was used to inoculate a supplemented (+ 1 mM DAP, + 1 mM lysine or both) or non-supplemented 1 mL aliquot of MOPS minimal media as described above. Single colonies of the PAO1 $\Delta dapB$ - pSEVA658-*dapB* strain was inoculated into 1 mL aliquots of MOPS minimal media with and without the addition of 1 mM 3MB. Cultures were then incubated for 1 hr at 37 °C with shaking at 165 rpm to ensure homogeneity. Subsequently, 200 μ L of each bacterial culture was added to a polystyrene Greiner CELLSTAR 96-well plate (Merck, NSW, Australia) in technical triplicates. The plate was then statically incubated at 37 °C for 22 hrs in a PerkinElmer Enspire 2300 Multilabel Reader with absorbance readings taken at 600 nm every 15 mins. Experiments were repeated with 3 biological replicates. Data were plotted using GraphPad Prism (version 8.4.3, GraphPad Software).

Protein Expression and Purification

The synthetic gene for PaDHDPR (*dapB*) was cloned into pET28a by Bioneer (Bioneer Pacific, Kew East, Vic, Australia). Proteins were recombinantly expressed in *E. coli* BL21 (DE3) cells and subsequently purified using immobilised metal affinity chromatography (IMAC) as previously described [17,26,37,38]. Briefly, recombinant protein expression was induced with the addition of 0.5 mM isopropyl β -D-1-thiogalactopyranoside in LB broth at 16 °C for 18 hrs for PaDHDPR or 37 °C for 4 hrs for EcDHDPS. Cells were harvested by centrifugation at $5,000 \times g$ at 4 °C before sonication in 20 mM Tris, 150 mM NaCl, 20 mM imidazole, pH 8.0. Recombinant His-tagged proteins were purified and desalted using a 5 mL IMAC column and

a 50 mL desalting column (BioRad Australia), respectively. Aliquots of PaDHDPR and EcDHDPS were stored at -80 °C in 20 mM Tris, 150 mM NaCl, pH 8.0.

Circular Dichroism (CD) Spectroscopy

The CD spectrum of PaDHDPR was obtained using an Aviv Model 420 CD spectrometer as previously described [39,40]. Briefly, protein was prepared in 20 mM NaH₂PO₄, 50 mM KF, pH 8.0 at 0.1 mg·mL⁻¹. Wavelength scans were performed between 190 and 250 nm in 1 nm increments at 20 °C, with a 4 sec averaging time using 1 mm quartz cuvettes. Data were fitted employing the CDPPro software incorporating the CONTINLL algorithm and the SP22X database [41,42].

Analytical Ultracentrifugation (AUC)

Sedimentation velocity experiments were conducted in a Beckman Coulter XL-A ultracentrifuge at 30 °C using a An-60 Ti rotor as previously described [12,26]. Briefly, double sector quartz cells were loaded with 380 µL of PaDHDPR at 0.9 mg·mL⁻¹ and 400 µL of reference buffer (20 mM Tris, 150 mM NaCl, pH 8.0). Absorbance readings were collected continuously at 230 nm, using a step size of 0.003 cm at 40,000 rpm. Solvent density, viscosity and partial specific volume were calculated using SEDNTERP [43]. Data were fitted to a continuous size distribution model [44] embedded in the SEDFIT analysis software (www.analyticalultracentrifugation.com).

Enzyme Kinetics

Kinetic analysis of PaDHDPR was performed using the DHDPS-DHDPR coupled assay as previously described [9,26,45]. Assays were performed at 37 °C with a total reaction volume of 0.8 mL in 1 cm acrylic cuvettes. Change in absorbance at 340 nm was measured using a Cary 4000 UV/Vis spectrophotometer. Pre-assay mixtures, containing all reagents but PaDHDPR, were incubated for 12 mins prior to addition of ASA. The reaction was initiated with the addition of PaDHDPR (final concentration of 0.16 µM), 1 min after the addition of ASA. For analysis of co-factor preference and substrate affinity, the Michaelis-Menten constant (K_M) was determined by simultaneously varying the ASA concentration (30 – 650 µM) against either NADH or NADPH concentration (16 – 250 µM). Initial velocity data were analysed using ENZFITTER (Biosoft, Cambridge, UK) and fitted to the ternary complex mechanism using Equation 1.

Equation 1:

$$v = (V_{\max} * A * B) / (K_{ia} * K_{M,B} + K_{M,A} * B + K_{M,B} * A + A * B)$$

Where v = initial velocity, V_{\max} = limiting maximal velocity, A = [co-factor], B = [DHDP], $K_{M,A}$ = limiting Michaelis-Menten constant for A, $K_{M,B}$ = limiting Michaelis-Menten constant for B, K_{ia} = dissociation constant for the enzyme:co-factor complex.

Microscale Thermophoresis (MST)

Affinity measurements were carried out using a Monolith NT.LabelFree MST instrument (NanoTemper Technologies) [26,39]. Aqueous solutions of 2,6-PDC (final concentrations of 0.6 μ M – 20 mM) was mixed 1:1 with PaDHDPR (final concentration of 10 μ M) pre-incubated with 150 μ M NAD⁺, 150 μ M NADP⁺ or water. All reactions were incubated for 30 mins at 37 °C before applying samples to Monolith NT Standard Untreated Capillaries (NanoTemper Technologies). Thermophoresis was measured at 37 °C with 5 sec/ 30 sec/5 sec laser off/on/off times. Experiments were conducted at 50% LED power and 40% MST IR-laser power. Data from three independently performed experiments were fitted to the single binding site model in the NT. MO Affinity Analysis software (version 2.3, NanoTemper Technologies) using the signal from Thermophoresis + T-Jump.

ACKNOWLEDGMENTS

T. P. S. C. acknowledges the National Health and Medical Research Council of Australia (APP1091976) and Australian Research Council (DE190100806) for funding support. M. A. P. would like to thank the Australian Research Council (DP150103313) for funding support. R. E. I. would like to acknowledge the Australian Government as a recipient of a Research Training Program Scholarship and the support of the British Society for Antimicrobial Chemotherapy for funding support. We thank Angela Wilks from Boston University for providing the original pEX18Tc plasmid and the De Lorenzo Lab, Centro Nacional de Biotecnología, Spain for providing the original pSEVA658 plasmid. We also thank the La Trobe University Comprehensive Proteomics Platform for providing infrastructure support.

AUTHOR CONTRIBUTIONS

R. E. I., L. J. B., M. A. P., J. M. S. and T. P. S. C. designed the experiments; R. E. I. and S. L. performed the experiments; R. E. I., S. L., J. M. S. and T. P. S. C. analysed the data; R. E. I. and T. P. S. C. wrote the paper; all authors revised the manuscript.

REFERENCES

1. Emerson J, Rosenfeld M, McNamara S, Ramsey B & Gibson RL (2002) *Pseudomonas aeruginosa* and other predictors of mortality and morbidity in young children with cystic fibrosis. *Pediatr Pulmonol* 34, 91–100.
2. Estahbanati HK, Kashani PP & Ghanaatpisheh F (2002) Frequency of *Pseudomonas aeruginosa* serotypes in burn wound infections and their resistance to antibiotics. *Burns* 28, 340–348.
3. Horcajada JP, Montero M, Oliver A, Sorlí L, Luque S, Gómez-Zorrilla S, Benito N & Grau S (2019) Epidemiology and treatment of multidrug-resistant and extensively drug-resistant *Pseudomonas aeruginosa* infections. *Clin Microbiol Rev* 32, e00031-19.
4. Palavutitotai N, Jitmuang A, Tongsai S, Kiratisin P & Angkasekwinai N (2018) Epidemiology and risk factors of extensively drug-resistant *Pseudomonas aeruginosa* infections. *PLoS ONE* 13, e0193431.
5. Impey RE, Hawkins DA, Sutton JM & Soares da Costa TP (2020) Overcoming intrinsic and acquired resistance mechanisms associated with the cell wall of Gram-negative bacteria. *Antibiotics (Basel)* 9, 623.
6. Hutton CA, Perugini MA & Gerrard JA (2007) Inhibition of lysine biosynthesis: an evolving antibiotic strategy. *Mol Biosyst* 3, 458–465.
7. Christoff RM, Gardhi CK, Soares da Costa TP, Perugini MA & Abbott BM (2019) Pursuing DHDPS: an enzyme of unrealised potential as a novel antibacterial target. *MedChemComm* 10, 1581–1588.
8. Impey RE & Soares da Costa TP (2018) Review: Targeting the biosynthesis and incorporation of amino acids into peptidoglycan as an antibiotic approach against Gram negative bacteria. *EC Microbiol* 14, 200–209.
9. Soares da Costa TP, Muscroft-Taylor AC, Dobson RCJ, Devenish SRA, Jameson GB & Gerrard JA (2010) How essential is the ‘essential’ active-site lysine in dihydrodipicolinate synthase? *Biochimie* 92, 837–845.
10. Devenish SRA, Blunt JW & Gerrard JA (2010) NMR studies uncover alternate substrates for dihydrodipicolinate synthase and suggest that dihydrodipicolinate reductase is also a dehydratase. *J Med Chem* 53, 4808–4812.

11. Soares da Costa TP, Christensen JB, Desbois S, Gordon SE, Gupta R, Hogan CJ, Nelson TG, Downton MT, Gardhi CK, Abbott BM, Wagner J, Panjikar S & Perugini MA (2015) Chapter Nine - Quaternary structure analyses of an essential oligomeric enzyme. In *Methods in Enzymology* (Cole JL, ed), pp. 205–223. Academic Press.
12. Peverelli MG, Costa TPS da, Kirby N & Perugini MA (2016) Dimerization of bacterial diaminopimelate decarboxylase is essential for catalysis. *J Biol Chem* 291, 9785–9795.
13. Dogovski C, Atkinson SC, Dommaraju SR, Downton M, Hor L, Moore S, Paxman JJ, Peverelli MG, Qiu TW & Reumann M (2012) Enzymology of bacterial lysine biosynthesis. In *Biochemistry (D Ekinici, ed.)* InTech Open Access Publisher, London, UK.
14. Gupta R, Hogan CJ, Perugini MA & Soares da Costa TP (2018) Characterization of recombinant dihydrodipicolinate synthase from the bread wheat *Triticum aestivum*. *Planta* 248, 381–391.
15. Fernandes R, Amador P & Prudêncio C (2013) β -Lactams: chemical structure, mode of action and mechanisms of resistance. *Rev Med Microbiol* 24, 7–17.
16. Kotra LP, Haddad J & Mobashery S (2000) Aminoglycosides: Perspectives on mechanisms of action and resistance and strategies to counter resistance. *Antimicrob Agents Chemother* 44, 3249–3256.
17. Impey RE, Panjikar S, Hall CJ, Bock LJ, Sutton JM, Perugini MA & Costa TPS da (2020) Identification of two dihydrodipicolinate synthase isoforms from *Pseudomonas aeruginosa* that differ in allosteric regulation. *FEBS J* 287, 386–400.
18. Liberati NT, Urbach JM, Miyata S, Lee DG, Drenkard E, Wu G, Villanueva J, Wei T & Ausubel FM (2006) An ordered, nonredundant library of *Pseudomonas aeruginosa* strain PA14 transposon insertion mutants. *PNAS* 103, 2833–2838.
19. Lee SA, Gallagher LA, Thongdee M, Staudinger BJ, Lippman S, Singh PK & Manoil C (2015) General and condition-specific essential functions of *Pseudomonas aeruginosa*. *PNAS* 112, 5189–5194.
20. Turner KH, Wessel AK, Palmer GC, Murray JL & Whiteley M (2015) Essential genome of *Pseudomonas aeruginosa* in cystic fibrosis sputum. *PNAS* 112, 4110–4115.
21. Poulsen BE, Yang R, Clatworthy AE, White T, Osmulski SJ, Li L, Penaranda C, Lander ES, Shores N & Hung DT (2019) Defining the core essential genome of *Pseudomonas aeruginosa*. *PNAS* 116, 10072–10080.
22. Skurnik D, Roux D, Aschard H, Cattoir V, Yoder-Himes D, Lory S & Pier GB (2013) A comprehensive analysis of *in vitro* and *in vivo* genetic fitness of *Pseudomonas*

- aeruginosa* using high-throughput sequencing of transposon libraries. *PLOS Pathog* 9, e1003582.
23. Chao MC, Abel S, Davis BM & Waldor MK (2016) The design and analysis of transposon-insertion sequencing experiments. *Nat Rev Microbiol* 14, 119–128.
 24. Hmelo LR, Borlee BR, Almblad H, Love ME, Randall TE, Tseng BS, Lin C, Irie Y, Storek KM, Yang JJ, Siehnel RJ, Howell PL, Singh PK, Tolker-Nielsen T, Parsek MR, Schweizer HP & Harrison JJ (2015) Precision-engineering the *Pseudomonas aeruginosa* genome with two-step allelic exchange. *Nat Protoc* 10, 1820–1841.
 25. Huang W & Wilks A (2017) A rapid seamless method for gene knockout in *Pseudomonas aeruginosa*. *BMC Microbiol* 17, 199.
 26. Christensen JB, Soares da Costa TP, Faou P, Pearce FG, Panjikar S & Perugini MA (2016) Structure and function of cyanobacterial DHDPS and DHDPR. *Sci Rep* 6, 37111.
 27. Coulter CV, Gerrard JA, Kraunsoe JAE & Pratt AJ (1999) *Escherichia coli* dihydrodipicolinate synthase and dihydrodipicolinate reductase: kinetic and inhibition studies of two putative herbicide targets. *J Pest Sci* 55, 887–895.
 28. Dommaraju SR, Dogovski C, Czabotar PE, Hor L, Smith BJ & Perugini MA (2011) Catalytic mechanism and cofactor preference of dihydrodipicolinate reductase from methicillin-resistant *Staphylococcus aureus*. *Arch Biochem Biophys* 512, 167–174.
 29. Girish TS, Sharma E & Gopal B (2008) Structural and functional characterization of *Staphylococcus aureus* dihydrodipicolinate synthase. *FEBS Lett* 582, 2923–2930.
 30. Scapin G, Reddy SG, Zheng R & Blanchard JS (1997) Three-dimensional structure of *Escherichia coli* dihydrodipicolinate reductase in complex with NADH and the inhibitor 2,6-pyridinedicarboxylate. *Biochemistry* 36, 15081–15088.
 31. Cirilli M, Zheng R, Scapin G & Blanchard JS (2003) The three-dimensional structures of the *Mycobacterium tuberculosis* dihydrodipicolinate reductase–NADH–2,6-PDC and –NADPH–2,6-PDC complexes. Structural and mutagenic analysis of relaxed nucleotide specificity. *Biochemistry* 42, 10644–10650.
 32. Jacobs MA, Alwood A, Thaipisuttikul I, Spencer D, Haugen E, Ernst S, Will O, Kaul R, Raymond C, Levy R, Chun-Rong L, Guenther D, Bovee D, Olson MV & Manoil C (2003) Comprehensive transposon mutant library of *Pseudomonas aeruginosa*. *PNAS* 100, 14339–14344.
 33. Xu J-Z, Yang H-K, Liu L-M, Wang Y-Y & Zhang W-G (2018) Rational modification of *Corynebacterium glutamicum* dihydrodipicolinate reductase to switch the nucleotide-

- cofactor specificity for increasing l-lysine production. *Biotechnology and Bioengineering* 115, 1764–1777.
34. Aparicio T, Lorenzo V de & Martínez-García E (2019) CRISPR/Cas9-enhanced ssDNA recombineering for *Pseudomonas putida*. *Micro Biotech* 12, 1076–1089.
 35. M9 minimal medium (standard) (2010) *Cold Spring Harb Protoc*.
 36. LaBauve AE & Wargo MJ (2012) Growth and laboratory maintenance of *Pseudomonas aeruginosa*. *Curr Prot Micro* 25, 6E.1.1-6E.1.8.
 37. Impey RE, Lee M, Hawkins DA, Sutton JM, Panjikar S, Perugini MA & Costa TPS da (2020) Mis-annotations of a promising antibiotic target in high-priority gram-negative pathogens. *FEBS Lett* 594, 1453–1463.
 38. Gupta R, Soares da Costa TP, Faou P, Dogovski C & Perugini MA (2018) Comparison of untagged and his-tagged dihydrodipicolinate synthase from the enteric pathogen *Vibrio cholerae*. *Pro Expr Purif* 145, 85–93.
 39. Soares da Costa TP, Desbois S, Dogovski C, Gorman MA, Ketaren NE, Paxman JJ, Siddiqui T, Zammit LM, Abbott BM, Robins-Browne RM, Parker MW, Jameson GB, Hall NE, Panjikar S & Perugini MA (2016) Structural determinants defining the allosteric inhibition of an essential antibiotic target. *Structure* 24, 1282–1291.
 40. Voss JE, Scally SW, Taylor NL, Atkinson SC, Griffin MDW, Hutton CA, Parker MW, Alderton MR, Gerrard JA, Dobson RCJ, Dogovski C & Perugini MA (2010) Substrate-mediated stabilization of a tetrameric drug target reveals Achilles heel in anthrax. *J Biol Chem* 285, 5188–5195.
 41. Sreerama N & Woody RW (2000) Estimation of protein secondary structure from circular dichroism spectra: comparison of CONTIN, SELCON, and CDSSTR methods with an expanded reference set. *Anal Biochem* 287, 252–260.
 42. Johnson WC (1999) Analyzing protein circular dichroism spectra for accurate secondary structures. *Proteins* 35, 307–312.
 43. Cole JL, Lary JW, Moody T & Laue TM (2008) Analytical ultracentrifugation: sedimentation velocity and sedimentation equilibrium. *Methods Cell Biol* 84, 143–179.
 44. Schuck P (2000) Size-distribution analysis of macromolecules by sedimentation velocity ultracentrifugation and lamm equation modeling. *Biophys. J.* 78, 1606–1619.
 45. Dogovski C, Dommaraju SR, Small LC & Perugini MA (2012) Comparative structure and function analyses of native and his-tagged forms of dihydrodipicolinate reductase from methicillin-resistant *Staphylococcus aureus*. *Pro Expr Purif* 85, 66–76.

FIGURE LEGENDS

Figure 1. The diaminopimelate (DAP) pathway. The pathway begins with DHDPS-catalysed condensation of ASA and pyruvate to HTPA, which is non-enzymatically dehydrated to DHDP. DHDP is further reduced to THDP by DHDPR. The pathway then diverges to one of four sub-pathways, dependent on the organism, before reconverging at the production of DAP. *Pseudomonas aeruginosa* utilises the succinyl sub-pathway (in bold). DAP can then be utilised in the crosslinking of the Gram-negative bacterial peptidoglycan layer, a target for antibiotics such as β -lactams. Lysine is produced from the decarboxylation of DAP by DAPDC for protein synthesis, which is targeted by current antibiotics including aminoglycosides, tetracyclines, macrolides and chloramphenicol. Image was produced using BioRender (www.BioRender.com).

Figure 2. Generation of *dapB* gene knockout in *Pseudomonas aeruginosa*. (A) Amplification of the 500 bp genomic DNA upstream and downstream of the *dapB* gene for ligation into the pEX18Tc plasmid. (B) PCR screening of 5 transformant colonies (1-5) showing successful integration of the pEX18Tc plasmid into the genome. Colonies integrated upstream of the *dapB* gene are shown by the ~1250 bp product (colonies 1, 4 & 5), whereas downstream integration is shown by the ~3000 bp product (colonies 2 & 3). (C) PCR screening of 6 PAO1 colonies after selection on tryptone yeast and sucrose media, compared to wildtype (WT) PAO1. The ~1000 bp band indicates a successful *dapB* knockout compared to the WT fragment at ~1900 bp.

Figure 3. Phenotypic assessment of PAO1 Δ *dapB* with and without supplementation. (A) Overnight cultures of wildtype PAO1 (PAO1 WT), PAO1 Δ *dapB* and PAO1 Δ *dapB* supplemented with 1 mM DAP and 1 mM lysine. Cultures of PAO1 Δ *dapB* - pSEVA658-*dapB* with and without *dapB* gene induction by addition of 1 mM *m*-toluic acid (3MB). The opaque appearance of the media indicates substantial bacterial growth. A 22-hour growth curve of (B) PAO1 WT (blue) and PAO1 Δ *dapB* with supplementation of 1 mM DAP (cyan), 1 mM lysine (red), 1mM DAP + 1 mM lysine (pink) and no supplementation (black, dashed); (C) PAO1 Δ *dapB* - pSEVA658-*dapB* is shown with and without 1 mM 3MB (green and purple, respectively) compared to PAO1 WT with 1 mM 3MB (black). Growth was assessed by optical density at 600 nm (Abs_{600nm}). Results shown are typical of at least three independent biological experiments.

Figure 4. Recombinant PaDHDPR characterisation. (A) SDS-PAGE analysis of purified PaDHDPR protein (lane 2) compared to the NEB Broad Range Molecular Weight (10-200 kDa) ladder (lane 1). (B) Circular dichroism spectrum for PaDHDPR indicates a mixed α/β fold. Experimental data (circle) was analysed using CDPro, utilising the SP22X CONTINLL database as the fit (line). (C) Analytical ultracentrifugation $c(s)$ sedimentation velocity experiments show a single species at ~ 5.5 S, which is indicative of a tetramer in solution. Residuals plotted as a function of radial position resulting from the $c(s)$ best fit. Data were plotted using GraphPad Prism (version 8.4.3, GraphPad software).

Figure 5. Michaelis-Menten kinetic profiles of recombinant PaDHDPR. Initial velocity ($\mu\text{mol} \cdot \text{min}^{-1} \cdot \text{mg}^{-1}$) of PaDHDPR plotted as a function of DHDP concentration with (A) NADPH (blue) or (B) NADH (black) used as the co-factor at varying concentrations [0.250 mM (\blacktriangle), 0.125 mM (\bullet), 0.065 mM (\blacklozenge), 0.032 mM (\blacksquare) and 0.016 mM (\bullet)]. Data were fitted to a ternary complex model using ENZFITTER software (version 2.0.18), which resulted in R^2 values of 0.98 and 0.95 for NADPH and NADH, respectively. Data are represented as mean \pm standard deviation (n=3).

Figure 6. Microscale thermophoresis of PaDHDPR against 2,6-PDC. Microscale thermophoresis affinity measurements of the binding of the substrate analogue 2,6-PDC to PaDHDPR pre-incubated with NADP^+ (blue), NAD^+ (black) or water (red), using the signal from thermophoresis + T-jump (\bullet). The solid lines represent the non-linear best fit to the single binding site model. Data were plotted using GraphPad Prism (version 8.4.3, GraphPad software). Data are represented as mean \pm standard deviation (n=3).

TABLES

Table 1. Primers used in *dapB* genetic allelic exchange protocol.

| Primer# | Sequence 5'-3' | Description |
|---------|---|--|
| 1&2 | 1: ggaaacagctatgacctgattacgGCCGTTGGCTTTCAGGTAGTCAGGC 2: tgagtggttttGGCGCTGCCGCACGTCGTCTTATTG | 500 bp upstream flanking region of the <i>dapB</i> gene, used for NEB Hi-Fi assembly* |
| 3&4 | 3: gtgcggcagcgccAAAACCACTCCACGCGGAACCCGGAC 4: agaggatccccgggtaccgagctcgCATCCGCCTCACCGGCGAAGGCGAG | 500 bp downstream flanking region of the <i>dapB</i> gene, used for NEB Hi-Fi assembly* |
| 5 | 5: GGCTCGTATGTTGTGTGGAATTGTG | Universal pEX primer |
| 6&7 | 6: GAGGATGCGAGTCAGGCGACG 7: AGAAGACCCTGTCGGTGAAGGTGC | Upstream and downstream of the <i>dapB</i> gene, used for colony PCR and sequencing confirmation |
| 8&9 | 8: taatggagtcagaccATGCATGCGACGTATAGCCGTAGTG 9: cctgcaggtcgactctagagTCAGCGTAGGCCGAGCAC | Amplification of <i>dapB</i> from PAO1, used for NEB Hi-Fi assembly* |

*For NEB Hi-Fi assembly reactions, lower case indicates homology regions used for cloning.

FIGURES

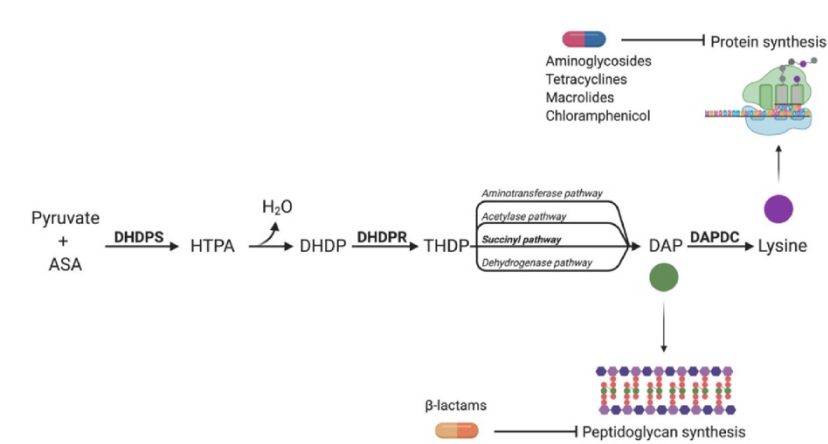


Figure 1

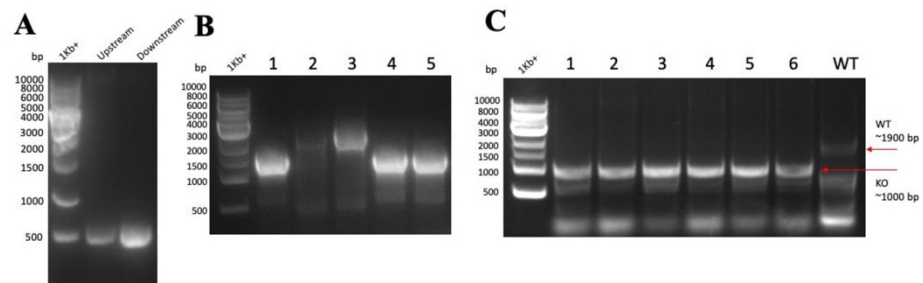


Figure 2

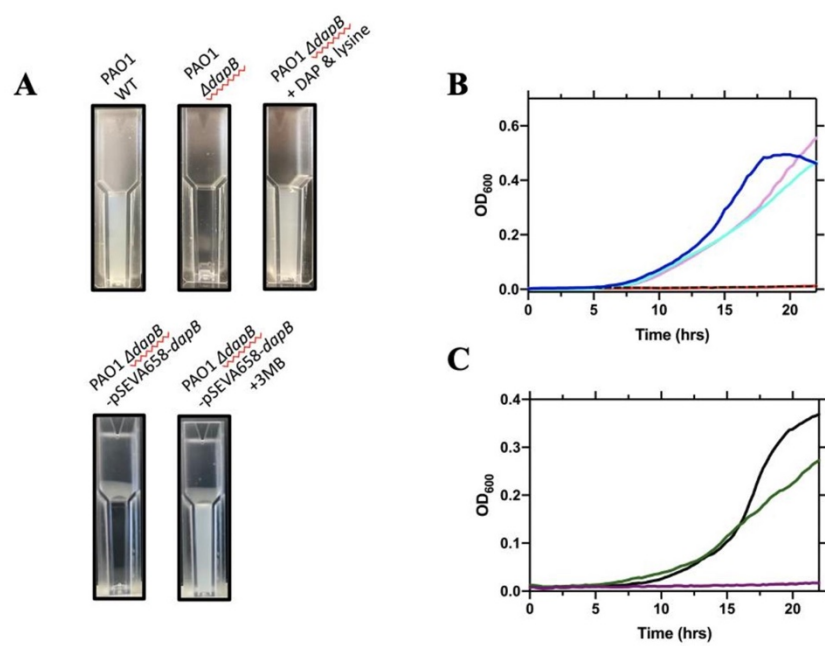


Figure 3

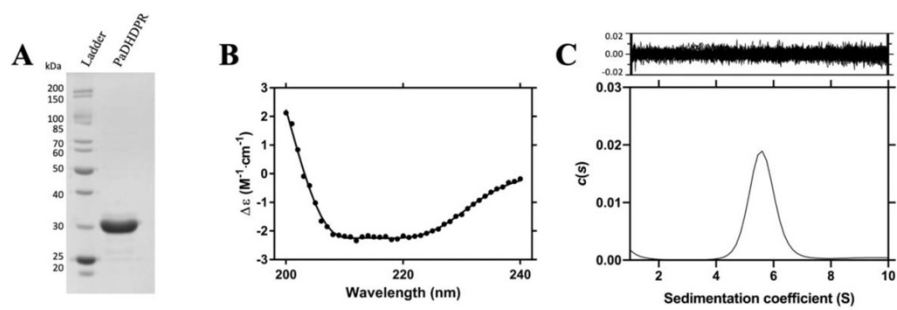


Figure 4

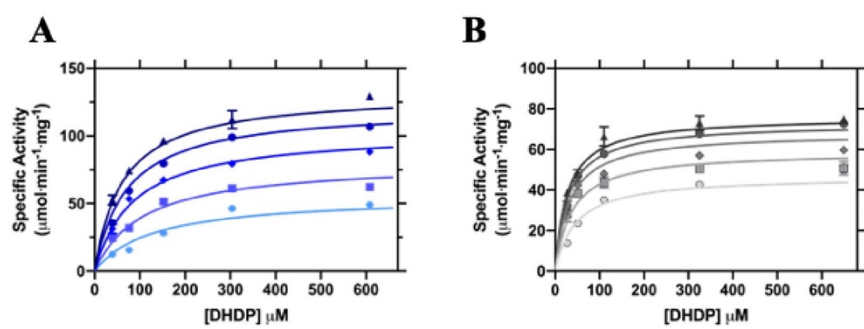


Figure 5

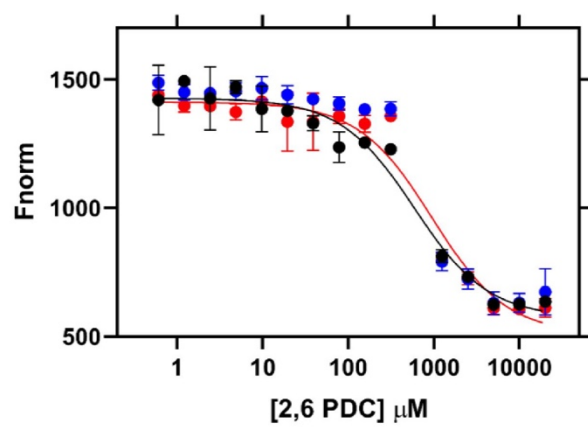


Figure 6

5 Discussion and Future Directions

The current rise in antibiotic resistance represents one of the biggest threats to global healthcare. To combat this, there is an urgent need for new antibiotics with novel modes of action. This thesis focuses on the potential antibiotic targets DHDPS and DHDPR within the DAP pathway, which are responsible for the biosynthesis of DAP and lysine, both crucial metabolites for bacterial survival [1,2]. Specifically, this thesis aimed to identify, validate and characterise DHDPS and DHDPR from important Gram-negative bacterial pathogens, namely *P. aeruginosa*, *A. baumannii* and *K. pneumoniae*. In this chapter, a discussion of the major findings will be summarised and how it provides insights into future antibiotic development targeting DHDPS and DHDPR from these clinically relevant pathogens. Furthermore, future directions will be discussed that may be useful in resolving unanswered questions in this field.

5.1 Final Discussion

5.1.1 Gene Mis-annotations

Gene mis-annotations arise from the incorrect assignment of gene function, either based on previous mis-annotations, sequence similarity or an overprediction of function [3]. All three bacteria, *P. aeruginosa*, *A. baumannii* and *K. pneumoniae*, had four annotated *dapA* genes each, which would indicate they encoded multiple DHDPS enzymes. This is unusual, as unlike plants, bacteria typically only have a single functional DHDPS enzyme [1,4]. In the case of *P. aeruginosa*, two of the four annotated genes were found to be functional DHDPS enzymes, resulting in a mis-annotation rate of 50% (Chapter 2). This was an important finding from not only a need to exclude non-DHDPS-encoding genes but also to ensure that no *bona fide* DHDPS enzymes were incorrectly excluded. If identification had relied on similarity alone, PaDHDPS1 could have been discounted as a functional DHDPS enzyme due to its low similarity to other characterised bacterial orthologues. Furthermore, in *A. baumannii* and *K. pneumoniae*, the *dapA* mis-annotation rate was found to be 75%, with only 1 in 4 of the annotated genes encoding an active DHDPS enzyme (Chapter 3). Subsequent investigation into the mis-annotated genes revealed the protein referred to as PaDapA4 was incorrectly annotated within the PDB as a DHDPS (PDB ID: 3NA8). PDB mis-annotations are particularly significant as computational groups can use deposited crystal structures for *in silico* chemical screens in the pursuit for new inhibitors. For example, DHDPR inhibitors were identified by

Paiva and colleagues using the available crystal structure for MtDHDPR [5]. While in this case the annotation was correct, similar investigations to identify DHDPS inhibitors using the crystal structure for PaDapA4 would have been a waste of valuable time and resources. Additionally, PaDapA3 had previously been demonstrated to have Pyr4H2C enzyme activity [6]. It is tempting to speculate that the protein referred to as KpDapA3 in Chapter 3 is also a Pyr4H2C enzyme given the high level of primary sequence homology. Perhaps the mis-annotation of the *P. aeruginosa* gene may have influenced the annotation of KpDapA3 as a DHDPS enzyme or *vice versa*. Whilst for the *dapA* genes described here, the complete 7-residue motif is indicative of a functional DHDPS enzyme, as more genes are discovered and annotated it would be valuable to investigate potential *dapA* genes lacking the full motif, including those listed above. If activity is observed, this could provide valuable insights into the evolution of the DHDPS mechanism, given the important roles that these residues play in catalytic activity.

This thesis highlights several mis-annotations of the *dapA* gene in clinically important Gram-negative bacteria. Worryingly, such mis-annotations are becoming more prevalent. In an investigation of mis-annotations in superfamilies, 10 of 37 superfamilies were found to have over 80% mis-annotation rates in one or more databases [3]. The impact of gene mis-annotations has been exemplified in a study that examined the germination of *A. thaliana* in cold temperatures by producing a transgenic mutant plant [7]. The mutation was believed to be in a single gene, with its identity being unclear [7]. Subsequent investigation revealed that this annotated single gene was actually two separate genes, with one encoding a key enzyme involved in protein degradation [7]. If this gene had remained mis-annotated as a single gene, it would have been impossible to define the protein degradation function and thus, its effect in cold temperature germination would have remained unclear [6]. Similarly, the annotation of the reverse open reading frames (ORF) for ubiquitin, another protein degradation enzyme, have been found to have numerous mis-annotations, significantly impacting the search of the correct forward sequence [8]. This substantially impacts the ability and ease of identifying the correct ORF, increasing the initial bioinformatic workload [8]. In some cases, it is impossible to assign the exact gene function based on similarity alone, so alternatively, a superfamily or domain designation can be made to imply function [3]. However, superfamily designation is not exempt from mis-annotations. In the instance of the enolase superfamily, several proteins were added as “mandelate racemase/muconate lactonising enzyme”, and without the designation of this superfamily, this would appear to be a multi-functional enzyme with both racemase and

lactonisation function that does not exist [3]. Mis-annotations also affect any subsequent annotation of similar genes, in what is known as the snowball effect [9]. Simply, this is when mis-annotated gene causes another unknown gene to be annotated identically, whether through automated processes or user error [9]. In turn, this causes a multitude of mis-annotated genes, and depending on the timing of the first mis-annotation, can dwarf the correctly annotated results [9].

5.1.1.1 DHDPS Signature Sequence Motif

To distinguish between the mis-annotated and *bona fide* *dapA* genes, we used a signature motif of the key DHDPS catalytic site residues. For *P. aeruginosa*, as mentioned, two of the four annotated genes were found to have all 7 key residues, and thus contained the signature motif. Further functional characterisation revealed that of the four encoded proteins, only these two proteins showed DHDPS activity *in vitro* and the ability to complement a *dapA* deficient *E. coli* strain. Similarly, for *K. pneumoniae*, all four genes were assessed for DHDPS function, with only KpDapA1 displaying DHDPS activity. In comparison, this was also the only annotated gene for *K. pneumoniae* that had the complete signature motif. Using this data, we were able to predict and verify the *bona fide* *dapA* gene for *A. baumannii*. This signature motif was originally used by Desbois and colleagues to confirm the absence of *dapA* genes in the fungi kingdom [9], however this is the first use of this to identify bacterial *dapA* genes among mis-annotations. This approach is similar to that used by Naumoff and colleagues for enzymes involved in nitrogen metabolism [11]. Specifically, they used previously ignored experimental data, a conserved motif and gene context to identify genes mis-annotated as ornithine carbamoyltransferases as actual putrescine carbamoyltransferases [11]. By validating the use of the signature motif for DHDPS enzymes in pathogenic bacteria, I have demonstrated an alternate gene annotation method for this promising antibiotic target with minimal experimental validation required. The other enzymes in the DAP pathway seem to show a lower mis-annotation rate, with a single annotated gene for DHDPR, DAP epimerase and DAP decarboxylase listed on the *Pseudomonas* genome database [12] (<https://www.pseudomonas.com/search/sequences>; DB version 18.1; searched 17 Nov 2020). Nevertheless, identifying a signature motif for these other enzymes would be valuable not only to correct any future mis-annotations that can quickly propagate, but would also allow for the identification of residues essential for catalytic activity that could be exploited for future inhibitor discovery efforts.

5.1.2 Gene Validation and Essentiality

Many antibiotic targets are the products of essential genes, with the rationale being if the bacteria are unable to survive without the gene, chemical inhibition of the gene product should have a similar effect [13]. Thus, several studies have been carried out in an attempt to identify essential genes in different bacterial genomes, including the Keio collection of *E. coli* single gene knockout mutants, leading to the largest collection of complete gene knockouts created to date [14]. However, generating complete gene knockouts is highly time and resource dependent, with essential genes also varying between bacterial species. As such, transposon libraries, which are generated by randomly inserting transposon DNA segments within a gene to disrupt its function, are now becoming more prevalent to assess gene essentiality [15]. Genes that do not tolerate insertions are considered essential for bacterial survival [15]. However, by inferring essentiality from an absence of successful transposon mutants, inherent problems can arise. The library is heavily dependent on the transposon used, the complexity of the library and the reliability of the sequencing and interpretation [16]. For instance, if a transposon is used that is sequence specific, only transposon mutants in genes with that specific sequence will be obtained, thus limiting the diversity [16]. The complexity is then determined by how many times each gene is disrupted, in which ideally each gene would have multiple insertions in different locations to determine essentiality [16]. Experimental design is also implicated in the determination of conditionally essential genes, with auxotrophs being unintentionally supplemented by rich optimal growth media [16]. In trying to determine if a gene represents a promising antibiotic target, this may wrongly classify a gene as non-essential, compared to a host infection environment in which supplementation may be unavailable [16]. Alternatively, some transposon libraries avoid this by using minimal media to grow their mutant bacterial strains [17]. Finally, the ORF of the gene needs to be accurately identified to interpret if the location of the insertion was adequate to determine essentiality [16]. Failure to do this can result in a gene being classified as non-essential [16]. An example of this is the *dapF* gene, which encodes for DAP epimerase [18]. In the *P. aeruginosa* PA14 Harvard transposon library, *dapF* is classified as non-essential as it has a successful transposon mutant with no observed growth defects (Mutant ID:48024) [19]. However, closer inspection of this insertion reveals that it is located two base pairs from the 3' end of the gene, and as such, it is unclear if this is enough to disrupt protein function. Mis-annotations, as described in Section 5.1.1, can also affect the validity of the conclusions, as a mis-annotated gene may be classed as non-essential, providing misleading information about the importance of the protein function for bacterial

survival [16]. These differences between transposon libraries can result in conflicting evidence, even within the same organism, as exemplified with the DAP pathway genes in Table 1. In summary, no consistent classification of essentiality is observed for 4 of the enzymes within the DAP pathway based on data from different transposon libraries.

Table 1. Essentiality classification of genes encoding DAP enzymes in *Pseudomonas aeruginosa* transposon libraries. “E” indicates essential, “N” non-essential and “C” conditional.

| | <i>dapA2</i> * | <i>dapB</i> | <i>dapF</i> | <i>lysA</i> |
|--------------------------------------|----------------|-------------|-------------|----------------|
| Liberati <i>et al.</i> , (2006) [19] | E | E | N | N |
| Skurnik <i>et al.</i> , (2013) [20] | E | N | N | N |
| Lee <i>et al.</i> , (2015) [21] | E | E | E | E |
| Turner <i>et al.</i> , (2015) [22] | E | E | E | N |
| Poulsen <i>et al.</i> , (2019) [23] | C | E | E | N [#] |

*No transposon data for *dapA1*

[#]A DAP decarboxylase gene was suggested to be essential, however this was a mis-annotated *lppl* gene

Due to this conflicting information, Chapter 4 of this thesis focused on generating a knockout of the DHDPR-encoding gene, *dapB*. By creating a single gene knockout, the potential limitations of a transposon library were avoided and the phenotype of *P. aeruginosa* lacking a functional DHDPR enzyme could be investigated. The resulting mutant strain was grown on minimal media, to control and avoid unintentional supplementation, and phenotypical assessment of growth rates indicated *dapB* was essential for bacterial replication in environments lacking supplemented DAP. Additionally, growth was rescued with supplementation of *meso*-DAP, but not with the final product of the pathway, lysine. This is assumed to be due to the conversion of the supplemented *meso*-DAP to lysine by DAP decarboxylase, the function of which should have remained unimpaired [1,24]. These results indicate that *meso*-DAP is essential for bacterial survival, thus supporting the investigation of DAP pathway enzymes as novel antibiotic targets. Previous research shed doubt on the essentiality of this pathway, with a single gene knockout of *PadapA2* resulting in no change in bacterial growth or virulence [25]. However, the study failed to address the presence of *PadapA1*, which encodes a functional DHDPS enzyme as shown in Chapter 2. Experiments into the essentiality of *PadapA1* and *PadapA2* are ongoing in the Soares da Costa laboratory.

Research should also be conducted into the essentiality of the DAP pathway genes in the other critical pathogens, *A. baumannii* and *K. pneumoniae*. While transposon libraries for both of these species list *dapA*, *dapB* and *dapF* as essential, and *lysA* as non-essential [26,27], there have been no complete gene knockout strains generated. Future investigations could include either genetic or transcriptional mutation of these genes to assess the phenotype, which will be described in Section 5.2.1.

5.1.3 Protein Structure and Function

Understanding protein structure and function is crucial for inhibitor development. In order to aid future structure activity relationship (SAR) optimisation of hit compounds, it is necessary to understand the key residues required for enzymatic activity. As previously mentioned, the foundation of current drug discovery efforts targeting DHDPS and DHDPR has been based on studies using EcDHDPS, EcDHDPR and MtDHDPR (Section 1.3.4). Furthermore, there have been no published inhibitors of any of the DAP pathway enzymes from *P. aeruginosa*, *A. baumannii* or *K. pneumoniae*. Accordingly, this thesis aimed to investigate the structure and function of DHDPS and DHDPR from these clinically important Gram-negative bacterial species. In Chapter 2, I demonstrated that although PaDHDPS1 and PaDHDPS2 share similar catalytic efficiencies, they differed in their allosteric inhibition by lysine. PaDHDPS1 displays an unusual allosteric site composition, with a glutamine residue in position 56, which had not been reported for any previously characterised DHDPS enzymes. Using site directed mutagenesis and homology modelling, I hypothesised that steric hinderance from this residue prevents lysine binding and thus inhibition. This expanded the current dogma of position 56 as an allosteric determinant to include a glutamine, which can now be applied to other DHDPS enzymes. Moreover, this has demonstrated that an allosteric inhibitor of PaDHDPS enzymes would have to overcome the steric hinderance of the glutamine, indicating that inhibitors, such as bis-lysine [28], may be ineffective.

Overall, these data suggests that narrow-spectrum inhibitors could be developed that target the allosteric site of DHDPS, whereas the active site represents a broad-spectrum target. To aid in this, DHDPS enzymes from *A. baumannii* and *K. pneumoniae* were functionally and structurally characterised (Chapter 3). While the crystal structure for AbDHDPS had already been deposited in the PDB (PDB ID: 3TAK) without accompanying functional data, I was able to crystallise and solve the structure of KpDHDPS (PDB ID: 6UE0). An overlay of the

EcDHDPS, KpDHDPS, AbDHDPS and PaDHDPS2 enzymes revealed similar orientations for the catalytic site residues (see Section 1.3.2.4). This further supports the idea that targeting the DHDPS active site should result in broad-spectrum inhibitors.

In addition to the characterisation of the DHDPS enzymes, the subsequent enzyme in the DAP pathway, DHDPR, from *P. aeruginosa* was also investigated (Chapter 4). DHDPR requires either NADH or NADPH as a co-factor for the donation of a hydrogen ion to complete the reduction of DHDP to THDP [29–31]. To investigate the co-factor specificity of PaDHDPR, its enzymatic rate was measured while titrating varying concentrations of both NADH and NADPH. This revealed that like EcDHDPR and MtDHDPR, PaDHDPR has dual co-factor specificity. This indicates that if inhibitors were to be designed against this co-factor binding site, they could potentially interact with either of the key residues involved in NADH and NADPH binding.

The order of substrate and co-factor binding for PaDHDPR was also explored as this could limit or expand potential chemical scaffolds. Previously, the order of substrate and co-factor binding had only been investigated for SaDHDPR and AvDHDPR, both of which demonstrated that NADH was required for the substrate analogue 2,6-PDC to bind [32,33]. Using microscale thermophoresis, I showed that 2,6-PDC can bind to the apo and co-factor bound forms of PaDHDPR, unlike previous studies (Chapter 4). It is currently unclear if the phenomenon observed for PaDHDPR is applicable to other DHDPR enzymes that have dual specificity, including EcDHDPR and MtDHDPR [29,34], and as such further investigation is required. Where inhibitors of SaDHDPR and AvDHDPR may be limited to scaffolds for a co-factor bound enzyme, our results demonstrate that a wider range of scaffolds could be investigated against the PaDHDPR enzyme, as this site is not co-factor dependent. Recent *in silico* modelling studies have revealed that two sulfonamide diuretics used for hypertension bind to the NADPH binding site of dihydrofolate reductase and are hypothesised to exert their antihypertensive effects through antibacterial control of the gut microbiome [35]. This highlights the potential of the co-factor binding site as a druggable site, and my research into PaDHDPR co-factor binding helps elucidate this process.

5.2 Future Directions

5.2.1 Genetic Manipulation and Investigation

The ultimate goal of chemical inhibition through drug development is to elicit a desired cellular phenotype [36], which in the case of antibiotics, is either bacterial growth inhibition or death. Genetic knockouts or knockdowns are used to assess if the desired phenotype is possible by removal of the target protein, prior to the identification of drug-like compounds [36]. Here we described the phenotypic characterisation of a *dapB* knockout in *P. aeruginosa*, which was shown to be lethal without adequate supplementation (Chapter 4). However, further investigation is required to fully ascertain the effects of DAP pathway alterations in *P. aeruginosa*. The knockout described in Chapter 4 was a seamless gene knockout, indicating that there is no partially functional enzyme remaining. While this was critical in determining the essentiality of the gene, future drug inhibition may fail to completely inhibit enzyme activity at desirable concentrations. To assess the effect of partial inhibition, enzyme activity has to be reduced but not completely eliminated *in vivo*. This could potentially be achieved by varying the expression of *dapB* using the complementation plasmid designed in Chapter 4, however it is unclear whether expression levels could be reduced sufficiently and accurately enough with this approach. Alternatively, to gain a more tightly regulated control of expression, known as “tuneable” expression, techniques such as RNA knockdown could be used. One method to generate RNA knockdowns within bacteria is through the generation of small RNA (sRNA) regulators, which have short 6-8 bp complementary regions to the mRNA of interest [37]. The binding of the sRNAs can then block translation by preventing interaction with the ribosome [37]. This allows for transcriptional control over the gene, without a complete knockout of function [37]. Sharma and colleagues demonstrated this protocol on a potential antibiotic target, *recA*, in *E. coli* [38]. By lowering the translation level of *recA*, phenotypic characterisation revealed diminished swarming motility that is implicated in pathogenesis, and increased susceptibility to the fluoroquinolone ciprofloxacin [38]. Importantly, prior to this research, *recA* had only been characterised using complete gene knockouts, where this study provided tuneable and a more diverse investigation into the *recA* deficient phenotype, potentially more accurately representing chemical inhibition [38].

While RNA knockdown alters gene expression at the mRNA level, CRISPRi allows for reduced expression at the genomic level. Traditional CRISPR gene modifications are inapplicable for most bacterial strains, however, CRISPRi has been optimised for several bacterial species including *E. coli* [39] and *B. subtilis* [40]. It involves an inactivated Cas9

nuclease (Cas9d) and the use of a single guide RNA homologous to the gene of interest [39,40]. Once both bind to the genome, RNA transcription elongation is blocked and the gene is silenced without modification [39,40]. More recently, this was optimised for use in *Pseudomonas putida* and is believed to be applicable to more clinically relevant *Pseudomonas* strains, including *P. aeruginosa* [41]. Using either RNA knockdown or CRISPRi on the *dapA* and *dapB* genes within *P. aeruginosa*, *A. baumannii* and *K. pneumoniae* would provide valuable insight into the physiological roles of these genes.

5.2.2 Phenotypic Characterisation of Mutant Strains

5.2.2.1 Assessment of Bacterial Fitness

The *dapB* knockout experiments described in Chapter 4 demonstrated the essentiality of DHDPR in *P. aeruginosa*. However, due to the lethality of the knockout, the effects of the absence of DHDPR on biological processes could not be further investigated. As mentioned previously, a drug may bind transiently or not completely inhibit the enzyme. Therefore, characterisation of so-called tuneable mutants mentioned above could help determine the expected phenotype of a partially inhibited bacterial strain.

In Chapter 4, we used minimal media with and without supplemented *meso*-DAP to assess for essentiality using growth curves. Whilst this is useful for demonstrating essentiality, more comprehensive growth curve experiments can be performed to further characterise a DHDPR deficiency. Such growth curve experiments typically involve altering the carbon source, nitrogen source and types of metal and antibiotic stress [42]. A comparison of the growth curves from these conditions can also lead to the identification of “co-fitness”, in which we can identify genes with a similar fitness pattern [42]. In the DAP pathway, the observation of co-fitness between each of the genes would suggest a similar phenotype could be observed with chemical inhibition of the different enzymes. However, typical growth curves represent bacterial growth while in media suspension, which is not always the most accurate mimic of a host environment. The pathogenic bacteria in this thesis, *P. aeruginosa*, *A. baumannii* and *K. pneumoniae*, tend to form biofilms, which significantly contribute to their pathogenicity and antibiotic resistance *in vivo* [43,44]. As such, it is important to assess biofilm formation in mutant strains. This can be done both qualitatively and quantitatively. Qualitative measurements include estimating the dry mass, total carbon mass, or crystal violet staining of adhered bacterial cultures. However, these methods assume a direct correlation of the substance

being measured to biofilm forming cells [45]. While more time consuming and laborious, quantitative methods involve direct cell counting by using techniques such as colony forming unit determination, flow cell counting or microscopy [45]. This eliminates the effect of extraneous variables such as cell debris from impacting the outcome [45]. Given that biofilms are implicated in up to 80% of chronic infections, agents that prevent biofilm formation are highly sought after [46]. Using the techniques described above, we can characterise the effects of mutations in the DAP pathway on biofilm formation. If it was observed that the bacteria were either unable to form a biofilm or there was a depletion in biofilm mass, this would indicate that there is a potential for DAP pathway inhibitors to be used as anti-biofilm agents. These agents, which may lack bactericidal effects alone, represent a promising avenue for adjuvant therapy to allow for the potentiation of existing antibiotics that are currently ineffective against biofilms [46].

As the DAP pathway plays an important role upstream of cell wall synthesis, future experiments should also investigate if there are any changes in cell wall permeability associated with DAP pathway mutants. To determine increases in cell membrane permeability, leakage of ATP, potassium and magnesium ions are often measured, as well as using electron micrographs to visualise the cell membrane [47]. Potassium and magnesium leakage can be measured via inductively coupled plasma mass spectrometry to determine the ion concentration within the supernatant of a bacterial culture [47]. Additionally, bioluminescence can be used to assess ATP leakage, using an interaction of the ATP in the supernatant with the fluorescent molecule luciferase [48]. Scanning electron micrographs then allow for visualisation of detailed morphology and the structure of bacterial cells [49]. Any changes in the cells resulting from the elimination of DAP pathway function could elucidate the mechanism of the antimicrobial effect observed. Moreover, an increase in cell wall permeability would indicate potential synergy with current antibiotics that cannot breach the cell membrane [50], as discussed later.

The relevance of these changes to survival rates, biofilm formation and cell wall permeability could also be assessed in a mouse infection model. Similar to what was performed for the *Yersinia pestis* *dapA* knockout [51], assessing the wildtype and mutant strains in a *P. aeruginosa* lung infection model would reveal the potential effects of chemical inhibition within a living system and reveal the propensity of mutant strains to scavenge the essential nutrients required.

5.2.2.2 Directed Inhibitor Screening

Historically, antibiotic screening methods involved whole cell screening assays, where drug-like fragments were screened against bacterial cultures and antibacterial activity was selected for with no knowledge of the cellular target [52]. Any potential hits were then optimised for improved pharmacological properties and potency [52]. This method is limited however, as many obsolete or toxic compounds are repeatedly identified [52]. Since significant advances have been made in genetic manipulation, antibiotic screening has now focused on more target directed approaches. A genetic knockout or knockdown of a gene can be used for two different screening techniques: determining the mode of action of a compound from a library screen or using a mutant strain to assess for synergy.

Whole cell assays using live bacteria are advantageous as any antibacterial compounds would have been able to bypass the intrinsic resistance afforded by the cell membrane and efflux pumps and exert their effects [52]. This enables researchers to begin lead optimisation with a compound that has known biological activity [52]. However, this method can result in the target of successful compounds being unknown. By having a mutant bacterial strain lacking a functional enzyme, in this case DHDPR, it would allow for the selection of DHDPR-specific inhibitors. As drug-like fragments are typically small, they can have off target effects that cause human toxicity if a human homologue is inhibited. Therefore, by determining DHDPR specificity, this would reduce the chances of toxicity. A caveat to this experiment is that external supplementation could not be used, as it would rescue other potential targets in the DAP pathway. The rescue plasmid described in Chapter 4 could be employed to overcome this issue. Successful examples of this approach include the determination of the mode of action for the antibiotic fosfomycin and the biocide triclosan. By screening a genetic library of *E. coli* mutants that conferred fosfomycin resistance, Marquardt and colleagues were able to determine that it targets the MurZ enzyme involved in peptidoglycan synthesis [53]. Moreover, triclosan was found to target fatty acid synthesis when screening against a mutant genomic library with a missense mutation in the *fabI* gene conferring resistance [54]. In another example, as opposed to starting with an inhibitor and determining the mode of action, natural product inhibitors of fatty acid synthesis in *S. aureus* were determined by screening compounds using antisense RNA against the mRNA of the key enzymes FabH and FabF and noting resistance [55].

As mentioned, this approach can also be used to assess for synergy with other antibiotic classes. Recently, there has been a resurgence in the investigation of compounds that re-sensitise

bacteria to known antibiotics [56]. This allows for the development of inhibitors that may lack antibacterial activity on their own but can be used in combination with existing drugs that would have otherwise been ineffective [56]. As the cell wall of Gram-negative bacteria represents a significant barrier [50], many synergistic strategies focus on permeabilising the cell wall to allow better passage of antibiotics. One example is the use of cell wall hydrolases, in which synergy is observed by enhanced penetration of existing antibiotics [57]. This is usually tested for using a checkerboard assay, in which two drugs are titrated against one another and observed for potentiation [58]. This has recently been optimised to test synergy of up to three drugs simultaneously using a diagonal plate set up [59]. These methods allow for specific DAP pathway inhibitors to be screened more thoroughly. However, until the mutant libraries described above can be generated, traditional drug discovery studies can still be conducted in the hopes of finding new inhibitory molecules.

5.2.3 Inhibitor Discovery

As described in Section 1.1, the discovery of several antibiotics was achieved using time and labour-intensive screens of natural product libraries for antibacterial activity [51]. With the technical advances in drug development, more streamlined methods are now available, including high throughput and *in silico* screening against a select target, both of which are applicable to identify inhibitors of DHDPS and DHDPR.

By definition, a high throughput screen allows for the assessment of many, often small, compounds against a bacterial culture or target for a desired phenotype, such as inhibition or cell death [60]. In the case of screening against a specific target, this process relies on the ability to accurately detect the desired phenotype in a high throughput manner, allowing quick determination of successful or unsuccessful compounds [60]. For DHDPS, this is possible using the colourimetric *o*-ABA assay, which was employed in Chapters 2 and 3 for the assessment of DHDPS activity [61]. For a high throughput DHDPS chemical screen, this assay can be used to assess for DHDPS inhibition, with a purple colour indicating a functional enzyme, while absence of colour indicates inhibition. In recent years, a high throughput chemical screen was performed against DHDPS using this assay, with the hit compound CT1-2 identified (Matthew Perugini, *pers. comms.* Appendix II). Structural optimisation of this hit compound resulted in CT1-5, a small molecule inhibitor with improved potency against EcDHDPS with a co-crystal structure showing binding within the active site (Tatiana Soares

da Costa, *pers. comms.*). As demonstrated in Chapter 3, there is a high level of structural similarity between the active site of EcDHDPS, PaDHDPS2, KpDHDPS and AbDHDPS. As such, to investigate if this structural similarity allowed for broad-spectrum inhibition of these bacterial DHDPS enzymes, I tested CT1-5 against PaDHDPS1&2, KpDHDPS and AbDHDPS *in vitro* (Figure 1). Minimal remaining catalytic activity was observed for the orthologues at 1 mM CT1-5, with an $IC_{50} < 0.5$ mM against all orthologues tested.

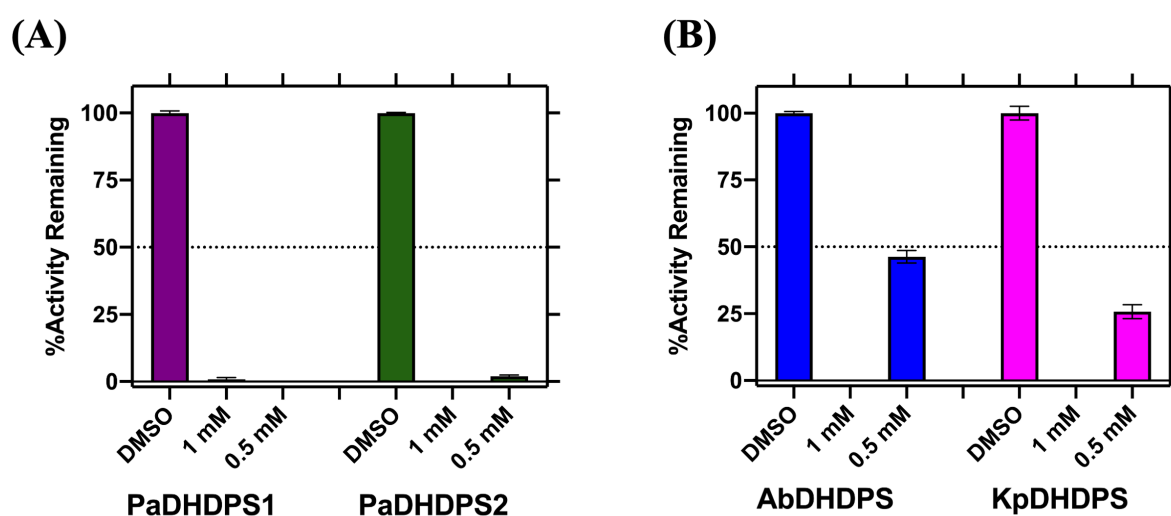


Figure 1. Inhibition of DHDPS enzymes by the active site inhibitor, CT1-5. Activity remaining (%) of (A) *P. aeruginosa* DHDPS isoforms 1 & 2 (PaDHDPS1 & PaDHDPS2) and (B) *K. pneumoniae* DHDPS (KpDHDPS) and *A. baumannii* DHDPS (AbDHDPS) in the DHDPS-DHDPR coupled assay when incubated with 1 mM CT1-5, 0.5 mM CT1-5 or 1% (v/v) DMSO as a vehicle control ($n=3$, \pm SD). Method is reported in Appendix III.

Previous inhibitor studies of DHDPS and DHDPR enzymes have shown some similarity in compounds that inhibit the active site of both enzymes (Section 1.3.4). This is in conjunction with previous research showing preliminary evidence for substrate channelling between DHDPS and DHDPR [62]. To this end, as CT1-5 was indicated as a DHDPS active site inhibitor, its inhibitory effects were also tested against PaDHDPR (Fig. 2). Complete inhibition was seen at both concentrations tested, indicating an $IC_{50} < 0.5$ mM, as observed with PaDHDPS1&2 above. Further investigation was conducted using antibacterial assays, with the minimal inhibitory concentration of CT1-5 determined against several *P. aeruginosa* strains (data courtesy of Tatiana Soares da Costa, *pers. comms.*, Appendix IV). Excitingly, growth

inhibition was observed for all strains tested with CT1-5, resulting in a lethal concentration of $64\ \mu\text{g}\cdot\text{ml}^{-1}$ regardless of the resistance profile. Moreover, this represents the first DAP pathway inhibitor with antibacterial activity, providing crucial information for future inhibitor optimisation. Continued investigation is still required to assess its potential broad-spectrum inhibition against *A. baumannii* and *K. pneumoniae* strains.

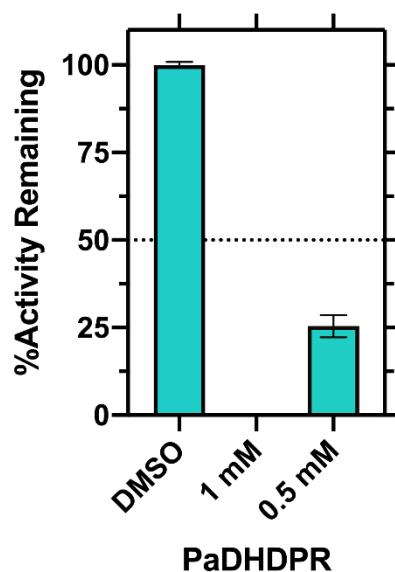


Figure 2. CT1-5 inhibition of PaDHDPR. *In vitro* inhibition of PaDHDPR with CT1-5. Activity remaining (%) of *P. aeruginosa* DHDPR (PaDHDPR) in the presence of 1 mM CT1-5, 0.5 mM CT1-5 or a DMSO control (n=3, \pm SD). Method is reported in Appendix III.

Whilst CT1-5 represents a promising compound for antibiotic development, further optimisation is required to improve its *in vitro* and *in vivo* potency. As described above, SAR optimisation can be used to investigate the effect of different functional groups and chemical extensions during analogue generation. Ideally, the expansion of CT1-5 within the binding pocket would increase potency by strengthening the interacting bonds, thus reducing disassociation [63–65]. As we have crystallised and refined the structure of KpDHDPS here (Chapter 3), this can now be utilised for co-crystallisation studies, alongside EcDHDPS, to identify any inter-species variation in inhibitor binding. Depending on the results obtained, this could allow for either an increase in broad-spectrum activity or species specificity. Alternatively, recent advancements in machine learning and simulation technology have increased the usability and accessibility of *in silico* screening as an alternate method of

optimisation. *In silico* screening provides the opportunity for both high throughput virtual screening of compound libraries, as well as lead optimisation through 3D pharmacophore mapping [66]. Pharmacophore mapping is the retrieval of similar novel compounds from a database that suit the 3D arrangement of functional groups required [66]. Improvements have been made to the search algorithms used in this process, making it one of the most successful tools in drug design and optimisation [66]. These optimisation tools can increase the potency of CT1-5 both *in vitro* and *in vivo* against various DHDPS and DHDPR enzymes. These tools also allow for increased species specificity by exploiting the enzymatic differences that have been demonstrated in this thesis.

5.3 Summary

Previous inhibition attempts of DHDPS and DHDPR enzymes have failed to result in compounds with antibacterial activity. We hypothesised that this could be due to a lack of knowledge surrounding the similarities and differences of DHDPS isoforms from pathogenic species. Therefore, this thesis aimed to identify, characterise and provide crucial tools for future drug discovery research against these pathogens. The studies described here were the first to utilise a key signature motif to identify bacterial DHDPS enzymes, among a variety of mis-annotated genes. This allows for more streamlined bioinformatic identification of *bona fide* DHDPS enzymes in the future, reducing the risk of a mis-annotated protein being investigated. Furthermore, the confirmed DHDPS enzymes from *P. aeruginosa*, *A. baumannii* and *K. pneumoniae* were structurally and functionally characterised, showing similarities and differences between species that can be considered and exploited for both narrow-spectrum and broad-spectrum inhibition. Finally, the DHDPR enzyme from *P. aeruginosa* was shown to be an essential protein for bacterial survival, indicating that chemical inhibition of the DAP pathway should result in a lethal phenotype. Altogether, this work significantly contributes to future DAP pathway inhibition attempts, including the optimisation of CT1-5 beyond *E. coli* and against these clinically relevant bacteria, in the pursuit for antibacterial agents with a novel mode of action to tackle our antibiotic resistance crisis.

5.4 References

- 1 Hutton CA, Perugini MA & Gerrard JA (2007) Inhibition of lysine biosynthesis: an evolving antibiotic strategy. *Mol Biosyst* **3**, 458–465.
- 2 Dogovski C, Atkinson SC, Dommaraju SR, Downton M, Hor L, Moore S, Paxman JJ, Peverelli MG, Qiu TW & Reumann M (2012) Enzymology of bacterial lysine biosynthesis. In *Biochemistry (D Ekinici, ed.)* InTech Open Access Publisher, London, UK.
- 3 Schnoes AM, Brown SD, Dodevski I & Babbitt PC (2009) Annotation error in public databases: misannotation of molecular function in enzyme superfamilies. *PLOS Comp Biol* **5**, e1000605.
- 4 Dogovski C, Gorman MA, Ketaren NE, Praszquier J, Zammit LM, Mertens HD, Bryant G, Yang J, Griffin MDW, Pearce FG, Gerrard JA, Jameson GB, Parker MW, Robins-Browne RM & Perugini MA (2013) From knock-out phenotype to three-dimensional structure of a promising antibiotic target from *Streptococcus pneumoniae*. *PLOS ONE* **8**, e83419.
- 5 Paiva AM, Vanderwall DE, Blanchard JS, Kozarich JW, Williamson JM & Kelly TM (2001) Inhibitors of dihydrodipicolinate reductase, a key enzyme of the diaminopimelate pathway of *Mycobacterium tuberculosis*. *Biochim Biophys Acta Protein Struct Mol Enzymol* **1545**, 67–77.
- 6 Sasai Y, Tozawa Y & Watanabe Y (2012) Identification and Characterization of d-Hydroxyproline Dehydrogenase and Δ^1 -Pyrroline-4-hydroxy-2-carboxylate Deaminase Involved in Novel l-Hydroxyproline Metabolism of Bacteria. *J Biol Chem* **287**, 32674–32688.
- 7 Majee M, Wu S, Salaita L, Gingerich D, Dirk LMA, Chappell J, Hunt AG, Vierstra R & Downie AB (2017) A misannotated locus positively influencing Arabidopsis seed germination is deconvoluted using multiple methods, including surrogate splicing. *Plant Gene* **10**, 74–85.
- 8 Linial M (2003) How incorrect annotations evolve – the case of short ORFs. *Trends Biotechnol* **21**, 298–300.
- 9 Jabbari K, Cruveiller S, Clay O, Le Saux J & Bernardi G (2004) The new genes of rice: a closer look. *Trends Plant Sci* **9**, 281–285.
- 10 Desbois S, John UP & Perugini MA (2018) Dihydrodipicolinate synthase is absent in fungi. *Biochimie* **152**, 73–84.

- 11 Naumoff DG, Xu Y, Glansdorff N & Labedan B (2004) Retrieving sequences of enzymes experimentally characterized but erroneously annotated: the case of the putrescine carbamoyltransferase. *BMC Genomics* **5**, 52.
- 12 Winsor GL, Griffiths EJ, Lo R, Dhillon BK, Shay JA & Brinkman FSL (2016) Enhanced annotations and features for comparing thousands of *Pseudomonas* genomes in the *Pseudomonas* genome database. *Nucleic Acids Res* **44**, D646-653.
- 13 Werneburg M, Zerbe K, Juhas M, Bigler L, Stalder U, Kaech A, Ziegler U, Obrecht D, Eberl L & Robinson JA (2012) Inhibition of lipopolysaccharide transport to the outer membrane in *Pseudomonas aeruginosa* by peptidomimetic antibiotics. *ChemBioChem* **13**, 1767–1775.
- 14 Baba T, Ara T, Hasegawa M, Takai Y, Okumura Y, Baba M, Datsenko KA, Tomita M, Wanner BL & Mori H (2006) Construction of *Escherichia coli* K-12 in-frame, single-gene knockout mutants: the Keio collection. *Mol Syst Biol* **2**, 2006.0008.
- 15 Cain AK, Barquist L, Goodman AL, Paulsen IT, Parkhill J & van Opijnen T (2020) A decade of advances in transposon-insertion sequencing. *Nat Rev Genet* **21**, 526–540.
- 16 Chao MC, Abel S, Davis BM & Waldor MK (2016) The design and analysis of transposon-insertion sequencing experiments. *Nat Rev Microbiol* **14**, 119–128.
- 17 Molina-Henares MA, Torre JDL, García-Salamanca A, Molina-Henares AJ, Herrera MC, Ramos JL & Duque E (2010) Identification of conditionally essential genes for growth of *Pseudomonas putida* KT2440 on minimal medium through the screening of a genome-wide mutant library. *Environ Micro* **12**, 1468–1485.
- 18 Richaud C & Printz C (1988) Nucleotide sequence of the *dapF* gene and flanking regions from *Escherichia coli* K12. *Nucleic Acids Res* **16**, 10367.
- 19 Liberati NT, Urbach JM, Miyata S, Lee DG, Drenkard E, Wu G, Villanueva J, Wei T & Ausubel FM (2006) An ordered, nonredundant library of *Pseudomonas aeruginosa* strain PA14 transposon insertion mutants. *Proc Nat Acad Sci* **103**, 2833–2838.
- 20 Skurnik D, Roux D, Aschard H, Cattoir V, Yoder-Himes D, Lory S & Pier GB (2013) A comprehensive analysis of *in vitro* and *in vivo* genetic fitness of *Pseudomonas aeruginosa* using high-throughput sequencing of transposon libraries. *PLOS Pathog* **9**, e1003582.
- 21 Lee SA, Gallagher LA, Thongdee M, Staudinger BJ, Lippman S, Singh PK & Manoil C (2015) General and condition-specific essential functions of *Pseudomonas aeruginosa*. *Proc Nat Acad Sci* **112**, 5189–5194.

- 22 Turner KH, Wessel AK, Palmer GC, Murray JL & Whiteley M (2015) Essential genome of *Pseudomonas aeruginosa* in cystic fibrosis sputum. *Prot Nat Acad Sci* **112**, 4110–4115.
- 23 Poulsen BE, Yang R, Clatworthy AE, White T, Osmulski SJ, Li L, Penaranda C, Lander ES, Shores N & Hung DT (2019) Defining the core essential genome of *Pseudomonas aeruginosa*. *Prot Nat Acad Sci* **116**, 10072–10080.
- 24 Peverelli MG, Costa TPS da, Kirby N & Perugini MA (2016) Dimerization of bacterial diaminopimelate decarboxylase is essential for catalysis. *J Biol Chem* **291**, 9785–9795.
- 25 Schnell R, Oehlmann W, Sandalova T, Braun Y, Huck C, Maringer M, Singh M & Schneider G (2012) Tetrahydrodipicolinate N-succinyltransferase and dihydrodipicolinate synthase from *Pseudomonas aeruginosa*: structure analysis and gene deletion. *PLOS ONE* **7**, e31133.
- 26 Wang N, Ozer EA, Mandel MJ & Hauser AR (2014) Genome-wide identification of *Acinetobacter baumannii* genes necessary for persistence in the lung. *mBio* **5**, e01163-14.
- 27 Ramage B, Erolin R, Held K, Gasper J, Weiss E, Brittnacher M, Gallagher L & Manoil C (2017) Comprehensive arrayed transposon mutant library of *Klebsiella pneumoniae* outbreak strain KPNIH1. *J Bacteriol* **199**, e00352-17.
- 28 Skovpen YV, Conly CJT, Sanders DAR & Palmer DRJ (2016) Biomimetic design results in a potent allosteric inhibitor of dihydrodipicolinate synthase from *Campylobacter jejuni*. *J Am Chem Soc* **138**, 2014–2020.
- 29 Cirilli M, Zheng R, Scapin G & Blanchard JS (2003) The three-dimensional structures of the *Mycobacterium tuberculosis* dihydrodipicolinate reductase–NADH–2,6-PDC and –NADPH–2,6-PDC complexes. Structural and mutagenic analysis of relaxed nucleotide specificity. *Biochemistry* **42**, 10644–10650.
- 30 Scapin G, Blanchard JS & Sacchettini JC (1995) Three-dimensional structure of *Escherichia coli* dihydrodipicolinate reductase. *Biochemistry* **34**, 3502–3512.
- 31 Reddy SG, Sacchettini JC & Blanchard JS (1995) Expression, purification, and characterization of *Escherichia coli* dihydrodipicolinate reductase. *Biochemistry* **34**, 3492–3501.
- 32 Christensen JB, Soares da Costa TP, Faou P, Pearce FG, Panjekar S & Perugini MA (2016) Structure and function of cyanobacterial DHDPS and DHDPR. *Sci Rep* **6**, 37111.

- 33 Dommaraju SR, Dogovski C, Czabotar PE, Hor L, Smith BJ & Perugini MA (2011) Catalytic mechanism and cofactor preference of dihydrodipicolinate reductase from methicillin-resistant *Staphylococcus aureus*. *Arch Biochem Biophys* **512**, 167–174.
- 34 Coulter CV, Gerrard JA, Kraunsoe JAE & Pratt AJ (1999) *Escherichia coli* dihydrodipicolinate synthase and dihydrodipicolinate reductase: kinetic and inhibition studies of two putative herbicide targets. *J Pest Sci* **55**, 887–895.
- 35 Kaur S, Bhattacharyya R & Banerjee D (2020) Hydrochlorothiazide and indapamide bind the NADPH binding site of bacterial dihydrofolate reductase: results of an in-silico study and their implications. *In Silico Pharmacol* **8**, 5.
- 36 Copeland RA (2013) *Evaluation of Enzyme Inhibitors in Drug Discovery: A Guide for Medicinal Chemists and Pharmacologists*, 2nd ed. John Wiley & Sons, Incorporated, Somerset, United States.
- 37 Gottesman S & Storz G (2011) Bacterial small RNA regulators: versatile roles and rapidly evolving variations. *Cold Spring Harb Perspect Biol* **3**, a003798.
- 38 Sharma V, Sakai Y, Smythe KA & Yokobayashi Y (2013) Knockdown of *recA* gene expression by artificial small RNAs in *Escherichia coli*. *Biochem Biophys Res Comm* **430**, 256–259.
- 39 Qi LS, Larson MH, Gilbert LA, Doudna JA, Weissman JS, Arkin AP & Lim WA (2013) Repurposing CRISPR as an RNA-guided platform for sequence-specific control of gene expression. *Cell* **152**, 1173–1183.
- 40 Peters JM, Colavin A, Shi H, Czarny TL, Larson MH, Wong S, Hawkins JS, Lu CHS, Koo B-M, Marta E, Shiver AL, Whitehead EH, Weissman JS, Brown ED, Qi LS, Huang KC & Gross CA (2016) A comprehensive, CRISPR-based functional analysis of essential genes in bacteria. *Cell* **165**, 1493–1506.
- 41 Batianis C, Kozaeva E, Damalas SG, Martín-Pascual M, Volke DC, Nikel PI & Santos VAPM dos (2020) An expanded CRISPRi toolbox for tunable control of gene expression in *Pseudomonas putida*. *Microb Biotech* **13**, 368–385.
- 42 Price MN, Wetmore KM, Waters RJ, Callaghan M, Ray J, Liu H, Kuehl JV, Melnyk RA, Lamson JS, Suh Y, Carlson HK, Esquivel Z, Sadeeshkumar H, Chakraborty R, Zane GM, Rubin BE, Wall JD, Visel A, Bristow J, Blow MJ, Arkin AP & Deutschbauer AM (2018) Mutant phenotypes for thousands of bacterial genes of unknown function. *Nature* **557**, 503–509.
- 43 Hall CW & Mah T-F (2017) Molecular mechanisms of biofilm-based antibiotic resistance and tolerance in pathogenic bacteria. *FEMS Microbiol Rev* **41**, 276–301.

- 44 Taylor PK, Yeung ATY & Hancock REW (2014) Antibiotic resistance in *Pseudomonas aeruginosa* biofilms: Towards the development of novel anti-biofilm therapies. *J Biotech* **191**, 121–130.
- 45 Wilson C, Lukowicz R, Merchant S, Valquier-Flynn H, Caballero J, Sandoval J, Okuom M, Huber C, Brooks TD, Wilson E, Clement B, Wentworth CD & Holmes AE (2017) Quantitative and qualitative assessment methods for biofilm growth: A mini-review. *Res Rev J Eng Technol* **6**, e2319-9873.
- 46 Monroe D (2007) Looking for chinks in the armor of bacterial biofilms. *PLOS Biology* **5**, e307.
- 47 Zhang YQ, Wu QP, Zhang JM & Yang XH (2011) Effects of ozone on membrane permeability and ultrastructure in *Pseudomonas aeruginosa*. *Journal of Applied Microbiology* **111**, 1006–1015.
- 48 Shama G & Malik DJ (2013) The uses and abuses of rapid bioluminescence-based ATP assays. *Int J Hyg Enviro Health* **216**, 115–125.
- 49 Diao HF, Li XY, Gu JD, Shi HC & Xie ZM (2004) Electron microscopic investigation of the bactericidal action of electrochemical disinfection in comparison with chlorination, ozonation and Fenton reaction. *Process Biochem* **39**, 1421–1426.
- 50 Impey RE, Hawkins DA, Sutton JM & Soares da Costa TP (2020) Overcoming intrinsic and acquired resistance mechanisms associated with the cell wall of Gram-negative bacteria. *Antibiotics (Basel)* **9**, 623.
- 51 Bland M, Eisele NA, Keleher LL, Anderson PE & Anderson DM (2011) Novel genetic tools for diaminopimelic acid selection in virulence studies of *Yersinia pestis*. *PLoS ONE* **6**, e17352.
- 52 Miesel L, Greene J & Black TA (2003) Genetic strategies for antibacterial drug discovery. *Nat Rev Gen* **4**, 442–456.
- 53 Marquardt JL, Siegele DA, Kolter R & Walsh CT (1992) Cloning and sequencing of *Escherichia coli* murZ and purification of its product, a UDP-N-acetylglucosamine enolpyruvyl transferase. *J Bacteriol* **174**, 5748–5752.
- 54 Heath RJ, Yu Y-T, Shapiro MA, Olson E & Rock CO (1998) Broad spectrum antimicrobial biocides target the FabI component of fatty acid synthesis. *J Biol Chem* **273**, 30316–30320.
- 55 Young K, Jayasuriya H, Ondeyka JG, Herath K, Zhang C, Kodali S, Galgoci A, Painter R, Brown-Driver V, Yamamoto R, Silver LL, Zheng Y, Ventura JI, Sigmund J, Ha S, Basilio A, Vicente F, Tormo JR, Pelaez F, Youngman P, Cully D, Barrett JF, Schmatz

- D, Singh SB & Wang J (2006) Discovery of FabH/FabF inhibitors from natural products. *Antimicrob Agents Chemother* **50**, 519–526.
- 56 Wright GD (2016) Antibiotic adjuvants: Rescuing antibiotics from resistance. *Trends Microbiol* **24**, 862–871.
- 57 Wittekind M & Schuch R (2016) Cell wall hydrolases and antibiotics: exploiting synergy to create efficacious new antimicrobial treatments. *Curr Opin Microbiol* **33**, 18–24.
- 58 Hsieh MH, Yu CM, Yu VL & Chow JW (1993) Synergy assessed by checkerboard a critical analysis. *Diag Microbiol Infect Dis* **16**, 343–349.
- 59 Cokol-Cakmak M, Bakan F, Cetiner S & Cokol M (2018) Diagonal method to measure synergy among any number of drugs. *JoVE* **136**, e57713.
- 60 Pereira DA & Williams JA (2007) Origin and evolution of high throughput screening. *Brit J Pharmacol* **152**, 53–61.
- 61 Yugari Y & Gilvarg C (1965) The condensation step in diaminopimelate synthesis. *J Biol Chem* **240**, 4710–4716.
- 62 Christensen JB (2017) Structure and interactions of enzymes functioning in the diaminopimelate biosynthesis pathway. *PhD Thesis, La Trobe University, Victoria, Australia*.
- 63 Nantasenamat C, Isarankura-Na-Ayudhya C, Naenna T & Prachayasittikul V (2009) A practical overview of quantitative structure-activity relationship. *EXCLI* **8**, 15.
- 64 Murray CW & Blundell TL (2010) Structural biology in fragment-based drug design. *Curr Opin Struct Biol* **20**, 497–507.
- 65 Thomas SE, Collins P, James RH, Mendes V, Charoensutthivarakul S, Radoux C, Abell C, Coyne AG, Floto RA, von Delft F & Blundell TL (2019) Structure-guided fragment-based drug discovery at the synchrotron: screening binding sites and correlations with hotspot mapping. *Philos T R Soc A* **377**, 20180422.
- 66 Wadood A, Shah L, Ahmad A, Hassan H & Shams S (2013) *In-silico* drug design: An approach which revolutionarised the drug discovery process. *OA Drug Design Deliv* **1**, 3.

Appendices

Appendix I

Review: Overcoming Intrinsic and Acquired Resistance Mechanisms Associated with the Cell Wall of Gram-Negative Bacteria

Copyright

This article was published in *Antibiotics*, Vol. 9(9), Impey, R. E., Hawkins, D. A., Sutton., J. M. & Soares da Costa, T. P., “Overcoming intrinsic and acquired resistance mechanisms associated with the cell wall of Gram-negative bacteria”, pp. 623, Copyright MDPI.

Under MDPI open access copyright policy, and the Creative Common CC BY licence, no permission is necessary for the reprinting of this article in this thesis.

Statement of Contribution

I confirm that Rachael Impey has made the following contributions:

- Conceptualisation and drafting of the manuscript (50%) in collaboration with Daniel Hawkins
- Preparation of figures
- Revisions of manuscript prior to acceptance

Tatiana Soares da Costa

Signed: —

Date: 14/12/2020

(Executive Author)

Review

Overcoming Intrinsic and Acquired Resistance Mechanisms Associated with the Cell Wall of Gram-Negative Bacteria

Rachael E. Impey ^{1,†}, Daniel A. Hawkins ^{1,†}, J. Mark Sutton ²  and Tatiana P. Soares da Costa ^{1,*}

¹ Department of Biochemistry and Genetics, La Trobe Institute for Molecular Science, La Trobe University, Melbourne, VIC 3086, Australia; reimpey@students.latrobe.edu.au (R.E.I.); daniel.hawkins@latrobe.edu.au (D.A.H.)

² National Infection Service, Research and Development Institute, Public Health England, Porton Down, Salisbury, Wiltshire SP4 0JG, UK; mark.sutton@phe.gov.uk

* Correspondence: T.SoaesdaCosta@latrobe.edu.au; Tel.: +61-3-9479-2227

† R.E.I. and D.A.H. are joint first authors.

Received: 2 September 2020; Accepted: 17 September 2020; Published: 19 September 2020



Abstract: The global increase in multi-drug-resistant bacteria is severely impacting our ability to effectively treat common infections. For Gram-negative bacteria, their intrinsic and acquired resistance mechanisms are heightened by their unique cell wall structure. The cell wall, while being a target of some antibiotics, represents a barrier due to the inability of most antibacterial compounds to traverse and reach their intended target. This means that its composition and resulting mechanisms of resistance must be considered when developing new therapies. Here, we discuss potential antibiotic targets within the most well-characterised resistance mechanisms associated with the cell wall in Gram-negative bacteria, including the outer membrane structure, porins and efflux pumps. We also provide a timely update on the current progress of inhibitor development in these areas. Such compounds could represent new avenues for drug discovery as well as adjuvant therapy to help us overcome antibiotic resistance.

Keywords: antibiotic discovery; antimicrobial resistance; cell wall; Gram-negative bacteria

1. Introduction

Antimicrobial resistance (AMR) represents one of the biggest threats facing modern medicine. If no action is taken, it is predicted that AMR will result in 10 million fatalities by the year 2050, which will largely be attributed to infections caused by Gram-negative bacteria (GNB) [1]. Depending on the level of resistance, GNB can be classified as either multi-drug resistant (MDR), extensively drug resistant (XDR) or pan-drug resistant (PDR), the latter displaying resistance to all antibiotic classes [2]. Recent studies have estimated that some nosocomial populations contain up to 34% XDR bacteria [3], with rising levels of XDR *Pseudomonas aeruginosa* being reported that are resistant to carbapenems as the last-resort antibiotic [4]. An alarming increase in clinical resistance has also been observed in *Acinetobacter baumannii* and *Klebsiella pneumoniae* [5]. This aligns with priority pathogen reports by the Centres for Disease Control and Prevention and the World Health Organisation, which highlight the urgent need for new antibiotics against these drug-resistant GNB [6,7]. Despite this, most new antibiotics, defined here as those that are in late-phase clinical trials, are variants of existing drugs or combinations of β -lactams and β -lactamase inhibitors, and as such, may still be subject to iterations of pre-existing resistance mechanisms [8].

One of the key mechanisms limiting antibiotic efficacy in GNB is the presence of a complex cell wall, consisting of an outer membrane and cytoplasmic membrane with differing physicochemical

properties, which are separated by a cross-linked peptidoglycan layer. This review will focus on the role that the cell wall plays in both intrinsic and acquired resistance mechanisms that limit the efficacy of many antibacterials in GNB, and the emerging novel strategies that are being developed to overcome them. Many of these focus on disrupting the complex mechanisms involved in the synthesis, assembly and maintenance of the dual-membrane system, which is essential to the integrity of GNB cells. Whilst this system is one of the major contributors to antibiotic resistance in GNB, there is a growing awareness that this might also be an Achilles' heel and provide important new targets for therapy.

2. Outer Membrane

Unlike Gram-positive bacteria, GNB have a hydrophobic outer membrane bilayer, containing lipopolysaccharide (LPS) molecules, phospholipids and outer membrane proteins (OMPs), including pore-forming proteins [9]. As such, this dynamic outer membrane acts as a barrier to several antibiotics that are typically effective against Gram-positive bacteria, such as vancomycin [10]. Most antimicrobials must traverse this outer membrane to reach their targets. Hydrophobic antibiotics, such as chloramphenicol and aminoglycosides, utilise a diffusion pathway through the lipids, but other hydrophobic and polar molecules may interact with LPS and have restricted entry [9,11]. Alterations of the outer membrane permeability influence the diffusion of hydrophobic antibiotics, which can result in poor uptake. For instance, in *P. aeruginosa*, mutations in the LPS transport pathway decreases membrane permeability, resulting in increased tobramycin resistance [11]. Hydrophilic antibiotics, including β -lactams, use channel proteins such as porins to gain entry into the periplasm [9,12], but molecules with cytoplasmic targets are restricted from entering the cytoplasm due to the inner membrane.

Alternatively, polymyxins and some cationic peptides exert their effects on the outer layer of the membrane itself by binding to the LPS and phospholipids, which destabilises the inner cell membrane [13]. Many bacteria that acquire polymyxin resistance through exposure to therapy, including *K. pneumoniae*, *Salmonella enterica*, *A. baumannii* and *P. aeruginosa*, exhibit overexpression of the *pmrCAB* operon (or species equivalent) [14–18]. One of the gene products, phosphoethanolamine transferase (PmrC), is responsible for the modification of lipid A [14–18]. This alteration lowers the negative charge of the LPS, resulting in varying levels of resistance to colistin and other polymyxins [14–18]. The regulatory complexes PmrAB, a two-component system (TCS) directly responsible for the regulation of PmrC, and PhoPQ have also been implicated in other lipid A resistance mechanisms [13,19,20]. This includes the addition of L-4-aminoarabinose, which reduces the dependency of LPS on the cross-bridging cations for stabilisation, and thus, blocks the self-promoted uptake ability of polymyxins [13,15]. The *pmrCAB* operon and/or the *arn* operon, which also mediate lipid modification, are proposed to play a role in intrinsic resistance to polymyxins in a number of clinical pathogens, including *Proteus mirabilis*, *Serratia marcescens*, *Burkholderia* spp. and *Yersinia* spp. [21–23]. The regulators of these lipid modifying enzymes mediate cell responses to different stresses and influence both drug resistance and virulence. Worryingly, these *pmrCAB* mutations can cause heteroresistance to polymyxins, including colistin. Heteroresistance occurs when a subpopulation of bacteria show resistance to certain antibiotics within a system that is generally considered to be susceptible [24,25]. Such phenomenon is often associated with breakdown in treatment and can lead to the proliferation of the resistant subpopulation and the emergence of a stable resistant strain, which may result in treatment failures [24,25]. Heteroresistance to colistin has been reported for several species, including *A. baumannii* [26], *K. pneumoniae* [27], *P. aeruginosa* [28], *Enterobacter cloacae* [29] and *Salmonella* spp. [30]. The mutations mentioned above and the role that they play in heteroresistance indicates that PmrAB could represent a relevant target for inhibitor development, which will be discussed below.

Significant interest has been focussed on another mechanism of acquired polymyxin resistance, mediated by a mobile colistin-resistance gene (*mcr-1*) and variants. This was originally described in *Escherichia coli* [31], but has been widely reported in other GNB isolates collected both before and after the original report [32]. The biochemical mechanism of resistance is similar to that mediated by PmrC as MCR1 protein is a probable phosphoethanolamine transferase, hypothesised to have originated

from an intrinsically resistant environmental strain (e.g., *Paenibacillus* spp.), but now disseminated globally due to its presence on a highly transmissible plasmid [31]. Another polymyxin resistance mechanism only described in *A. baumannii* is the complete loss of the LPS, mediated by disabling mutations in one of the *lpxACD* genes [33]. Further examples of outer membrane resistance include the up-regulation of the OMP OprH in *P. aeruginosa*, contributing to both aminoglycoside and colistin resistance [34], as well as resistance mediated by mutations in regulators of membrane stress responses in a variety of species [35–37].

Targeting outer membrane permeability has been considered an underexploited approach to enhance antibiotic susceptibility and prolong the effectiveness of first-line treatments in the clinic. Current treatments that improve membrane permeability based on synergy between licensed antibiotics involve either polymyxin B or colistin (polymyxin E) [38]. While polymyxins have shown promising synergistic effects in vitro against GNB, the overall concern lies with their associated nephrotoxic effects [39]. Despite this, MDR *A. baumannii* infections still rely heavily on the use of polymyxins as a primary treatment given the lack of alternative effective therapeutics [39]. There has been renewed interest in developing further polymyxin derivatives as candidate therapies, with considerable work taking place to optimise efficacy, reduce cytotoxicity and address issues with intrinsic and adaptive resistance [40].

One of the most well-known membrane permeabilisers, polymyxin B nonapeptide (PMBN) (Figure 1), has been used in in vitro studies since its discovery in 1992 [41]. Despite the lack of antibacterial activity, PMBN's ability to permeabilise the membrane allows resistant bacteria to be re-sensitised to several classes of antibiotics [41,42]. Moreover, reduced toxicity has been observed in animal models when compared to polymyxin B [43,44]. Thus, PMBN has become a valuable benchmark and building block for the development of polymyxin derivatives. Indeed, a polymyxin B analogue, SPR741 (originally named NAB741, Figure 1), displays synergy with rifampicin and clarithromycin in murine infections, and it has since completed phase I clinical trials [43,45]. Furthermore, the analogue SPR206 (Figure 1), which progressed from phase I clinical trials, displays antibacterial activity against several MDR GNB [46]. Despite historical concerns about nephrotoxicity, recent polymyxin analogues such as SPR206 do not appear to have cytotoxic effects, showing promise for future investigation into polymyxin-like compounds as potential membrane permeabilisers.

Recent development of other cyclic peptides termed octapeptins, which also permeabilise the outer membrane as at least part of their mechanism of action, has generated promising in vitro data even against MDR GNB strains that are resistant to polymyxins [47–49]. Octapeptins are structurally related to polymyxins, with analogues including octapeptin C4 (Figure 1) showing significant promise [49]. Indeed, where a 1000-fold reduction in antibacterial activity was observed for *K. pneumoniae* after continuous exposure to polymyxins B and E (colistin) in resistance studies, only a 4-fold decrease was seen for octapeptin C4 in the same timeframe [47]. Although a great effort has been made to elucidate the mode of action of these octapeptins, further investigation is needed to fully explore their potential as antibiotic treatments or adjuvants [47–49]. Recently, the non-profit funder, Carb-X, invested heavily in the ongoing research into octapeptins [50]. In other related strategies, an attempt to overcome already existing polymyxin resistance has been pursued through the investigation of the small molecule inhibitor dephostatin (Figure 1) [51]. Dephostatin has been shown to disrupt the signalling of TCSs, including PmrAB as previously described, and in doing so, re-sensitises *Salmonella* spp. to colistin and reduces virulence in both cell-based assays and animal models [51].

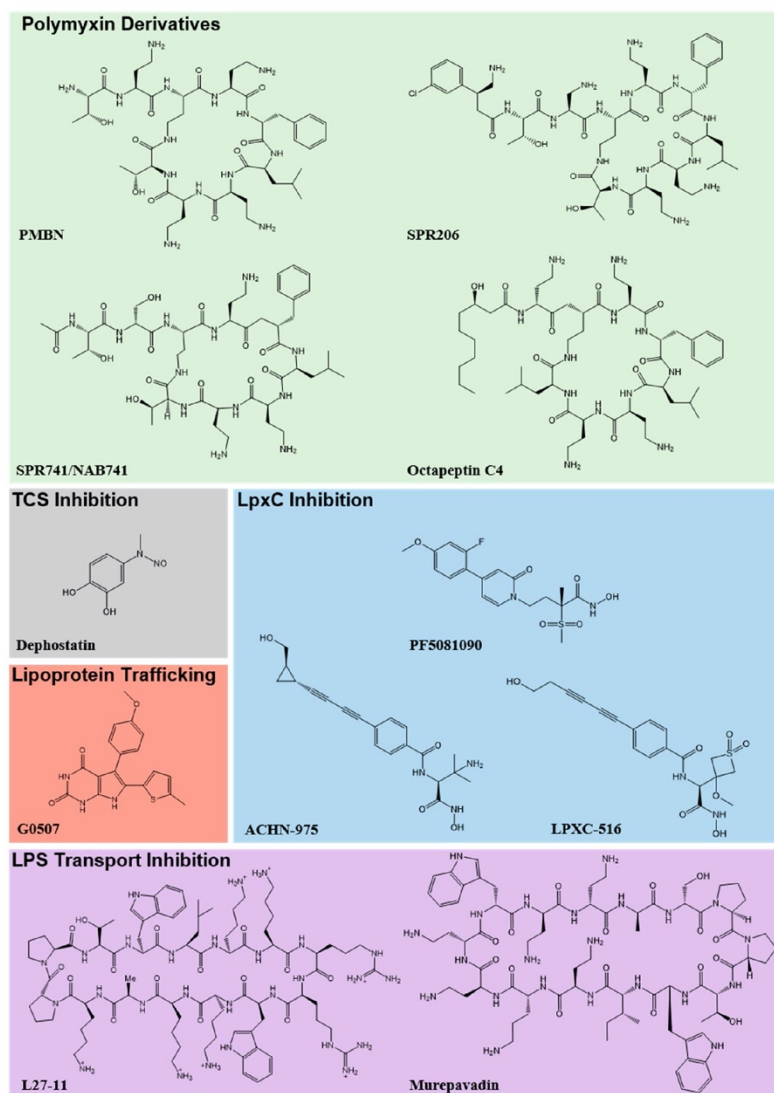


Figure 1. Outer Membrane Inhibitors. Polymyxin analogues (green), two-component system (TCS) (grey), lipoprotein trafficking (red), LpxC (blue) and LPS transport (purple) inhibitors. PMBN has been well characterised as a combinatorial agent that allows the disruption to the cell membrane to potentiate current antibiotics. SPR741/NAB741 and SPR206 are polymyxin B analogues that have lowered toxicity compared to the parent compound. Octapeptin C4 is structurally similar to polymyxins but has shown a slowed resistance profile compared to the parent compounds of polymyxins B and E. Dephostatin exhibits anti-virulence properties against *Salmonella* spp. by inhibiting both SsrA-SsB and PmrB-PmrA TCSs. G0507 is an inhibitor of the LolCDE ABC transporter in lipoprotein trafficking. PF5081090 and ACHN-975 were designed as LpxC inhibitors with efficacy in murine infection models against *P. aeruginosa*. LPXC-516 is an analogue of ACHN-975. L27-11 and murepavadin are macrocyclic peptidomimetic compounds that inhibit the enzyme LptD in the LPS transport pathway.

Alternative strategies have looked at targeting the major component of the outer membrane, the LPS layer. There are two main approaches for targeting the LPS layer—lipid A biosynthesis or LPS transport to the outer membrane. LpxC is the best characterised enzyme and a key regulator of lipid A biosynthesis, which is generally conserved across all GNB [52]. Research into LpxC inhibitors began before the discovery of the enzyme. However, early attempts were abandoned due to the lack of broad-spectrum activity [52]. Two lead compounds, PF5081090 and ACHN-975 (Figure 1), were developed by Pfizer and Achaogen, respectively, with both showing activity against *P. aeruginosa* in murine models [53,54]. ACHN-975 (Figure 1) is the only known LpxC inhibitor to have completed phase 1 clinical trials, but has not progressed further [55]. Analogues of ACHN-975 have been developed since, with LPXC-516 (Figure 1) showing the most promising activity against GNB, including *Enterobacteriaceae* [56]. However, concerns over cardiovascular toxicity have halted the development of these compounds [56].

In *A. baumannii*, mutational studies of the lipid biosynthetic enzymes LpxA, LpxC and LpxD unexpectedly revealed that LPS was not essential for growth, at least in this organism. On the contrary, a loss of functional LPS enzymes resulted in increased resistance to azithromycin, rifampicin and vancomycin [57]. Although mutations in these genes have resulted in colistin resistance [33,58], they have also been associated with a loss of fitness. This is linked to avirulence in a *Galleria melonella* model, coupled with increased biocide susceptibility [58]. Based on such observations, the LpxC inhibitor, PF5081090 (Figure 1), has been suggested as an anti-virulence strategy and repurposed as a synergistic agent to re-sensitise *A. baumannii* to current antibiotics through the permeabilisation of the outer membrane [59].

Beyond the biosynthetic pathway, the translocation of lipid A across the cytoplasmic membrane and transport of the LPS to the outer membrane mediated by the multi-protein Lpt complex are also attractive targets. Inhibition of this pathway was shown using a macrocyclic peptidomimetic compound (L27-11, Figure 1) that targets the LptD enzyme on the outer membrane [60], and displays antibacterial activity against *P. aeruginosa* [61]. Other macrocyclic peptides have also been used to target LptD in clinical trials. Murepavadin (Figure 1) demonstrated excellent in vitro efficacy against >1000 clinical MDR *P. aeruginosa* strains before successfully completing phases I and II clinical trials [62]. Investigation into intravenous administration was halted at phase III due to increased hepatic toxicity [63]. However, preclinical research into inhaled murepavadin is ongoing. Harrison et al. recently demonstrated that other mutants in this transport pathway resulted in aminoglycoside hypersensitivity in *P. aeruginosa* [64]. This study noted that mutations in the LptG enzyme could potentially interfere with the dimerisation of its LptB counterpart [64], highlighting its potential as a novel antibiotic target. A recent study has examined the role of the membrane transporter PbgA as a target for drug development and have identified its encoding gene to be essential for LPS biogenesis in *E. coli* [65]. Lipoprotein transporters, including the LolABCDE enzyme complex, have also been screened as novel targets. Recently, Nickerson et al. discovered a pyrrolpyrimidinedione inhibitor of LolCDE (G0507, Figure 1), which inhibits *E. coli* growth [66].

An additional target of interest is the Mla complex, which is responsible for maintaining the LPS-phospholipid asymmetry of the outer membrane. In a similar way to Lpt and Lol, this forms a multi-protein complex spanning the periplasm and is thought to remove mislocalised phospholipid from the outer leaflet, thus helping to maintain the integrity of the membrane barrier [67]. Mutations in the genes that encode the outer membrane MlaA protein, which closely associates with OmpC, a periplasmic protein MlaC, and an inner membrane ABC transporter MlaFEDB, have been shown to disrupt barrier function and could suggest these are potential targets for drug development. Interestingly, serial passage of a uropathogenic *E. coli* strain in the presence of arenicin-3 resulted in MlaC-associated resistance mutations, with the results supported by TraDIS data that showed enrichment of transposon mutations in mlaABCDEF in selected populations [68]. This suggests that MlaC could be the target for arenicin-3 and/or that enhanced activity of genes in this operon are a response to outer membrane disruption.

3. Peptidoglycan Layer and Inner Membrane

While the outer membrane represents a barrier to antibacterial compounds, it is only part of the mechanism of resistance in the cell wall complex. The peptidoglycan layer, which is found spanning the periplasmic space, is commonly used as a target for antibiotics due to its absence in humans. However, it has been hypothesised that the recycling of the peptidoglycan building blocks, often up-regulated in response to antibiotics, can activate secondary resistance mechanisms [69]. This includes the displacement of the UDP-MurNac-pentapeptide by anhydromuropeptides that are accumulated during β -lactam treatment [69]. In turn, this can disrupt the AmpR gene repression, causing the up-regulation of the β -lactamase AmpC and altered regulation of the MexEF efflux pump, which will be discussed in Section 5 [69].

There have been serious concerns over increasing reports of resistance to antibiotics that target the peptidoglycan layer. One approach to negate such resistance mechanisms is to move upstream of the peptidoglycan layer and look at the synthesis of its components. A promising antibiotic target is the diaminopimelate (DAP) pathway [70–74]. The DAP pathway is responsible for the production of *meso*-diaminopimelate (*meso*-DAP) and L-lysine, which are critical building blocks for cell wall and protein synthesis [75–77]. Inhibition of enzymes in the DAP pathway could result in a two-pronged approach of inactivation, effectively combining two modes of action, and thus, circumventing resistance. Other upstream targets include the well-studied MurF enzyme, responsible for the ligation of the D-Ala-D-Ala peptide on the cross-linking of the peptidoglycan layer [78]. We have recently published a review that describes the current status of targeting these, and other upstream pathways [79].

Unlike the outer membrane, the inner membrane is a phospholipid bilayer containing several enzymes responsible for energy metabolism and other important cellular processes [80]. Aside from any direct role in mediating resistance in GNB, especially working in synergy with the outer membrane, it remains a postulated target as it is the site of action for polymyxins [81].

4. Porins

The outer membrane provides a high level of protection against unwanted substances; however, it also limits the passive uptake of nutrients. To overcome this, bacteria use water filled pores, known as porins, to span the membrane, allowing the movement of size-specific hydrophilic compounds [82]. Porins consist of a β -barrel structure, with hydrophobic amino acids facing into the outer membrane, and hydrophilic amino acids facing inwards, creating a pore to attract and allow transport of hydrophilic molecules across the membrane [83]. Porins can be monomeric, but are often found in trimers to enhance stability, with each unit hypothesised to function independently [83]. Porins are also known to form part of a tripartite structure of efflux pump proteins, which will be discussed in Section 5.

While there are porins that allow the transport of specific solutes, general diffusion channels are the ones most commonly associated with antibiotic resistance [82,84]. It is important to note that by some definitions, *P. aeruginosa* does not have a general diffusion porin, with the major OMP, OprF, being considered an outer membrane channel [85]. Nevertheless, OprF and other similar channels will be referred to as porins here.

Porin-mediated antibiotic resistance can be as simple as having a limited number of porins within the bacterial genome or controlling expression of selected porins. In a clinical isolate of *K. pneumoniae*, a nonsense mutation resulted in a translation error in the OmpK36 porin, compensated by up-regulation of other selective porins to maintain essential transport functions [86]. This is believed to have contributed to the development of resistance to all carbapenems tested [87]. The intrinsic resistance of *P. aeruginosa* is partly attributed to the more stringent exclusion criteria of its main porins such as OprF, which limits the penetration of antibiotics into the cell [88,89].

Structural modifications to porins can also confer antibiotic resistance. One example is the in-frame deletion of loop 7 of the *P. aeruginosa* OprD porin that results in carbapenem resistance, while still retaining its ability to transport arginine [90]. In *Salmonella enterica* serotype Typhimurium, changes in disulphide bond formation within the periplasm upon exposure to oxidative stress can regulate the

opening and closing of the outer membrane porins OmpA and OmpC, resulting in increased resistance to β -lactams [91]. In *K. pneumoniae*, a premature stop codon in the OmpK35 porin is proposed to prevent the insertion into the membrane by blocking C-terminal anchoring [86]. This, combined with extended spectrum β -lactamases, resulted in carbapenem resistance in multiple Chilean clinical isolates [86]. This is also seen in other *Enterobacteriaceae* species [86]. While these porin alterations may decrease overall viability under non-selective conditions, the mutations will often be propagated under the selection pressure of otherwise lethal antibiotics.

As some of the major OMPs, porins have been implicated in other roles. For instance, OmpA (and its orthologue OprF in *P. aeruginosa*) is involved in the attachment of pathogenic bacteria to epithelial cells during infection [92]. It also plays a role in the stabilisation of the membrane, with its C-terminal non-covalently bound to the peptidoglycan layer [93,94]. Absence of OprF in *P. aeruginosa* can promote biofilm formation through the up-regulation of biofilm mediators such as bis-(3'-5')-cyclic dimeric guanosine monophosphate [95]. While these roles do not contribute to resistance by blocking entry to the cell, these mechanisms can have indirect effects on the resistance profile of GNB by contributing to biofilm-dependence.

These alternate functions of porins are of interest for drug development. Using computational techniques, Vila-Ferr s et al. were able to design a cyclic hexapeptide that inhibits OmpA in both reference and clinical strains of *A. baumannii*, *E. coli* and *P. aeruginosa* [96]. While this inhibitor, AOA-2 (Figure 2), did not have antibacterial activity directly, it was able to reduce the attachment of bacteria to epithelial cells and subsequently reduce bacterial load in the lungs, spleen and blood culture in a murine sepsis model [96]. It is believed that this approach reduces the bacteria's ability to evade the host's immune system, allowing more time to clear the infection [96]. Nie et al. have written a timely review discussing non-antibiotic options for OmpA inhibition of MDR infections [97].

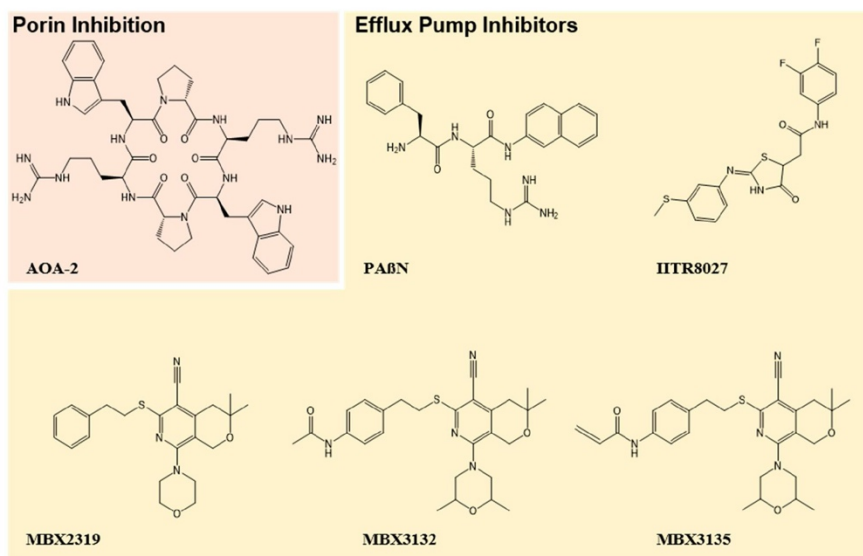


Figure 2. Porin and Efflux Pump Inhibitors. Porin (orange) and efflux pump (yellow) inhibitors. AOA-2 represents a promising inhibitor of the porin OmpA in *P. aeruginosa*. PA N inhibits the MexAB-OprM efflux pump, whilst the efflux pump inhibitor IITR8027 has been used to re-sensitise *A. baumannii* to fluoroquinolones. MBX2319 acts upon the RND-type efflux pumps in *P. aeruginosa*. Its analogues, MBX3132 and MBX3135, were shown to have improved potency and stability.

Rather than examining inhibition of porins themselves, a study by Haglan et al. examined the OMP assembly as a possible antibiotic target. The β -barrel structure of OMPs, including porins, are formed through an interaction network with β -barrel assembly machine (Bam) proteins [98]. This study looked at targeting the BamABCDE complex via the inhibition of BamD with a peptide sequence, derived from BamA. This resulted in growth defects in terms of colony size and colony forming units, as well as increased susceptibility to antibiotics that are typically unable to traverse the outer membrane [98]. As such, the interaction of BamD with BamA and porins such as OmpA, presents a promising new antibiotic target that would inhibit the OMPs from within [98]. There has also been considerable interest in targeting the outer membrane porins, such as TolC, associated with tripartite efflux pump systems as discussed below.

5. Efflux Pumps

The key to maintaining cellular homeostasis is to regulate the uptake of essential nutrients and solutes, whilst simultaneously expelling waste products and harmful substances. This process is governed by efflux pumps, which are membrane bound proteins that are found ubiquitously in bacteria [99,100]. Efflux pumps are responsible for the extrusion of a variety of solutes including fatty acids, heavy metals, antiseptics, detergents, virulence factors, toxins and most notably, antibiotics [101]. They can be specific to a single compound, class of antibiotics or have the ability to expel a number of structurally diverse classes of drugs (so called multi-drug efflux pumps), presenting a major problem in the fight against antibiotic resistance [101,102].

To extend through the GNB cell wall, some efflux pumps form tripartite assemblies from the inner membrane to the outer membrane [103]. This assembly consists of an inner membrane transporter protein, an OMP and a periplasmic membrane fusion protein [104]. Tripartite efflux pumps systems are associated mainly with the resistance-nodulation-cell division (RND) efflux superfamily [101], with some examples also from the ATP-binding cassette (ABC) family [105] and major facilitator superfamily (MFS) [103,104]. The most notable RND-type efflux pump is AcrAB-TolC from the *Enterobacteriaceae* family, covering important pathogens such as *E. coli*, *K. pneumoniae* and *Salmonella* spp. [106]. Homologous RND-type pumps are present in other GNB families, with relevant examples from *P. aeruginosa* (MexAB-OprM, MexCD-OprJ, MexEF-OprN and MexXY-OprM), *Campylobacter* spp. (CmeABC), *A. baumannii* (AdeABC) and *Neisseria* spp. (MtrCDE) [106]. Collectively, these tripartite RND efflux pumps have been shown to mediate resistance to a broad range of antibiotics, covering many classes, due to their overlapping substrate profiles [106–109]. Interestingly, the OMPs of tripartite assemblies are commonly the same or similar across different efflux pumps [103,110]. TolC is a well-characterised example and has been reported to contribute to resistance to many antibiotics and antiseptics including β -lactams, chloramphenicol, fluoroquinolones, novobiocin, tetracycline and macrolides in the *Enterobacteriaceae* family [103,111,112]. The utilisation of TolC (or species equivalent) across various efflux pumps and bacterial families highlights the potential of OMPs as targets for the development of broad-spectrum compounds [103,104,113].

Providing clear evidence of the ability of efflux pumps to increase resistance to different drugs, OqxAB-TolC, a plasmid-borne efflux pump of the RND-family from *E. coli*, was transconjugated by Hansen et al. into *S. enterica* serotype Typhimurium, *K. pneumoniae*, *Enterobacter aerogenes* and *Kluyvera* sp., resulting in decreased susceptibility to ciprofloxacin, olaquinox and chloramphenicol [114]. This was also shown for *E. cloacae*, in which genetic manipulation of the RND efflux pump AcrB linked its activity to both virulence and resistance to multiple antibiotic classes [115]. Reported mutations of efflux pump genes, such as those encoding the Mex efflux pumps from *P. aeruginosa*, have illustrated that antibiotic susceptibility is able to be restored, providing a possible avenue for the reinvigoration of current antibiotics [108].

Regulation of efflux pumps is complex and tightly controlled by a cross-talking set of regulatory pathways that involve the utilisation of TCSs and/or positive or negative transcriptional regulators to respond to a range of stimuli [116,117]. Common examples of TCSs that regulate the expression of MDR efflux pumps are AdeSR in *A. baumannii*, CpxAR in *Enterobacteriaceae* and AmgRS in *P. aeruginosa*.

In the context of an antibiotic stress response, TCSs induce overexpression of efflux pump genes to ensure the removal of the target antibiotic [118]. The regulation of AcrAB-TolC in *E. coli*, *Salmonella* spp. and *Klebsiella* spp. is achieved by repressors and global transcriptional regulators of efflux pump associated genes [106]. In this instance, a member of the TetR family of transcriptional repressors, AcrR, is responsible for the prevention of overexpression of *acrAB* under normal growth conditions. Therefore, mutations in *acrR* result in the overexpression of AcrAB-TolC, leading to MDR phenotypes in *E. coli* and *Salmonella* isolates [119,120]. AcrR has also been identified as a repressor of other regulatory complexes, including MarAB and SoxS, as summarised by Ferrand and colleagues [121]. Mutations in another regulatory gene, *mexR*, have been shown to increase expression of the associated MexAB-OprM efflux system in *P. aeruginosa* isolates [122]. Other similar repressors, including RamR and OqxR, have also been linked to efflux pump regulation and overexpression, resulting in antimicrobial resistance for multiple species [121]. Environmental factors can also stimulate the overexpression of efflux pumps and can include oxidative stress, antibiotic application as well as the presence of specific ligands. The latter is evident in *E. coli* with the multiple antibiotic operon, Mar [106,123]. Furthermore, either direct mutations or mutations in the Tet-R family regulator of the MFS family efflux pump *smvA* in *K. pneumoniae*, *P. mirabilis*, *E. cloacae* and *S. enterica* serotype Typhimurium are associated with increased biocide resistance, including to chlorhexidine [124–126] and acriflavine [127]. Efflux pump regulatory pathways have been noted to be interwoven into many other regulatory processes that promote bacterial virulence such as biofilm formation, quorum sensing and membrane permeability [110,128,129].

Due to their broad substrate specificity, efflux pumps have long been considered a promising target for adjuvant development, aiming to re-sensitise bacteria to a number of antibiotics. The relatively recent structural elucidation of major tripartite pumps in MDR clinical pathogens has assisted in the development and optimisation of inhibitors. The most well-characterised efflux pump inhibitor (EPI) is phenylalanine-arginine beta-naphthylamide (PAβN) (Figure 2), which inhibits the MexAB-OprM efflux pump and related RND-family pumps in clinically relevant pathogens, including *P. aeruginosa* [130,131]. However, PAβN has limited clinical use as the high concentrations required for treatment results in off-target cytotoxicity to the host [132]. EPIs that function through dissipation of the proton motive force, including cyanide *m*-chlorophenylhydrazine (CCCP), are also cytotoxic [133]. Whilst these compounds may be used as research tools for in vitro antibiotic testing, neither are useful for clinical use. Unfortunately, this drawback seems to apply to most EPI development, with no inhibitors successfully completing clinical trials to date. Recently, a promising small molecule inhibitor (IITR8027, Figure 2) of proton driven *A. baumannii* efflux pumps has re-sensitised MDR bacteria to ciprofloxacin, despite displaying no antibacterial activity on its own [134]. Additionally, IITR8027 showed no cytotoxicity at the reported minimum effective concentration for ciprofloxacin potentiation [134]. The novel pyranopyradine inhibitor MBX2319 (Figure 2) has been shown to potentiate current antibiotics through inhibition of the AcrAB efflux pump in *E. coli*; however, the lack of potency and stability were major drawbacks [135]. A subsequent study used MBX2319 as a scaffold to produce analogues with enhanced potency and stability [136]. Analogues MBX3132 and MBX3135 (Figure 2) were able to inhibit more than one type of RND efflux pump in *E. coli*, whilst retaining activity against a panel of *Enterobacteriaceae* [137]. Such broad-spectrum efflux pumps inhibitors without associated toxicity may have significant value in potentiating the efficacy of multiple classes of antibiotics.

6. Combinatorial Approaches

Resistance phenotypes in bacteria can be due to the presence of single genes (e.g., carbapenemases) or, more commonly, a combination of different resistance mechanisms. For instance, in the case of carbapenem resistance, porin down-regulation results in resistance to imipenem but only in combination with increased efflux will it result in resistance to both meropenem and doripenem [138]. Often loss of a specific porin is also combined with up-regulation of an enzyme, such as AmpC, which is capable of degrading the carbapenem, albeit with relatively poor turnover [139]. In *P. aeruginosa*, mutations in either the *mexT* or *mexS* genes can decrease porin OprD expression, whilst concurrently increasing

MexEF-OprN expression, which leads to resistance to imipenem, quinolones and chloramphenicol [140]. Many of these intrinsic mechanisms are coupled with other adaptive resistance mechanisms, for example carbapenemase expression, AmpC overexpression and target alteration [141]. For instance, a MDR *E. coli* strain has been found to have decreased permeability to and increased efflux of ciprofloxacin, coupled with a mutation in DNA gyrase, further increasing its resistance [103]. Transient or constitutive up-regulation of efflux pump expression may be a common first response in many bacteria to treatment with an antibiotic and be an essential stepping stone to the development of target-site resistance mutations [142]. Biofilms also play a key role in phenotypic antibiotic resistance, which has been extensively covered and will not be discussed here [143–148]. It is this interconnected network of resistance mechanisms that allows for bacteria to become resistant to an extensive range of antibiotics, and as such, development of effective therapeutics should aim to take a multi-targeted approach.

A combinatorial approach of inhibitors may be the key to overcoming antibacterial resistance. Making antibiotic analogues that are efflux resistant to prevent the initial efflux-mediated resistance response may be an attractive approach to reducing the emergence of resistance. Similarly, the combination of a membrane permeabilising agent with an efflux pump inhibitor may have benefits in lowering EPI concentration to minimise cytotoxicity and potentiate a broader range of antibiotic agents that would otherwise have been sensitive to efflux. Utilising the EPI PAβN and the membrane permeabiliser PMBN, Ferrer-Espada et al. were able to improve the activity of azithromycin by 2000-fold with 1 µg/mL PMBN [149]. Interestingly, this could not be achieved with the EPI alone [149]. Ideally, if the right efflux pump inhibitor was developed, mammalian toxicity could be significantly reduced by lowering the dose required with compounds like PMBN.

Further combinatorial approaches have focused on the utilisation of adjuvant compounds. Such adjuvants typically have no antibacterial activity on their own but can result in synergistic responses in combination with current antibiotics [150]. Several studies have shown the potential for adjuvants to potentiate antibiotics that are specific to Gram-positive bacteria to treat resistant strains of GNB [151,152]. This was achieved in one paper by adding anthracyclines to rifampicin and linezolid, whereby the combination resulted in increased susceptibility to both *A. baumannii* and *E. coli* [151]. Any of the aforementioned approaches that target the cell wall have the potential to be used in combination to revitalise our current antibiotic arsenal or to act as a stand-alone antibacterial agent (Figure 3).

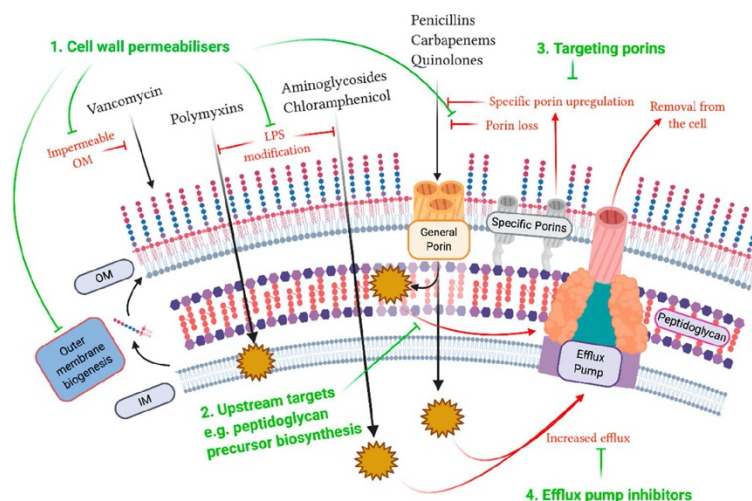


Figure 3. Novel Approaches to Bypass Resistance Mechanisms. Shown in green are the potential approaches for overcoming antibiotic resistance mechanisms associated with the cell wall in Gram-negative

bacteria that have been discussed in this review. (1) The first of approach is using compounds to disrupt and permeabilise the cell wall, including targeting outer membrane biogenesis and transport or by using non-antibacterial polymyxin compounds that increase susceptibility to current antibiotics. (2) Targets upstream of the peptidoglycan layer, such as the biosynthesis of peptidoglycan precursors, represent potential new modes of action that may be able to circumvent pre-existing resistance mechanisms. (3) Porin inhibition is an attractive antibiotic target, which can reduce bacterial virulence, thereby aiding in clearance of the infection by the immune system. (4) As almost all antibiotic classes are susceptible to efflux, efflux pump inhibitors aim to block the extrusion of antibiotics, thus increasing their active concentration within the cell. Figure was generated using [BioRender.com](https://www.biorender.com).

7. Conclusions

AMR represents a major threat to our ability to treat and prevent common infections. A major contributor to this resistance is the intricate membrane system of GNB, which is a potent barrier to the uptake of existing and new antibacterial agents. This includes impermeability due to the outer membrane composition and porin selectivity, as well as increased efflux from the cell. Furthermore, by understanding membrane synthesis and maintenance, we can examine potential new avenues for the development of adjuvant therapies. Here, we have described several examples of these, including membrane permeabilisation agents, targeting porin alternate functions and efflux pump inhibitors, which can be employed as new modes of action alone or in combinatorial treatments. By highlighting this as a challenge-led approach, as we have done here, we can open up avenues to revitalise our current antibiotic arsenal as well as stimulate the development of new agents to tackle the global antibiotic resistance crisis.

Author Contributions: Conceptualization, R.E.I., D.A.H., J.M.S. and T.P.S.d.C.; writing—original draft preparation, R.E.I. and D.A.H.; writing—review and editing, J.M.S. and T.P.S.d.C.; supervision, T.P.S.d.C.; project administration, T.P.S.d.C.; funding acquisition, T.P.S.d.C. All authors have read and agreed to the published version of the manuscript.

Funding: This research was funded by the National Health and Medical Research Council of Australia, grant number APP1091976, and the Australian Research Council, grant number DE190100806.

Acknowledgments: R.E.I. would like to acknowledge the Australian Government as a recipient of a Research Training Program scholarship and the British Society for Antimicrobial Chemotherapy. D.A.H. would like to acknowledge La Trobe University as a recipient of the La Trobe Research Training Program scholarship.

Conflicts of Interest: The authors declare no conflict of interest.

References

1. O'Neill, J. *Tackling Drug-Resistant Infections Globally: Final Report and Recommendations*; Wellcome Trust: London, UK, 2016.
2. Magiorakos, A.-P.; Srinivasan, A.; Carey, R.B.; Carmeli, Y.; Falagas, M.E.; Giske, C.G.; Harbarth, S.; Hindler, J.F.; Kahlmeter, G.; Olsson-Liljequist, B.; et al. Multidrug-Resistant, extensively drug-resistant and pandrug-resistant bacteria: An international expert proposal for interim standard definitions for acquired resistance. *Clin. Microbiol. Infect.* **2012**, *18*, 268–281. [[CrossRef](#)]
3. Pattnaik, D.; Panda, S.S.; Singh, N.; Sahoo, S.; Mohapatra, I.; Jena, J. Multidrug resistant, extensively drug resistant and pan drug resistant Gram-negative bacteria at a tertiary care centre in Bhubaneswar. *Int. J. Community Med. Public Health* **2019**, *6*, 567–572. [[CrossRef](#)]
4. De Rosa, A.; Mutters, N.T.; Mastroianni, C.M.; Kaiser, S.J.; Günther, F. Distribution of carbapenem resistance mechanisms in clinical isolates of XDR *Pseudomonas aeruginosa*. *Eur. J. Clin. Microbiol. Infect. Dis.* **2019**, *38*, 1547–1552. [[CrossRef](#)] [[PubMed](#)]
5. Nichols, L. Death from pan-resistant superbug. *Autops. Case Rep.* **2019**, *9*, e2019106. [[CrossRef](#)] [[PubMed](#)]
6. Tacconelli, E.; Carrara, E.; Savoldi, A.; Harbarth, S.; Mendelson, M.; Monnet, D.L.; Pulcini, C.; Kahlmeter, G.; Kluytmans, J.; Carmeli, Y.; et al. Discovery, research, and development of new antibiotics: The WHO priority list of antibiotic-resistant bacteria and tuberculosis. *Lancet Infect. Dis.* **2018**, *18*, 318–327. [[CrossRef](#)]

7. Centers for Disease Control and Prevention (U.S.). *Antibiotic Resistance Threats in the United States, 2019*; U.S. Department of Health and Human Services: Atlanta, GA, USA, CDC; 2019.
8. Silver, L.L. Challenges of antibacterial discovery. *Clin. Microbiol. Rev.* **2011**, *24*, 71–109. [\[CrossRef\]](#)
9. Delcour, A.H. Outer membrane permeability and antibiotic resistance. *Biochim. Biophys. Acta* **2009**, *1794*, 808–816. [\[CrossRef\]](#)
10. Blair, J.M.A.; Webber, M.A.; Baylay, A.J.; Ogbolu, D.O.; Piddock, L.J.V. Molecular mechanisms of antibiotic resistance. *Nat. Rev. Microbiol.* **2015**, *13*, 42–51. [\[CrossRef\]](#)
11. Schurek, K.N.; Marr, A.K.; Taylor, P.K.; Wiegand, I.; Semenec, L.; Khaira, B.K.; Hancock, R.E.W. Novel genetic determinants of low-level aminoglycoside resistance in *Pseudomonas aeruginosa*. *Antimicrob. Agents Chemother.* **2008**, *52*, 4213–4219. [\[CrossRef\]](#)
12. Zgurskaya, H.I.; López, C.A.; Gnanakaran, S. Permeability barrier of Gram-negative cell envelopes and approaches to bypass it. *ACS Infect. Dis.* **2015**, *1*, 512–522. [\[CrossRef\]](#)
13. Trimble, M.J.; Mlynářčík, P.; Kolář, M.; Hancock, R.E.W. Polymyxin: Alternative mechanisms of action and resistance. *Cold Spring Harb. Perspect. Med.* **2016**, *6*, a025288. [\[CrossRef\]](#) [\[PubMed\]](#)
14. Choi, M.-J.; Ko, K.S. Mutant prevention concentrations of colistin for *Acinetobacter baumannii*, *Pseudomonas aeruginosa* and *Klebsiella pneumoniae* clinical isolates. *J. Antimicrob. Chemother.* **2014**, *69*, 275–277. [\[CrossRef\]](#) [\[PubMed\]](#)
15. Gunn, J.S.; Lim, K.B.; Krueger, J.; Kim, K.; Guo, L.; Hackett, M.; Miller, S.I. PmrA-PmrB-regulated genes necessary for 4-aminoarabinose lipid A modification and polymyxin resistance. *Mol. Microbiol.* **1998**, *27*, 1171–1182. [\[CrossRef\]](#) [\[PubMed\]](#)
16. Arroyo, L.A.; Herrera, C.M.; Fernandez, L.; Hankins, J.V.; Trent, M.S.; Hancock, R.E.W. The pmrCAB operon mediates polymyxin resistance in *Acinetobacter baumannii* ATCC 17978 and clinical isolates through phosphoethanolamine modification of lipid A. *Antimicrob. Agents Chemother.* **2011**, *55*, 3743–3751. [\[CrossRef\]](#)
17. Beceiro, A.; Llobet, E.; Aranda, J.; Bengoechea, J.A.; Doumith, M.; Hornsey, M.; Dhanji, H.; Chart, H.; Bou, G.; Livermore, D.M.; et al. Phosphoethanolamine modification of lipid A in colistin-resistant variants of *Acinetobacter baumannii* mediated by the pmrAB two-component regulatory system. *Antimicrob. Agents Chemother.* **2011**, *55*, 3370–3379. [\[CrossRef\]](#)
18. Macfarlane, E.L.A.; Kwasnicka, A.; Hancock, R.E.W. Role of *Pseudomonas aeruginosa* PhoP-PhoQ in resistance to antimicrobial cationic peptides and aminoglycosides. *Microbiology* **2000**, *146*, 2543–2554. [\[CrossRef\]](#)
19. Gunn, J.S.; Miller, S.I. PhoP-PhoQ activates transcription of pmrAB, encoding a two-component regulatory system involved in *Salmonella typhimurium* antimicrobial peptide resistance. *J. Bacteriol.* **1996**, *178*, 6857–6864. [\[CrossRef\]](#)
20. Wand, M.E.; Sutton, J.M. Mutations in the two component regulator systems PmrAB and PhoPQ give rise to increased colistin resistance in *Citrobacter* and *Enterobacter* spp. *J. Med. Microbiol.* **2020**, *69*, 521–529. [\[CrossRef\]](#)
21. Poirel, L.; Jayol, A.; Nordmann, P. Polymyxins: Antibacterial activity, susceptibility testing, and resistance mechanisms encoded by plasmids or chromosomes. *Clin. Microbiol. Rev.* **2017**, *30*, 557–596. [\[CrossRef\]](#)
22. Olaitan, A.O.; Morand, S.; Rolain, J.-M. Mechanisms of polymyxin resistance: Acquired and intrinsic resistance in bacteria. *Front. Microbiol.* **2014**, *5*, 643. [\[CrossRef\]](#)
23. Marceau, M.; Sebbane, F.; Ewann, F.; Collyn, F.; Lindner, B.; Campos, M.A.; Bengoechea, J.-A.; Simonet, M. The pmrF polymyxin-resistance operon of *Yersinia pseudotuberculosis* is upregulated by the PhoP-PhoQ two-component system but not by PmrA-PmrB, and is not required for virulence. *Microbiology* **2004**, *150*, 3947–3957. [\[CrossRef\]](#) [\[PubMed\]](#)
24. Sherman, E.X.; Wozniak, J.E.; Weiss, D.S. Methods to evaluate colistin heteroresistance in *Acinetobacter baumannii*. *Methods Mol. Biol.* **2019**, *1946*, 39–50. [\[CrossRef\]](#) [\[PubMed\]](#)
25. Band, V.I.; Weiss, D.S. Heteroresistance: A cause of unexplained antibiotic treatment failure? *PLoS Pathog.* **2019**, *15*, e1007726. [\[CrossRef\]](#) [\[PubMed\]](#)
26. Li, J.; Rayner, C.R.; Nation, R.L.; Owen, R.J.; Spelman, D.; Tan, K.E.; Liolios, L. Heteroresistance to colistin in multidrug-resistant *Acinetobacter baumannii*. *Antimicrob. Agents Chemother.* **2006**, *50*, 2946–2950. [\[CrossRef\]](#) [\[PubMed\]](#)
27. Jayol, A.; Nordmann, P.; Brink, A.; Poirel, L. Heteroresistance to Colistin in *Klebsiella pneumoniae* associated with alterations in the PhoPQ regulatory system. *Antimicrob. Agents Chemother.* **2015**, *59*, 2780–2784. [\[CrossRef\]](#) [\[PubMed\]](#)

28. Lin, J.; Xu, C.; Fang, R.; Cao, J.; Zhang, X.; Zhao, Y.; Dong, G.; Sun, Y.; Zhou, T. Resistance and heteroresistance to colistin in *Pseudomonas aeruginosa* isolates from Wenzhou, China. *Antimicrob. Agents Chemother.* **2019**, *63*, e00556-19. [\[CrossRef\]](#)
29. Guérin, F.; Isnard, C.; Sinel, C.; Morand, P.; Dhalluin, A.; Cattoir, V.; Giard, J.-C. Cluster-dependent colistin hetero-resistance in *Enterobacter cloacae* complex. *J. Antimicrob. Chemother.* **2016**, *71*, 3058–3061. [\[CrossRef\]](#)
30. Hjort, K.; Nicoloff, H.; Andersson, D.I. Unstable tandem gene amplification generates heteroresistance (variation in resistance within a population) to colistin in *Salmonella enterica*. *Mol. Microbiol.* **2016**, *102*, 274–289. [\[CrossRef\]](#)
31. Liu, Y.-Y.; Wang, Y.; Walsh, T.R.; Yi, L.-X.; Zhang, R.; Spencer, J.; Doi, Y.; Tian, G.; Dong, B.; Huang, X.; et al. Emergence of plasmid-mediated colistin resistance mechanism MCR-1 in animals and human beings in China: A microbiological and molecular biological study. *Lancet Infect. Dis.* **2016**, *16*, 161–168. [\[CrossRef\]](#)
32. Doumith, M.; Godbole, G.; Ashton, P.; Larkin, L.; Dallman, T.; Day, M.; Day, M.; Muller-Pebody, B.; Ellington, M.J.; de Pinna, E.; et al. Detection of the plasmid-mediated mcr-1 gene conferring colistin resistance in human and food isolates of *Salmonella enterica* and *Escherichia coli* in England and Wales. *J. Antimicrob. Chemother.* **2016**, *71*, 2300–2305. [\[CrossRef\]](#)
33. Moffatt, J.H.; Harper, M.; Harrison, P.; Hale, J.D.F.; Vinogradov, E.; Seemann, T.; Henry, R.; Crane, B.; St Michael, F.; Cox, A.D.; et al. Colistin resistance in *Acinetobacter baumannii* is mediated by complete loss of lipopolysaccharide production. *Antimicrob. Agents Chemother.* **2010**, *54*, 4971–4977. [\[CrossRef\]](#) [\[PubMed\]](#)
34. Young, M.L.; Bains, M.; Bell, A.; Hancock, R.E. Role of *Pseudomonas aeruginosa* outer membrane protein OprH in polymyxin and gentamicin resistance: Isolation of an OprH-deficient mutant by gene replacement techniques. *Antimicrob. Agents Chemother.* **1992**, *36*, 2566–2568. [\[CrossRef\]](#) [\[PubMed\]](#)
35. Zhai, Y.-J.; Sun, H.-R.; Luo, X.-W.; Liu, J.-H.; Pan, Y.-S.; Wu, H.; Yuan, L.; Liang, J.; He, D.-D.; Hu, G.-Z. CpxR regulates the colistin susceptibility of *Salmonella Typhimurium* by a multitarget mechanism. *J. Antimicrob. Chemother.* **2020**. [\[CrossRef\]](#) [\[PubMed\]](#)
36. Muller, C.; Plésiat, P.; Jeannot, K. A two-component regulatory system interconnects resistance to polymyxins, aminoglycosides, fluoroquinolones, and β -lactams in *Pseudomonas aeruginosa*. *Antimicrob. Agents Chemother.* **2011**, *55*, 1211–1221. [\[CrossRef\]](#)
37. Telke, A.A.; Olaitan, A.O.; Morand, S.; Rolain, J.-M. soxRS induces colistin hetero-resistance in *Enterobacter asburiae* and *Enterobacter cloacae* by regulating the *acrAB-tolC* efflux pump. *J. Antimicrob. Chemother.* **2017**, *72*, 2715–2721. [\[CrossRef\]](#)
38. Shinohara, D.R.; Menegucci, T.C.; Fedrigo, N.H.; Migliorini, L.B.; Carrara-Marroni, F.E.; Maria dos Anjos, M.; Cardoso, C.L.; Nishiyama, S.A.B.; Tognim, M.C.B. Synergistic activity of polymyxin B combined with vancomycin against carbapenem-resistant and polymyxin-resistant *Acinetobacter baumannii*: First in vitro study. *J. Med. Microbiol.* **2019**, *68*, 309–315. [\[CrossRef\]](#)
39. Lenhard, J.R.; Bulman, Z.P.; Tsuji, B.T.; Kaye, K.S. Shifting gears: The future of polymyxin antibiotics. *Antibiotics* **2019**, *8*, 42. [\[CrossRef\]](#)
40. Velkov, T.; Roberts, K.D.; Thompson, P.E.; Li, J. Polymyxins: A new hope in combating Gram-negative superbugs? *Future Med. Chem.* **2016**, *8*, 1017–1025. [\[CrossRef\]](#)
41. Vaara, M. Agents that increase the permeability of the outer membrane. *Microbiol. Rev.* **1992**, *56*, 395–411. [\[CrossRef\]](#)
42. Ofek, I.; Cohen, S.; Rahmani, R.; Kabha, K.; Tamarkin, D.; Herzig, Y.; Rubinstein, E. Antibacterial synergism of polymyxin B nonapeptide and hydrophobic antibiotics in experimental Gram-negative infections in mice. *Antimicrob. Agents Chemother.* **1994**, *38*, 374–377. [\[CrossRef\]](#)
43. Vaara, M. Polymyxin derivatives that sensitize Gram-negative bacteria to other antibiotics. *Molecules* **2019**, *24*, 249. [\[CrossRef\]](#) [\[PubMed\]](#)
44. Danner, R.L.; Joiner, K.A.; Rubin, M.; Patterson, W.H.; Johnson, N.; Ayers, K.M.; Parrillo, J.E. Purification, toxicity, and antitendotoxin activity of polymyxin B nonapeptide. *Antimicrob. Agents Chemother.* **1989**, *33*, 1428–1434. [\[CrossRef\]](#) [\[PubMed\]](#)
45. Zurawski, D.V.; Reinhart, A.A.; Alamneh, Y.A.; Pucci, M.J.; Si, Y.; Abu-Taleb, R.; Shearer, J.P.; Demons, S.T.; Tyner, S.D.; Lister, T. SPR741, an antibiotic adjuvant, potentiates the *in vitro* and *in vivo* activity of rifampin against clinically relevant extensively drug-resistant *Acinetobacter baumannii*. *Antimicrob. Agents Chemother.* **2017**, *61*, e01239-17. [\[CrossRef\]](#) [\[PubMed\]](#)

46. Spero Reports Preliminary Findings from Phase 1 Clinical Trial of SPR206 and Plans to Advance Program with Alliance Partners Everest Medicines and the Department of Defense. Available online: <https://investors.sperotherapeutics.com/news-releases/news-release-details/spero-reports-preliminary-findings-phase-1-clinical-trial-spr206> (accessed on 21 April 2020).
47. Pitt, M.E.; Cao, M.D.; Butler, M.S.; Ramu, S.; Ganesamoorthy, D.; Blaskovich, M.A.T.; Coin, L.J.M.; Cooper, M.A. Octapeptin C4 and polymyxin resistance occur via distinct pathways in an epidemic XDR *Klebsiella pneumoniae* ST258 isolate. *J. Antimicrob. Chemother.* **2019**, *74*, 582–593. [\[CrossRef\]](#) [\[PubMed\]](#)
48. Velkov, T.; Gallardo-Godoy, A.; Swarbrick, J.D.; Blaskovich, M.A.; Elliott, A.G.; Han, M.; Thompson, P.E.; Roberts, K.D.; Huang, J.X.; Becker, B.; et al. Structure, function, and biosynthetic origin of octapeptin antibiotics active against extensively drug-resistant Gram-negative bacteria. *Cell Chem. Biol.* **2018**, *25*, 380–391. [\[CrossRef\]](#) [\[PubMed\]](#)
49. Blaskovich, M.A.T.; Pitt, M.E.; Elliott, A.G.; Cooper, M.A. Can octapeptin antibiotics combat extensively drug-resistant (XDR) bacteria? *Expert Rev. Anti-Infect Ther.* **2018**, *16*, 485–499. [\[CrossRef\]](#) [\[PubMed\]](#)
50. CARB-X Funds University of Queensland to Accelerate the Development of a New Class of Last-Resort Antibiotics to Treat Deadly Superbug Infections. Carb-X. Available online: <https://carb-x.org/carb-x-news/carb-x-funds-university-of-queensland-to-accelerate-the-development-of-a-new-class-of-last-resort-antibiotics-to-treat-deadly-superbug-infections> (accessed on 8 May 2020).
51. Tsai, C.N.; MacNair, C.R.; Cao, M.P.T.; Perry, J.N.; Magolan, J.; Brown, E.D.; Coombes, B.K. Targeting two-component systems uncovers a small-molecule inhibitor of *Salmonella* virulence. *Cell Chem. Biol.* **2020**, *27*, 793–805. [\[CrossRef\]](#)
52. Erwin, A.L. Antibacterial drug discovery targeting the lipopolysaccharide biosynthetic enzyme LpxC. *Cold Spring Harb. Perspect. Med.* **2016**, *6*, a025304. [\[CrossRef\]](#)
53. Tomaras, A.P.; McPherson, C.J.; Kuhn, M.; Carifa, A.; Mullins, L.; George, D.; Desbonnet, C.; Eidem, T.M.; Montgomery, J.I.; Brown, M.F.; et al. LpxC inhibitors as new antibacterial agents and tools for studying regulation of lipid A biosynthesis in Gram-negative pathogens. *mBio* **2014**, *5*, e01551-14. [\[CrossRef\]](#)
54. Krause, K.M.; Haglund, C.M.; Hebner, C.; Serio, A.W.; Lee, G.; Nieto, V.; Cohen, F.; Kane, T.R.; Machajewski, T.D.; Hildebrandt, D.; et al. Potent LpxC inhibitors with *in vitro* activity against multidrug-resistant *Pseudomonas aeruginosa*. *Antimicrob. Agents Chemother.* **2019**, *63*, e00977-19. [\[CrossRef\]](#)
55. A Study to Assess the Safety, Tolerability, and Pharmacokinetics of ACHN-975 in Healthy Volunteers—ClinicalTrials.gov. Available online: <https://clinicaltrials.gov/ct2/show/NCT01597947> (accessed on 29 April 2020).
56. Cohen, F.; Aggen, J.B.; Andrews, L.D.; Assar, Z.; Boggs, J.; Choi, T.; Dozzo, P.; Easterday, A.N.; Haglund, C.M.; Hildebrandt, D.J.; et al. Optimization of LpxC inhibitors for antibacterial activity and cardiovascular safety. *ChemMedChem* **2019**, *14*, 1560–1572. [\[CrossRef\]](#)
57. García-Quintanilla, M.; Carretero-Ledesma, M.; Moreno-Martínez, P.; Martín-Peña, R.; Pachón, J.; McConnell, M.J. Lipopolysaccharide loss produces partial colistin dependence and collateral sensitivity to azithromycin, rifampicin and vancomycin in *Acinetobacter baumannii*. *Int. J. Antimicrob. Agents* **2015**, *46*, 696–702. [\[CrossRef\]](#) [\[PubMed\]](#)
58. Wand, M.E.; Bock, L.J.; Bonney, L.C.; Sutton, J.M. Retention of virulence following adaptation to colistin in *Acinetobacter baumannii* reflects the mechanism of resistance. *J. Antimicrob. Chemother.* **2015**, *70*, 2209–2216. [\[CrossRef\]](#) [\[PubMed\]](#)
59. García-Quintanilla, M.; Caro-Vega, J.M.; Pulido, M.R.; Moreno-Martínez, P.; Pachón, J.; McConnell, M.J. Inhibition of LpxC increases antibiotic susceptibility in *Acinetobacter baumannii*. *Antimicrob. Agents Chemother.* **2016**, *60*, 5076–5079. [\[CrossRef\]](#) [\[PubMed\]](#)
60. Werneburg, M.; Zerbe, K.; Juhas, M.; Bigler, L.; Stalder, U.; Kaech, A.; Ziegler, U.; Obrecht, D.; Eberl, L.; Robinson, J.A. Inhibition of lipopolysaccharide transport to the outer membrane in *Pseudomonas aeruginosa* by peptidomimetic antibiotics. *ChemBioChem* **2012**, *13*, 1767–1775. [\[CrossRef\]](#)
61. Vetterli, S.U.; Moehle, K.; Robinson, J.A. Synthesis and antimicrobial activity against *Pseudomonas aeruginosa* of macrocyclic β -hairpin peptidomimetic antibiotics containing N-methylated amino acids. *Bioorg. Med. Chem.* **2016**, *24*, 6332–6339. [\[CrossRef\]](#)
62. Martin-Loeches, I.; Dale, G.E.; Torres, A. Murepavadin: A new antibiotic class in the pipeline. *Expert Rev. Anti-Infect. Ther.* **2018**, *16*, 259–268. [\[CrossRef\]](#)

63. Provenzani, A.; Hospodar, A.R.; Meyer, A.L.; Leonardi Vinci, D.; Hwang, E.Y.; Butrus, C.M.; Polidori, P. Multidrug-resistant gram-negative organisms: A review of recently approved antibiotics and novel pipeline agents. *Int. J. Clin. Pharm.* **2020**, *42*, 1016–1025. [\[CrossRef\]](#)
64. Harrison, L.B.; Fowler, R.C.; Abdalhamid, B.; Selmecki, A.; Hanson, N.D. lptG contributes to changes in membrane permeability and the emergence of multidrug hypersusceptibility in a cystic fibrosis isolate of *Pseudomonas aeruginosa*. *Microbiol. Open* **2019**, *8*, e844. [\[CrossRef\]](#)
65. Clairfeuille, T.; Buchholz, K.R.; Li, Q.; Verschuere, E.; Liu, P.; Sangaraju, D.; Park, S.; Noland, C.L.; Storek, K.M.; Nickerson, N.N.; et al. Structure of the essential inner membrane lipopolysaccharide–PbgA complex. *Nature* **2020**, *584*, 479–483. [\[CrossRef\]](#)
66. Nickerson, N.N.; Jao, C.C.; Xu, Y.; Quinn, J.; Skippington, E.; Alexander, M.K.; Miu, A.; Skelton, N.; Hankins, J.V.; Lopez, M.S.; et al. A novel inhibitor of the LolCDE ABC transporter essential for lipoprotein trafficking in Gram-negative bacteria. *Antimicrob. Agents Chemother.* **2018**, *62*, e02151–17. [\[CrossRef\]](#) [\[PubMed\]](#)
67. Shrivastava, R.; Chng, S.-S. Lipid trafficking across the Gram-negative cell envelope. *J. Biol. Chem.* **2019**, *294*, 14175–14184. [\[CrossRef\]](#) [\[PubMed\]](#)
68. Elliott, A.G.; Huang, J.X.; Neve, S.; Zuegg, J.; Edwards, I.A.; Cain, A.K.; Boinett, C.J.; Barquist, L.; Lundberg, C.V.; Steen, J.; et al. An amphipathic peptide with antibiotic activity against multidrug-resistant Gram-negative bacteria. *Nat. Commun.* **2020**, *11*, 3184. [\[CrossRef\]](#) [\[PubMed\]](#)
69. Domínguez-Gil, T.; Molina, R.; Alcorlo, M.; Hermoso, J.A. Renew or die: The molecular mechanisms of peptidoglycan recycling and antibiotic resistance in Gram-negative pathogens. *Drug Resist. Update* **2016**, *28*, 91–104. [\[CrossRef\]](#) [\[PubMed\]](#)
70. Impey, R.E.; Lee, M.; Hawkins, D.A.; Sutton, J.M.; Panjikar, S.; Perugini, M.A.; Soares da Costa, T.P. Mis-annotations of a promising antibiotic target in high-priority gram-negative pathogens. *FEBS Lett.* **2020**, *594*, 1453–1463. [\[CrossRef\]](#)
71. Impey, R.E.; Panjikar, S.; Hall, C.J.; Bock, L.J.; Sutton, J.M.; Perugini, M.A.; Soares da Costa, T.P. Identification of two dihydrodipicolinate synthase isoforms from *Pseudomonas aeruginosa* that differ in allosteric regulation. *FEBS J.* **2020**, *287*, 386–400. [\[CrossRef\]](#)
72. Soares da Costa, T.P.; Christensen, J.B.; Desbois, S.; Gordon, S.E.; Gupta, R.; Hogan, C.J.; Nelson, T.G.; Downton, M.T.; Gardhi, C.K.; Abbott, B.M.; et al. Chapter Nine—Quaternary Structure Analyses of an Essential Oligomeric Enzyme. In *Methods in Enzymology*; Cole, J.L., Ed.; Analytical Ultracentrifugation; Academic Press: Cambridge, MA, USA, 2015; Volume 562, pp. 205–223.
73. Christoff, R.M.; Gardhi, C.K.; da Costa, T.P.S.; Perugini, M.A.; Abbott, B.M. Pursuing DHDPs: An enzyme of unrealised potential as a novel antibacterial target. *Med. Chem. Commun.* **2019**, *10*, 1581–1588. [\[CrossRef\]](#)
74. Soares da Costa, T.P.; Desbois, S.; Dogovski, C.; Gorman, M.A.; Ketaren, N.E.; Paxman, J.J.; Siddiqui, T.; Zammit, L.M.; Abbott, B.M.; Robins-Browne, R.M.; et al. Structural determinants defining the allosteric inhibition of an essential antibiotic target. *Structure* **2016**, *24*, 1282–1291. [\[CrossRef\]](#)
75. Hutton, C.A.; Perugini, M.A.; Gerrard, J.A. Inhibition of lysine biosynthesis: An evolving antibiotic strategy. *Mol. Biosyst.* **2007**, *3*, 458–465. [\[CrossRef\]](#)
76. Christensen, J.B.; Soares da Costa, T.P.; Faou, P.; Pearce, F.G.; Panjikar, S.; Perugini, M.A. Structure and function of cyanobacterial DHDPs and DHDPR. *Sci. Rep.* **2016**, *6*, 37111. [\[CrossRef\]](#)
77. Gupta, R.; Soares da Costa, T.P.; Faou, P.; Dogovski, C.; Perugini, M.A. Comparison of untagged and his-tagged dihydrodipicolinate synthase from the enteric pathogen *Vibrio cholerae*. *Protein Expr. Purif.* **2018**, *145*, 85–93. [\[CrossRef\]](#) [\[PubMed\]](#)
78. Anderson, M.S.; Eveland, S.S.; Onishi, H.R.; Pompliano, D.L. Kinetic mechanism of the *Escherichia coli* UDPMurNAC-tripeptide d-alanyl-d-alanine-adding enzyme: Use of a glutathione s-transferase fusion. *Biochemistry* **1996**, *35*, 16264–16269. [\[CrossRef\]](#) [\[PubMed\]](#)
79. Impey, R.E.; Soares da Costa, T.P. Review: Targeting the biosynthesis and incorporation of amino acids into peptidoglycan as an antibiotic approach against Gram negative bacteria. *EC Microbiol.* **2018**, *14*, 200–209.
80. Silhavy, T.J.; Kahne, D.; Walker, S. The bacterial cell envelope. *Cold Spring Harb. Perspect. Biol.* **2010**, *2*. [\[CrossRef\]](#)
81. Falagas, M.E.; Kasiakou, S.K.; Saravolatz, L.D. Colistin: The revival of polymyxins for the management of multidrug-resistant Gram-negative bacterial infections. *Clin. Infect. Dis.* **2005**, *40*, 1333–1341. [\[CrossRef\]](#)

82. Fernández, L.; Hancock, R.E.W. Adaptive and mutational resistance: Role of porins and efflux pumps in drug resistance. *Clin. Microbiol. Rev.* **2012**, *25*, 661–681. [\[CrossRef\]](#)
83. Vergalli, J.; Bodrenko, I.V.; Masi, M.; Moynié, L.; Acosta-Gutiérrez, S.; Naismith, J.H.; Davin-Regli, A.; Ceccarelli, M.; van den Berg, B.; Winterhalter, M.; et al. Porins and small-molecule translocation across the outer membrane of Gram-negative bacteria. *Nat. Rev. Microbiol.* **2020**, *18*, 164–176. [\[CrossRef\]](#)
84. Choi, U.; Lee, C.-R. Distinct roles of outer membrane porins in antibiotic resistance and membrane integrity in *Escherichia coli*. *Front. Microbiol.* **2019**, *10*, 953. [\[CrossRef\]](#)
85. Chevalier, S.; Bouffartigues, E.; Bodilis, J.; Maillot, O.; Lesouhaitier, O.; Feuilloley, M.G.J.; Orange, N.; Dufour, A.; Cornelis, P. Structure, function and regulation of *Pseudomonas aeruginosa* porins. *FEMS Microbiol. Rev.* **2017**, *41*, 698–722. [\[CrossRef\]](#)
86. Wozniak, A.; Villagra, N.A.; Undabarrena, A.; Gallardo, N.; Keller, N.; Moraga, M.; Román, J.C.; Mora, G.C.; García, P. Porin alterations present in non-carbapenemase-producing *Enterobacteriaceae* with high and intermediate levels of carbapenem resistance in Chile. *J. Med. Microbiol.* **2012**, *61*, 1270–1279. [\[CrossRef\]](#)
87. García-Fernández, A.; Miriagou, V.; Papagiannitsis, C.C.; Giordano, A.; Venditti, M.; Mancini, C.; Carattoli, A. An ertapenem-resistant extended-spectrum- β -lactamase-producing *Klebsiella pneumoniae* clone carries a novel OmpK36 porin variant. *Antimicrob. Agents Chemother.* **2010**, *54*, 4178–4184. [\[CrossRef\]](#) [\[PubMed\]](#)
88. Nikaido, H.; Nikaido, K.; Harayama, S. Identification and characterization of porins in *Pseudomonas aeruginosa*. *J. Biol. Chem.* **1991**, *266*, 770–779. [\[PubMed\]](#)
89. Bellido, F.; Martin, N.L.; Siehnell, R.J.; Hancock, R.E. Reevaluation, using intact cells, of the exclusion limit and role of porin OprF in *Pseudomonas aeruginosa* outer membrane permeability. *J. Bacteriol.* **1992**, *174*, 5196–5203. [\[CrossRef\]](#) [\[PubMed\]](#)
90. Kos, V.N.; McLaughlin, R.E.; Gardner, H.A. Identification of unique in-frame deletions in OprD among clinical isolates of *Pseudomonas aeruginosa*. *Pathog. Dis.* **2016**, *74*, ftw031. [\[CrossRef\]](#) [\[PubMed\]](#)
91. van der Heijden, J.; Reynolds, L.A.; Deng, W.; Mills, A.; Scholz, R.; Imami, K.; Foster, L.J.; Duong, F.; Finlay, B.B. *Salmonella* rapidly regulates membrane permeability to survive oxidative stress. *mBio* **2016**, *7*, e01238-16. [\[CrossRef\]](#) [\[PubMed\]](#)
92. Krishnan, S.; Prasadarao, N.V. Outer membrane protein A and OprF: Versatile roles in Gram-negative bacterial infections. *FEBS J.* **2012**, *279*, 919–931. [\[CrossRef\]](#)
93. Woodruff, W.A.; Hancock, R.E. *Pseudomonas aeruginosa* outer membrane protein F: Structural role and relationship to the *Escherichia coli* OmpA protein. *J. Bacteriol.* **1989**, *171*, 3304–3309. [\[CrossRef\]](#)
94. De Mot, R.; Vanderleyden, J. The C-terminal sequence conservation between OmpA-related outer membrane proteins and MotB suggests a common function in both Gram-positive and Gram-negative bacteria, possibly in the interaction of these domains with peptidoglycan. *Mol. Microbiol.* **1994**, *12*, 333–334. [\[CrossRef\]](#)
95. Bouffartigues, E.; Moscoso, J.A.; Duchesne, R.; Rosay, T.; Fito-Boncompagni, L.; Gicquel, G.; Maillot, O.; Bénard, M.; Bazire, A.; Brenner-Weiss, G.; et al. The absence of the *Pseudomonas aeruginosa* OprF protein leads to increased biofilm formation through variation in c-di-GMP level. *Front. Microbiol.* **2015**, *6*, 630. [\[CrossRef\]](#)
96. Vila-Farrés, X.; Parra-Millán, R.; Sánchez-Encinales, V.; Varese, M.; Ayerbe-Algaba, R.; Bayó, N.; Guardiola, S.; Pachón-Ibáñez, M.E.; Kotev, M.; García, J.; et al. Combating virulence of Gram-negative bacilli by OmpA inhibition. *Sci. Rep.* **2017**, *7*, 1–11. [\[CrossRef\]](#)
97. Nie, D.; Hu, Y.; Chen, Z.; Li, M.; Hou, Z.; Luo, X.; Mao, X.; Xue, X. Outer membrane protein A (OmpA) as a potential therapeutic target for *Acinetobacter baumannii* infection. *J. Biomed. Sci.* **2020**, *27*, 26. [\[CrossRef\]](#)
98. Hagan, C.L.; Wzorek, J.S.; Kahne, D. Inhibition of the β -barrel assembly machine by a peptide that binds BamD. *Proc. Natl. Acad. Sci. USA* **2015**, *112*, 2011–2016. [\[CrossRef\]](#) [\[PubMed\]](#)
99. Van Bambeke, F.; Michot, J.-M.; Tulkens, P.M. Antibiotic efflux pumps in eukaryotic cells: Occurrence and impact on antibiotic cellular pharmacokinetics, pharmacodynamics and toxicodynamics. *J. Antimicrob. Chemother.* **2003**, *51*, 1067–1077. [\[CrossRef\]](#) [\[PubMed\]](#)
100. Van Bambeke, F.; Glupczynski, Y.; Plésiat, P.; Pechère, J.C.; Tulkens, P.M. Antibiotic efflux pumps in prokaryotic cells: Occurrence, impact on resistance and strategies for the future of antimicrobial therapy. *J. Antimicrob. Chemother.* **2003**, *51*, 1055–1065. [\[CrossRef\]](#) [\[PubMed\]](#)
101. Venter, H.; Mowla, R.; Ohene-Agyei, T.; Ma, S. RND-type drug efflux pumps from Gram-negative bacteria: Molecular mechanism and inhibition. *Front. Microbiol.* **2015**, *6*, 377. [\[CrossRef\]](#)
102. Marquez, B. Bacterial efflux systems and efflux pumps inhibitors. *Biochimie* **2005**, *87*, 1137–1147. [\[CrossRef\]](#)

103. Du, D.; Wang-Kan, X.; Neuberger, A.; van Veen, H.W.; Pos, K.M.; Piddock, L.J.V.; Luisi, B.F. Multidrug efflux pumps: Structure, function and regulation. *Nat. Rev. Microbiol.* **2018**, *16*, 523–539. [\[CrossRef\]](#)
104. Neuberger, A.; Du, D.; Luisi, B.F. Structure and mechanism of bacterial tripartite efflux pumps. *Res. Microbiol.* **2018**, *169*, 401–413. [\[CrossRef\]](#)
105. Lubelski, J.; Konings, W.N.; Driessen, A.J.M. Distribution and physiology of ABC-type transporters contributing to multidrug resistance in bacteria. *Microbiol. Mol. Biol. Rev.* **2007**, *71*, 463–476. [\[CrossRef\]](#)
106. Weston, N.; Sharma, P.; Ricci, V.; Piddock, L.J.V. Regulation of the AcrAB-TolC efflux pump in *Enterobacteriaceae*. *Res. Microbiol.* **2018**, *169*, 425–431. [\[CrossRef\]](#)
107. Lomovskaya, O.; Lee, A.; Hoshino, K.; Ishida, H.; Mistry, A.; Warren, M.S.; Boyer, E.; Chamberland, S.; Lee, V.J. Use of a genetic approach to evaluate the consequences of inhibition of efflux pumps in *Pseudomonas aeruginosa*. *Antimicrob. Agents Chemother.* **1999**, *43*, 1340–1346. [\[CrossRef\]](#) [\[PubMed\]](#)
108. Morita, Y.; Komori, Y.; Mima, T.; Kuroda, T.; Mizushima, T.; Tsuchiya, T. Construction of a series of mutants lacking all of the four major mex operons for multidrug efflux pumps or possessing each one of the operons from *Pseudomonas aeruginosa* PAO1: MexCD-OprJ is an inducible pump. *FEMS Microbiol. Lett.* **2001**, *202*, 139–143. [\[CrossRef\]](#) [\[PubMed\]](#)
109. Dreier, J.; Ruggerone, P. Interaction of antibacterial compounds with RND efflux pumps in *Pseudomonas aeruginosa*. *Front. Microbiol.* **2015**, *6*. [\[CrossRef\]](#) [\[PubMed\]](#)
110. Li, X.-Z.; Plésiat, P.; Nikaido, H. The challenge of efflux-mediated antibiotic resistance in Gram-negative bacteria. *Clin. Microbiol. Rev.* **2015**, *28*, 337–418. [\[CrossRef\]](#) [\[PubMed\]](#)
111. Nishino, K.; Latifi, T.; Groisman, E.A. Virulence and drug resistance roles of multidrug efflux systems of *Salmonella enterica* serovar Typhimurium. *Mol. Microbiol.* **2006**, *59*, 126–141. [\[CrossRef\]](#)
112. Kobayashi, N.; Nishino, K.; Yamaguchi, A. Novel macrolide-specific ABC-type efflux transporter in *Escherichia coli*. *J. Bacteriol.* **2001**, *183*, 5639–5644. [\[CrossRef\]](#)
113. Iyer, R.; Moussa, S.H.; Tommasi, R.; Miller, A.A. Role of the *Klebsiella pneumoniae* TolC porin in antibiotic efflux. *Res. Microbiol.* **2019**, *170*, 112–116. [\[CrossRef\]](#)
114. Hansen, L.H.; Jensen, L.B.; Sørensen, H.I.; Sørensen, S.J. Substrate specificity of the OqxAB multidrug resistance pump in *Escherichia coli* and selected enteric bacteria. *J. Antimicrob. Chemother.* **2007**, *60*, 145–147. [\[CrossRef\]](#)
115. Guérin, F.; Lallement, C.; Isnard, C.; Dhalluin, A.; Cattoir, V.; Giard, J.-C. Landscape of resistance-nodulation-cell division (RND)-type efflux pumps in *Enterobacter cloacae* complex. *Antimicrob. Agents Chemother.* **2016**. [\[CrossRef\]](#)
116. Hernando-Amado, S.; Blanco, P.; Alcalde-Rico, M.; Corona, F.; Reales-Calderón, J.A.; Sánchez, M.B.; Martínez, J.L. Multidrug efflux pumps as main players in intrinsic and acquired resistance to antimicrobials. *Drug Resist. Update* **2016**, *28*, 13–27. [\[CrossRef\]](#)
117. Blanco, P.; Hernando-Amado, S.; Reales-Calderon, J.A.; Corona, F.; Lira, F.; Alcalde-Rico, M.; Bernardini, A.; Sanchez, M.B.; Martinez, J.L. Bacterial multidrug efflux pumps: Much more than antibiotic resistance determinants. *Microorganisms* **2016**, *4*, 14. [\[CrossRef\]](#) [\[PubMed\]](#)
118. Housseini, B.; Issa, K.; Phan, G.; Broutin, I. Functional mechanism of the efflux pumps transcription regulators from *Pseudomonas aeruginosa* based on 3D structures. *Front. Mol. Biosci.* **2018**, *5*. [\[CrossRef\]](#) [\[PubMed\]](#)
119. Olliver, A.; Vallé, M.; Chaslus-Dancla, E.; Cloeckaert, A. Role of an *acrR* mutation in multidrug resistance of in vitro-selected fluoroquinolone-resistant mutants of *Salmonella enterica* serovar Typhimurium. *FEMS Microbiol. Lett.* **2004**, *238*, 267–272. [\[CrossRef\]](#) [\[PubMed\]](#)
120. Webber, M.A.; Talukder, A.; Piddock, L.J.V. Contribution of mutation at amino acid 45 of AcrR to *acrB* expression and ciprofloxacin resistance in clinical and veterinary *Escherichia coli* isolates. *Antimicrob. Agents Chemother.* **2005**, *49*, 4390–4392. [\[CrossRef\]](#)
121. Ferrand, A.; Vergalli, J.; Pagès, J.-M.; Davin-Regli, A. An intertwined network of regulation controls membrane permeability including drug influx and efflux in *Enterobacteriaceae*. *Microorganisms* **2020**, *8*, 833. [\[CrossRef\]](#)
122. Ziha-Zarif, I.; Llanes, C.; Köhler, T.; Pechere, J.-C.; Plésiat, P. In vivo emergence of multidrug-resistant mutants of *Pseudomonas aeruginosa* overexpressing the active efflux system MexA-MexB-OprM. *Antimicrob. Agents Chemother.* **1999**, *43*, 287–291. [\[CrossRef\]](#)
123. Cohen, S.P.; Hächler, H.; Levy, S.B. Genetic and functional analysis of the multiple antibiotic resistance (*mar*) locus in *Escherichia coli*. *J. Bacteriol.* **1993**, *175*, 1484–1492. [\[CrossRef\]](#)

124. Wand, M.E.; Jamshidi, S.; Bock, L.J.; Rahman, K.M.; Sutton, J.M. SmvA is an important efflux pump for cationic biocides in *Klebsiella pneumoniae* and other *Enterobacteriaceae*. *Sci. Rep.* **2019**, *9*, 1–11. [\[CrossRef\]](#)
125. Guérin, F.; Gravey, F.; Plésiat, P.; Aubourg, M.; Beyrouthy, R.; Bonnet, R.; Cattoir, V.; Giar, J.-C. The transcriptional repressor smvr is important for decreased chlorhexidine susceptibility in *Enterobacter cloacae* complex. *Antimicrob. Agents Chemother.* **2019**, *64*, e01845-19, /aac/64/1/AAC.01845-19.atom. [\[CrossRef\]](#)
126. Pelling, H.; Bock, L.J.; Nzakizwanayo, J.; Wand, M.E.; Denham, E.L.; MacFarlane, W.M.; Sutton, J.M.; Jones, B.V. Derepression of the smvA efflux system arises in clinical isolates of *Proteus mirabilis* and reduces susceptibility to chlorhexidine and other biocides. *Antimicrob. Agents Chemother.* **2019**, *63*, e01535-19. [\[CrossRef\]](#)
127. Villagra, N.A.; Hidalgo, A.A.; Santiviago, C.A.; Saavedra, C.P.; Mora, G.C. SmvA, and not AcrB, is the major efflux pump for acriflavine and related compounds in *Salmonella enterica* serovar Typhimurium. *J. Antimicrob. Chemother.* **2008**, *62*, 1273–1276. [\[CrossRef\]](#) [\[PubMed\]](#)
128. Laborda, P.; Alcalde-Rico, M.; Blanco, P.; Martínez, J.L.; Hernando-Amado, S. Novel inducers of the expression of multidrug efflux pumps that trigger *Pseudomonas aeruginosa* transient antibiotic resistance. *Antimicrob. Agents Chemother.* **2019**, *63*, e01095-19. [\[CrossRef\]](#) [\[PubMed\]](#)
129. Reza, A.; Sutton, J.M.; Rahman, K.M. Effectiveness of efflux pump inhibitors as biofilm disruptors and resistance breakers in Gram-negative (ESKAPEE) bacteria. *Antibiotics* **2019**, *8*, 229. [\[CrossRef\]](#) [\[PubMed\]](#)
130. Renau, T.E.; Léger, R.; Flamme, E.M.; Sangalang, J.; She, M.W.; Yen, R.; Gannon, C.L.; Griffith, D.; Chamberland, S.; Lomovskaya, O.; et al. Inhibitors of efflux pumps in *Pseudomonas aeruginosa* potentiate the activity of the fluoroquinolone antibacterial levofloxacin. *J. Med. Chem.* **1999**, *42*, 4928–4931. [\[CrossRef\]](#)
131. Lomovskaya, O.; Warren, M.S.; Lee, A.; Galazzo, J.; Fronko, R.; Lee, M.; Blais, J.; Cho, D.; Chamberland, S.; Renau, T.; et al. Identification and characterization of inhibitors of multidrug resistance efflux pumps in *Pseudomonas aeruginosa*: Novel agents for combination therapy. *Antimicrob. Agents Chemother.* **2001**, *45*, 105–116. [\[CrossRef\]](#)
132. Watkins, W.J.; Landaverry, Y.; Léger, R.; Litman, R.; Renau, T.E.; Williams, N.; Yen, R.; Zhang, J.Z.; Chamberland, S.; Madsen, D.; et al. The relationship between physicochemical properties, *in vitro* activity and pharmacokinetic profiles of analogues of diamine-containing efflux pump inhibitors. *Bioorg. Med. Chem. Lett.* **2003**, *13*, 4241–4244. [\[CrossRef\]](#)
133. Osei Sekyere, J.; Amoako, D.G. Carbonyl cyanide m-chlorophenylhydrazine (CCCP) reverses resistance to colistin, but not to carbapenems and tigecycline in multidrug-resistant *Enterobacteriaceae*. *Front. Microbiol.* **2017**, *8*, 228. [\[CrossRef\]](#)
134. Bhattacharyya, T.; Sharma, A.; Akhter, J.; Pathania, R. The small molecule IITR08027 restores the antibacterial activity of fluoroquinolones against multidrug-resistant *Acinetobacter baumannii* by efflux inhibition. *Int. J. Antimicrob. Agents* **2017**, *50*, 219–226. [\[CrossRef\]](#)
135. Opperman, T.J.; Kwasny, S.M.; Kim, H.-S.; Nguyen, S.T.; Houseweart, C.; D'Souza, S.; Walker, G.C.; Peet, N.P.; Nikaido, H.; Bowlin, T.L. Characterization of a novel pyranopyridine inhibitor of the AcrAB efflux pump of *Escherichia coli*. *Antimicrob. Agents Chemother.* **2014**, *58*, 722–733. [\[CrossRef\]](#)
136. Nguyen, S.T.; Kwasny, S.M.; Ding, X.; Cardinale, S.C.; McCarthy, C.T.; Kim, H.-S.; Nikaido, H.; Peet, N.P.; Williams, J.D.; Bowlin, T.L.; et al. Structure–Activity relationships of a novel pyranopyridine series of Gram-negative bacterial efflux pump inhibitors. *Bioorg. Med. Chem.* **2015**, *23*, 2024–2034. [\[CrossRef\]](#)
137. Sjuts, H.; Vargiu, A.V.; Kwasny, S.M.; Nguyen, S.T.; Kim, H.-S.; Ding, X.; Ornik, A.R.; Ruggerone, P.; Bowlin, T.L.; Nikaido, H.; et al. Molecular basis for inhibition of AcrB multidrug efflux pump by novel and powerful pyranopyridine derivatives. *Prot. Nat. Acad. Sci. USA* **2016**, *113*, 3509–3514. [\[CrossRef\]](#) [\[PubMed\]](#)
138. Nicolau, D.P. Carbapenems: A potent class of antibiotics. *Expert Opin. Pharm.* **2008**, *9*, 23–37. [\[CrossRef\]](#) [\[PubMed\]](#)
139. Aghazadeh, M.; Hojabri, Z.; Mahdian, R.; Nahaei, M.R.; Rahmati, M.; Hojabri, T.; Pirzadeh, T.; Pajand, O. Role of efflux pumps: MexAB-OprM and MexXY(-OprA), AmpC cephalosporinase and OprD porin in non-metallo- β -lactamase producing *Pseudomonas aeruginosa* isolated from cystic fibrosis and burn patients. *Infect. Genet. Evol.* **2014**, *24*, 187–192. [\[CrossRef\]](#) [\[PubMed\]](#)
140. Sobel, M.L.; Neshat, S.; Poole, K. Mutations in PA2491 (mexS) promote MexT-dependent mexEF-oprN expression and multidrug resistance in a clinical strain of *Pseudomonas aeruginosa*. *J. Bacteriol. Res.* **2005**, *187*, 1246–1253. [\[CrossRef\]](#) [\[PubMed\]](#)

141. Breidenstein, E.B.M.; de la Fuente-Núñez, C.; Hancock, R.E.W. *Pseudomonas aeruginosa*: All roads lead to resistance. *Trends Microbiol.* **2011**, *19*, 419–426. [[CrossRef](#)] [[PubMed](#)]
142. Coyne, S.; Courvalin, P.; Périchon, B. Efflux-mediated antibiotic resistance in *Acinetobacter* spp. *Antimicrob. Agents Chemother.* **2011**, *55*, 947–953. [[CrossRef](#)]
143. Højby, N.; Bjarnsholt, T.; Givskov, M.; Molin, S.; Ciofu, O. Antibiotic resistance of bacterial biofilms. *Int. J. Antimicrob. Agents* **2010**, *35*, 322–332. [[CrossRef](#)]
144. Hall, C.W.; Mah, T.-F. Molecular mechanisms of biofilm-based antibiotic resistance and tolerance in pathogenic bacteria. *FEMS Microbiol. Rev.* **2017**, *41*, 276–301. [[CrossRef](#)]
145. Saxena, P.; Joshi, Y.; Rawat, K.; Bisht, R. Biofilms: Architecture, resistance, quorum sensing and control mechanisms. *Indian J. Microbiol.* **2019**, *59*, 3–12. [[CrossRef](#)]
146. Roy, R.; Tiwari, M.; Donelli, G.; Tiwari, V. Strategies for combating bacterial biofilms: A focus on anti-biofilm agents and their mechanisms of action. *Virulence* **2018**, *9*, 522–554. [[CrossRef](#)]
147. Singh, S.; Singh, S.K.; Chowdhury, I.; Singh, R. Understanding the mechanism of bacterial biofilms resistance to antimicrobial agents. *Open Microbiol. J.* **2017**, *11*, 53–62. [[CrossRef](#)] [[PubMed](#)]
148. Belanger, C.R.; Mansour, S.C.; Pletzer, D.; Hancock, R.E.W. Alternative strategies for the study and treatment of clinical bacterial biofilms. *Emerg. Top. Life Sci.* **2017**, *1*, 41–53. [[CrossRef](#)]
149. Ferrer-Espada, R.; Shahrour, H.; Pitts, B.; Stewart, P.S.; Sánchez-Gómez, S.; Martínez-de-Tejada, G. A permeability-increasing drug synergizes with bacterial efflux pump inhibitors and restores susceptibility to antibiotics in multi-drug resistant *Pseudomonas aeruginosa* strains. *Sci. Rep.* **2019**, *9*, 3452. [[CrossRef](#)] [[PubMed](#)]
150. Wright, G.D. Antibiotic adjuvants: Rescuing antibiotics from resistance. *Trends Microbiol.* **2016**, *24*, 862–871. [[CrossRef](#)]
151. Cox, G.; Koteva, K.; Wright, G.D. An unusual class of anthracyclines potentiate Gram-positive antibiotics in intrinsically resistant Gram-negative bacteria. *J. Antimicrob. Chemother.* **2014**, *69*, 1844–1855. [[CrossRef](#)]
152. Corbett, D.; Wise, A.; Langley, T.; Skinner, K.; Trimby, E.; Birchall, S.; Doral, A.; Sandiford, S.; Williams, J.; Warn, P.; et al. Potentiation of antibiotic activity by a novel cationic peptide: Potency and spectrum of activity of SPR741. *Antimicrob. Agents Chemother.* **2017**, *61*, e00200-17. [[CrossRef](#)]



© 2020 by the authors. Licensee MDPI, Basel, Switzerland. This article is an open access article distributed under the terms and conditions of the Creative Commons Attribution (CC BY) license (<http://creativecommons.org/licenses/by/4.0/>).

Appendix II - High throughput chemical screen method

A high throughput screen of a library of 87,648 compounds was conducted against recombinant EcDHDPS enzyme by the Walter and Eliza Hall Institute High Throughput Chemical Screening Facility (Melbourne, Australia). The *o*-aminobenzaldehyde (*o*-ABA) colourimetric assay was employed to assess DHDPS activity via the production of a purple chromophore measured spectrophotometrically at 540 nm [1]. For the primary screen, reactions comprised 0.5 mg·mL⁻¹ EcDHDPS, 0.5 mM sodium pyruvate and 0.5 mM ASA. Library compounds were added at final concentrations of 20 mM, with DMSO concentrations kept at a final concentration of 0.4% (v/v). Reactions were incubated at 25 °C for 15 mins after the addition of ASA, before the addition of HCl to a final concentration of 350 mM was added to stop the reaction. *o*-ABA was subsequently added to a final concentration of 0.44 mg·mL⁻¹, plates incubated at room temperature for 1 hour, and absorbance quantified at 540 nm. DMSO was used as a positive control, whilst negative controls lacked the substrate ASA. For the secondary screen, 11-point dose response curves were generated using the same reactions as described above. A counter screen was conducted using the same set-up without the inclusion library compounds before the addition of 350 mM HCl. Library compounds were then added after the reaction was stopped, followed by *o*-ABA to a final concentration of 0.44 mg·mL⁻¹. The plates were subsequently incubated at room temperature for 1 hour, and absorbance quantified at 540 nm.

Appendix III – CT1-5 Inhibition Determination

The DHDPS-DHDPR coupled assay was used to assess the inhibitory effect of CT1-5 against recombinant PaDHDPS1, PaDHDPS2, AbDHDPS, KpDHDPS and PaDHDPR enzymes, as previously described [2–4]. CT1-5 was dissolved in DMSO to a concentration of 100 mM and 50 mM, before being used at a final concentration of 1 mM and 0.5 mM within the reaction. To assess DHDPS inhibition, all assays were performed in triplicate and incubated with CT1-5 for 12 minutes at 37 °C prior to the addition of ASA for initiation of the reaction. DHDPS enzymes were used at a final concentration of 5 $\mu\text{g}\cdot\text{ml}^{-1}$, while EcDHDPR was kept in a 10-fold molar excess. To assess DHDPR inhibition, pre-assay mixtures, containing all reagents but PaDHDPR and CT1-5, were incubated for 12 minutes prior to the addition of ASA at a final concentration of 50 μM and incubated for 1 minute. CT1-5 was added to the reaction immediately prior to initiation with PaDHDPR (final concentration 5 $\mu\text{g}\cdot\text{ml}^{-1}$). EcDHDPS was kept at a 10-fold molar excess. The vehicle control used was 1% (v/v) DMSO. Substrate turnover was measured via the oxidation of NADPH at $\text{Abs}_{340\text{nm}}$ ($\epsilon_{340\text{nm}} = 6220 \text{ M}^{-1} \text{ cm}^{-1}$).

Appendix IV – CT1-5 Minimum Inhibitory Concentration

A broth microdilution method was used to determine the minimum inhibitory concentration (MIC) of CT1-5 against *P. aeruginosa* strains as defined by the Clinical Laboratory Standards Institute [5]. Specifically, 1×10^5 colony forming units per ml were inoculated using tryptic soy broth in 96 well plates with CT1-5 concentrations ranging from 256 – 0.25 $\mu\text{g}\cdot\text{ml}^{-1}$. Plates were incubated at 37 °C for 20 hours. Growth was assessed by measuring the absorbance at 600 nm. The MIC values was defined as the lowest concentration of CT1-5 where no bacterial growth was observed. Experiments were repeated with 3 biological replicates.

Appendix References

- 1 Yugari Y & Gilvarg C (1965) The condensation step in diaminopimelate synthesis. *J Biol Chem* **240**, 4710–4716.
- 2 Dobson RCJ, Devenish SRA, Turner LA, Clifford VR, Pearce FG, Jameson GB & Gerrard JA (2005) Role of arginine 138 in the catalysis and regulation of *Escherichia coli* dihydrodipicolinate synthase. *Biochemistry* **44**, 13007–13013.
- 3 Impey RE, Panjikar S, Hall CJ, Bock LJ, Sutton JM, Perugini MA & Soares da Costa TP (2019) Identification of two dihydrodipicolinate synthase isoforms from *Pseudomonas aeruginosa* that differ in allosteric regulation. *FEBS J*.
- 4 Impey RE, Lee M, Hawkins DA, Sutton JM, Panjikar S, Perugini MA & Costa TPS da (2020) Mis-annotations of a promising antibiotic target in high-priority gram-negative pathogens. *FEBS Lett* **594**, 1453–1463.
- 5 Wiegand I, Hilpert K & Hancock REW (2008) Agar and broth dilution methods to determine the minimal inhibitory concentration (MIC) of antimicrobial substances. *Nat Prot* **3**, 163–175.